Photoresponsive Modulation of a Freshwater Phytoplankton Community by Bacterial Lipopeptides

Dissertation

To Fulfill the

Requirements for the Degree of

„doctor rerum naturalium“ (Dr. rer. nat.)

Submitted to the Council of the Faculty

of Biological Sciences

of the Friedrich Schiller University Jena

by M. Sc. Colette Kurth

born on 18th October 1988 in Gelsenkirchen

Die Forschungsarbeit im Rahmen dieser Dissertation wurde von 08.2014 bis 07.2016 am Leibniz-Institut für Naturstoff-Forschung und Infektionsbiologie e.V. – Hans-Knöll-Institut in der Nachwuchsgruppe „Sekundärmetabolismus räuberischer Bakterien“ unter der Betreuung von Prof. Dr. Markus Nett in Jena durchgeführt. Von 08.2016 bis 06.2018 wurde sie am Institut für Anorganische und Analytische Chemie der Friedrich-Schiller-Universität Jena in der Abteilung „Bioorganische Analytik“ unter der Betreuung von Prof. Dr. Markus Nett und Prof. Dr. Georg Pohnert durchgeführt.

Gutachter 1: Prof. Dr. Markus Nett, Technische Universität Dortmund

Gutachter 2: Prof. Dr. Erika Kothe, Friedrich-Schiller-Universität Jena

Gutachter 3: Prof. Dr. Dieter Spiteller, Universität Konstanz

Tag der öffentlichen Verteidigung: 09.01.2019

Table of contents

1 Introduction

1.1 Chemical mediators in complex biosystems

Small molecules are an integral part of the language of (microbial) life. They mediate interactions that strongly affect community organization, population structure and ecosystem function.[1] The assumption that the majority of low molecular weight organic compounds secreted by microbes actually act as cell-signaling molecules in the environment,[2] reflects their ecological significance. Chemical mediators influence every aspect of life and determine whether an organism will feed on, be eaten by, mate with, be infected by, chase, evade or defend against other organisms next to it. These cues are extremely powerful and act within and between species of all kingdoms of life. A demonstrative example are male crabs, which attempt to mate with a bath sponge or stone, if soaked with the pheromones of a receptive female.[3,4] Mating in crustaceans is highly dependent on chemical mediators, that do not only enable mate finding from a far distance, but also prevent cannibalism during mating time.[1,5] Pheromone-based intraspecific communication has been known for decades and countless other examples could be named, especially from insects.[6–8] Chemically mediated interspecific interactions are often more difficult to assess, but are ecologically just as important. One example is the settlement and metamorphosis of coral larvae that are highly depend on chemical cues secreted by crustose coralline algae. While bacterial biofilms may induce metamorphosis in the larvae, only algal exudates seem to also induce settlement, which is indispensable for the juveniles' survival.[9] This further reflects the specificity of the interaction. Another example highlighting the importance of interkingdom communication for a species' success, is the interaction between the macroalga *Ulva mutabilis* and its symbiotic bacteria. Morphogenesis and growth of the alga absolutely depend on the combination of two bacterial species.[10,11] Without their exudates, *U. mutabilis* gametes cannot differentiate and form calamitous callus-like structures. The described examples delineate positive interactions, but negative interactions are just as impressive. For instance, diatoms were found to release polyunsaturated aldehydes upon predation that will accumulate in the herbivores' gonads and thereby hinder their reproductive success.[12] All these examples illustrate the tremendous role of chemical mediators in intra- and interspecies interactions. The nature of the involved molecules is amazingly diverse and often remains unknown, due to low concentrations, rapid degradation or complex cocktails that trigger a certain reaction, instead of a pure compound.[1] Unravelling the complex interactions based on these compounds is an intriguing prospect that will help understanding community structures and their changes. This is especially important with respect to climate change. Being

able to predict and/or direct community shifts may help reducing its negative effects on various ecosystems.

1.2 Interactions between diatoms and bacteria

Diatoms and bacteria have been coexisting in aquatic habitats for more than 200 million years.[13] Their long coevolution is even reflected in the diatoms' genomes that include an astonishing high level (≥5%) of bacterial genes acquired via horizontal gene transfer.[14] It is thus not surprising that diatoms and bacteria have developed intimate interactions. These are based on chemical mediators of known and unknown nature.[15] Nutrient exchange is common and often represents the basis for mutualistic interactions. One prominent example of such metabolic cross-feeding are bacteria that provide vitamin B_{12} to diatoms and obtain photosynthetically fixed carbon in exchange.[16] More than 50% of all algae are vitamin B_{12} auxotrophs and thus absolutely depend on an external supply.[16] The vitamin is required for methionine synthesis by organisms that do not harbor a vitamin B_{12}-independent methionine synthase. That is why diatoms either have to omit their requirement for vitamin B_{12} or to acquire it from bacteria which are able to produce it *de novo*. Another intimate interaction has been described between the diatom *Pseudo-nitzschia multiseries* and associated *Sulfitobacter* species.[17] The bacteria were found to use endogenous as well as diatom-secreted tryptophan for the biosynthesis of the hormone indole-3-acetic acid. This compound promotes algal cell division and further acts as signaling molecule between both species. In return, the diatoms excrete organosulfur compounds that are metabolized by the bacteria, supporting their growth. The interaction is highly complex and specific, with different bacteria having no inducing growth effect on *P. multiseries*.

Only relatively few bacterial genera are found in association with diatoms and most of them belong to the Proteobacteria and Bacteroidetes.[13,18–20] This leads to the assumption that the involved interactions are rather species-specific.[21] Indeed, transplant experiments showed that bacteria that had a beneficial effect on their native host, would have a negative, i.e. parasitic, effect on some "foreign" diatoms.[20] It appears that diatoms can select and cultivate the bacteria that will be most beneficial to them. This happens within the phycosphere, which is the zone directly surrounding the algal cell.[22,23] The phycosphere is confined from the surrounding fluid in that it does not mix. It therefore readily accumulates metabolites secreted by the algal cell. A unique aquatic microenvironment is created, that will attract certain bacteria and become a hotspot for interkingdom interactions. The involved metabolites produced by both partners are

often lipophilic to amphiphilic. This characteristic (i) minimizes their diffusive loss and (ii) may facilitate their uptake by either partner.[13]

Considering the facts that diatoms are responsible for about 20% of total primary production on Earth[24] and that their proliferation is significantly influenced by co-occurring bacteria, diatom-bacteria interactions appear to be of global importance. Their study will enrich our understanding on the occurrence of algal blooms, a recurrent phenomenon with significant ecological implications.

1.3 Diatoms and their need for iron

Some 30 years ago, it was postulated that primary productivity in the ocean is essentially limited by iron in a way that phytoplankton cannot take advantage of the excess surface nitrate and phosphate.[25,26] This would, at least partly, cause high nutrient-low chlorophyll regions that cover >20% of the Earth's oceans.[27] These regions are characterized by rather constant phytoplankton biomass, while spring blooms are rare and macronutrients are never absolutely depleted. It was further suggested that iron fertilization of the ocean should result in massive phytoplankton blooms, especially in these regions.[28] This "iron hypothesis" could indeed be confirmed in numerous large-scale experiments.[29]

The reason for this apparent insatiable need for iron lies in the fact that life on Earth originated in an anaerobic atmosphere. Under these conditions, the transition metal mainly occurs in the oxidation state Fe^{2+} (ferrous iron), which is soluble (0.1 M at pH 7) and highly bioavailable. Under aerobic conditions, however, iron mainly occurs as Fe^{3+} (ferric iron), which is extremely insoluble (1.4×10^{-9} M at pH 7) and therefore hardly bioavailable.[30] Besides its high abundance and bioavailability in the pre-photosynthetic era, iron also exhibits a unique redox and coordination chemistry, which promoted its incorporation into proteins as versatile co-factor. Examples of iron-containing prosthetic groups are the widely distributed and functionally diverse iron-sulfur clusters and hemes (iron-porphyrin clusters).[31] Around 10% of all characterized enzymes and over 80% of known oxidoreductases use iron, mainly in their catalytic centers.[32] As a result, iron is involved in many biological key processes, including photosynthesis, respiration, N_2 fixation, the tricarboxylic acid cycle and DNA biosynthesis and has become indispensable for virtually all life.[33] There are only extremely few organisms that do not require iron for survival, such as *Borrelia burgdorferi*, the causative agent of lyme disease,[34] and *Lactobacillus plantarum*.[35] The onset of photosynthesis, led to an increase of

oxygen levels in the atmosphere which gradually decreased the bioavailability of iron. As a consequence, organisms had to evolve elaborate strategies in order to access this vital element and ensure their survival.

In most of the large-scale iron fertilization experiments conducted in the ocean, diatoms clearly dominated the observed phytoplankton blooms.[29] They thus must possess particularly efficient iron uptake und storage mechanisms, resulting in such competitive advantage. Originally, phytoplankton was assumed to primarily use dissolved uncomplexed iron, Fe', which appears to be highly bioavailable. Fe' binds to surface ligands, and subsequently gets internalized by transfer across the plasma membrane.[36] A recent study in the diatom *Phaeodactylum tricornutum* revealed that the involved iron starvation-induced proteins (ISIPs) are actually phytotransferrins.[37] These glycoproteins bind Fe^{3+} along with CO_3^{2-}, accumulate at the cell surface and get internalized via endocytosis. Then, the carbonate anion is protonated and Fe^{3+} is reduced, disrupting the complex and releasing the iron into the cell. This iron uptake strategy is under thermodynamic control and proportional to the concentration of Fe'.[38] The fact that more than 99% of the dissolved iron in the ocean is complexed to organic ligands[39] suggests that Fe' is too scarce to satisfy the need of phytoplankton for iron. Thus other strategies must exist. For diatoms, a reductive iron uptake mechanism was suggested.[40] This has been well-characterized for the yeast *Saccharomyces cerevisiae* and the corresponding homologous genes have been identified in several diatoms.[41] Extracellular Fe^{3+}-complexes are dissociated via reduction at the cell surface by specialized flavohemoproteins (Fre). Fe^{2+} is subsequently reoxidized by a multi-copper oxidase (Fet) and transported across the cell membrane by a permease (Ftr).[42] A relationship between iron limitation and need for copper was assessed in several diatoms, further corroborating the assumption that such reductive iron uptake mechanism occurs.[43,44] This iron uptake strategy has the advantage that most iron species present in the ocean, even ferrisiderophores (i.e., iron-bound siderophores),[45] can be used as iron sources. Diatoms are also able to take up ferrisiderophores as a complex, without prior iron reduction.[46] This involves binding of the ferrisiderophore to the cell surface and subsequent endocytosis-mediated uptake and delivery to the chloroplast.

External iron supply usually reaches the ocean either via rivers or, more importantly, via aeolian dust transport from the great deserts of the Earth.[47] This often means that long periods of severe iron paucity will be followed by short intervals of iron abundance. Bloom-forming diatoms were found to use maxi-ferritins for iron storage,[48] which certainly contribute to their success in persisting long periods under chronically low iron concentrations and rapidly dominating

blooms once iron becomes abundant. Their way to cope with the intricate iron bioavailability makes diatoms arguably the most successful group of eukaryotic phytoplankton in the ocean. Associated bacteria have a major influence on iron speciation by secreting photoreactive siderophores. Once they have complexed Fe^{3+}, these molecules readily undergo photooxidative cleavage, thereby releasing Fe^{2+} into the environment.[49] This solubilized iron is highly bioavailable to phytoplankton[50] and should be taken up via ISIP-mediated endocytosis in diatoms. Bacteria can thus significantly support algal iron uptake and growth. Considering the severity of iron paucity and the ecological importance of diatoms in most aquatic ecosystems, such photoreactive siderophore-based diatom-bacteria interactions are of fundamental importance and have the potential to shape planktic communities.

1.4 Siderophore-mediated iron uptake in bacteria

Bacteria have developed different strategies to overcome the challenge of poor iron availability, one of the most important being the production of siderophores (Greek: iron carriers). Siderophores are small molecules (500-1500 Da) that exhibit extremely strong affinity towards Fe^{3+}. They are typically secreted by bacteria and fungi under low iron stress in order to scavenge iron from the environment and provide it to the cell.[51] Siderophores often use catecholate, hydroxamate and/or α-hydroxy carboxylate moieties for coordinating the iron, as negatively charged oxygen atoms strongly interact with Fe^{3+} (Fig. 1). Other functional groups that include nitrogen or sulfur as donor atoms may also be used, but have lower selectivity towards Fe^{3+}.[51] Most siderophores harbor three bidentate ligands, resulting in a hexadentate coordination of the iron atom. This appears to be the optimal denticity, satisfying the six coordination sites of Fe^{3+}. However, there are numerous examples of siderophores with less than six coordination sites, such as vibrioferrin,[52] pyochelin,[53] and rhodotorulic acid.[54] In these cases a single siderophore molecule cannot achieve full Fe^{3+} coordination saturation. Consequently, the usual metal to ligand (L) ratio of 1:1 has to be modified to e.g. Fe_2L_3, $FeL(H_2O)_2^+$, $Fe_2L_2(H_2O)_4^{2+}$, etc.[54]

There are over 500 different siderophores,[51] delineating their importance in nature. In the microbial world, competition for iron is tough and efficient siderophore usage is crucial. In order to ensure iron uptake under different environmental conditions (pH, [Fe], occurrence of competitors, etc.), many microorganisms are able to produce more than one siderophore. The acquisition of xenosiderophores (i.e., siderophores produced by other species) represents another approach to ensure sufficient iron uptake by the own species. It is also known as siderophore piracy. *Pseudomonas aeruginosa*, for instance is able to produce pyochelin and

pyoverdine. In addition to these siderophores, the bacterium possesses specific uptake systems for enterobactin, citrate, ferrioxamine and ferrichrome as xenosiderophores.[55,56]

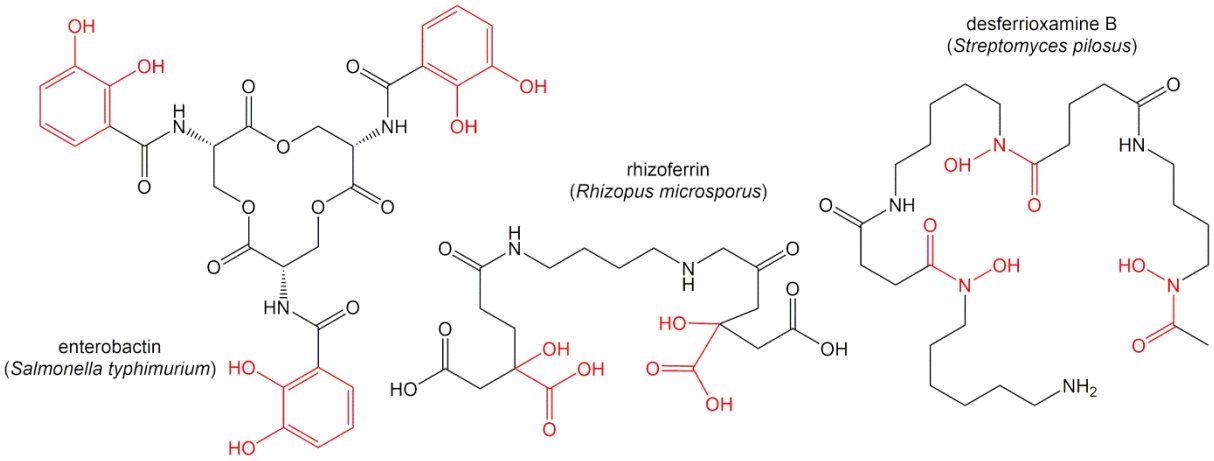

Fig. 1: Selected examples of catecholate, α-hydroxy carboxylate and hydroxamate type siderophores. The organisms from which these siderophores were first isolated are set in parentheses.

In Gram-negative bacteria, where two membranes have to be crossed, the uptake of ferrisiderophores involves several steps.[57] First, high-affinity outer membrane receptors recognize the complexes and mediate their transport into the periplasmic space. This process is activated by the Ton complex, which comprises the integral membrane protein ExbB and the membrane-anchored proteins ExbD and TonB. TonB undergoes a conformational change, driven by the proton-motive force that is mediated by ExbB and ExbD. It thereby interacts with the outer membrane receptor, initiating transport. Once in the periplasmic space, the ferrisiderophore is loaded onto the periplasmic-binding protein component of an ABC transporter. Delivery to the cytoplasm is executed by the permease component of the ABC transporter using ATP.

In Gram-positive bacteria siderophore-mediated iron uptake is less well-studied, but there seem to be similarities with the mechanisms described for Gram-negatives. Lipoprotein siderophore-binding proteins have been identified, which are anchored to the membrane, bind siderophores and import Fe-siderophores via a permease and an ATPase.[58] Interestingly, these lipoproteins were found to bind not only the ferrisiderophores, but also iron-free siderophores. This enables a siderophore-shuttle mechanism, where a ferrisiderophore delivers Fe^{3+} to the lipoprotein-bound iron-free siderophore, which is subsequently transported into the cell. Alternatively, the iron-free siderophore is displaced from the lipoprotein to allow ferrisiderophore binding and uptake.[59] The utility of binding an iron-free siderophore in the first place is questionable. A

possible explanation is that a variety of Fe^{3+} species could be caught in that way. Also, iron-free siderophores usually reach far higher concentrations at the cell surface than ferrisiderophores. The siderophore-shuttle mechanism may thus maximize iron-uptake efficiency by transferring Fe^{3+} from the ferrisiderophore to the iron-free siderophore without requiring its reduction.[58,59]

In order to fulfill its biological function, iron needs to be released from the siderophore once inside the cell.[60] The most efficient way seems to be the reduction of Fe^{3+} to Fe^{2+}, which reduces the affinity. Another possibility is the hydrolysis of the siderophore, which however has the major disadvantage that the siderophore cannot be reused.

1.5 Biosynthesis of siderophores

Most siderophores are synthesized by nonribosomal peptide synthetases (NRPSs).[61] These large enzymes are modularly organized. NRPSs assemble complex peptides of great structural and biological diversity, including siderophores, toxins, pigments, antibiotics, cytostatics, and immunosuppressants. NRPSs are widely distributed in bacteria and fungi.[62] Peptide synthesis takes place in an assembly line-like mechanism, where each NRPS module incorporates a selected substrate into the peptide (Fig. 2). Not only the 20 proteinogenic amino acids, but a plentitude of monomers, including nonproteinogenic, carboxy, *N*-methylated and D-amino acids have been identified as potential substrates and thus represent the building blocks of nonribosomal peptides.[64] As the number, order and identity of NRPS modules determine the structure of the synthesized peptide, NRPSs are also referred to as “protein templates”.[65] Each NRPS module comprises at least three domains: the adenylation (A), the thiolation (T) and the condensation (C) domain. The A domain is responsible for substrate recognition and activation to the corresponding aminoacyl adenylate. This instable intermediate is transferred to the T domain that functions as carrier protein for the growing acyl chain. The C domain catalyzes the peptide bond formation between the substrates. The final module of a NRPS usually exhibits an additional thioesterase (TE) domain that cleaves the product off the enzyme. Some modules may harbor additional domains, such as epimerization or cyclization domains to further modify the substrate’s structure.

Fig. 2 shows the NRPS-dependent biosynthetic assembly of cupriachelin,[66] which is the central molecule of the present study. Decanoic acid acts as biosynthetic starter unit and was proposed

to originate from fatty acid metabolism, where it is already present in the activated form. The following peptide synthesis largely follows the NRPS enzymatic logic.

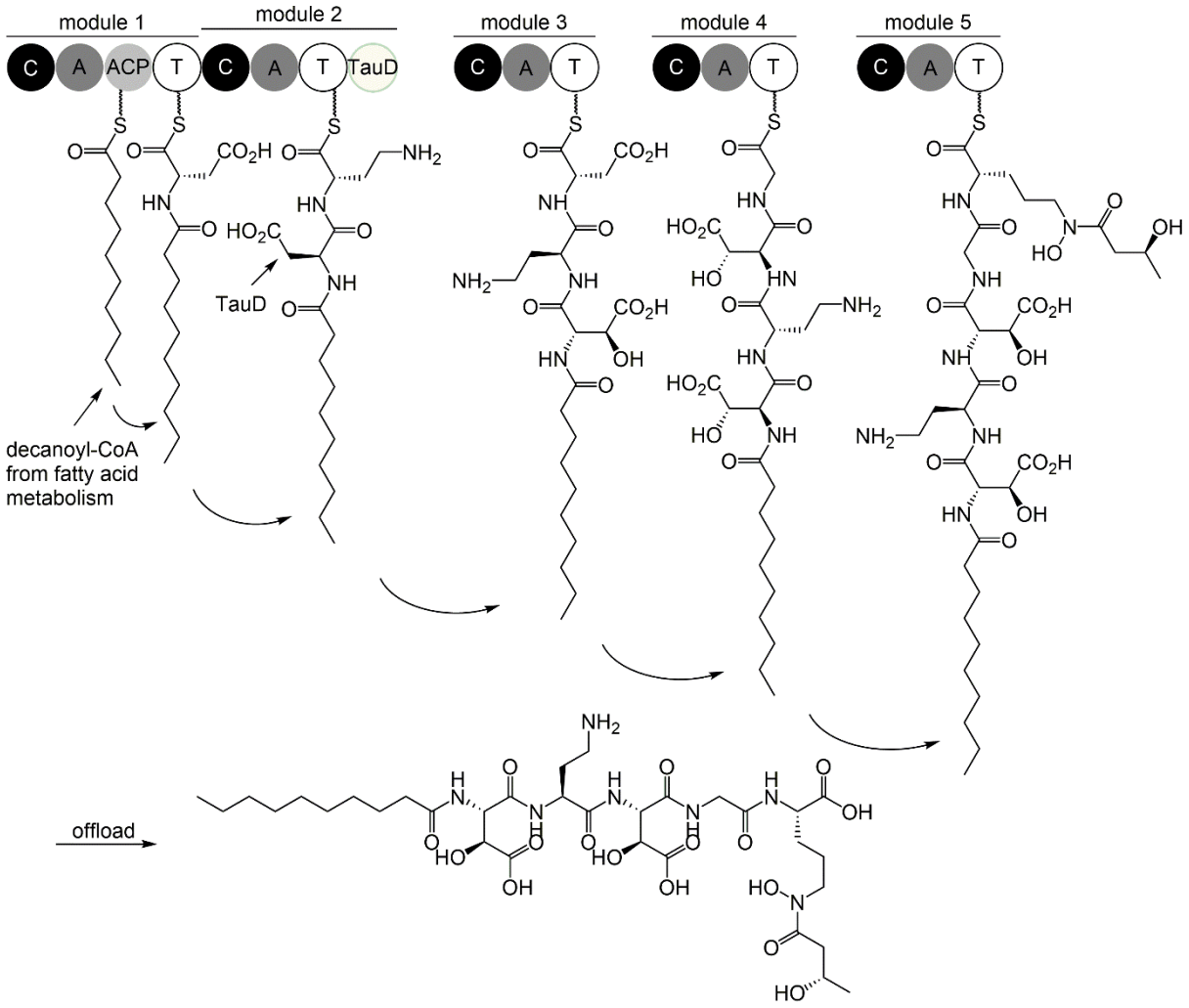

Fig. 2: NRPS-dependent biosynthesis of the siderophore cupriachelin. Domain notations: C, condensation; A, adenylation; ACP, acyl carrier protein; T, thiolation; TauD, hydroxylase. Modified after Kreutzer et al.[66]

In some cases, siderophore biosynthesis is catalyzed by NRPS-independent synthetases. Siderophores produced by these enzymes are not polypeptides, but are assembled from dicarboxylic and diamine or amino alcohol units. Aerobactin was the first siderophore found to be produced by an NRPS-independent siderophore (NIS) biosynthesis pathway[67,68] and remained the only example for almost one decade. Nowadays it has become apparent that NIS biosynthesis pathways are not uncommon and can be found in many bacterial species.[69] Examples of NISs include vibrioferrin,[70] rhizobactin,[71] achromobactin,[72] and alcaligin.[73] Aerobactin biosynthesis has been well-characterized[67,68] and exemplifies the NIS biosynthesis

pathway (Fig. 3).[74] The aerobactin cluster consists of five genes, *iucABCD* and *iutA*, the latter encoding a receptor protein. IucD is a flavin-dependent monooxygenase that hydroxylates the ε-amino group of lysine. IucB, an acyl transferase, subsequently catalyzes the ε-N-acetylation. IucA and IucC finally condensate the modified lysine to citric acid, yielding aerobactin. The biosynthesis of other NISs employs at least one enzyme with significant sequence similarity to either IucA or IucC.[69]

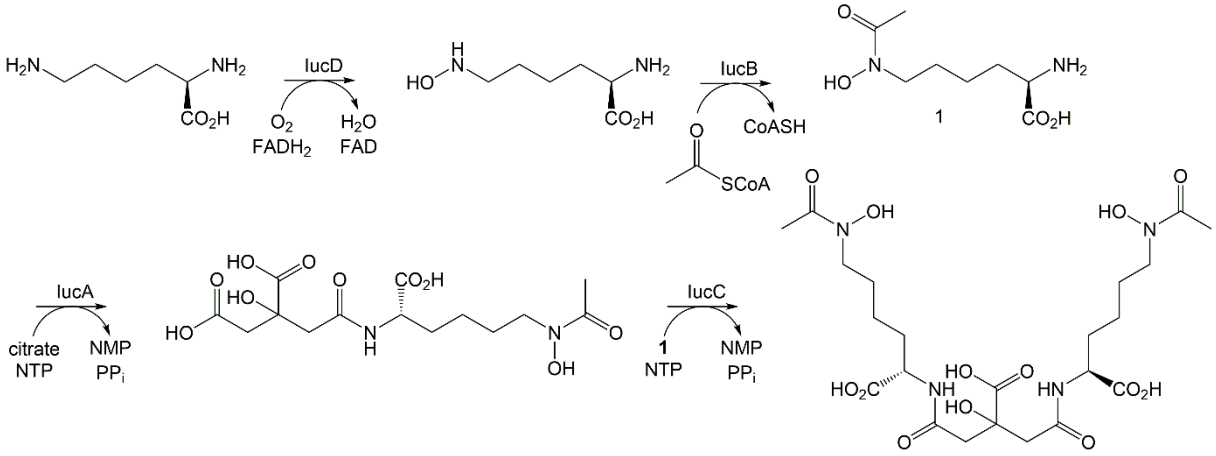

Fig. 3: Aerobactin assembly exemplifying NRPS-independent siderophore biosynthesis. Modified after Challis.[69]

1.6 Transcriptional regulation of siderophore biosynthesis

As delineated before, iron is indispensable for many biological key processes and its deprivation can be fatal for an organism. On the other hand, iron over-abundance can be just as dangerous. Free soluble iron is toxic to cells by catalyzing the formation of reactive oxygen species (ROS) in the Haber-Weiss reaction:

$$(1)\ Fe^{3+} + O_2^{-\bullet} \rightleftharpoons Fe^{2+} + O_2$$

$$(2)\ Fe^{2+} + H_2O_2 \rightleftharpoons Fe^{3+}\ OH^{\bullet} + OH^{-}$$

ROS target all biological macromolecules and thus represent a serious threat to the cell. They can directly attack polyunsaturated fatty acids in cell membranes, resulting in decreased membrane fluidity and disruption of membrane-bound proteins. Further, ROS tackle the base and sugar moieties of DNA, leading to single- and double-strand breaks. The oxidation of proteins represents another cell damage caused by ROS. All these modifications are deleterious to the cell, leading to loss of function of membranes and proteins, mutations and eventually to cell death.[75] Life-sustaining, but potentially toxic, iron thus represents an element that requires

a well-balanced homeostasis. Tight regulation of iron uptake, storage and consumption are absolutely essential for the survival of every organism.[33] In many bacteria, this regulation is mediated by the ferric uptake regulator (Fur). In the "classical" model (Fig. 4), Fur acts as transcriptional repressor.[76] When intracellular iron concentrations are high, *apo*-Fur binds Fe^{2+}, thereby dimerizes, and the *holo*-protein blocks the transcription of its target genes by binding to their promoter regions. Fur has been found to regulate over 90 genes in *Escherichia coli*[77] and can thus be regarded as global regulator. Besides genes that are directly associated to iron metabolism, various genes related e.g. to swarming, toxin production or defense against oxygen radicals were found to be controlled by Fur.[78] The protein interacts with the DNA by binding to a region within the promoter called Fur-box. This was initially described as a conserved 19 bp inverted repeat sequence (5'-GATAATGATAATCATTATC-3').[79] However, there is recent evidence that the sequence recognized by Fur is actually highly degenerate. Fur was found to recognize DNA via base readout only to a limited degree, while shape readout appeared much more important.[80] A narrow minor groove in the DNA, typical of AT-rich regions, was found to be identified by Lys15 of Fur. The order of A and T base pairs, as well as the base pairs in between, however, allowed random variations.[80] This enables Fur to recognize an array of different target sequences, which seems plausible for a global regulator. Besides acting as transcriptional repressor, Fur may also act as activator.[81] While iron uptake genes are generally repressed by Fur when iron is abundant, many genes encoding iron-using proteins are upregulated. This is indirectly mediated by small regulatory RNAs, such as RyhB (Fig. 4). The 90-nt RNA was initially discovered in *E. coli*[82] and homologs have been found in numerous bacteria.[83] RyhB itself is negatively regulated by Fur. When iron is abundant, Fur represses RyhB transcription and translation of non-essential iron-using proteins can occur. However, when iron is limited, RyhB is transcribed and pairs with the mRNA of its target genes, blocking their translation. The RNA-protein complexes are rapidly degraded and no gene product is formed.

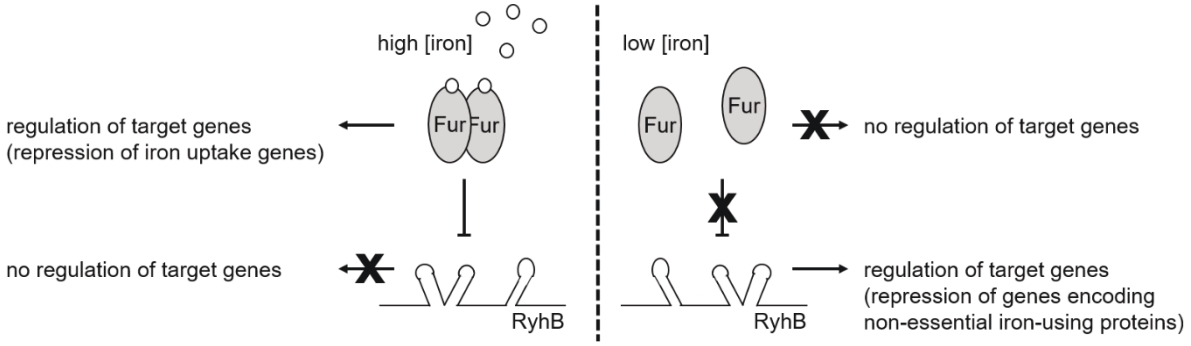

Fig. 4: Interplay of the transcription factor Fur and the small regulatory RNA RyhB in gene regulation. When the iron concentration is high, Fur represses many genes, including *ryhB*. When the iron concentration is low, Fur repression is relieved and *ryhB* is expressed, blocking the transcription of its target genes. Modified after Porcheron and Dozois.[83]

Iron homeostasis is vital and is based on Fur in numerous Gram-negatives and Gram-positives with low genomic GC content. Gram-positives with high genomic GC content use regulators of the diphtheria toxin repressor (DtxR) family instead of Fur.[84] Even though proteins of both families show very low sequence similarity, they are structurally and functionally analogous. Upon binding of a divalent metal iron, DtxR, just like Fur, undergoes a conformational change, dimerizes and binds to the DNA as transcription factor.[85]

1.7 Photoreactive lipopeptide siderophores

Many siderophores known from the marine environment are photoreactive. Once they have complexed Fe^{3+}, these siderophores will immediately get cleaved upon sunlight (UV light) exposure. The iron thereby gets reduced and released into the environment. Photoreactivity of marine siderophores was first described for aquachelins (Fig. 5).[49] Numerous other examples followed, including marinobactins,[86] synechobactins,[87] loihichelins,[88] ochrobactins,[89] petrobactin,[90] vibrioferrin,[52] and imaqobactin.[91] The photoreactive cleavage mechanism has not been fully resolved to date, but the presence of an α-hydroxy carboxylate function (usually β-hydroxy aspartate[92] or citrate) seems crucial in this context. It is known that the absorption of a photon leads to a ligand-to-metal charge transfer.[49] The loss of an electron destabilizes the siderophore which will finally result in its dissociation. Depending on the site of cleavage, the photoproduct may exhibit similar (e.g., petrobactin,[90] aerobactin[93]) or weaker (e.g., aquachelin[49]) affinity towards Fe^{3+} compared to the parent siderophore, or may even completely lose its ability to bind iron (e.g., vibrioferrin[52]).

Besides photoreactivity, amphiphilicity is another important feature of many marine siderophores. Bacteria often produce several derivatives of an amphiphilic siderophore, where the (non-variable) Fe^{3+}-binding peptidic headgroup is appended by fatty acid side chains of varying lengths. The relative size of the fatty acid chain compared to the peptidic head group is crucial for the secretion behavior of the siderophore. Hydrophobic siderophores, such as amphibactins, will mostly remain cell-associated.[94] In contrast, siderophores with longer peptidic headgroups, such as loihichelins with eight amino acids compared to fatty acid chains of only C_{10}-C_{14}, are rather hydrophilic and will be excreted into the surroundings of the cell.[86] Amphiphilicity further entails self-assembly of the molecules, either to micelles (for iron-free siderophores) or to vesicles (for ferrisiderophores).[86] This behavior has been suggested to (i) protect the siderophores from proteolytic cleavage, (ii) prolong their residence time in the vicinity of the producing cell and/or (iii) concentrate iron around the cell.[95]

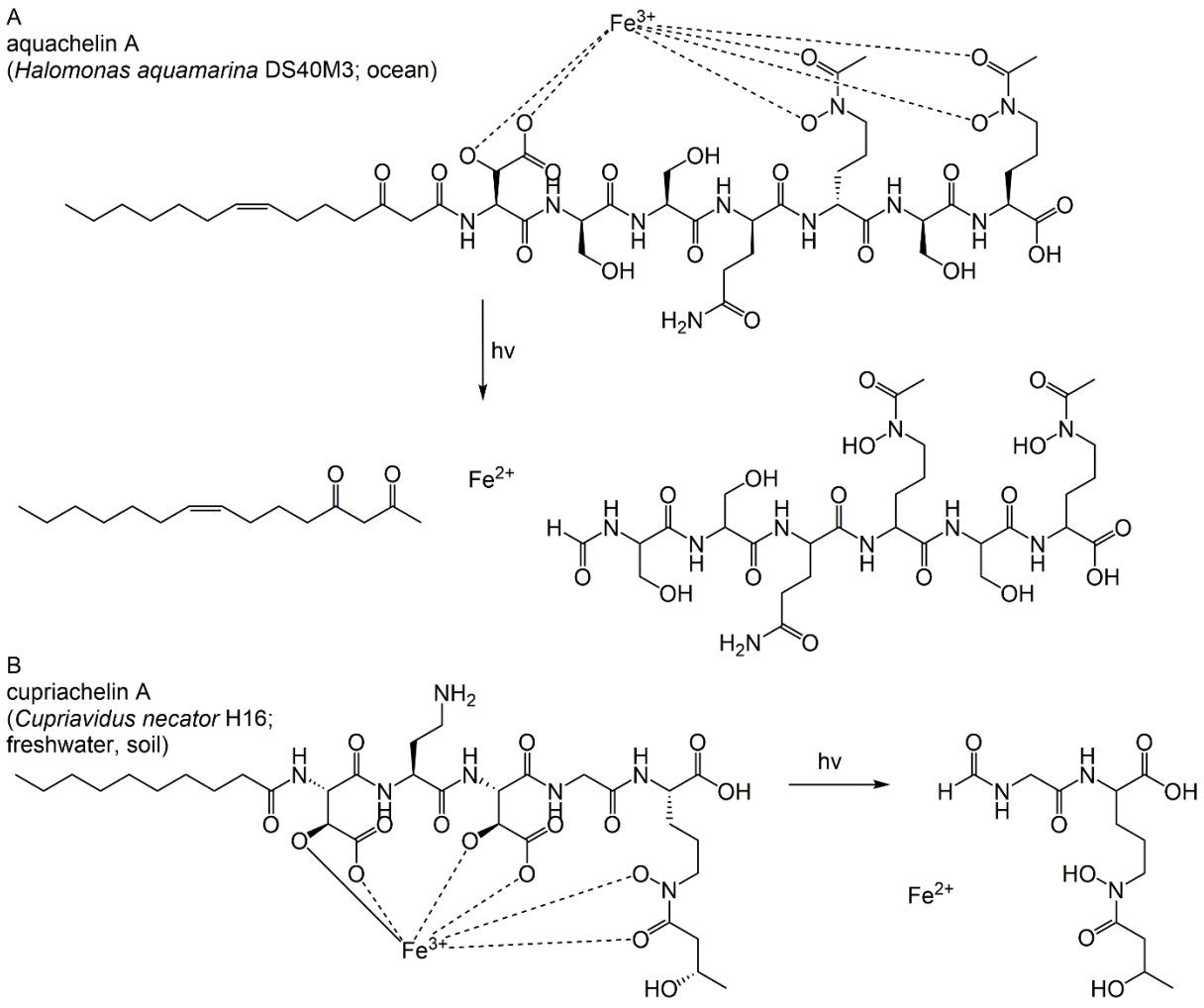

Fig. 5: Aquachelins (A) and cupriachelins (B) as examples of photoreactive lipopeptide siderophores. Upon UV-light exposure, the ferrisiderophores are cleaved, yielding photoproducts and soluble Fe^{2+}.

Considering their photoreactive and amphiphilic characteristics, marine siderophores are intriguing molecules that play a major role in iron cycling in marine environments. The release of solubilized iron into the environment, rather than into the cells of the siderophore producer, raises questions for the primary function of these molecules. Obviously, the siderophore-solubilized iron becomes available to the whole microbial community. A photoreactive siderophore-based mutualism could be demonstrated between heterotrophic bacteria and phytoplankton, where the bacteria obtained photosynthetically fixed carbon in exchange for the shared iron.[50] Such mutualism represents a possible explanation, why bacteria produce siderophores that do not only ascertain the own iron supply, but also "feed" others. Few studies have been carried out to further corroborate this "carbon for iron mutualism". Also, little is known about the chemical mediators involved in these bacteria-phytoplankton interactions. Bacteria maximally profit of iron sharing, if the corresponding partners are mutualists and non-mutualists are excluded. This means that bacteria should be able to distinguish between their interaction partners. Mutualists may notify their presence to the bacteria by certain exudates, which may in turn trigger bacterial photoreactive siderophore biosynthesis.

Photoreactive lipopeptide siderophores are widely distributed amongst marine bacteria where they represent the basis for various planktic interactions. Considering the scarcity of iron in the ocean, they can be expected to have a major impact on the composition of planktic communities. Recently, photoreactive lipopeptide siderophores were also discovered from a freshwater bacterium.[66] The cupriachelins (Fig. 5) from *Cupriavidus necator* H16 suggest that photoreactive siderophores may be similarly important in freshwater, as they are in the oceans.

2 Scope of the study

Numerous studies on photoreactive lipopeptide siderophores from marine bacteria indicate that these molecules have a fundamental effect on iron cycling in the ocean. This includes the light-induced release of solubilized iron into the environment, which entails interspecies interactions and thereby determines the composition of the plankton community. In freshwater environments, however, such molecules were only recently discovered and have barely been investigated with respect to their ecological impacts.

An important aspect to be studied, is the occurrence of photoreactive lipopeptide siderophores in freshwater. This will allow first conclusions about their ecological relevance. The discovery of cupriachelins, the first photoreactive lipopeptide siderophores originating from a freshwater bacterium, adumbrates that these molecules may be just as important in freshwater, as they are in the ocean. However, it is also possible that cupriachelin is an exception and that its photoreactive properties rather represent an evolutionary relict without ecological significance. The discovery of novel freshwater photoreactive lipopeptide siderophores would thus represent a first step towards recognizing their role in these environments and represents a major objective of this study.

Furthermore, the study of bacterial-algal interactions based on these siderophores is crucial for assessment of their ecological relevance. The "carbon for iron mutualism" has been demonstrated in the marine environment.[50] If photoreactive lipopeptide siderophores also occur in freshwater, it is well-conceivable that they will entail similar planktic interactions as their marine counterparts. In this study, the interaction between the β-proteobacterium *C. necator* H16 and the pennate diatom *Navicula pelliculosa* is investigated (Fig. 6). Both organisms were chosen for their ubiquitous occurrence in freshwater. The cupriachelin-producer *C. necator* H16 grows heterotrophically under the chosen laboratory conditions and thus depends on external organic carbon sources, which could be provided by symbiotic phytoplankton. The genome of *C. necator* H16 is fully sequenced,[96,97] which represents another advantage to use it as model organism. *N. pelliculosa* is available as axenic culture from the SAG culture collection (SAG 1050-3). Thus, the effect of other diatom-associated bacteria on the studied interaction can be ruled out. The hypothesized "carbon for iron mutualism" between *C. necator* H16 and *N. pelliculosa* suggests that the organisms will have a positive growth effect on each other. In this study, the question whether the diatom can induce bacterial siderophore production will also be addressed. An affirmative answer would further corroborate the "carbon for iron mutualism"

by suggesting that the diatom profits from cupriachelin in such an extent, that it further induces its biosynthesis in order to maximize its own benefit.

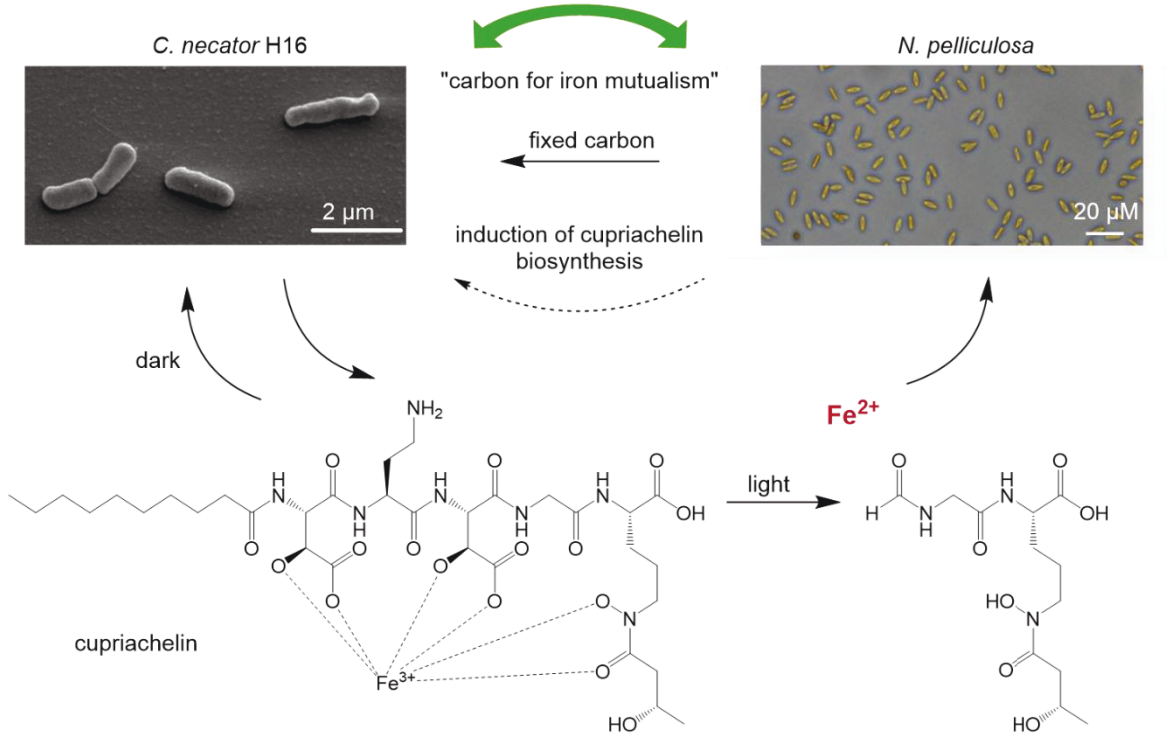

Fig. 6: Hypothesized cupriachelin-based interaction between *C. necator* H16 and *N. pelliculosa*. The heterotrophic siderophore-producing bacterium provides iron to the photoautotrophic algae, which provides fixed carbon in exchange.

The results of this thesis should give valuable insight into iron cycling in freshwater environments. It is one of the first studies addressing photoreactive siderophores in these environments, aiming at assessing their ecological significance.

3 Manuscripts

Manuscript A:

Kurth C, Schieferdecker S, Athanasopolou K, Seccareccia I, Nett M

Variochelins, lipopeptide siderophores from *Variovorax boronicumulans* discovered by genome mining. *Journal of Natural Products* 79 (2016): 865-872.

Variochelins, photoreactive lipopeptide siderophores, were isolated from the freshwater bacterium *Variovorax boronicumulans*. Such siderophores are well-known from the marine environment, where they have been attributed a major role in iron cycling. In freshwater, variochelins are the second photoreactive lipopeptide siderophores discovered, suggesting that these molecules may play a similar ecological role in these environments as they do in the ocean.

Colette Kurth annotated the variochelin gene cluster, isolated variochelins, performed chemical analyses as well as photoreactivity experiments and wrote the final manuscript (65%). Sebastian Schieferdecker conducted the stereochemical analyses (10%). Kalliopi Athanasopoulou assisted the isolation of variochelins (4%). Ivana Seccareccia carried out siderophore screening studies (1%). Prof. Dr. Markus Nett designed the research project, carried out bioinformatic analyses, performed the structure elucidation and edited the final manuscript (20%).

Manuscript B:

Kurth C, Wasmuth I, Wichard T, Pohnert G, Nett M

Algae induce siderophore biosynthesis in the freshwater bacterium *Cupriavidus necator* H16. Submitted.

Cupriavidus necator H16 produces the photoreactive siderophore cupriachelin which is hypothesized to provide solubilized iron not only to the siderophore producer, but to the whole planktic community. Cupriachelin should thus be highly beneficial for phytoplankton. This study demonstrates that the diatom *Naviculla pelliculosa* can induce cupriachelin biosynthesis in *C. necator* H16, corroborating a “carbon for iron mutualism”.

Colette Kurth constructed cupriachelin biosynthesis reporter strains, performed β-galactosidase and DNA-protein pulldown assays, performed atomic absorption spectroscopy (AAS) measurements, conducted statistical data analysis and wrote the final manuscript (80%). Ina Wasmuth assisted β-galactosidase assays, DNA-protein pulldown assays and statistical data analysis (5%). Dr. Thomas Wichard guided statistical data analyses (2.5%). Prof. Dr. Georg Pohnert contributed to research design (2.5%). Prof. Dr. Markus Nett designed the research project and edited the final manuscript (10%).

Manuscript C:

Kurth C, Kage H, Nett M

Siderophores as molecular tools in medical and environmental applications. *Organic & Biomolecular Chemistry* 14 (2016): 8212-8227.

Medical and environmental applications of siderophores are reviewed. The potential of photoreactive lipopeptide siderophores to shape planktic communities is discussed with respect to the biocontrol of harmful algal blooms.

Colette Kurth wrote the section “Non-medical applications of siderophores” (33.3%). Dr. Hirokazu Kage wrote the section “Medical applications” (33.3%). Prof. Dr. Markus Nett wrote the introduction and edited the final manuscript (33.3%).

_____

Prof. Dr. Markus Nett

3.1 Manuscript A

Kurth C, Schieferdecker S, Athanasopolou K, Seccareccia I, Nett M

Variochelins, lipopeptide siderophores from *Variovorax boronicumulans* discovered by genome mining. *Journal of Natural Products* 79 (2016): 865-872.

JOURNAL OF NATURAL PRODUCTS

Article

pubs.acs.org/jnp

Variochelins, Lipopeptide Siderophores from *Variovorax boronicumulans* Discovered by Genome Mining

Colette Kurth,[†] Sebastian Schieferdecker,[†] Kalliopi Athanasopoulou,[†] Ivana Seccareccia,[†] and Markus Nett*[,†,‡]

[†]Leibniz Institute for Natural Product Research and Infection Biology e.V., Hans-Knöll-Institute, Beutenbergstraße 11a, 07745 Jena, Germany

[‡]Department of Biochemical and Chemical Engineering, Technical Biology, Technical University Dortmund, Emil-Figge-Straße 66, 44227 Dortmund, Germany

Supporting Information

ABSTRACT: Photoreactive siderophores have a major impact on the growth of planktonic organisms. To date, these molecules have mainly been reported from marine bacteria, although evidence is now accumulating that some terrestrial bacteria also harbor the biosynthetic potential for their production. In this paper, we describe the genomics-driven discovery and characterization of variochelins, lipopeptide siderophores from the bacterium *Variovorax boronicumulans*, which thrives in soil and freshwater habitats. Variochelins are different from most other lipopeptide siderophores in that their biosynthesis involves a polyketide synthase. We demonstrate that the ferric iron complex of variochelin A possesses photoreactive properties and present the MS-derived structures of two degradation products that emerge upon light exposure.

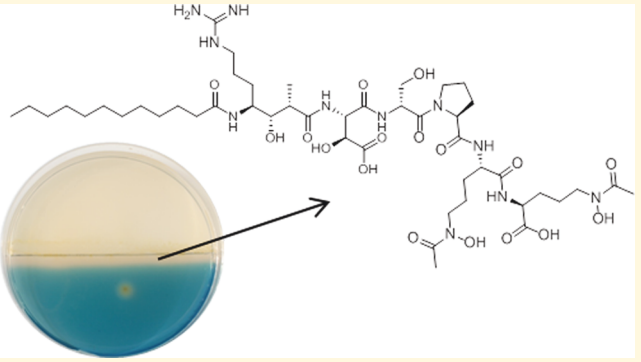

Iron is an essential nutrient for virtually all forms of life. It plays a crucial role in many key biological processes, such as photosynthesis, respiration, N_2 fixation, methanogenesis, oxygen transport, gene regulation, and DNA biosynthesis.[1] Despite its abundance in Earth's crust, iron's biological availability is severely limited in aerobic environments, in part due to the formation of insoluble oxides or hydroxides.[2] In order to secure sufficient iron uptake, many bacteria and fungi secrete low molecular weight compounds, so-called siderophores, which have an extremely high affinity toward ferric iron.[3,4] After binding of the metal, the resulting complex is actively transported back into the cell, where the metal is released by a reductive or hydrolytic mechanism.[5]

Siderophores not only support the growth of the producing organism but also play a significant role in the structuring of microbial communities.[6−9] Moreover, some lipopeptide siderophores were shown to serve as chemical mediators for bacteria−algal interactions in the oceans.[10] These molecules are often distinguished by iron-binding α-hydroxycarboxylate ligand groups.[11] The latter absorb photons in the presence of UV light, thereby triggering a ligand-to-metal charge transfer reaction.[10,12] As a result, ferrous iron is released into the environment, which is then available for direct uptake by surrounding microalgae.[13] Since the latter provide organic nutrients in exchange, the bacterial siderophore producers still benefit from their resource expenditure for siderophore biosynthesis.[14] This mutualism has important ecological implications and possibly contributes to the occurrence of algal blooms.[15]

The production of photoreactive siderophores has been reported from taxonomically distinct genera of marine bacteria, such as *Halomonas*, *Marinobacter*, *Ochrobactrum*, *Synechococcus*, and *Vibrio*.[16−19] The widespread occurrence of these natural products suggests that the carbon-for-iron exchange is a common feature of bacteria−algal interactions. Recently, three classes of photoreactive lipopeptide siderophores were isolated from nonmarine strains.[20−22] While the cupriachelins are produced by a freshwater bacterium possibly having a biological function similar to their marine counterparts,[20] taiwachelin and serobactins are made by rhizosphere bacteria.[21,22] These findings raise questions concerning not only the ecological significance of photoreactivity and amphiphilicity in a soil environment but also whether additional nonrecognized producers of such siderophores exist.

Here, we report our recent results on the discovery of novel lipopeptide siderophores from terrestrial bacteria. Using a genome mining strategy,[23−26] we analyzed various strains for the presence of genes that are involved in the biosynthesis of such compounds. This approach resulted in the identification of the genus *Variovorax* as a potential source of structurally new siderophores. Subsequent screening efforts, which were guided

Received: October 19, 2015
Published: March 29, 2016

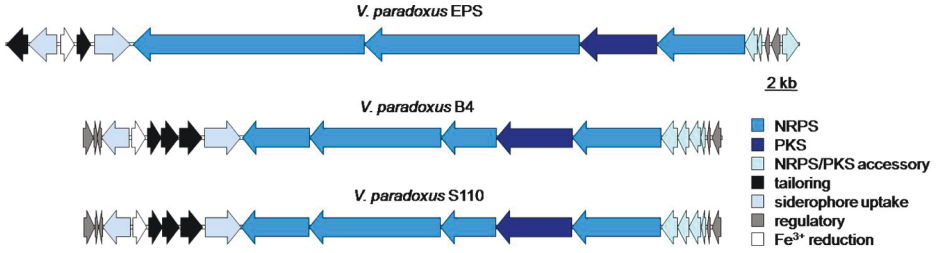

Figure 1. Putative siderophore biosynthesis gene clusters in bacteria of the genus *Variovorax*.

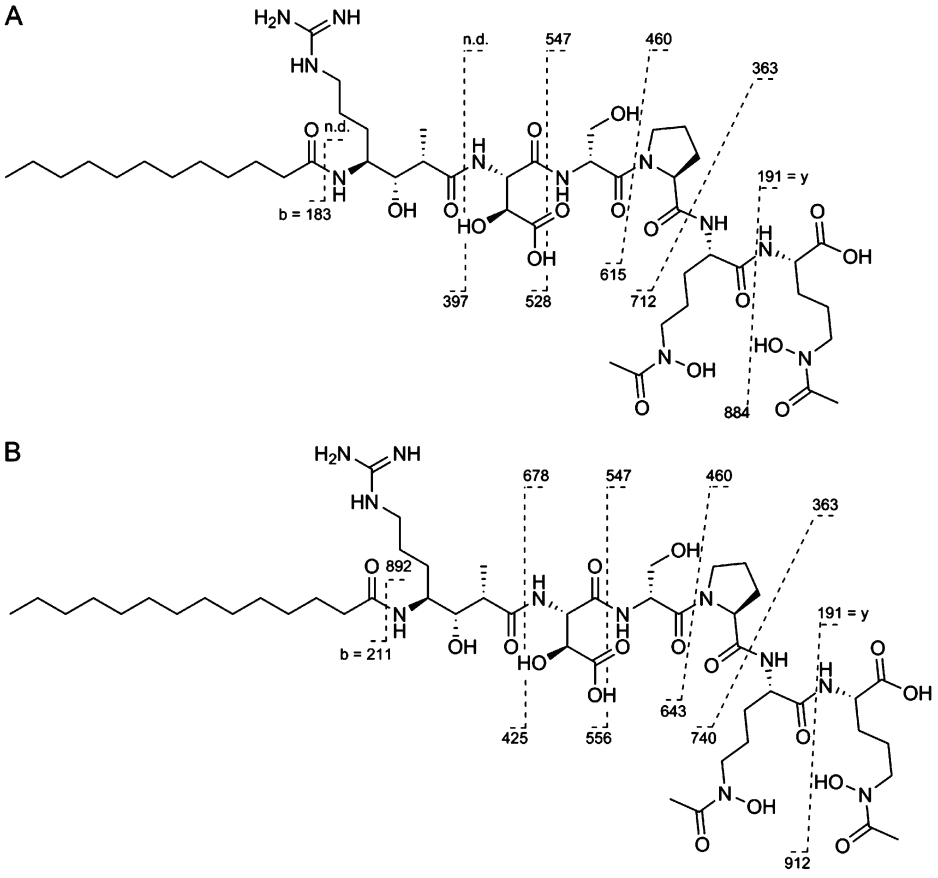

Figure 2. Structures of variochelin A (A) and variochelin B (B). The dashed lines through the structures show the "y" and "b" fragments obtained in a tandem MS experiment. The depicted numbers indicate the corresponding m/z values.

by the chrome azurol S (CAS) assay,[27] led to the isolation of variochelins A and B from the bacterium *Variovorax boronicumulans*. The structures of the two natural products were elucidated by NMR and MS measurements as well as Marfey's analysis. We present and discuss the gene cluster involved in variochelin biosynthesis and evaluate the photoreactive properties of variochelin A.

RESULTS AND DISCUSSION

Genome Mining and Siderophore Screening. A common structural motif of photoreactive acyl peptide siderophores is the presence of one or more β-hydroxyaspartate residues. Biosynthetically, these moieties derive from aspartate, which is incorporated into the respective siderophore by a nonribosomal peptide synthetase (NRPS) and, subsequently, subjected to an enzymatic oxidation reaction to introduce the β-hydroxy moiety.[28,29] The oxidation is carried out by an α-ketoglutarate-dependent dioxygenase, which is very similar to the well-studied taurine dioxygenase (TauD).[20,30] In order to identify siderophore gene clusters with these features, BLASTP homology searches were conducted using an aspartate-activating NRPS adenylation domain as well as a TauD-like protein from cupriachelin biosynthesis as probes. Cross-searches against the fatty acyl-AMP ligase (FAAL) domain from taiwachelin biosynthesis or, alternatively, the starter condensation domain from cupriachelin biosynthesis were used to narrow down the initial results to siderophore loci that possess genetic hallmarks of fatty acid incorporation.[31] The hits that were retrieved from this combined analysis were validated by bioinformatic software to confirm the predictions concerning the molecular architecture of the encoded natural products.[32] In this way, we identified a total of 16 nonmarine strains that were likely to produce acyl peptide siderophores with a β-hydroxyaspartate motif (Table S1). After excluding those strains whose biosynthetic potential had already been confirmed in previous investigations,[20−22] 13 strains remained, covering six different genera. Among the newly identified

DOI: 10.1021/acs.jnatprod.5b00932
J. Nat. Prod. 2016, 79, 865−872

Table 1. NMR Spectroscopic Data for Variochelin A in DMSO-d_6

pos.	δ_C, type		δ_H (J in Hz)	HMBC[a]	pos.	δ_C, type		δ_H (J in Hz)	HMBC[a]
N^{δ}-acetyl-N^{δ}-hydroxyornithine					β-hydroxyaspartic acid				
C1	173.4, C				C23	168.4, C			
C2	51.6, CH		4.17, dt (7.8, 4.4)	1, 3	C24	55.0, CH		4.74, dd (9.1, 2.7)	23, 25, 26, 27
C3	29.0, CH_2	a:	1.70, m	2, 4, 5	C25	70.1, CH		4.51, d (2.7)	23, 24, 26
		b:	1.56, m	2, 4, 5	C26	173.0, C			
C4	22.9, CH_2		1.53, m	2, 3, 5	N4			7.75, d (9.1)	24, 25, 27
C5	46.5, CH_2		3.48, m	3, 4	4-amino-7-guanidino-3-hydroxy-2-methylheptanoic acid				
C6	170.3, C				C27	175.5, C			
C7	20.3, CH_3		1.95, s	6	C28	41.8, CH		2.49, m	27, 29, 34
N1			8.08, d (7.8)	8	C29	73.3, CH		3.56, m	27, 28, 30, 31, 34
	N^{δ}-acetyl-N^{δ}-hydroxyornithine				C30	49.5, CH		3.66, m	29, 31, 32, 36
C8	171.4, C				C31	27.5, CH_2		1.22, m	29, 30, 32
C9	51.6, CH		4.35, m	8, 11	C32	25.1, CH_2	a:	1.44, m	30, 31, 33
C10	29.8, CH_2	a:	1.61, m	9, 11, 12			b:	1.36, m	30, 31, 33
		b:	1.50, m	9, 11, 12	C33	40.8, CH_2	a:	3.10, m	31, 32, 35
C11	22.8, CH_2		1.53, m	9, 10, 12			b:	3.02, m	31, 32, 35
C12	46.8, CH_2		3.48, m	10, 11	C34	11.3, CH_3		1.00, d (6.9)	27, 28, 29
C13	170.3, C				C35	156.5, C			
C14	20.3, CH_3		1.96, s	13	N5			7.56, d (9.2)	29, 30, 36
N2			7.96, d (8.7)	15	N6			7.40, t (5.8)	33
	proline					dodecanoic acid			
C15	171.3, C				C36	172.1, C			
C16	59.7, CH		4.38, dd (8.4, 3.7)	15, 17, 18	C37	35.5, CH_2		2.07, t (7.4)	36, 38, 39
C17	29.8, CH_2	a:	2.05, m	15, 16	C38	25.4, CH_2		1.47, m	36, 37, 39, 40
		b:	1.83, m	16	C39	28.7, CH_2		1.23, m	n.r.[b]
C18	24.1, CH_2		1.49, m	17, 19	C40	28.8, CH_2		1.23, m	n.r.
C19	47.0, CH_2		3.48, m	17, 18, 20	C41	29.0, CH_2		1.23, m	n.r.
	serine				C42	29.1, CH_2		1.23, m	n.r.
C20	168.5, C				C43	29.0, CH_2		1.23, m	n.r.
C21	52.8, CH		4.65, q (7.4)	20, 22, 23	C44	29.0, CH_2		1.23, m	n.r.
C22	61.8, CH_2		3.48, d (7.4)	20, 21	C45	31.3, CH_2		1.23, m	n.r.
N3			7.72, d (7.4)	21, 23	C46	22.1, CH_2		1.26, m	45, 47
					C47	14.0, CH_3		0.85, t (7.0)	45, 46

[a]HMBC correlations, optimized for 7.7 Hz, are from proton(s) stated to the indicated carbon. [b]n.r., not resolved.

producers, the genus *Variovorax* appeared to be of particular interest. Unlike the known acyl peptide siderophore gene clusters,[29] the loci in the three *Variovorax paradoxus* strains include distinctive polyketide synthase (PKS) genes (Figure 1). A thorough inspection of the NRPS and PKS domain architecture and substrate specificities[32−36] unveiled the close relatedness of the biosynthetic enzymes in *V. paradoxus* B4 and *V. paradoxus* S110, suggesting that they catalyze the production of structurally identical molecules (Table S2). In contrast, the gene cluster of *V. paradoxus* EPS clearly differs from the other two loci in size and gene organization. A total of 10 NRPS and PKS modules in the EPS assembly line outnumbers the six modules from B4 and S110 and indicates the biosynthesis of a significantly larger siderophore (Table S3).

To test the secretion of iron-chelating metabolites, we subjected five *Variovorax* strains available in our laboratory to a modified CAS assay, in which the siderophore detection is spatially separated from the growth area of the respective bacterium.[37] All five strains produced an orange halo in the CAS zone of the agar plate (Figure S1), thereby indicating the release of iron-chelating agents.[27] A comparison of the different halo sizes in three independently conducted experiments revealed that *V. boronicumulans* BAM-48 consistently gave the strongest assay response when compared to the other strains. Since the bacterium also grew vigorously under established siderophore production conditions (data not shown),[20,21] we decided to carry out the following chemical investigations with this organism.

Isolation and Structure Determination of Variochelins. In order to induce siderophore biosynthesis in *V. boronicumulans* BAM-48, the bacterium was cultivated in H-3 minimal medium under iron starvation conditions. Secreted metabolites were recovered from the fermentation broth by adsorption onto XAD-2 resin. After removal of the supernatant, the resin was eluted with methanol to release the bound molecules. The resulting extract was concentrated and subjected to HPLC. Two peaks in the metabolic profile corresponded to iron-chelating compounds, as evidenced by a positive response of the respective fractions in the liquid CAS assay (Figure S2).[27] The associated compounds were isolated and subjected to ESIMS. Distinctive pseudomolecular ions appeared at m/z 1074 $[M + H]^+$ for compound **1** and m/z 1102 $[M + H]^+$ for compound **2**, respectively. A preliminary inspection of their ^1H NMR spectra suggested both metabolites to be acyl peptides.

High-resolution ESIMS of variochelin A (**1**) yielded m/z 1074.6040 for the $[M + H]^+$ ion, indicating a molecular formula of $C_{47}H_{83}N_{11}O_{17}$. The constituents in the peptidic headgroup of **1** and their connectivity were initially deduced by tandem mass spectrometry.[38] A sequential loss of 191, 172, 97, 87, and

DOI: 10.1021/acs.jnatprod.5b00932
J. Nat. Prod. 2016, 79, 865−872

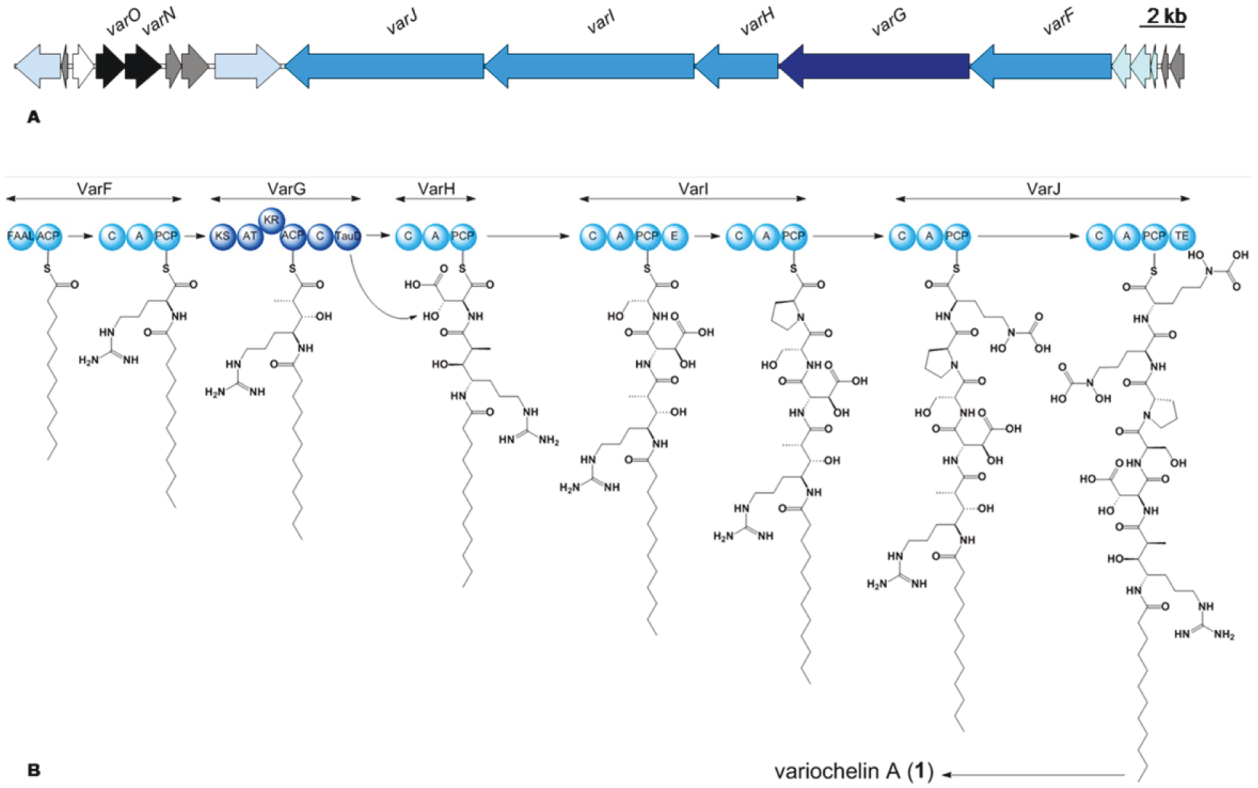

Figure 3. Organization of the variochelin biosynthesis cluster (for annotations see Table S4) (A). Molecular assembly line deduced from *varF*–*varJ* and proposed biosynthesis of **1** (B). Domain annotation: FAAL, fatty acyl-AMP ligase; ACP, acyl carrier protein; C, condensation; A, adenylation; PCP, peptidyl carrier protein; KS, ketosynthase; AT, acyltransferase; KR, ketoreductase; TauD, hydroxylase; E, epimerization; TE, thioesterase.

131 mass units during MALDI-TOF/TOF fragmentation was attributed to an amino acid sequence of N^{δ}-acetyl-N^{δ}-hydroxyornithine, N^{δ}-acetyl-N^{δ}-hydroxyornithine, proline, serine, and β-hydroxyaspartic acid from the carboxylate terminus (Figure 2A, Figure S3). The configurations of the amino acid residues were determined by Marfey's method upon acidic hydrolysis of **1**.[39] This analysis established the proline residue to be in L configuration, whereas the serine was found to be D-configured (Figures S4, S5). Marfey's method also revealed the presence of *threo*-β-hydroxyaspartic acid. The elution order of the diastereomeric pairs of L-FDAA-derivatized *threo*-β-hydroxyaspartic acid had previously been shown to be D → L under reversed-phase conditions.[40] The variochelin A hydrolysate contained only one single peak of the correct mass upon conversion with L-FDAA, which eluted at the same retention time as the second peak of L-FDAA-derivatized D,L-*threo*-β-hydroxyaspartic acid (Figure S6). Therefore, we concluded that, out of the four possible stereoisomers of β-hydroxyaspartic acid, the L-*threo* form is present in **1**. Despite repeated attempts, the derivatization of the released ornithine units with L-FDAA failed. To determine the configuration of these amino acid residues, we treated the hydrolysate of **1** with (1*R*,2*S*,5*R*)-2-isopropyl-5-methylcyclohexyl carbonochloridate. Co-chromatography of the resulting ornithine carbamate against synthetic standards eventually established the L configuration for both N^{δ}-acetyl-N^{δ}-hydroxyornithine moieties in **1** (Figure S7).

The amino acid sequence that had been inferred from the interpretation of the tandem mass spectra was subsequently confirmed by NMR data (Table 1, Figures S8–S12). To elucidate the full structure of **1**, we then focused on carbon C35, which had not been assigned yet and was distinguished by its chemical shift at 156.5 ppm. This value was lower than those observed for the amide carbonyl groups and could not be traced to an aromatic moiety. Instead a comparison with literature data strongly suggested that C35 is part of a guanidino group.[41−43] HMBC interactions then enabled the identification of a 4-amino-7-guanidino-3-hydroxy-2-methylheptanoate fragment. The relative stereochemistry of the three chiral centers in this moiety was deduced as (28*S**,29*S**,30*S**) by selective NOESY experiments. Upon irradiation at the resonance frequency of H34, an NOE was observed with H30, but not with H29. Likewise, irradiation on H28 revealed an NOE with H29, but not with H30. Eventually, it was shown by long-range correlations from H24 and NH4 to C27 that the unusual γ-amino acid was connected to the β-hydroxyaspartate residue of **1**. The remaining nonassigned signals in the ^{1}H and ^{13}C spectra were distinctive of an unbranched acyl chain. The latter was attributed to a dodecanoyl residue in consideration of the molecular formula of **1**. HMBC interactions from H30 and NH5 to C36 linked the acyl moiety with the rest of the molecule and, thereby, established the complete structure of **1**.

The sum formula of variochelin B (**2**) was calculated as $C_{49}H_{87}N_{11}O_{17}$ from its high-resolution mass. Tandem mass spectrometry revealed the same y fragments as those observed during the fragmentation of **1**. However, the corresponding b fragments were increased by 28 mass units each (Figure 2B). MS and NMR data (Figures S13, S14) suggested that both variochelins differ in their fatty acid tail, with **2** featuring a tetradecanoic acid residue. A ^{13}C NMR spectrum recorded with an inverse-gated decoupling pulse sequence[44] confirmed the presence of 14 carbons in the alkyl chain of **2**.

Variochelin Gene Cluster and Biosynthetic Model. The guanidino-containing γ-amino acid that is present in both

DOI: 10.1021/acs.jnatprod.5b00932
J. Nat. Prod. 2016, 79, 865−872

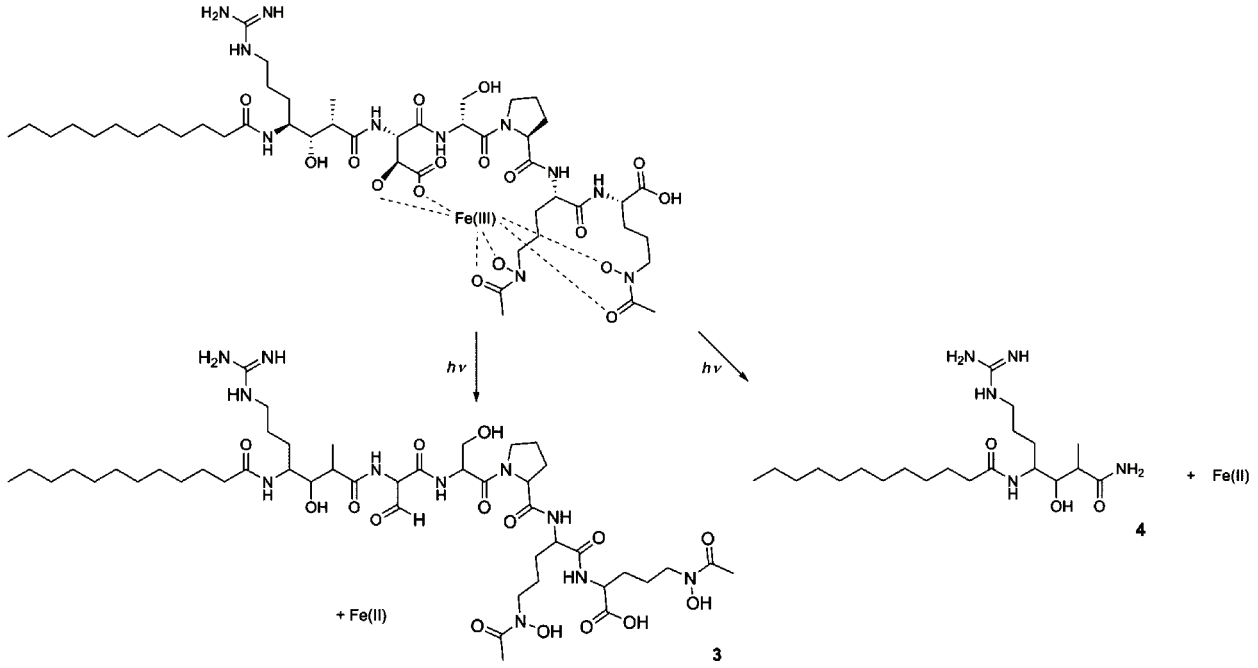

Figure 4. Proposed reaction scheme for the photolysis of ferric **1**. The depicted cleavage products **3** and **4** were detected by HRESIMS. The complexed ferric iron is likely to be reduced via ligand-to-metal charge transfer.

variochelins can be biosynthetically rationalized as the product of a decarboxylative Claisen condensation of arginine and methylmalonate, which is then subject to a β-keto reduction. This scenario suggests the involvement of a PKS and could indicate that the variochelin gene cluster is organizationally closely related to the siderophore loci that were previously discovered in the three *V. paradoxus* strains. To find out whether this assumption is correct, we sequenced and annotated the entire genome of *V. boronicumulans* BAM-48. Gene clusters with a putative role in secondary metabolism were identified using antiSMASH 3.0.1.[32] Out of the seven loci detected, only one met the defined criteria for the biosynthesis of an acyl peptide with a β-hydroxy aspartate motif. The cluster boundaries that had been predicted by antiSMASH 3.0.1 were manually refined on the basis of functional annotations, gene distances, and GC content shifts.[25] According to this analysis, the variochelin (*var.*) locus (Figure 3A) consists of 18 genes, covers 43.2 kb of contiguous DNA, and displays a significant similarity to the *V. paradoxus* siderophore clusters. However, substrate specificity predictions suggest different metabolic products (Tables S2, S3).[33−36] The seven NRPS and PKS modules encoded by *varF*, *varG*, *varH*, *varI*, and *varJ* are assumed to assemble the molecular backbones of **1** and **2** (Figure 3B). The biosynthesis would hence start with the activation of dodecanonoic (or tetradecanoic) acid by the FAAL domain of VarF. It then follows the collinear logic of assembly line enzymology, where the activated substrates are incorporated into a linear oligomer by successive condensation steps.[25,45] The PKS VarG contains the typical β-ketoacylsynthase (KS), acyl transferase (AT), and acyl carrier protein (ACP) domains, as well as a ketoreductase (KR) domain. Each NRPS module harbors the complete set of condensation (C), adenylation (A), and peptidyl carrier protein (PCP) domains. The TauD domain of VarG would be responsible for the hydroxylation of the incorporated aspartic acid residue. Additionally, VarI harbors an epimerization (E) domain, which would be required for the stereochemical inversion of L-serine. The domain architecture is hence consistent with the experimentally deduced configurations. Although Marfey's analysis provided no information on the stereochemistry of the 4-amino-7-guanidino-3-hydroxy-2-methylheptanoate moiety, the missing E domain in VarF strongly suggests an L configuration for the primary arginine building block. We thus propose an (28*S*,29*S*,30*S*) absolute configuration for **1** and **2**. Once the chain elongation is completed, the terminal thioesterase (TE) domain in VarJ releases the newly synthesized lipopeptide.

The *var.* cluster also features several accessory proteins that are essential for the proper functioning of the NRPS and PKS enzymes. Small MbtH-like proteins, such as VarC, are assumed to influence amino acid activation by NRPS,[46] whereas the role of type II thioesterases, such as VarD, lies in the removal of aberrant intermediates that may block the NRPS/PKS assembly line. Furthermore, type II thioesterases are possibly involved in substrate selection and in product release.[47] The phosphopantetheinyl transferase VarE is essential to convert the carrier protein domains of the NRPS and PKS from the inactive *apo* into the active, substrate-binding *holo* forms.[48] VarN and VarO were annotated as L-ornithine 5-monooxygenase and N^{δ}-hydroxyornithine acetyltransferase, respectively. Similar to the homologous IucD and IucB in aerobactin biosynthesis,[49] the two enzymes are assumed to act in a concerted manner to generate the hydroxamate ligand groups in variochelins. The remaining genes that are located in the *var* cluster are likely involved in siderophore transport. Uptake of ferric iron−variochelin complexes should occur via the TonB-dependent receptor VarK and possibly also via the peptide transporter VarR. Intracellular iron release from the siderophore would then be mediated by the ferric iron reductase VarP.[50] VarB, VarL, and VarQ are homologues of FecR, a protein responsible for the regulation of Fe^{3+}-dicitrate uptake in *Escherichia coli*.[51] Together with the encoded sigma-factors VarA and VarM, we expect these proteins to regulate gene expression within the cluster depending on iron availability.

DOI: 10.1021/acs.jnatprod.5b00932
J. Nat. Prod. 2016, 79, 865−872

Complexing Properties and Photoreactivity of 1. The variochelins possess three bidentate ligand groups for the coordination of metal ions, including an α-hydroxycarboxylate (i.e., the β-hydroxyaspartate residue) and two hydroxamate functions. To test the complexing properties of **1**, the compound was treated with an equimolar quantity of a metal salt and directly subjected to HR-MS. This analysis revealed that **1** is capable of forming monomeric 1:1 complexes with Fe^{3+} and Ga^{3+} (Figure S15). No masses corresponding to Mn^{2+}, Co^{2+}, Ni^{2+}, Cu^{2+}, or Zn^{2+} complexes could be detected, and we also did not observe any complex formation of **1** in the presence of boron salts. The observed discrimination between divalent and trivalent metal ions and the iron-responsive production suggest a siderophore function for **1**.

Depending on their coordination state, bidentate ligand groups are sensitive to light exposure. While hydroxamates are in general photochemically stable, catechols are prone to photooxidation in the absence of metal coordination, but stable once bound to ferric iron.[52] In contrast, α-hydroxy acid moieties are stable in their metal-free form, but undergo light-induced oxidation after complexation to ferric iron.[10,11] In order to test the photostability of **1**, we exposed an aqueous solution of its ferric iron complex to direct sunlight and analyzed product formation via LCESIMS. Two photoproducts exhibited ions at m/z 1026.5862 $[M - H]^-$ and m/z 414.3440 $[M + H]^+$, respectively (Figures S16, S17). The predicted sum formula for the first photoproduct is consistent with an aldehyde (**3**) resulting from a decarboxylation of the β-hydroxyaspartate residue in **1**.[53] The second photoproduct (**4**) is suggested to result from a more extensive cleavage reaction (Figure 4). Despite thorough analysis we did not detect the mass of a peptide fragment lacking the fatty acid tail. In a parallel experiment, we confirmed the light-induced ligand-to-metal charge transfer reaction, which leads to a reduction of the coordinated ferric iron. Samples of Fe^{3+}-variochelin A that were exposed to sunlight gradually turned red in the presence of the Fe^{2+}-trapping agent bathophenantrolinedisulfonate (BPDS). Absorption at 535 nm increased from 0.004 ± 0.001 to 0.0438 ± 0.001 within 4 h of light exposure. The negative control that was shielded from light remained colorless in the same time period. Here, the absorption at 535 nm increased from 0.0027 ± 0.001 to 0.0032 ± 0.001.

In summary, we herein report the discovery of a new class of acyl peptides from the bacterium *V. boronicumulans* BAM-48. Although the variochelins show typical hallmarks of marine siderophores, the producing strain originates from soil,[54] where it was shown to contribute to plant growth.[55] After taiwachelin[21] and the serobactins,[22] the variochelins represent the third class of photoreactive lipopeptide siderophores that are produced by plant-associated bacteria. Amphiphilic siderophores that might be added to this group include corrugatin and ornicorrugatin from *Pseudomonas* spp.,[56] ornibactins from *Burkholderia* spp.,[57] and rhizobactin 1021 from *Sinorhizobium meliloti*,[58] even though the photoreactivity of these compounds still awaits experimental confirmation. The occurrence of such siderophores in bacteria thriving in the vicinity of plants raises two possible conclusions: amphiphilicity and/or photoreactivity are somewhat beneficial in the rhizosphere or the chemical properties inherent to these siderophores represent an evolutionary relic. It is noteworthy in this context that bacteria of the genus *Variovorax* are also commonly found in freshwater habitats,[59] where an ecological advantage of amphiphilicity and photoreactivity would be plausible.[3]

During the preparation of this article, an NRPS-PKS assembly line with a domain architecture almost identical to that of *V. boronicumulans* BAM-48 was reported from the bacterium *V. paradoxus* P4B.[60] A product from this assembly line named variobactin A possesses the same molecular formula as variochelin A. However, the structure of variobactin A was proposed as a cyclic depsipeptide[60] with an amino acid sequence that deviates from that of variochelin A.

EXPERIMENTAL SECTION

General Experimental Procedures. LC-MS experiments were conducted on an Accela UHPLC system equipped with a C_{18} column (Betasil C_{18}, 150 × 2.1 mm, 3 μm; Thermo Scientific) coupled to a Finnigan Surveyor PDA Plus detector (Thermo Scientific). For metabolic profiling, a gradient of acetonitrile (ACN) in water + 0.1% formic acid and a flow rate of 0.2 mL/min were used. The ACN concentration was increased from 5% to 98% within 16 min, was kept for 3 min at 98%, and was subsequently decreased to 5% within 14 min. High-resolution mass determination was carried out on an Exactive mass spectrometer (Thermo Scientific). One- and two-dimensional MALDI-TOF/MS data using postsource decay were acquired on a Bruker Ultraflex spectrometer (Bruker Daltonics). NMR spectra were recorded at 300 K on a Bruker Avance III 500 MHz spectrometer with DMSO-d_6 as solvent and internal standard. The solvent signals were referenced to δ_H 2.50 ppm and δ_C 39.5 ppm.

Siderophore Screening. CAS agar plates were prepared as previously reported.[27,37] Half of the CAS agar layer was cut out, and the gap was filled with iron-free H-3 mineral medium (1.0 g/L aspartic acid, 2.3 g/L KH_2PO, 2.57 g/L Na_2HPO_4, 1.0 g/L NH_4Cl, 0.5 g/L $MgSO_4 \cdot 7H_2O$, 0.5 g/L $NaHCO_3$, 0.01 g/L $CaCl_2 \cdot 2H_2O$, and 5 mL/L SL-6 trace element solution).[61] *V. boronicumulans* BAM-48, *V. paradoxus* 351, B13-0-1 D, *V. paradoxus* B4, *V. paradoxus* S110, and *V. soli* GH9-3 were streaked out on the H-3 half of the plates. The secretion of iron-complexing metabolites was detected by a color change from blue to orange in the CAS half of the plates after incubation at 30 °C.

Isolation of Variochelins. *V. boronicumulans* BAM-48 was grown in a 10 L scale in iron-free H-3 mineral medium.[61] The strain was shaken (130 rpm) at 30 °C for 5 days. The culture supernatant was then separated from the cells by centrifugation (8000 rpm) and extracted with 150 g/L XAD-2 (Supelco). The resin was thoroughly washed with distilled water before the adsorbed metabolites were eluted with MeOH. The eluate was dried under vacuum, resuspended in 1 mL of MeOH, and initially fractionated by flash column chromatography over Polygoprep 60-50 C_{18} (Macherey-Nagel) using an increasing concentration of MeOH in water. CAS-positive fractions were further purified by high-performance liquid chromatography on a Shimadzu UFLC liquid chromatography system equipped with a Nucleodur C_{18} HTec column (VP 250 × 10 mm, 5 μm; Macherey-Nagel) using a MeOH–H_2O gradient from 50% to 100% over 20 min and keeping 100% MeOH for 10 min, with 0.1% trifluoroacetic acid.

*Variochelin A (**1**):* ^{1}H and ^{13}C NMR data (DMSO-d_6, 500 and 125 MHz, respectively), see Table 1; HRESIMS m/z 1074.6040 $[M + H]^+$ calcd for $C_{47}H_{84}N_{11}O_{17}$ 1074.6041.

*Variochelin B (**2**):* ^{1}H NMR (DMSO-d_6, 500 MHz) δ 8.08 (1H, d, J = 7.8 Hz, NH-1), 7.96 (1H, d, J = 8.7 Hz, NH-2), 7.75 (1H, d, J = 9.1 Hz, NH-4), 7.72 (1H, d, J = 7.4 Hz, NH-3), 7.56 (1H, d, J = 9.2 Hz, NH-5), 7.40 (1H, t, J = 5.8 Hz, NH-6), 4.74 (1H, dd, J = 9.1, 2.7 Hz, H-24), 4.65 (1H, q, J = 7.4 Hz, H-21), 4.51 (1H, d, J = 2.7 Hz, H-25), 4.38 (1H, dd, J = 8.4, 3.7 Hz, H-16), 4.35 (1H, m, H-9), 4.17 (1H, dt, J = 7.8, 4.4 Hz, H-2), 3.66 (1H, m, H-30), 3.56 (1H, m, H-29), 3.48 (2H, m, H-5), 3.48 (2H, m, H-12), 3.48 (2H, m, H-19), 3.48 (2H, d, J = 7.4 Hz, H-22), 3.10 (1H, m, H-33a), 3.02 (1H, m, H-33b), 2.49 (1H, m, H-28), 2.07 (2H, t, J = 7.4 Hz, H-37), 2.05 (1H, m, H-17a), 1.96 (3H, s, H-14), 1.95 (3H, s, H-7), 1.83 (1H, m, H-17b), 1.70 (1H, m, H-3a), 1.61 (1H, m, H-10a), 1.56 (1H, m, H-3b), 1.53 (2H, m, H-4), 1.53 (2H, m, H-11), 1.50 (1H, m, H-10b), 1.49 (2H, m, H-18), 1.47 (2H, m, H-38), 1.44 (1H, m, H-32a), 1.36 (1H, m, H-32b), 1.26 (2H, m, H-48), 1.23 (2H, m, H-39), 1.23 (2H, m, H-40), 1.23 (2H, m, H-41), 1.23 (2H, m, H-42), 1.23 (2H, m, H-43), 1.23 (2H, m, H-44),

DOI: 10.1021/acs.jnatprod.5b00932
J. Nat. Prod. 2016, 79, 865–872

1.23 (2H, m, H-45), 1.23 (2H, m, H-46), 1.23 (2H, m, H-47), 1.22 (2H, m, H-31), 1.00 (3H, d, J = 6.9 Hz, H-34), 0.85 (3H, t, J = 7.0 Hz, H-49); ^{13}C NMR (DMSO-d_6, 125 MHz) δ 175.5 (C, C-27), 173.4 (C, C-1), 173.0 (C, C-26), 172.1 (C, C-36), 171.4 (C, C-8), 171.3 (C, C-15), 170.3 (C, C-6), 170.3 (C, C-13), 168.5 (C, C-20), 168.4 (C, C-23), 156.5 (C, C-35), 73.3 (CH, C-29), 70.1 (CH, C-25), 61.8 (CH_2, C-22), 59.7 (CH, C-16), 55.0 (CH, C-24), 52.8 (CH, C-21), 51.6 (CH, C-2), 51.6 (CH, C-9), 49.5 (CH, C-30), 47.0 (CH_2, C-19), 46.8 (CH_2, C-12), 46.5 (CH_2, C-5), 41.8 (CH, C-28), 40.8 (CH_2, C-33), 35.5 (CH_2, C-37), 31.3 (CH_2, C-47), 29.8 (CH_2, C-10), 29.8 (CH_2, C-17), 29.1 (CH_2, C-42), 29.0 (CH_2, C-3), 29.0 (CH_2, C-41), 29.0 (CH_2, C-43), 29.0 (CH_2, C-44), 29.0 (CH_2, C-45), 29.0 (CH_2, C-46), 28.8 (CH_2, C-40), 28.7 (CH_2, C-39), 27.5 (CH_2, C-31), 25.4 (CH_2, C-38), 25.1 (CH_2, C-32), 24.1 (CH_2, C-18), 22.9 (CH_2, C-4), 22.8 (CH_2, C-11), 22.1 (CH_2, C-48), 20.3 (CH_3, C-7), 20.3 (CH_3, C-14), 14.0 (CH_3, C-49), 11.3 (CH_3, C-34); HRESIMS m/z 1102.6357 $[M + H]^+$ calcd for $C_{49}H_{88}N_{11}O_{17}$ 1102.6354.

Amino Acid Analysis by Marfey's Method. Amino acid configurations were determined following acid hydrolysis and derivatization with Marfey's reagent (1-fluoro-2,4-dinitrophenyl-5-L-alanine amide, L-FDAA, Sigma-Aldrich)[39] by coelution experiments with L-FDAA-derivatized amino acids. For this purpose, 1 mg of purified **1** was dissolved in 500 μL of concentrated HI and heated at 110 °C for 8 h. The solution was lyophilized, and the dried hydrolysate was resuspended in 50 μL of water and 20 μL of aqueous $NaHCO_3$ (1 M). Derivatization was carried out with 100 μL of L-FDAA (1% w/v in acetone) at 40 °C for 1 h. Afterward the reaction was quenched with 20 μL of HCl (1 M). The products were lyophilized and prepared for LCHRMS analysis by dissolving in MeOH. Standards for co-chromatography were prepared by reacting 50 μL of an aqueous amino acid solution (50 mM) with 20 μL of $NaHCO_3$ (1 M) and 100 μL of L-FDAA (1% w/v in acetone) at 40 °C for 1 h. The dried reaction mixture was dissolved in MeOH and subsequently analyzed by LCHRMS.

Configurational Analysis of the Released Ornithine Residues. Triphosgene (0.065 mmol) and pyridine (0.45 mmol) were added to a solution of (−)-menthol (0.13 mmol) in 3 mL of DCM in an ice bath. The solution was stirred for 30 min and subsequently allowed to warm to room temperature. The stirring was continued for 30 min. The resulting (1*R*,2*S*,5*R*)-2-isopropyl-5-methylcyclohexyl carbonochloridate was used directly for derivatization. For this purpose, D- and L-ornithine standards (0.2 mmol) or hydrolyzed **1** was dissolved in a 2:1 DMSO−H_2O mixture (3 mL) in the presence of $NaHCO_3$ (0.2 mmol) and added to the (1*R*,2*S*,5*R*)-2-isopropyl-5-methylcyclohexyl carbonochloridate solution. After stirring for 1 h at room temperature, the samples were lyophilized, dissolved in MeOH, and analyzed by HRLCMS.

Genome Sequencing, Assembly, and Annotation. Genomic DNA of *V. boronicumulans* BAM-48 was isolated via phenol chloroform extraction. The purity, quality, and size of the bulk gDNA preparation were assessed according to DOE-JGI guidelines.[44] Sequencing was performed at GATC Biotech AG (Konstanz, Germany) by means of single-molecule real-time sequencing.[62] The sequences extracted from the resulting data set were assembled using the hierarchical genome assembly process.[63] Variochelin biosynthesis genes were first identified using antiSMASH 3.0.1.[32] Refinement of the cluster analysis was conducted as previously described.[25,45] The annotated nucleotide sequence for the variochelin gene cluster has been deposited in GenBank under accession number KT900023.

Photoreactivity Tests. Photoreactivity tests of variochelins were performed as previously described.[20] Reduction of the complexed ferric iron to ferrous iron was investigated via the bathophenanthrolinedisulfonic acid assay. Each reaction contained 100 μM variochelin A, 10 μM $FeCl_3$, and 40 μM BPDS (Sigma-Aldrich) in PBS buffer (pH 7.5). The reactions were either exposed to sunlight or kept in the dark for 4 h. The formation of $Fe(BPDS)_3^{2+}$ was monitored before and after exposure to sunlight/darkness by measuring the absorption at 535 nm using a Genesys 10 UV spectrophotometer (Thermo). The experiments were run in duplicate. In order to identify photolysis products, a 2 mM solution of ferric **1** in PBS buffer (pH 7.5) was exposed to sunlight for 6 h. An identical solution that was shielded from sunlight served as a negative control. After photoexposure, both samples were dried in vacuo. The samples were then taken up in 100 μL of MeOH and analyzed by HRESIMS.

■ ASSOCIATED CONTENT

Supporting Information

The Supporting Information is available free of charge on the ACS Publications website at DOI: 10.1021/acs.jnatprod.5b00932.

Complete annotation of the *Variovorax* siderophore gene clusters, including GenBank accession numbers; testing of *Variovorax* strains in the CAS assay; HPLC purification of **1** and **2**; MS data and NMR spectra of **1** and **2**; amino acid analysis; photoreactivity test of ferric **1** (PDF)

■ AUTHOR INFORMATION

Corresponding Author

*Phone: +49 231 7554742. Fax: +49 7557489. E-mail: markus.nett@bci.tu-dortmund.de.

Notes

The authors declare no competing financial interest.

■ ACKNOWLEDGMENTS

This project was supported by the Collaborative Research Center ChemBioSys (CRC 1127 ChemBioSys) and funded by the Deutsche Forschungsgemeinschaft (DFG). We thank A. Perner and H. Heinecke (Hans-Knöll-Institute Jena, Department of Biomolecular Chemistry) for recording high-resolution ESIMS and NMR spectra. We also thank M. Poetsch (Hans-Knöll-Institute Jena, Department of Molecular and Applied Microbiology) for MALDI-TOF/TOF measurements.

■ REFERENCES

(1) Andrews, S. C.; Robinson, A. K.; Rodríguez-Quiñones, F. *FEMS Microbiol Rev.* **2003**, *27*, 215−237.
(2) Shaked, Y.; Erel, Y.; Sukenik, A. *Environ. Sci. Technol.* **2002**, *36*, 460−467.
(3) Sandy, M.; Butler, A. *Chem. Rev.* **2009**, *109*, 4580−4595.
(4) Hider, R. C.; Kong, X. *Nat. Prod. Rep.* **2010**, *27*, 637−657.
(5) Hopkinson, B. M.; Morel, F. M. M. *BioMetals* **2009**, *22*, 659−669.
(6) Matthijs, S.; Tehrani, K. A.; Laus, G.; Jackson, R. W.; Cooper, R. M.; Cornelis, P. *Environ. Microbiol.* **2007**, *9*, 425−434.
(7) D'Onofrio, A.; Crawford, J. M.; Stewart, E. J.; Witt, K.; Gavrish, E.; Epstein, S.; Clardy, J.; Lewis, K. *Chem. Biol.* **2010**, *17*, 254−264.
(8) Traxler, M. F.; Seyedsayamdost, M. R.; Clardy, J.; Kolter, R. *Mol. Microbiol.* **2012**, *86*, 628−644.
(9) Böttcher, T.; Clardy, J. *Angew. Chem., Int. Ed.* **2014**, *53*, 3510−3513.
(10) Barbeau, K.; Rue, E. L.; Bruland, K. W.; Butler, A. *Nature* **2001**, *413*, 409−413.
(11) Butler, A.; Theisen, R. M. *Coord. Chem. Rev.* **2010**, *254*, 288−296.
(12) Küpper, F. C.; Carrano, C. J.; Kuhn, J.-U.; Butler, A. *Inorg. Chem.* **2006**, *45*, 6028−6033.
(13) Yarimizu, K.; Polido, G.; Gärdes, A.; Carter, M. L.; Hilbern, M.; Carrano, C. J. *Metallomics* **2014**, *6*, 1156−1163.
(14) Amin, S. A.; Green, D. H.; Hart, M. C.; Küpper, F. C.; Sunda, W. G.; Carrano, C. J. *Proc. Natl. Acad. Sci. U. S. A.* **2009**, *106*, 17071−17076.
(15) Amin, S. A.; Parker, M. S.; Armbrust, E. V. *Microbiol. Mol. Biol. Rev.* **2012**, *76*, 667−684.
(16) Gauglitz, J. M.; Zhou, H.; Butler, A. *J. Inorg. Biochem.* **2012**, *107*, 90−95.

(17) Martinez, J. S.; Zhang, G. P.; Holt, P. D.; Jung, H.-T.; Carrano, C. J.; Haygood, M. G.; Butler, A. *Science* **2000**, *287*, 1245−1247.
(18) Ito, Y.; Butler, A. *Limnol. Oceanogr.* **2005**, *50*, 1918−1923.
(19) Homann, V. V.; Sandy, M.; Tincu, J. A.; Templeton, A. S.; Tebo, B. M.; Butler, A. *J. Nat. Prod.* **2009**, *72*, 884−888.
(20) Kreutzer, M. F.; Kage, H.; Nett, M. *J. Am. Chem. Soc.* **2012**, *134*, 5415−5422.
(21) Kreutzer, M. F.; Nett, M. *Org. Biomol. Chem.* **2012**, *10*, 9338−9343.
(22) Rosconi, F.; Davyt, D.; Martínez, V.; Martínez, M.; Abin-Carriquiry, J. A.; Zane, H.; Butler, A.; de Souza, E. M.; Fabiano, E. *Environ. Microbiol.* **2013**, *15*, 916−927.
(23) Zerikly, M.; Challis, G. L. *ChemBioChem* **2009**, *10*, 625−633.
(24) Gross, H. *Appl. Microbiol. Biotechnol.* **2007**, *75*, 267−277.
(25) Nett, M. In *Progress in Chemistry of Organic Natural Products*; Kinghorn, D. A.; Falk, H.; Kobayashi, J., Eds.; Springer: Switzerland, 2014; Vol. *99*, pp 199−246.
(26) Kleigrewe, K.; Almaliti, J.; Tian, I. Y.; Kinnel, R. B.; Korobeynikov, A.; Monroe, E. A.; Duggan, B. M.; Di Marzo, V.; Sherman, D. H.; Dorrestein, P. C.; Gerwick, L.; Gerwick, W. H. *J. Nat. Prod.* **2015**, *78*, 1671−1682.
(27) Schwyn, B.; Neilands, J. B. *Anal. Biochem.* **1987**, *160*, 47−56.
(28) Kem, M. P.; Naka, H.; Iinishi, A.; Haygood, M. G.; Butler, A. *Biochemistry* **2015**, *54*, 744−752.
(29) Kem, M. P.; Butler, A. *BioMetals* **2015**, *28*, 445−459.
(30) Singh, G. M.; Fortin, P. D.; Koglin, A.; Walsh, C. T. *Biochemistry* **2008**, *47*, 11310−11320.
(31) Zane, H. K.; Naka, H.; Rosconi, F.; Sandy, M.; Haygood, M. G.; Butler, A. *J. Am. Chem. Soc.* **2014**, *136*, 5615−5618.
(32) Weber, T.; Blin, K.; Duddela, S.; Krug, D.; Kim, H. U.; Bruccoleri, R.; Lee, S. Y.; Fischbach, M. A.; Müller, R.; Wohlleben, W.; Breitling, R.; Takano, E.; Medema, M. H. *Nucleic Acids Res.* **2015**, *43*, W237−W243.
(33) Bachmann, B. O.; Ravel, J. *Methods Enzymol.* **2009**, *458*, 181−217.
(34) Stachelhaus, T.; Mootz, H. D.; Marahiel, M. A. *Chem. Biol.* **1999**, *6*, 493−505.
(35) Challis, G. L.; Ravel, J.; Townsend, C. A. *Chem. Biol.* **2000**, *7*, 211−224.
(36) Baranašić, D.; Zucko, J.; Diminic, J.; Gacesa, R.; Long, P. F.; Cullum, J.; Hranueli, D.; Starcevic, A. *J. Ind. Microbiol. Biotechnol.* **2014**, *41*, 461−467.
(37) Milagres, A. M.; Machuca, A.; Napoleao, D. *J. Microbiol. Methods* **1999**, *37*, 1−6.
(38) Papayannopoulos, I. A. *Mass Spectrom. Rev.* **1995**, *14*, 49−73.
(39) Marfey, P. *Carlsberg Res. Commun.* **1984**, *49*, 591−596.
(40) Fujii, K.; Ikai, Y.; Mayumi, T.; Oka, H.; Suzuki, M.; Harada, K. *Anal. Chem.* **1997**, *69*, 3346−3352.
(41) Fuchs, S. W.; Sachs, C. C.; Kegler, C.; Nollmann, F. I.; Karas, M.; Bode, H. B. *Anal. Chem.* **2012**, *84*, 6948−6955.
(42) Bosello, M.; Zeyadi, M.; Kraas, F. I.; Linne, U.; Xie, X.; Marahiel, M. A. *J. Nat. Prod.* **2013**, *76*, 2282−2290.
(43) Johnston, C. W.; Wyatt, M. A.; Li, X.; Ibrahim, A.; Shuster, J.; Southam, G.; Magarvey, N. A. *Nat. Chem. Biol.* **2013**, *9*, 241−243.
(44) Berger, S.; Braun, S. In *200 and More NMR Experiments*; Wiley-VCH: Weinheim, 2004; pp 318−320.
(45) Schieferdecker, S.; König, S.; Weigel, C.; Dahse, H.-M.; Werz, O.; Nett, M. *Chem. - Eur. J.* **2014**, *20*, 15933−15940.
(46) Felnagle, E. A.; Barkei, J. J.; Park, H.; Podevels, A. M.; McMahon, M. D.; Drott, D. W.; Thomas, M. G. *Biochemistry* **2010**, *49*, 8815−8817.
(47) Kotowska, M.; Pawlik, K. *Appl. Microbiol. Biotechnol.* **2014**, *98*, 7735−7746.
(48) Lambalot, R. H.; Gehring, A. M.; Flugel, R. S.; Zuber, P.; LaCelle, M.; Marahiel, M. A.; Reid, R.; Khosla, C.; Walsh, C. T. *Chem. Biol.* **1996**, *3*, 923−936.
(49) Challis, G. L. *ChemBioChem* **2005**, *6*, 601−611.
(50) Matzanke, B. F.; Anemüller, S.; Schünemann, V.; Trautwein, A. X.; Hantke, K. *Biochemistry* **2004**, *43*, 1386−1392.
(51) Braun, V.; Killmann, H. *Trends Biochem. Sci.* **1999**, *24*, 104−109.
(52) Barbeau, K.; Rue, E. L.; Trick, C. G.; Bruland, K. W.; Butler, A. *Limnol. Oceanogr.* **2003**, *48*, 1069−1078.
(53) Grabo, J. E.; Chrisman, M. A.; Webb, L. M.; Baldwin, M. J. *Inorg. Chem.* **2014**, *53*, 5781−5787.
(54) Miwa, H.; Ahmed, I.; Yoon, J.; Yokota, A.; Fujiwara, T. *Int. J. Syst. Evol. Microbiol.* **2008**, *58*, 286−289.
(55) Liu, Z. H.; Cao, Y. M.; Zhou, Q. W.; Guo, K.; Ge, F.; Hou, J. Y.; Hu, S. Y.; Yuan, S.; Dai, Y. J. *Biodegradation* **2013**, *24*, 855−864.
(56) Matthijs, S.; Budzikiewicz, H.; Schäfer, M.; Wathelet, B.; Cornelis, P. *Z. Naturforsch., C: J. Biosci.* **2008**, *63*, 8−12.
(57) Stephan, H.; Freund, S.; Beck, W.; Jung, G.; Meyer, J. M.; Winkelmann, G. *BioMetals* **1993**, *6*, 93−100.
(58) Smith, M. J.; Shoolery, J. N.; Schwyn, B.; Holden, I.; Neilands, J. B. *J. Am. Chem. Soc.* **1985**, *107*, 1739−1743.
(59) Satola, B.; Wübbeler, J. H.; Steinbüchel, A. *Appl. Microbiol. Biotechnol.* **2013**, *97*, 541−560.
(60) Johnston, C. W.; Skinnider, M. A.; Wyatt, M. A.; Li, X.; Ranieri, M. R. M.; Yang, L.; Zechel, D. L.; Ma, B.; Magarvey, N. A. *Nat. Commun.* **2015**, *6*, 8421.
(61) Pfennig, N. *Arch. Microbiol.* **1974**, *100*, 197−206.
(62) Eid, J.; Fehr, A.; Gray, J.; Luong, K.; Lyle, J.; Otto, G.; Peluso, P.; Rank, D.; Baybayan, P.; Bettman, B.; Bibillo, A.; Bjornson, K.; Chauduri, B.; Christians, F.; Cicero, R.; Clark, S.; Dalal, R.; deWinter, A.; Dixon, J.; Foquet, M.; Gaertner, A.; Hardenbol, P.; Heiner, C.; Hester, K.; Holden, D.; Kearns, G.; Kong, X.; Kuse, R.; Lacroix, Y.; Lin, S.; Lundquist, P.; Ma, C.; Marks, P.; Maxham, M.; Murphy, D.; Park, I.; Pham, T.; Phillips, M.; Roy, J.; Sebra, R.; Shen, G.; Sorenson, J.; Tomaney, A.; Travers, K.; Trulson, M.; Vieceli, J.; Wegener, J.; Wu, D.; Yang, A.; Zaccarin, D.; Zhao, P.; Zhong, F.; Korlach, J.; Turner, S. *Science* **2009**, *323*, 133−138.
(63) Chin, C. S.; Alexander, D. H.; Marks, P.; Klammer, A. A.; Drake, J.; Heiner, C.; Clum, A.; Copeland, A.; Huddleston, J.; Eichler, E. E.; Turner, S. W.; Korlach, J. *Nat. Methods* **2013**, *10*, 563−569.

DOI: 10.1021/acs.jnatprod.5b00932
J. Nat. Prod. 2016, 79, 865−872

Supporting Information

Variochelins, lipopeptide siderophores from *Variovorax boronicumulans* discovered by genome mining

*Colette Kurth, Sebastian Schieferdecker, Kalliopi Athanasopoulou, Ivana Seccareccia, and Markus Nett**

Table of Contents

Figure S1. Response of *Varivorax paradoxus* B4 (a), *V. paradoxus* S110 (b), *V. paradoxus* 351, B13-0-1 D (c), *V. boronicumulans* BAM-48 (d), and *V. soli* GH9-3 (e) in the CAS assay. Plate (f) shows a negative control.

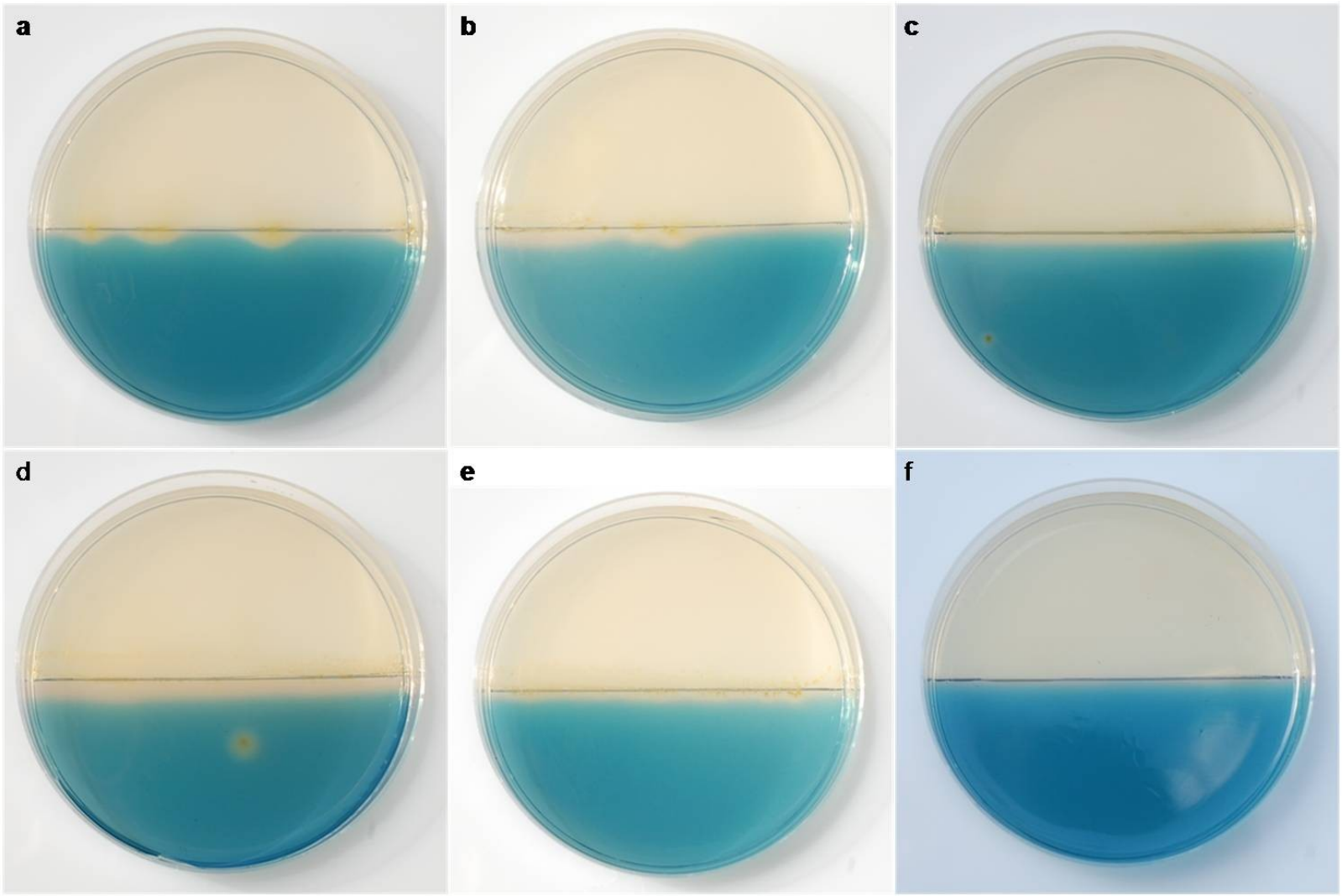

Figure S2. HPLC separation of variochelin A (**1**) and B (**2**) monitored at 190 nm (A). Both compounds were positive in the liquid CAS assay (B).

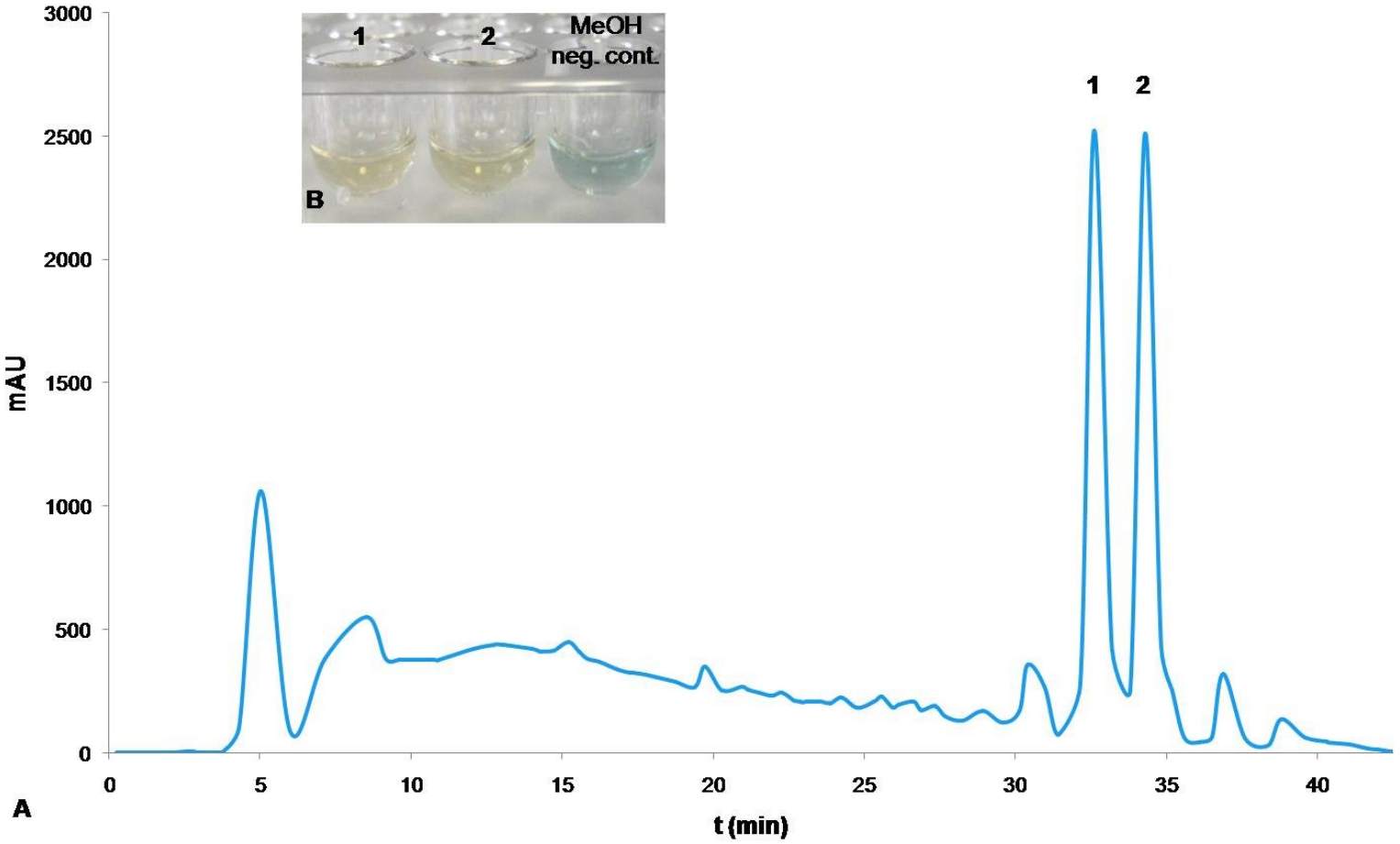

Figure S3. MALDI-TOF/TOF spectrum of variochelin A (**1**).

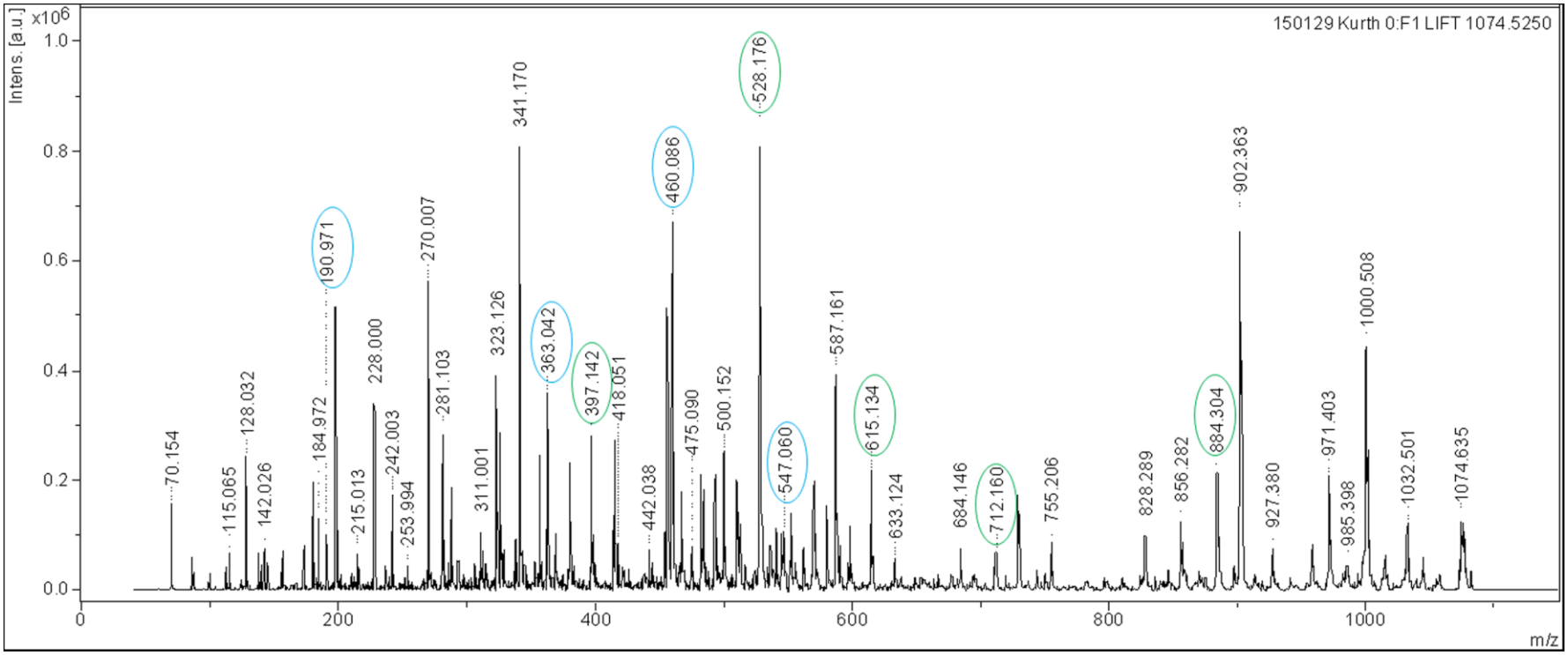

Figure S4. Marfey's analysis of the proline residue in **1**. Extracted ion chromatograms of Marfey products after HI cleavage of **1** (A), from commercial L-proline (B) and D-proline (C).

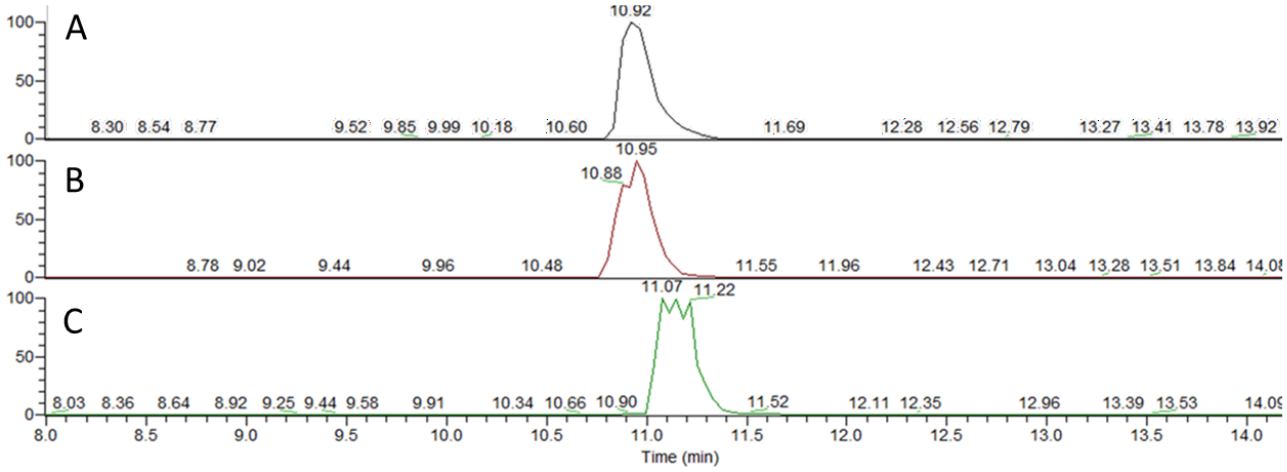

Figure S5. Marfey's analysis of the serine residue in **1**. Extracted ion chromatograms of Marfey products after HI cleavage of **1** (A), from commercial L-serine (B) and D-serine (C).

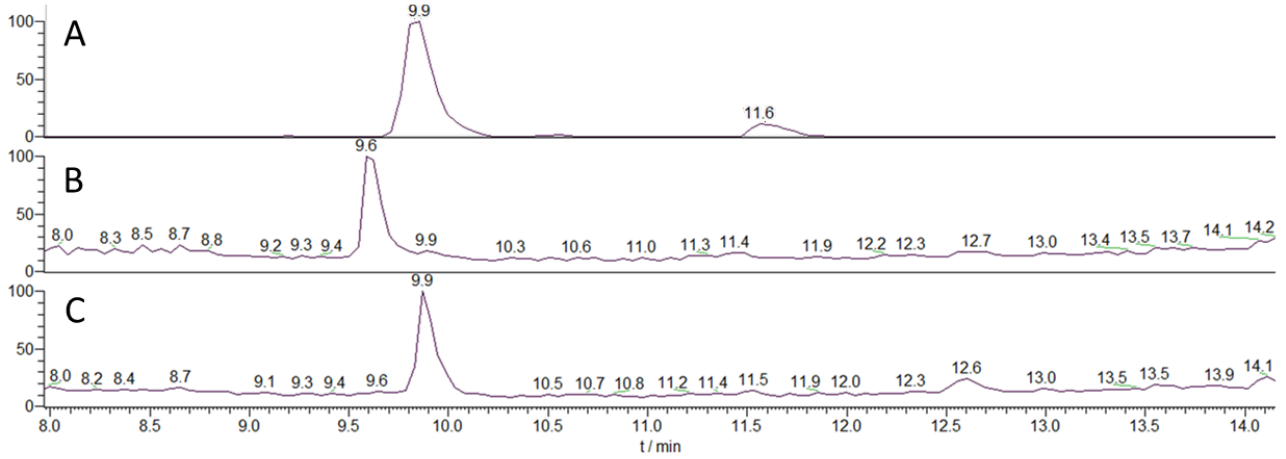

Figure S6. Marfey's analysis of the *β*-hydroxyaspartic acid residue in **1**. UV profiles of Marfey products after HI cleavage of **1** (A) and from commercial D/L-*threo*-*β*-hydroxyaspartic acid (B).

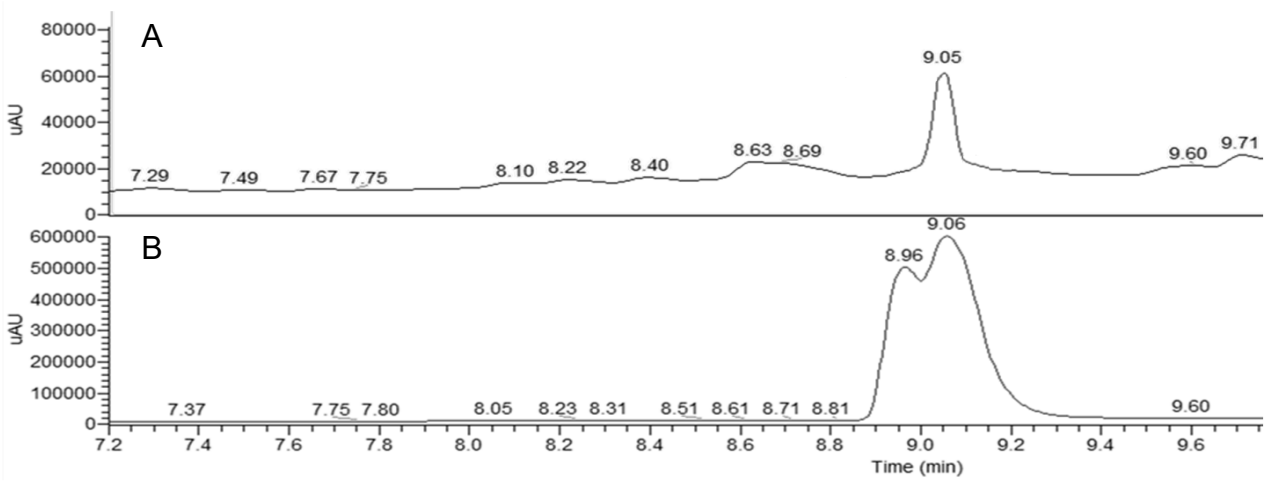

Figure S7. Configurational analysis of the ornithine residues in **1**. Extracted ion chromatograms of bis-carbamate products after HI cleavage of **1** (A), from commercial D/L-ornithine (B), and from L-ornithine (C).

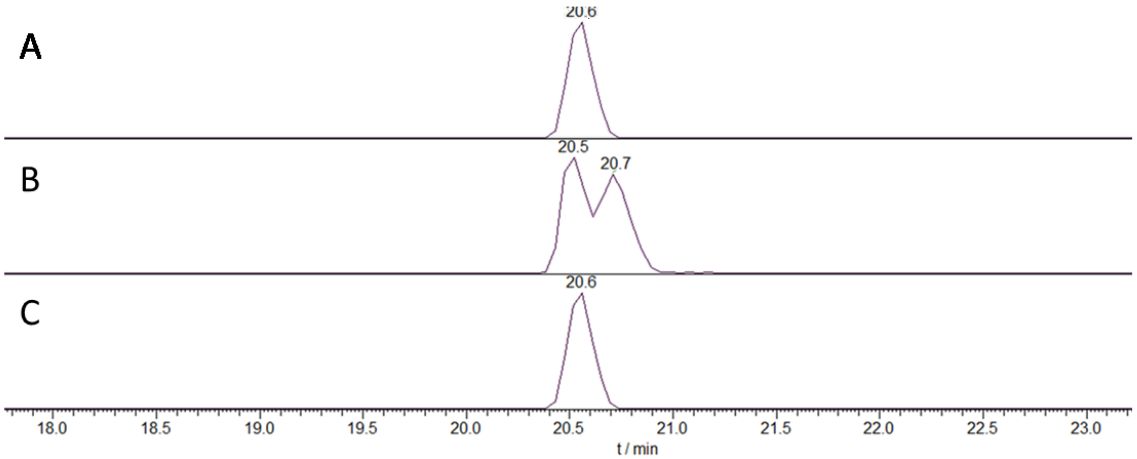

Figure S8. ^{1}H NMR (500 MHz) spectrum of **1** in DMSO-d_6

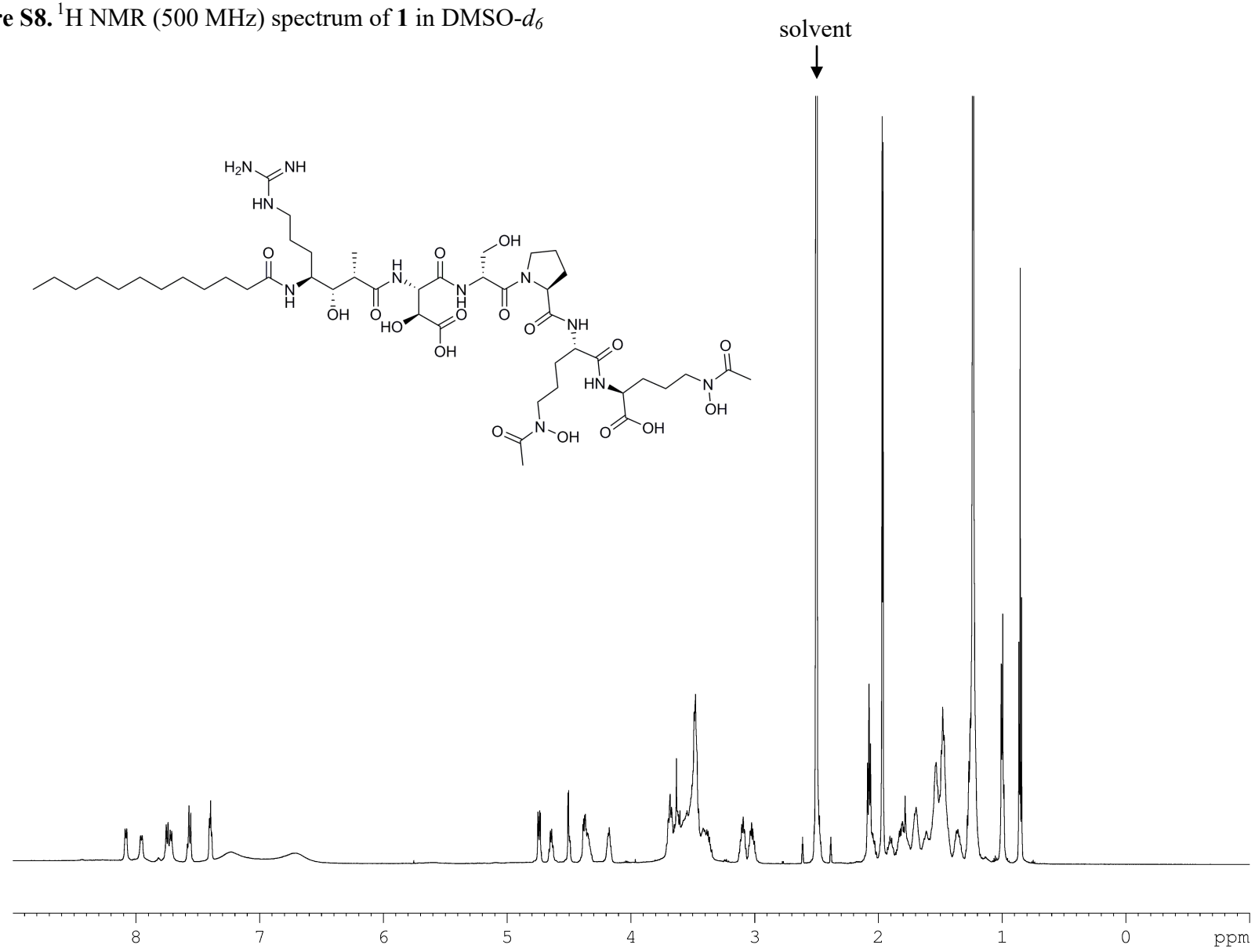

Figure S9. ^{1}H-decoupled ^{13}C NMR (125 MHz) spectrum of **1** in DMSO-d_6

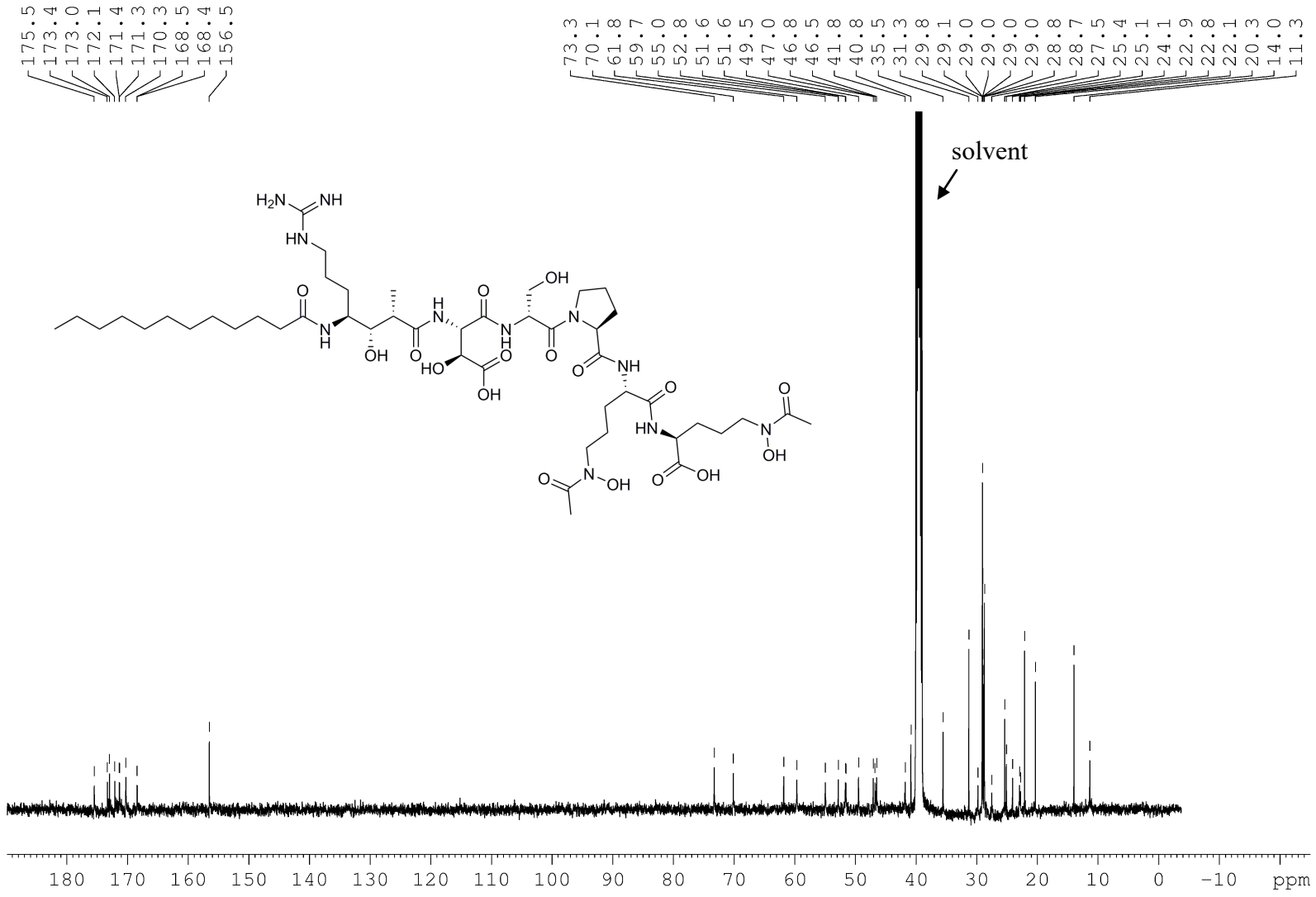

Figure S10. ^{1}H, ^{1}H COSY spectrum (500 MHz) of **1** in DMSO-d_6

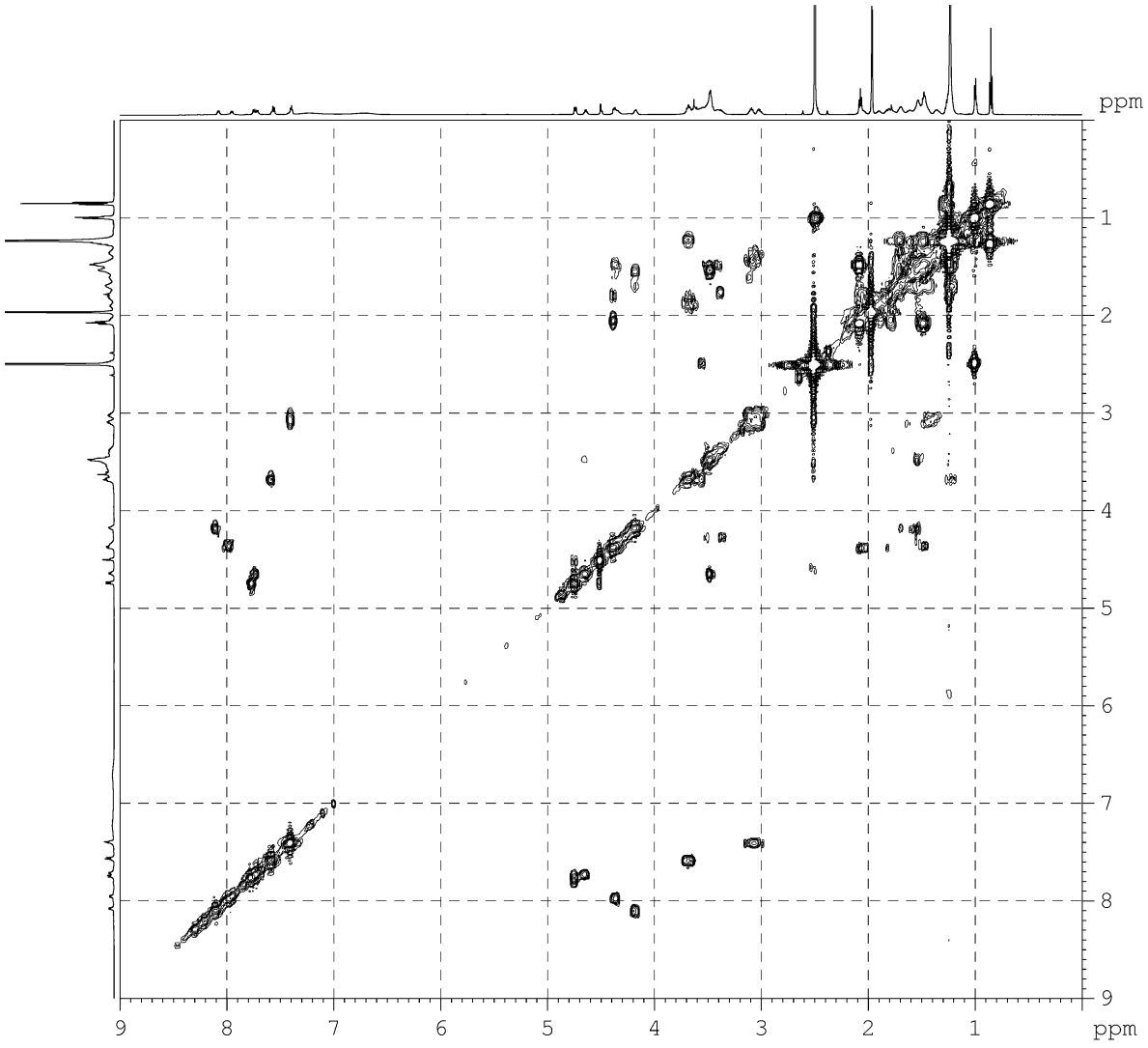

Figure S11. ^{1}H, ^{13}C HSQC (500 MHz) spectrum of **1** in DMSO-d_6

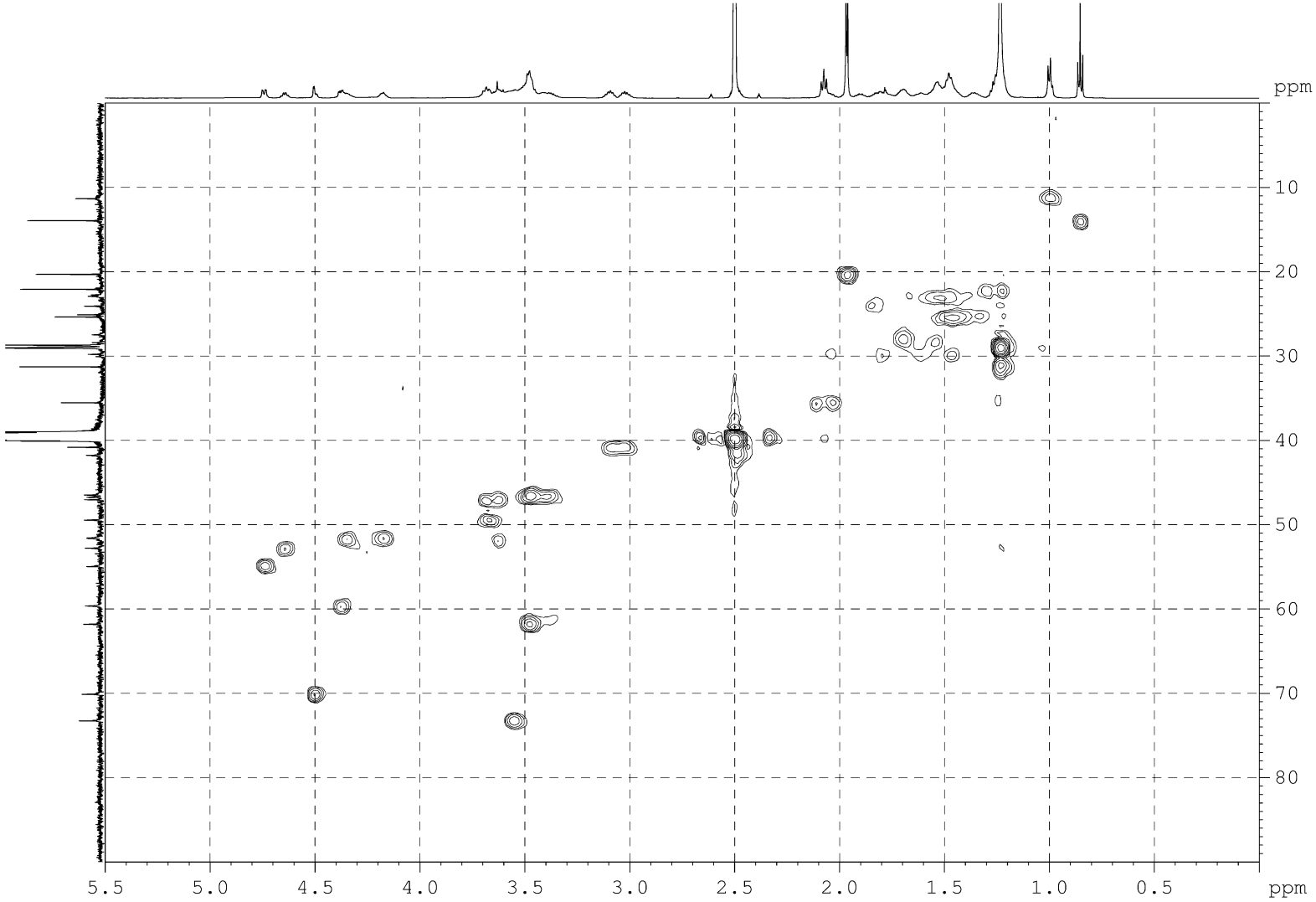

Figure S12. ^{1}H, ^{13}C HMBC (500 MHz) spectrum of **1** in DMSO-d_6

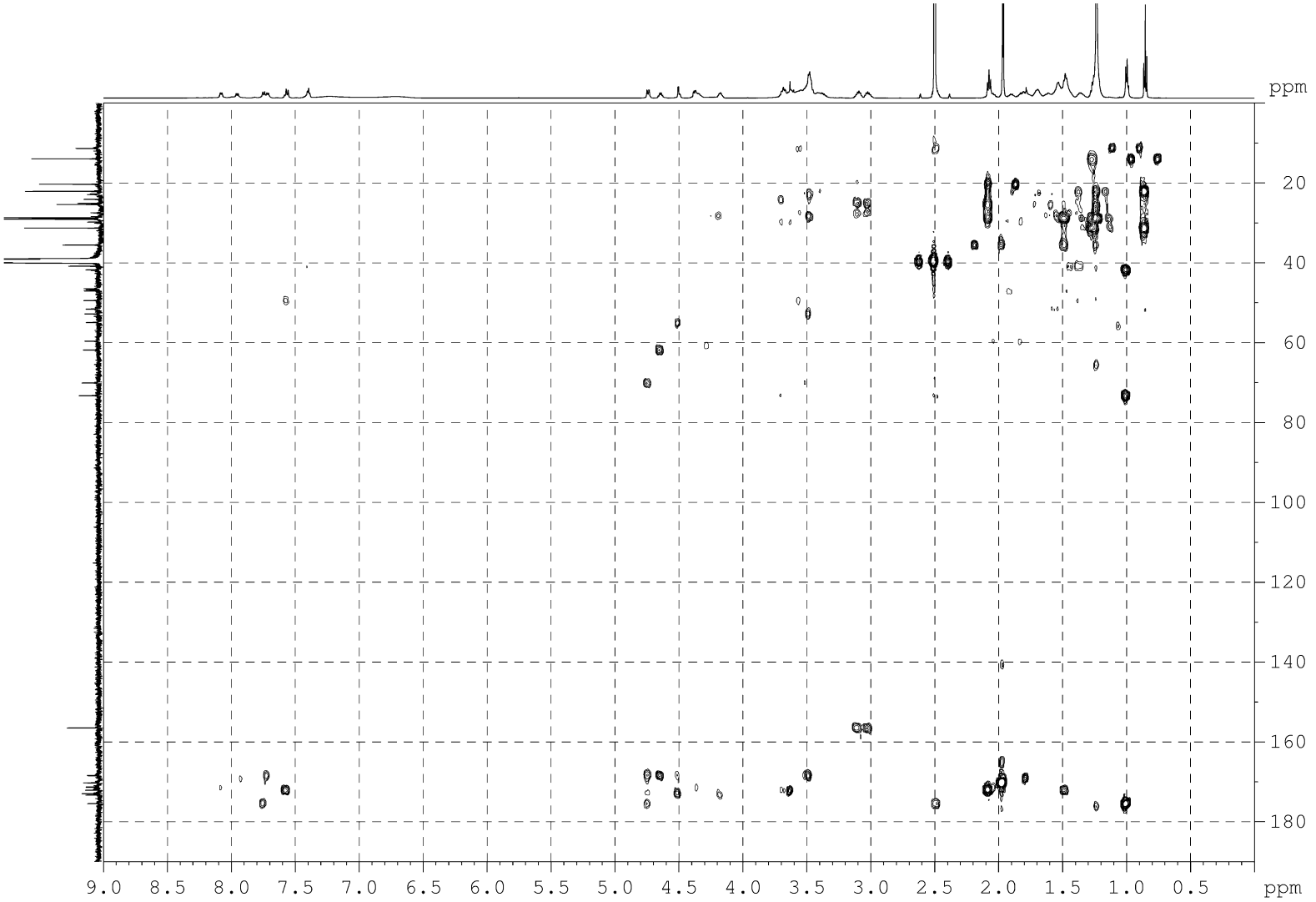

Figure S13. ^{1}H NMR (500 MHz) spectrum of **2** in DMSO-d_6

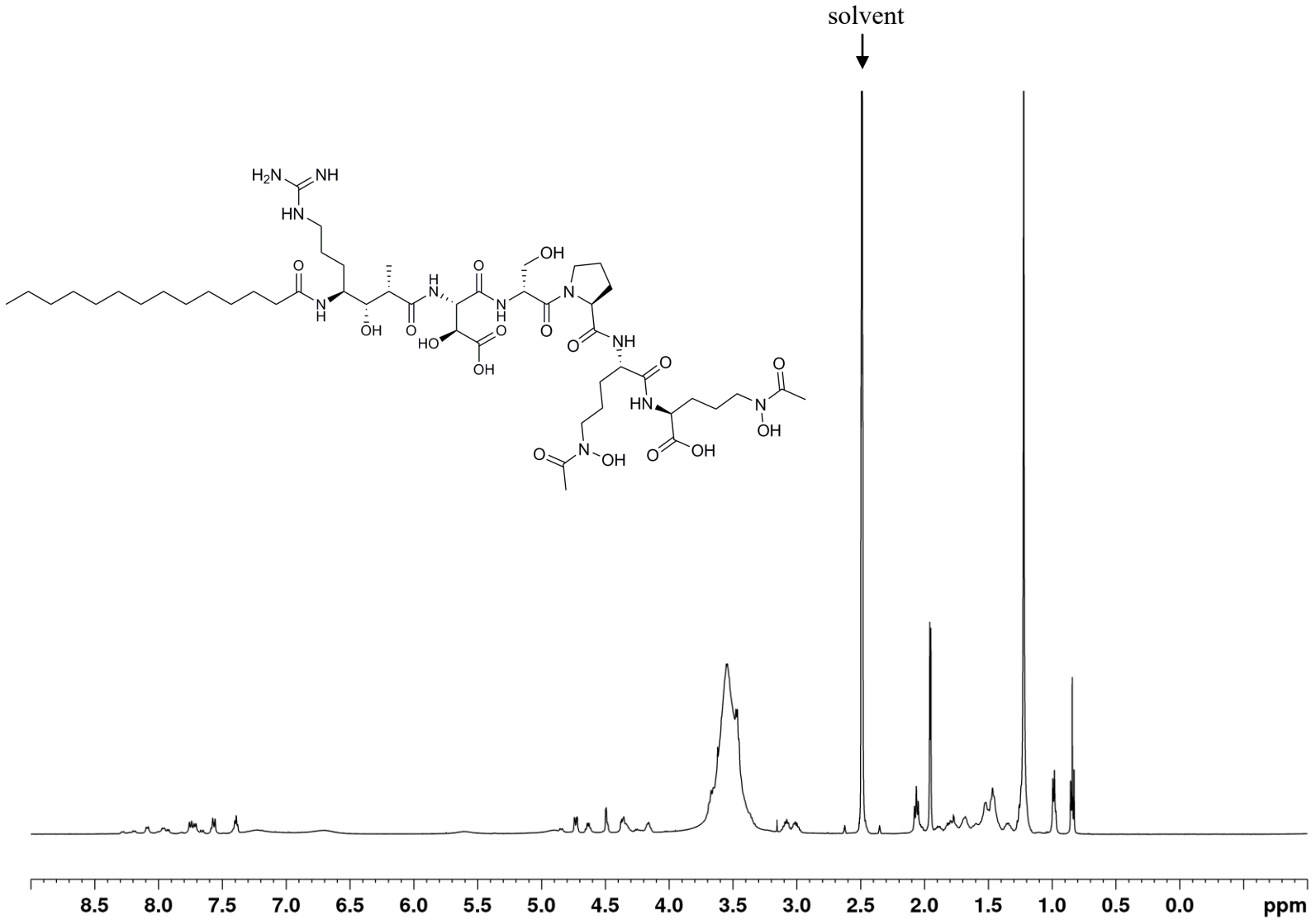

Figure S14. ^{1}H-decoupled ^{13}C NMR (125 MHz) spectrum of **2** in DMSO-d_6

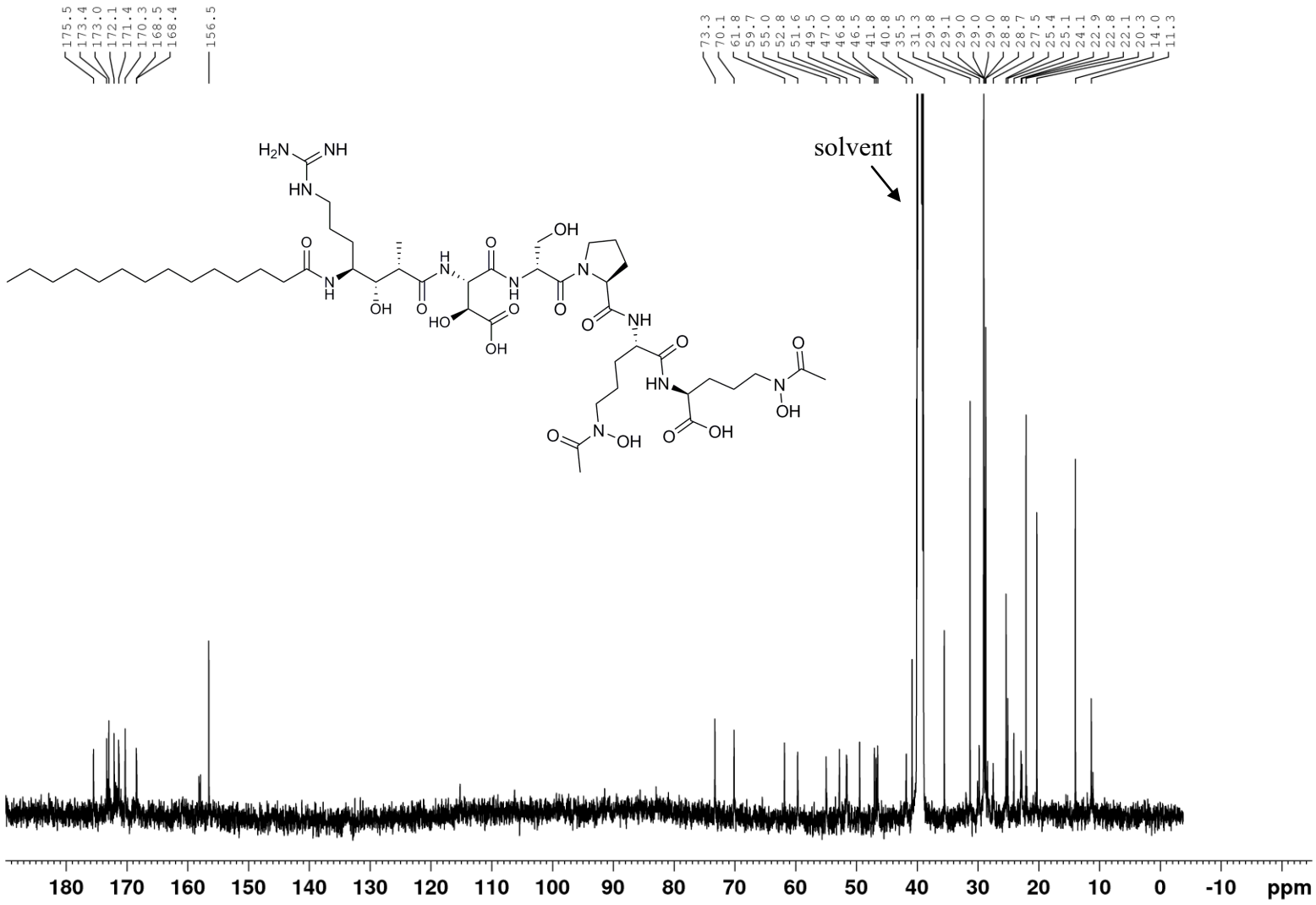

Figure S15. HR-ESI-MS spectra of variochelin A as a free ligand (top), and in complex with Fe^{3+} (middle) and Ga^{3+} (bottom).

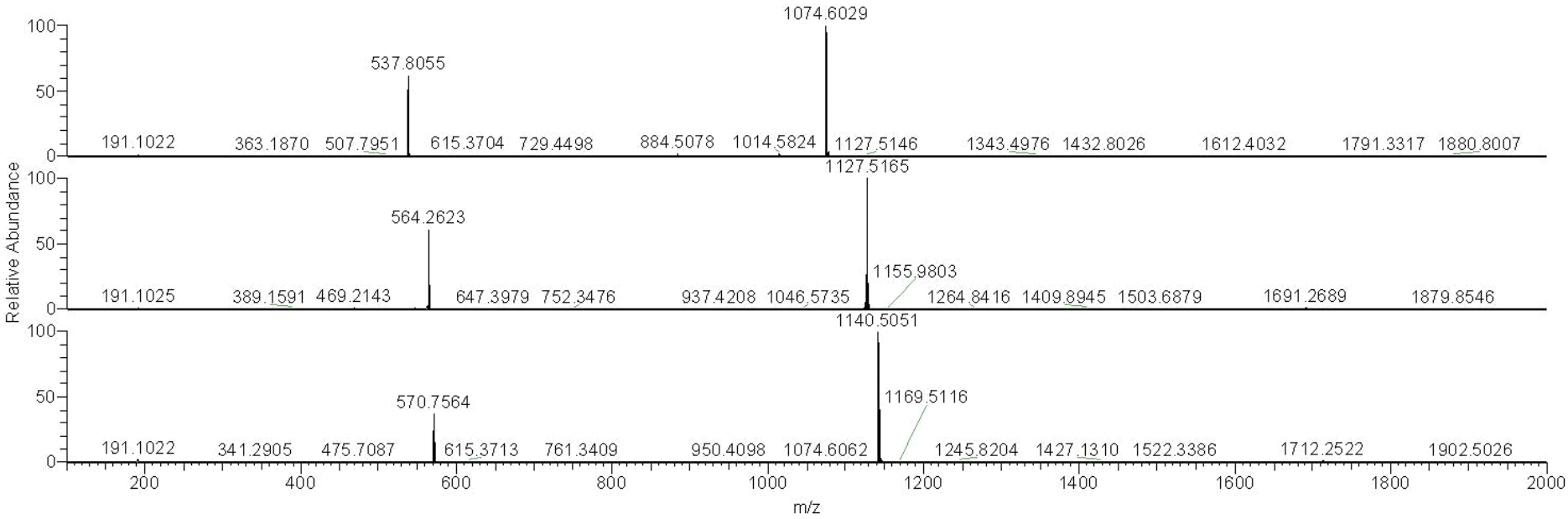

Figure S16. Photoreactivity test. LC-HR-MS of Fe(III)-variochelin A exposed to sunlight (A) and stored in the dark (B). The fragments of pseudomolecular ions with *m/z* 1026 $[M - H]^-$ and *m/z* 414 $[M + H]^+$ are only observed after light exposure.

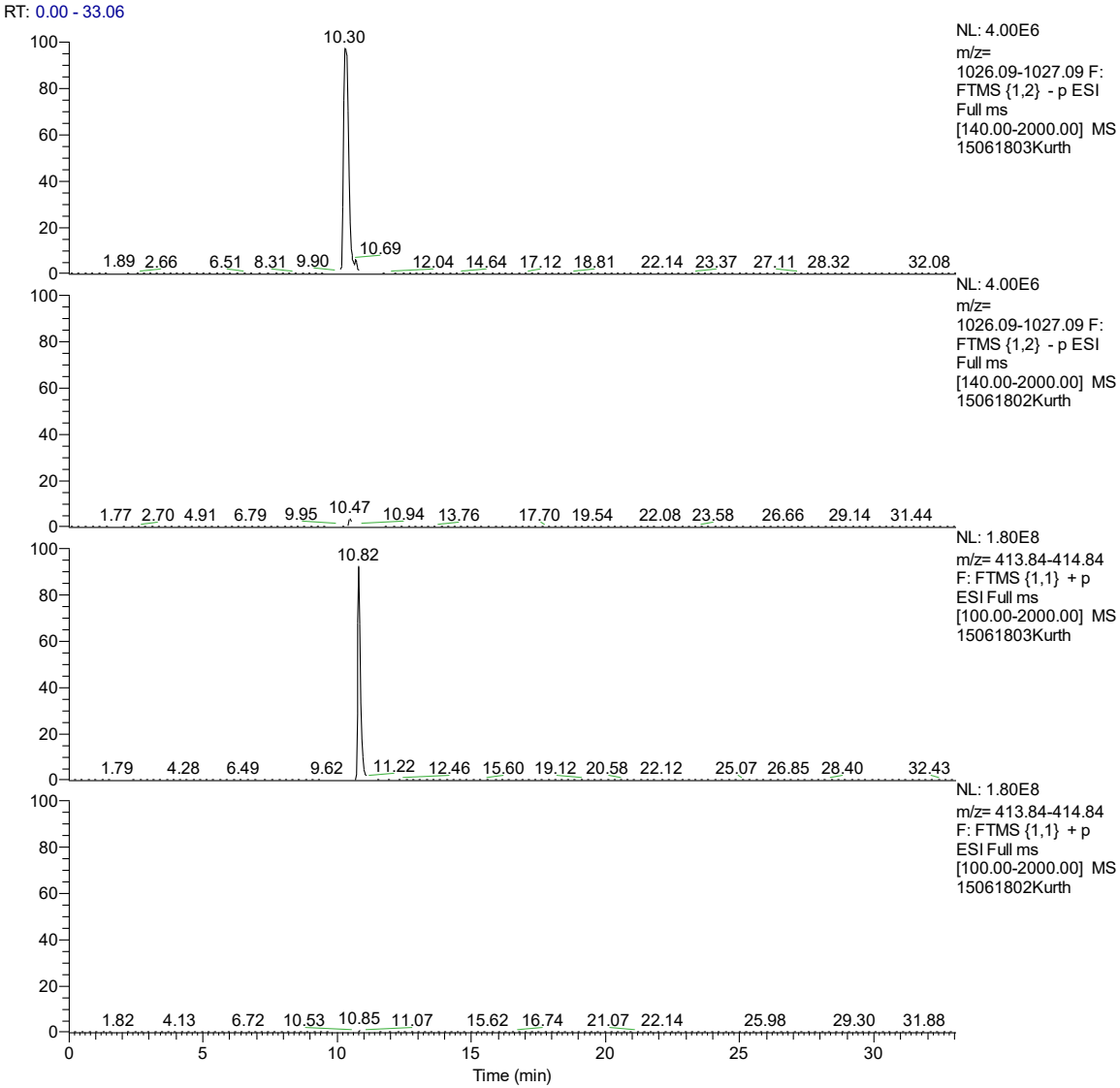

Figure S17. HR-ESI-MS spectra of the two Fe(III)-variochelin A fragment detected after light exposure.

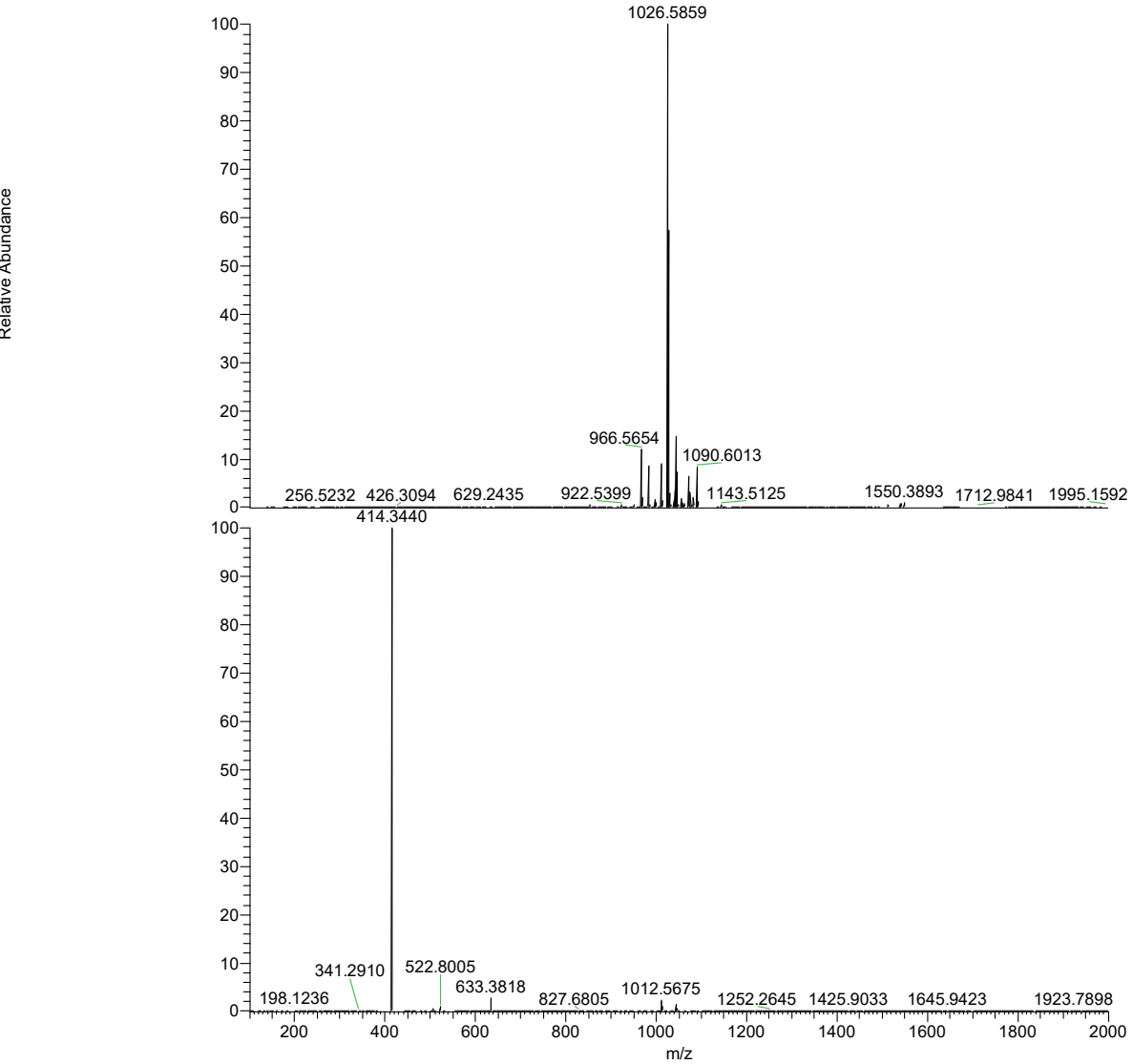

Composition (calculated): $C_{46}H_{80}N_{11}O_{15}$
Theoretical mass: 1026.5830
Delta (ppm): 2.838

Composition (calculated): $C_{21}H_{44}O_3N_5$
Theoretical mass: 414.3439
Delta (ppm): 0.133

Figure S18. HR-ESI-MS spectrum of variochelin B.

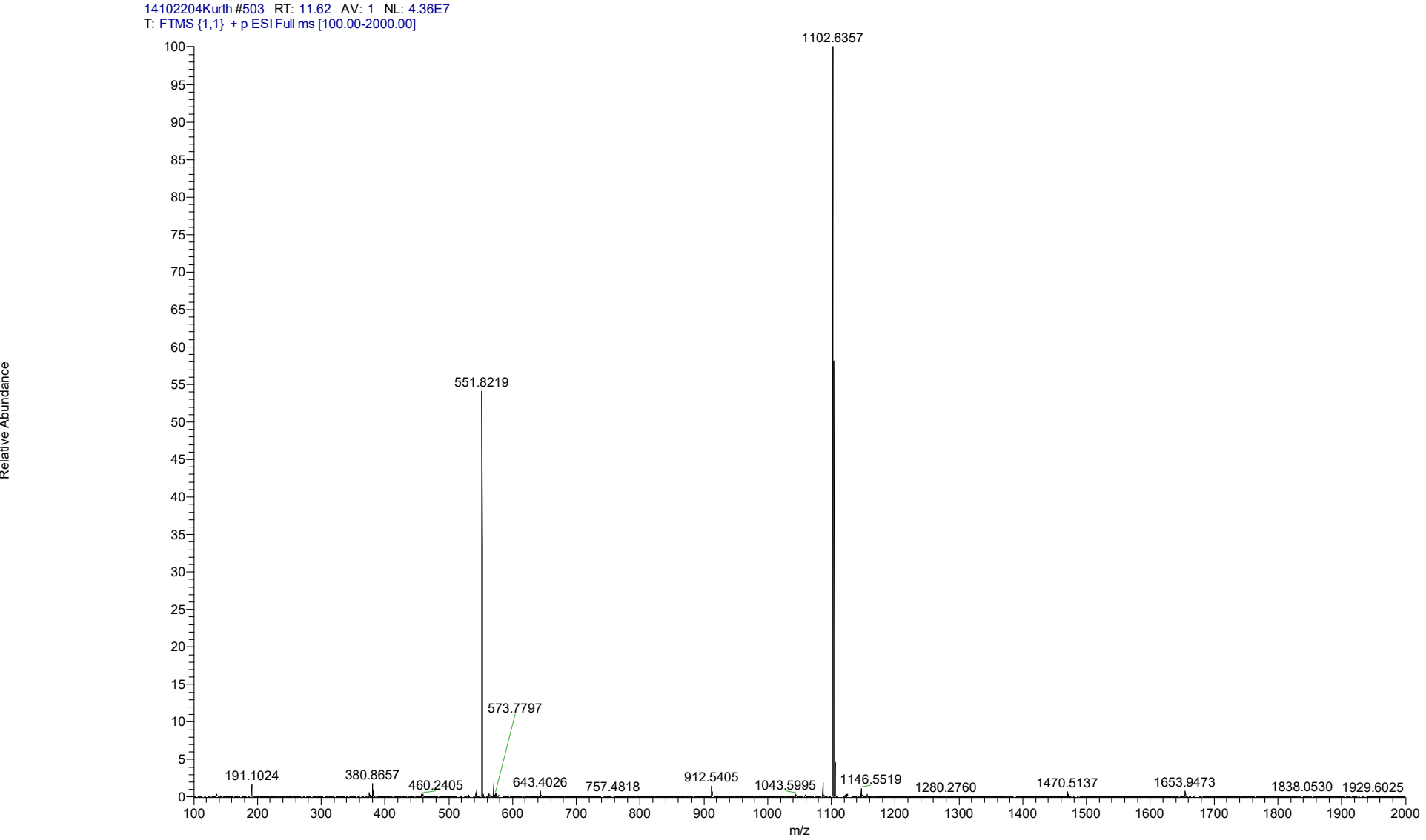

Table S1. Soil and freshwater bacteria that are assumed to produce photoreactive acyl peptide siderophore.

	CucG A domain homolog (Identity [%])	CucF TauD domain homolog (Identity [%])	CucF starter C domain homolog (Identity [%])	TaiD FAAL domain homolog (Identity [%])	Predicted siderophore	Reference[1]
Achromobacter spanius CGMCC9173	WP_050444824 (51)	WP_050444825 (71)	-	WP_050444825 (71)	new	
Burkholderia sordidicola S170	WP_051887899 (42)	WP_051887896 (68)	-	WP_051887899 (56)	new	
Cupriavidus basilensis OR16	EHP40329 (38)	EHP40328 (73)	-	EHP40327 (76)	taiwachelin	[21]
Cupriavidus gilardii CR3	WP_053823544 (44)	ALD92493 (45)	-	WP_053823547 (52)	new	
Cupriavidus necator H16	WP_011617407 (100)	WP_011617408 (100)	WP_011617408 (100)	-	cupriachelin	[20]
Cupriavidus sp. amp6	WP_051320452 (44)	WP_051320452 (94)	WP_051320452 (83)	-	cupriachelin	[20]
Cupriavidus sp. SK-4	EYS85590 (97)	EYS85589 (99)	EYS85589 (97)	-	cupriachelin	[20]
Cupriavidus sp. WS	WP_020206421 (46)	WP_020206420 (75)	-	WP_020206420 (72)	taiwachelin	[21]
Cupriavidus taiwanensis LMG 19424	WP_012356046 (47)	WP_012356045 (73)	-	WP_012356045 (100)	taiwachelin	[21]
Herbaspirillum seropedicae Z67	AKN68207 (43)	AKN68207 (71)	-	AKN68207 (36)	serobactin	[22]
Janthinobacterium agaricidamnosum NBRC 102515	CDG82376 (43)	CDG82376 (72)	-	CDG82375 (57)	new	
Ralstonia pickettii DTP0602	AGW94292 (93)	AGW94293 (98)	AGW94293 (93)	-	cupriachelin	[20]
Ralstonia sp. GA3-3	EON20600 (99)	EON20601 (100)	EON20601 (99)	-	cupriachelin	[20]
Variovorax paradoxus B4	WP_021008405 (40)	WP_021008410 (42)	-	WP_021008409 (55)	new	
Variovorax paradoxus EPS	WP_013542707 (37)	ADU35203 (55)	-	WP_013542707 (55)	new	
Variovorax paradoxus S110	WP_015866520 (41)	WP_015866525 (42)	-	WP_015866524 (56)	new	

[1]see main manuscript

Table S2. Annotation of siderophore gene clusters from *Variovorax paradoxus* B4 and *V. paradoxus* S110.

Gene	Protein accession no. (GenBank)	Size (aa)	Proposed function (domain architecture)	Predicted substrate specificity[1]
VAPA_1c38580 / Vapar_3733	WP_021008396 / WP_015866511	206 / 207	DNA-directed RNA polymerase sigma-70 factor	
VAPA_1c38590 /Vapar_3734	WP_021008397 / WP_015866512	72 / 72	anti-FecI sigma factor FecR	
VAPA_1c38600 / Vapar_3735	WP_021008398 / WP_015866513	78 / 78	hypothetical protein	
VAPA_1c38610 / Vapar_3736	WP_021008399 / WP_015866514	563 / 563	peptide transporter	
VAPA_1c38620 / Vapar_3737	WP_021008400 / WP_015866515	281 / 281	ferric iron reductase	
VAPA_1c38630 / Vapar_3738	WP_021008401 / WP_015866516	281 / 281	*N*-hydroxyornithine formyltransferase	
VAPA_1c38640 / Vapar_3739	WP_021008402 / WP_015866517	344 / 344	*N*-hydroxyornithine acetyltransferase	
VAPA_1c38650 / Vapar_3740	WP_021008403 / WP_015866518	450 / 439	ornithine *N*-monooxygenase	
VAPA_1c38660 / Vapar_3741	WP_021008404 / WP_015866519	722 / 723	TonB-dependent receptor	
VAPA_1c38670 / Vapar_3742	WP_021008405 / WP_015866520	1357 / 1358	non-ribosomal peptide synthetase (C-A-PCP-TE)	aspartic acid
VAPA_1c38680 / Vapar_3743	WP_021008406 / WP_015866521	2625 / 2626	non-ribosomal peptide synthetase (C-A-PCP-E-C-A-PCP)	N^{δ}-hydroxyornithine + threonine
VAPA_1c38690 / Vapar_3744	WP_021008407 / WP_015866522	1113 / 1110	non-ribosomal peptide synthetase (C-A-PCP)	serine
VAPA_1c38700 / Vapar_3745	WP_021008408 / WP_015866523	1520 / 1520	polyketide synthase (KS-AT-KR-ACP)	malonyl-CoA
VAPA_1c38710 / Vapar_3746	WP_021008409 / WP_015866524	1771 / 1776	non-ribosomal peptide synthetase (FAAL-ACP-C-A-PCP)	fatty acid + N^{δ}-formyl-N^{δ}-hydroxyornithine
VAPA_1c38720 / Vapar_3747	WP_021008410 / WP_015866525	330 / 330	TauD-like hydroxylase	
VAPA_1c38730 / Vapar_3748	WP_021008411 / WP_015866526	229 / 229	4'-phosphopantetheinyl transferase	
VAPA_1c38740 / Vapar_3749	WP_021008412 / WP_015866527	245 / 246	type II thioesterase	
VAPA_1c38750 / Vapar_3750	WP_021008413 / WP_015866528	85 / 85	MbtH domain-containing protein	
VAPA_1c38760 / Vapar_3751	WP_021008414 / WP_015866529	67 / 67	anti-FecI sigma factor FecR	
VAPA_1c38770 / Vapar_3752	WP_021008415 / WP_015866530	181 / 181	DNA-directed RNA polymerase sigma-70 factor	

[1]according to references [32-36] in the main manuscript

Table S3. Annotation of the siderophore gene cluster from *Variovorax paradoxus* EPS.

Gene	Protein accession no. (GenBank)	Size (aa)	Proposed function (domain architecture)	Predicted substrate specificity[1]
Varpa_4319	WP_013542699	433	ornithine *N*-monooxygenase	
Varpa_4320	WP_013542700	559	peptide transporter	
Varpa_4321	WP_013542701	288	ferric iron reductase	
Varpa_4322	WP_013542702	280	*N*-hydroxyornithine formyltransferase	
Varpa_4323	WP_013542703	721	TonB-dependent siderophore receptor	
Varpa_4324	WP_013542704	4633	non-ribosomal peptide synthetase (C-A-PCP-C-A-PCP-C-A-PCP-C-A-PCP-TE)	N^{δ}-hydroxyornithine + N^{δ}-formyl-N^{δ}-hydroxyornithine + threonine +serine
Varpa_4325	WP_013542705	4313	non-ribosomal peptide synthetase (C-A-PCP-C-A-PCP-C-A-PCP-C-A-PCP)	N^{δ}-formyl-N^{δ}-hydroxyornithine + threonine + threonine + glycine
Varpa_4326	WP_013542706	1542	polyketide synthase (KS-AT-KR-ACP)	malonyl-CoA
Varpa_4327	WP_013542707	1766	non-ribosomal peptide synthetase (FAAL-ACP-C-A-PCP)	fatty acid + N^{δ}-formyl-N^{δ}-hydroxyornithine
Varpa_4328	WP_013542708	249	type II thioesterase	
Varpa_4329	WP_013542709	84	MbtH domain-containing protein	
Varpa_4330	WP_013542710	82	anti-FecI sigma factor FecR	
Varpa_4331	WP_013542711	179	DNA-directed RNA polymerase sigma-70 factor	
Varpa_4332	WP_013542712	321	4'-phosphopantetheinyl transferase	

[1]according to references [32-36] in the main manuscript

Tables S4. Annotation of the variochelin gene cluster from *Variovorax boronicumulans* BAM-48.

Gene	Size of protein (aa)	Proposed function (domain architecture)	Predicted substrate specificity[1]
varR	560	peptide transporter	
varQ	78	anti-FecI sigma factor FecR	
varP	262	ferric iron reductase	
varO	369	*N*-hydroxyornithine acetyltransferase	
varN	440	ornithine *N*-monooxygenase	
varM	193	RNA polymerase subunit sigma-24	
varL	343	anti-FecI sigma factor FecR	
varK	816	TonB-dependent receptor	
varJ	2459	nonribosomal peptide synthetase (C-A-PCP-C-A-PCP-TE)	N^{δ}-hydroxyornithine + N^{δ}-hydroxyornithine
varI	2586	nonribosomal peptide synthetase (C-A-PCP-E-C-A-PCP)	serine + proline
varH	1035	nonribosomal peptide synthetase (C-A-PCP)	aspartic acid
varG	2351	polyketide synthase (KS-AT-KR-ACP-C-TauD)	malonyl-CoA
varF	1756	nonribosomal peptide synthetase (FAAL-ACP-C-A-PCP)	fatty acid + arginine
varE	234	4'-phosphopantetheinyl transferase	
varD	249	type II thioesterase	
varC	81	MbtH domain-containing protein	
varB	82	anti-FecI sigma factor FecR	
varA	178	DNA-directed RNA polymerase sigma-70 factor	

[1]according to references [32-36] in the main manuscript

3.2 Manuscript B

Kurth C, Wasmuth I, Wichard T, Pohnert G, Nett M

Algae induce siderophore biosynthesis in the freshwater bacterium *Cupriavidus necator* H16. Submitted.

Colette Kurth,[a] Ina Wasmuth,[b] Thomas Wichard,[b] Georg Pohnert,[b] and Markus Nett[c]#

Algae Induce Siderophore Biosynthesis in the Freshwater Bacterium *Cupriavidus necator* H16

[a]Leibniz Institute for Natural Product Research and Infection Biology, Hans Knöll Institute, Beutenbergstr. 11a, 07745 Jena, Germany

[b]Institute of Inorganic and Analytical Chemistry, Friedrich Schiller University, Lessingstrasse 8, D-07743 Jena, Germany

[c]Department of Biochemical and Chemical Engineering, Laboratory of Technical Biology, TU Dortmund University, Emil-Figge-Strasse 66, 44227 Dortmund, Germany

Corresponding author: Markus Nett, markus.nett@tu-dortmund.de, +49 231 7554742

ACKNOWLEDGEMENT

This project was supported by the Collaborative Research Center ChemBioSys (CRC1127 ChemBioSys) and funded by the Deutsche Forschungsgemeinschaft. We thank T. Kindel (Hans Knöll Institute Jena, Department for Molecular and Applied Microbiology) for MALDI-TOF/TOF measurements.

ABSTRACT

Cupriachelin is a photoreactive lipopeptide siderophore produced by the freshwater bacterium *Cupriavidus necator* H16. In the presence of sunlight, the iron-loaded siderophore undergoes photolytic cleavage, thereby releasing solubilized iron into the environment. This iron is not only available to the siderophore producer, but also to the surrounding microbial community. In this study, the cupriachelin-based interaction between *C. necator* H16 and the freshwater diatom *Navicula pelliculosa* was investigated. A reporter strain of the bacterium was constructed to study differential expression levels of the cupriachelin biosynthesis gene *cucJ* in response to varying environmental conditions. Not only iron starvation, but also culture supernatants of *N. pelliculosa* were found to induce cupriachelin biosynthesis. The transcription factors involved in this differential gene expression were identified using DNA-protein pulldown assays. Besides the well-characterized ferric uptake regulator (Fur), a two-component system was found to tune the expression of cupriachelin biosynthesis genes in the presence of diatom supernatants.

33 **KEYWORDS**

34 photoreactive siderophores, bacteria-diatom interactions, freshwater, differential gene expression,

35 transcription factors

INTRODUCTION

Iron is involved in many biologically vital processes and is indispensable for virtually all forms of life (Andrews et al. 2003). It is highly abundant, yet hardly bioavailable in most ecosystems due to the formation of insoluble ferric oxides and hydroxides. Therefore, iron often represents a limiting factor for microbial growth. Microorganisms have evolved different strategies to overcome this challenge, one of the most well-known being the production of siderophores (Hider and Kong 2010; Kurth et al. 2016a). Siderophores are small molecular weight compounds that have a strong affinity towards ferric iron (Fe^{3+}). Once secreted from the producing cell, they rapidly coordinate the metal and are then taken back up into the cell by active transport. In the cytoplasm, the iron is usually released from the siderophore by a reductive or hydrolytic mechanism (Schalk and Guillon 2013).

A different mode of siderophore-mediated iron acquisition was described from marine organisms. Some marine bacteria produce siderophores, of which the iron-bound complexes are prone to photolytic cleavage in the presence of sunlight. The complexed iron is thereby reduced and released into the environment (Barbeau et al. 2001). The production of photoreactive siderophores appears to be widely distributed in marine bacteria (Barbeau et al. 2001, 2002; Ito and Butler 2005; Martin et al. 2006; Homann et al. 2009; Amin et al. 2009b; Butler and Theisen 2010; Robertson et al. 2018). An essential characteristic of these molecules is the presence of an α-hydroxycarboxylate function that confers the photoreactivity (Barbeau et al. 2001). Furthermore, many of these siderophores feature a fatty acid side chain. The latter was proposed to increase the residence time of the siderophore and to concentrate iron around the cell, which seems plausible in aquatic environments, where diffusion plays a significant role (Martinez 2000). Recently, photoreactive acyl siderophores have also been reported from freshwater bacteria. The finding of the

cupriachelins (Kreutzer et al. 2012) and the variochelins (Kurth et al. 2016b) indicates that photoreactive siderophores are even more widespread in the environment than previously thought.

The light-induced release of soluble and, thus, bioavailable iron has a major impact on environmental iron cycling. Since aquatic bacteria often live in tight relationships with phytoplankton species (Kouzuma and Watanabe 2015; Seymour et al. 2017), siderophore-mediated biotic interactions are highly likely as well. Indeed, Amin et al. (2009b) demonstrated that the dinoflagellate *Scrippsiella trochoidea* can utilize iron, which is released from a photoreactive siderophore produced by associated bacteria. They further found that the bacterial siderophore producers receive exudates from the dinoflagellate, which serve as sources of carbon and energy. The described interaction was referred to as "carbon-for-iron" paradigm (Amin et al. 2009a) and can be regarded as mutualistic. It is conceivable that such iron sharing is a common phenomenon amongst plankton. Because iron represents a major limiting factor for the growth of phytoplankton species (Blain et al. 2007), an association with producers of photoreactive siderophores would represent an important ecological advantage.

In this study, the cupriachelin-based interaction between the freshwater bacterium *Cupriavidus necator* H16 and the diatom *Navicula pelliculosa* was investigated. The latter was chosen for this analysis because of its wide global distribution in freshwater environments. A natural co-occurrence of *N. pelliculosa* and *C. necator* H16 appeared hence conceivable. We hypothesized that *N. pelliculosa* could trigger the production of cupriachelin and that the concomitant communication could rely on signal molecules secreted by the diatom (Fig. 1). To probe this scenario, we constructed a reporter of cupriachelin biosynthesis gene expression. We show that not only iron starvation, but also culture supernatants of *N. pelliculosa* induce cupriachelin biosynthesis. Furthermore, we analyzed the transcription factors involved in the regulation of

cupriachelin biosynthesis by DNA-protein-pulldown assays. In addition to the well-known ferric uptake regulator (Fur) a two-component system was found to tune the expression of cupriachelin biosynthesis genes.

MATERIALS AND METHODS

Growth conditions of algal and bacterial strains. *N. pelliculosa* was obtained from the SAG culture collection (SAG 1050-3, Göttingen, Germany). The diatom was grown in static, non-shaking culture in cell culture flasks (50 mL/125 mL, Sarstedt) at 18 °C in modified WC medium (36.8 mg/L $CaCl_2$ x 2 H_2O, 37 mg/L $MgSO_4$ x 7 H_2O, 12.6 mg/L $NaHCO_3$, 11.4 mg/L K_2HPO_4 x 3 H_2O, 85 mg/L $NaNO_3$, 21.2 mg/L Na_2O_3Si x 5 H_2O, 115 mg/L TES, 4.36 mg/L $EDTANa_2$, 0.01 mg/L $CuSO_4$ x 5 H_2O, 0.022 mg/L $ZnSO_4$ x 7 H_2O, 0.01 mg/L $CoCl_2$ x 6 H_2O, 0.18 mg/L $MnCl_2$ x 4 H_2O, 0.006 mg/L Na_2MoO_4 x 2 H_2O, 1 mg/L H_3BO_3, 0.1 mg/L thiamine HCl, 0.0005 mg/L biotin, 0.0005 mg/L cyanocobalamin). Ferric chloride was added to the medium at different concentrations corresponding to iron-limited (0.15 µM) and iron-replete (10 µM) conditions. The light was provided by a "JBL Solar Reptil Sun T8" tube covering the UV-Vis range from 200-800 nm. A light regime of 12:12 (light/dark) with 30–50 µmol/m^2/s light intensity was used. Growth was monitored by daily microscopic cell counts. For this purpose, micrographs were taken every day on ten randomly chosen spots of every cell culture flask, and the number of cells per monitored area (~72,000 µm^2) was counted using ImageJ (Schindelin et al. 2012). Seed cultures consisted of *N. pelliculosa* cells in their exponential growth phase and constituted 2% (v/v) of the final culture volume. Under these conditions, *N. pelliculosa* reached stationary phase after ~ 2 weeks. For cultivation of *C. necator* H16, H-3 mineral medium (2.3 g/L KH_2PO, 2.57 g/L Na_2HPO_4, 1.0 g/L NH_4Cl, 0.5 g/L $MgSO_4$ × 7 H_2O, 0.5 g/L $NaHCO_3$, 0.01 g/L $CaCl_2$ × 2 H_2O and 5 mL/L SL-6 trace element solution (0.1 g/L $ZnSO_4$ × 7 H_2O, 0.03 g/L $MnCl_2$ × 4 H_2O, 0.3 g/L H_3BO_3, 0.2 g/L $CoCl_2$ × 6 H_2O, 0.01 g/L CuCl2 × 2 H_2O, 0.02 g/L $NiCl_2$ × 6 H_2O, 0.03 g/L Na_2MoO_4 × 2 H_2O)) supplemented with 1 g/L aspartate was used as standard growth medium. When required, iron was added as $FeCl_3$ to different concentrations. Cultures were vigorously shaken at 28 °C. For

cultivation of *C. necator* H16 with culture supernatants of *N. pelliculosa*, a 1:1 mixture of H-3 mineral medium and filter-sterilized (0.2 µM) algal culture supernatant supplemented with 2% fructose was used. The control consisted of modified WC medium supplemented with 2% fructose. The described cultivation conditions were used for β-galactosidase assays, as well as for DNA-protein pulldown assays. *Escherichia coli* strains were cultivated at 37 °C in lysogeny broth (LB). When required, antibiotics were added to the following concentrations: 100 µg ampicillin/mL and 25 µg chloramphenicol/mL.

Construction of the reporter and control strains. Plasmids used in this study are listed in Table 1. The broad host range expression vector pRANGER-BTB-3 was used as the backbone for all constructed plasmids. First, *araC* was removed from the plasmid by *Bsa*XI digestion and religation yielding pCK01. The β-galactosidase gene *lacZ*, obtained from *Xmn*I digestion of pMLB1034 (ATCC 37222), was introduced into the *Eco*RV restriction site of the plasmid resulting in pCK02. Three different promoters were subsequently cloned in front of *lacZ*. (i) The arabinose-inducible promoter *araBp* was PCR-amplified along with *araC* from pRANGER-BTB-3 using the primers *araBp*_F (5'-cccgggtataggaacttcgaagcagctc-3') and *araBp*_R (5'-cccgggttctcctttactcatgctagcc-3'). It was then cloned into pJET1.2/blunt (Thermo Fisher Scientific), introduced into chemically competent *E. coli* DH5α and sequenced. The genes *araBp* and *araC* were cut out from pJET1.2/blunt using *Sma*I and cloned into the *Sma*I site of pCK02, resulting in pCK03. (ii) The constitutive promoter *tacp* (Fukui et al. 2011) was amplified via PCR from pGEX-6P-2 with the primers *tacp*_F (5'-cccgggttggccgattcattaatgcag-3') and *tacp*_R (5'-cccgggtagtataggggacatgaatactg-3'). Cloning of *tacp* into pCK02 was performed as previously described for *araBp*, resulting in pCK04. (iii) *cucJp* is the 1037 bp upstream region of *h16_b1683*, which encodes an enzyme involved in cupriachelin biosynthesis (Kreutzer et al. 2012). It was

amplified via PCR from *C. necator* H16 genomic DNA using the primers *cucJp*_F (5'-cccgggctaggtgccgacggctttac-3') and *cucJp*_R (5'-cccgggcataggctgcgtcattgggtc-3'). Cloning of *cucJp* into pCK02 was performed as previously described for *araBp*, resulting in pCK05. The plasmids pCK02, pCK03, pCK04 and pCK05 were introduced into *C. necator* H16 via electroporation. Electrocompetent cells were prepared by growing *C. necator* H16 in LB medium to an OD_{600} of 0.4. The cells were then placed on ice for 20 min, harvested by centrifugation (5 min, 2,627 x *g*, 4 °C), washed twice with 10% glycerol and resuspended in 10% glycerol. After electroporation (2500 V, 200 Ω, 25 µF), the transformed cells were allowed to regenerate for 150 min shaking at 30 °C in super optimal broth with catabolite repression (2% tryptone, 0.5% yeast extract, 10 mM NaCl, 2.5 mM KCl, 10 mM $MgCl_2$, 20 mM glucose). *C. necator*:pCK03 was plated on LB agar containing 10 mM arabinose and 0.1 mg/mL X-Gal to confirm the production of β-galactosidase in the host strain. The *C. necator* reporter strain harboring pCK05 was subsequently used for β-galactosidase assays, along with the control strains harboring pCK02 (negative control) and pCK04 (positive control).

Measuring of iron concentration in media and algal culture supernatants. The iron concentration in media and supernatants was determined on a contrAA 700 high-resolution continuum source atomic absorption spectrometer (AAS, Analytik Jena, Germany) using graphite tubes (Hermenau et al. 2018).

β-Galactosidase assay. The reporter strain was grown in 50 mL volumes under the respective conditions. A culture volume of 2-4 mL was harvested by centrifugation (1 min, 15,700 x *g*, room temperature) for each assay and resuspended in 200 µL phosphate-buffered saline pH 7.4 (8 g/L NaCl, 0.2 g/L KCl, 1.44 g Na_2HPO_4, 0.24 g KH_2PO_4). The β-galactosidase assay was performed

as previously described by Griffith and Wolf (2002), with the exception that microplates were incubated at 28 °C instead of room temperature.

Statistical analyses. For β-galactosidase assays, reporter stains were cultivated as triplicates for every treatment. *N. pelliculosa* was cultivated in biological triplicates. Every supernatant of the diatom culture was split into three samples and added to the reporter strains, resulting in nine replicates for each data point. Outliers were identified according to Dixon's Q test at the 95% confidence interval and eliminated from the analysis. Statistical significance of results was assessed via one-way ANOVA with Tukey´s post hoc for pairwise comparisons ($p < 0.05$) using VassarStats for statistical computation (Lowry 2018).

DNA-protein pulldown assay. *C. necator* H16 was cultivated in 500 mL cultures under the respective conditions. After having reached stationary growth phase, cells were harvested by centrifugation (10 min, 9,500 x *g*, 4°C), washed with 20 mL washing buffer (10 mM Tris-HCl pH 7.5, 5% glycerol, 2 mM EDTA, 120 mM NaCl) and resuspended in 2 mL BS/THES buffer (Jutras et al. 2012). Cells were lysed via sonication (7 x 40% pulsed cycles of 1 min with 20% power and 1 min break in between the cycles) using a Bandelin Sonopuls HD 2070. Cell debris was separated from the soluble protein by centrifugation (30 min, 30,000 × *g*, 4 °C). The DNA fragment containing *cucJp* was amplified using *cucJp*_R and 5'-biotinylated *cucJp*_F. The DNA-protein pulldown assay was then performed as previously described (Jutras et al. 2012). Briefly, the DNA fragment containing *cucJp* was attached to Dynabeads M-280 Streptavidin (Thermo Fisher Scientific) by mixing 200 µL of beads resuspended in 2x B/W buffer (Jutras et al. 2012) and 200 µL PCR product for 20 min. The bead-probe complex was then washed three times with TE buffer (1 mM EDTA, 10 mM TrisCl, pH 8.0), two times with BS/THES buffer und once with BS/THES buffer supplemented with Poly(dI-dC) (i.e., poly(deoxyinosinic-deoxycytidylic) acid). The

supernatant of the bacterial cell lysate was added to the beads resuspended in BS/THES buffer supplemented with Poly(dI-dC) and mixed for 30 min at RT. This step was repeated at 4 °C. The bead-probe-protein complex was then washed five times with BS/THES buffer supplemented with Poly(dI-dC) and two times with BS/THES buffer in order to remove unspecifically bound proteins. Target proteins were finally eluted using increasing NaCl concentrations (200-1000 mM).

Protein analysis. Proteins were initially analyzed via SDS-PAGE using 4-20% Mini-PROTEAN® TGX™ Gels (Bio-Rad). Electrophoresis was performed in Mini-PROTEAN® Tetra Cells (Bio-Rad) at 180 V for 30 min. Coomassie staining of the gel was conducted following the protocol of Dyballa and Metzger (2009). Protein bands of interest were excised from the gel and treated after the protocol of Shevchenko et al. (1996) with slight modifications. Briefly, protein bands were destained, and proteins were reduced with dithiothreitol and iodoacetamide before in-gel digestion with trypsin. The resulting peptides were analyzed on an Ultraflex MALDI-TOF/TOF mass spectrometer (Bruker Daltonics).

RESULTS

Generation and testing of reporter strains. To investigate the effect of varying environmental conditions on cupriachelin biosynthesis, we constructed *C. necator* H16 reporter strains harboring plasmids with the β-galactosidase gene *lacZ*. Initially, an arabinose-inducible promoter was cloned in front of the reporter gene and the corresponding plasmid, pCK03, was introduced into *C. necator*. When plated on LB agar containing arabinose and X-Gal, *C. necator*:pCK03 formed blue colonies, confirming the production of recombinant β-galactosidase (Fig. S1). In contrast, the negative control strain *C. necator*:pCK02, which does not harbor any promoter in front of *lacZ*, formed white colonies on the same medium. The latter strain was also used as negative control for the β-galactosidase assay. *C. necator*:pCK04, which harbors the constitutive promoter *tacp* (Fukui et al. 2011), served as positive control. For the actual cupriachelin biosynthesis reporter strain, *cucJp* was inserted in front of *lacZ*, yielding pCK05. The gene *cucJ* encodes a nonribosomal peptide synthetase, which is required for the assembly of cupriachelin (Kreutzer et al. 2012), and its transcription level was thus expected to mirror the level of cupriachelin biosynthesis.

Effect of iron concentrations on transcription levels of *cucJ*. The iron concentration in the growth medium measured by AAS was found to have a major effect on transcription levels of *cucJ* in *C. necator* (Fig. 2). On the second day after inoculation, reporter strain cultures grown under iron deficiency (≤ 1 µM Fe) showed significantly higher β-galactosidase activities compared to cultures supplied with higher iron concentrations. The iron concentration in the growth medium correlates with the measured β-galactosidase activity. It became apparent that iron concentrations below 1 µM highly induce siderophore biosynthesis, while β-galactosidase activities of cultures grown with 10 µM to 500 µM iron are comparatively low. Interestingly, the increased expression

of *cucJ* in low-iron media was short-lived. On the third day after inoculation, the cultures showed only negligible differences in β-galactosidase activity.

Effect of *N. pelliculosa* culture supernatants on transcription levels of *cucJ*. To test a possible effect of *N. pelliculosa* supernatants on the expression level of *cucJ*, the diatom was grown under iron starvation (0.15 µM Fe) and iron repletion (10 µM Fe) to stationary phase (Fig. S2). AAS measurements revealed that *N. pelliculosa* sequestered most iron present in the medium during that time. The remaining iron concentrations in the culture supernatants after cultivation were 0.07 µM ± 0.003 µM and 0.56 µM ± 0.090 µM for iron starvation and iron repletion conditions, respectively. For the β-galactosidase assay, *C. necator* reporter strains were inoculated into a 1:1 mixture of fresh H-3 mineral medium and *N. pelliculosa* supernatant. The iron concentration in the latter had been adjusted to 0.65 µM (0.56 µM + 0.090 µM). In doing so, the effect of varying iron concentrations on *cucJ* expression levels could be eliminated, and the observed differences in reporter gene transcription levels could be ascribed to metabolites secreted by the diatom. Since *C. necator* grew slowly in the given media composition (data not shown), β-galactosidase assays were performed only on days 3 and 4 after inoculation. The results show that, regardless of iron concentration, the addition of diatom supernatants had a significant impact on the β-galactosidase activity in the reporter strain (Fig. 3). Supernatants from *N. pelliculosa* cultures that had been grown under iron-replete conditions strongly induced β-galactosidase activity in the reporter strains compared to the medium control on both days. The same increase in β-galactosidase activity, but one day delayed, was observed in the reporter strains incubated with culture supernatants grown under iron starvation (Fig. 3).

Transcriptional regulation of cupriachelin biosynthesis. Following the assessment of differential gene expression of *cucJ* in the β-galactosidase assay, we set out to identify the

responsible transcription factors. For this purpose, a DNA-protein pulldown assay was performed. Briefly, a DNA fragment comprising *cucJp* was generated and incubated with cell lysates of *C. necator* H16 to allow transcription factors to bind to *cucJp*. After several washing steps, bound proteins were eluted from the DNA and analyzed via SDS-PAGE and MALDI-TOF/MS. In this way, the ferric uptake regulator (Fur) protein H16_A3143 was found to be involved in the transcriptional regulation of cupriachelin biosynthesis (Fig. S3). The protein was present in *C. necator* H16 cells grown under iron starvation (no added iron) and iron-replete conditions (190 µM Fe). Interestingly, when the bacterium was cultivated with algal supernatants, the DNA-protein pull down assay revealed a second transcription factor, H16_A1372, binding to *cucJp* (Fig. 4). H16_A1372 is annotated as a response regulator of the NarL family. NarL response regulators harbor a characteristic helix-turn-helix motif in their DNA-binding domain, which is also present in H16_A1372 (Kohlmann 2015). Besides the response regulator, four other proteins were identified in this DNA-protein pulldown assay (Fig. 4). They include proteins involved in energy metabolism (dihydrolipoyl dehydrogenase) and nucleotide biosynthesis (dihydroorotase, aspartate carbamoyltransferase). Since an unspecific or indirect binding with *cucJp* cannot be ruled out, these proteins were not further considered in this study.

DISCUSSION

The production of siderophores by microorganisms depends on several environmental conditions, one of the most important being the availability of iron. Siderophore biosynthesis is generally upregulated under low iron stress, which was also confirmed for the production of cupriachelin in this study. Iron concentrations ≤ 1 μM increased the transcription level of the reporter gene compared to higher iron concentrations (Fig. 2). Interestingly, β-galactosidase activity was also observed with iron concentrations as high as 500 μM. Since iron concentrations > 190 μM are known to abolish cupriachelin production (Kreutzer et al. 2012), it is possible that the biosynthesis is also regulated post-transcriptionally. Such control at the mRNA level has been recognized to play a pivotal role in prokaryotic gene expression (Papenfort and Vogel 2009), but its identification remains challenging due to different constraints (Livny and Waldor 2007). Another observation was the short persistence of the increased expression of *cucJ* in low-iron media (Fig. 2). A possible explanation might be that cupriachelin is only produced under severe iron starvation. Once a sufficient intracellular iron concentration is reached, *C. necator* H16 may switch to the production of a metabolically less costly siderophore, as previously reported for *Pseudomonas* spp. (Dumas et al. 2013). A gene cluster for the biosynthesis of an auxiliary siderophore is indeed present in the genome of *C. necator* H16 (Schwartz et al. 2003).

Besides the environmental iron concentration, cell density has a major influence on siderophore transcription levels (Niehus et al. 2017). Siderophore production is generally most effective when iron concentrations are low, and cell densities are high. This is because higher cell densities entail higher siderophore production rates and, concurrently, higher chances for cells to encounter iron-siderophore complexes. Quorum sensing mediates this concentration-dependent mechanism of siderophore biosynthesis in *Pseudomonas aeruginosa* (Stintzi et al. 1998), and it is conceivable

273 that this may be true also for other bacteria. When iron availability is very low, cells grow poorly
274 and benefit less from producing siderophores. The poor growth may explain why lower
275 transcription levels of the reporter gene were measured when bacteria had been grown without any
276 iron supplementation compared to the cases when small amounts of iron (0.4 μM, 1 μM) had been
277 added to the cultures (Fig. 2).

278 A third factor influencing siderophore biosynthesis is the presence of iron-competing strains
279 (Niehus et al. 2017). As secreted molecules, siderophores may be considered as public goods,
280 especially when non-producers possess receptors and transporters for the uptake of the
281 corresponding siderophore (Niehus et al. 2017). Photoreactive siderophores indeed are particular
282 in this context. Their photolytic cleavage yields free Fe(II) that will rapidly reoxidize to a soluble,
283 bioavailable form of iron, *i.e.* Fe(III)' (the sum of all inorganic Fe(III)-hydrolysis species), under
284 aerobic conditions (Bruland and Rue 2001; Amin et al. 2012). To which extent iron is shared with
285 other organisms or used by the producer is an important aspect that has to be considered. The
286 cupriachelin gene cluster encodes a TonB-dependent receptor (Kreutzer et al. 2012), suggesting
287 that the Fe-cupriachelin complex can be taken up by the bacterium, at least in the dark. The genome
288 of *C. necator* H16 further exhibits a ferrous iron uptake system (H16_B0083-H16_B0085)
289 (Cartron et al. 2006; Kreutzer et al. 2012) that may be used for the uptake of the photochemically
290 released Fe(II). However, fast reoxidation to Fe(III)' under aerobic conditions and the apparent
291 lack of a ferric iron uptake system in the bacterial genome, reduce the chance for cupriachelin-
292 based iron uptake in sunlight. This leads to the assumption that cupriachelin will deliver iron to *C.*
293 *necator* H16 mainly in the dark, while potentially providing iron to other organisms in the light
294 (Fig. 1). Producing such siderophore would only make sense, if the other organisms are mutualists,

295 providing other benefits to *C. necator* H16. Considering the "iron-for-carbon" paradigm (Amin et
296 al. 2009a), mutualistic iron sharing of *C. necator* H16 with phytoplankton seems possible.

297 Especially diatoms, which have been coexisting with bacteria in aquatic environments for more
298 than 200 million years, appear to form specific interactions with bacteria (Amin et al. 2012). These
299 encompass, e.g. the exchange of iron (Amin et al. 2009a), vitamins (Croft et al. 2005), nitrogen
300 (Foster et al. 2011) and dissolved organic carbon (Haynes et al. 2007). Interactions typically take
301 place within the phycosphere, i.e., the zone directly surrounding microalgae (Seymour et al. 2017)
302 and macroalgae (Wichard 2016). Here, algae can "cultivate" their bacteria by secreting metabolites
303 that will attract certain microorganisms. The phycosphere does not mix with the surrounding fluids
304 and readily accumulates metabolites. The resulting accumulation of microorganisms in microscale
305 patches throughout aquatic environments (Blackburn et al. 1998) can favor cooperation by keeping
306 cooperators and metabolites together. This is reinforced by the production of metabolites with
307 rather a low diffusivity. For siderophores, it was found that low habitat structuring and severe iron
308 starvation, conditions that prevail in aquatic environments, favor the production of siderophores
309 with low diffusivity (Kümmerli et al. 2014; Boiteau et al. 2016). All this leads to the assumption
310 that aquatic photoreactive siderophores are public goods, but stay in the close vicinity of the
311 producing organism and thereby share their iron only with a fine selection of mutualists. It seems
312 plausible that the metabolically closely linked organisms will influence each other on different
313 levels. The observed increase of reporter gene transcription levels after treatment with *N.*
314 *pelliculosa* culture supernatants (Fig. 3) corroborates this assumption. The fact that culture
315 supernatants of iron-replete algae had a greater inducing effect on cupriachelin biosynthesis than
316 those of iron-starved algae, can be explained by the different growth behavior of the algal cultures.
317 In the presence of 10 µM iron, *N. pelliculosa* generally reached higher cell densities compared to

0.15 µM iron (Fig. S2). This difference in growth is probably also reflected in the amount of secreted metabolites and, thereby, in the inducing effect on cupriachelin transcription levels. The induction of cupriachelin biosynthesis will likely maximize the amount of iron *N. pelliculosa* can obtain from *C. necator* H16 and result in an important growth advantage for the alga. It illustrates the importance of microbial interactions for the success of a species.

In this study, we used the promoter region of *cucJ*, a gene involved in cupriachelin biosynthesis, to determine cupriachelin transcription levels and regulation. *CucJp* harbors a Fur box (AATGAGAATGATTATCA) (Fillat 2014), and it is therefore not surprising that we identified Fur (H16_A3143) to bind to the promoter in the DNA-protein pulldown assay. Fur is widely distributed in bacteria and regulates transcription of many genes related to iron metabolism. When iron concentration within the cell is high, a*po*-Fur binds Fe^{2+} and dimerizes. The resulting *holo*-protein then binds to Fur boxes of the corresponding promoters and, thereby, blocks the RNA polymerase binding site (de Lorenzo et al. 1987). In this classical model, Fur acts as a transcriptional repressor that prevents the transcription of siderophore biosynthesis genes, when the intracellular iron concentration is high. Fur is autoregulated, binding to its promoter and thus preventing its transcription when it is already abundant (Delany et al. 2002). This ensures a homogeneous distribution of the transcription factor and ensures an adequate response to environmental stimuli (Watnick et al. 1997). In our assays, Fur could be found in both iron-deplete and iron-replete cultures of *C. necator* H16, illustrating the constitutive expression of the *fur* gene (*h16_a3143*). There is increasing evidence that Fur does not only act as a transcriptional repressor but also as an activator (Massé et al. 2007). It can thus be regarded as a global regulator of gene expression in many bacteria.

When *C. necator* H16 was grown with culture supernatants of *N. pelliculosa*, we identified a second transcription factor binding to *cucJp*. This protein, H16_A1372, was previously characterized as a global regulator of energy and carbon metabolism in *C. necator* H16 (Kohlmann 2015). It is a response regulator of the NarL family. H16_A1372 seemed more abundant in *C. necator* H16 samples that had been grown with *N. pelliculosa* culture supernatants, rather than in the control samples grown with modified WC medium (Fig. 4). Since transcription levels of the reporter gene were upregulated under the former conditions, we hypothesize that H16_A1372 acts as a transcriptional activator. Regulation of siderophore biosynthesis and uptake by two-component systems has been reported before (Dean and Poole 1993; Liao et al. 1996), but seems relatively rare compared to the regulation by Fur. Also, this is the first report of a NarL-type response regulator involved siderophore biosynthesis regulation to our knowledge. The interplay between Fur and H16_A1372 may be crucial for the fine-tuning of cupriachelin transcription levels but remains elusive so far. Further studies need to be conducted to unravel the underlying mechanisms.

In summary, cupriachelin biosynthesis was found to be highly dependent on environmental conditions. These include varying iron concentrations, but also the presence of other microorganisms, such as the diatom *N. pelliculosa*. To our knowledge, this is the first report of an alga manipulating siderophore biosynthesis in a bacterium. Photoreactive siderophores have a major influence on iron cycling in aquatic environments and have the potential to shape planktic communities. Considering the importance of plankton dynamics for climate change and the formation of toxic algal blooms (Hallegraeff 2010), the fundamental understanding of such interactions is of major interest.

REFERENCES

Amin SA, Green DH, Hart MC, et al (2009a) Photolysis of iron-siderophore chelates promotes bacterial-algal mutualism. Proc Natl Acad Sci 106:17071–17076. doi: 10.1073/pnas.0905512106

Amin SA, Green DH, Küpper FC, Carrano CJ (2009b) Vibrioferrin, an unusual marine siderophore: Iron binding, photochemistry, and biological implications. Inorg Chem 48:11451–11458. doi: 10.1021/ic9016883

Amin SA, Parker MS, Armbrust EV (2012) Interactions between diatoms and bacteria. Microbiol Mol Biol Rev 76:667–684. doi: 10.1128/MMBR.00007-12

Andrews SC, Robinson AK, Rodríguez-Quiñones F (2003) Bacterial iron homeostasis. FEMS Microbiol Rev 27:215–237. doi: 10.1016/S0168-6445(03)00055-X

Barbeau K, Rue EL, Bruland KW, Butler A (2001) Photochemical cycling of iron in the surface ocean mediated by microbial iron(III)-binding ligands. Nature 413:409–413. doi: 10.1038/35096545

Barbeau K, Zhang G, Live DH, Butler A (2002) Petrobactin, a photoreactive siderophore produced by the oil-degrading marine bacterium *Marinobacter hydrocarbonoclasticus*. J Am Chem Soc 124:378–379. doi: 10.1021/ja0119088

Blackburn N, Fenchel T, Mitchell J (1998) Microscale nutrient patches in planktonic habitats shown by chemotactic bacteria. Science 282:2254–2256. doi: 10.1126/science.282.5397.2254

Blain S, Quéguiner B, Armand L, et al (2007) Effect of natural iron fertilization on carbon sequestration in the Southern Ocean. Nature 446:1070–1074. doi: 10.1038/nature05700

Boiteau RM, Mende DR, Hawco NJ, et al (2016) Siderophore-based microbial adaptations to iron scarcity across the eastern Pacific Ocean. Proc Natl Acad Sci 113:14237–14242. doi: 10.1073/pnas.1608594113

Bruland KW, Rue EL (2001) Analytical methods for the determination of concentrations and speciation of iron. In: Turner DK, Hunter KA (eds) The biogeochemistry of seawater. Wiley

Butler A, Theisen RM (2010) Iron(III)–siderophore coordination chemistry: Reactivity of marine siderophores. Coord Chem Rev 254:288–296. doi: 10.1016/j.ccr.2009.09.010

Cartron ML, Maddocks S, Gillingham P, et al (2006) Feo – transport of ferrous iron into bacteria. BioMetals 19:143–157. doi: 10.1007/s10534-006-0003-2

Croft MT, Lawrence AD, Raux-Deery E, et al (2005) Algae acquire vitamin B12 through a symbiotic relationship with bacteria. Nature 438:90–93. doi: 10.1038/nature04056

de Lorenzo V, Wee S, Herrero M, Neilands JB (1987) Operator sequences of the aerobactin operon of plasmid ColV-K30 binding the ferric uptake regulation (fur) repressor. J Bacteriol 169:2624–2630. doi: 10.1128/jb.169.6.2624-2630.1987

Dean CR, Poole K (1993) Expression of the ferric enterobactin receptor (PfeA) of *Pseudomonas aeruginosa*: involvement of a two-component regulatory system. Mol Microbiol 8:1095–1103. doi: 10.1111/j.1365-2958.1993.tb01654.x

Delany I, Spohn G, Pacheco A-BF, et al (2002) Autoregulation of *Helicobacter pylori* Fur revealed by functional analysis of the iron-binding site: Autoregulation of *H. pylori* Fur protein. Mol Microbiol 46:1107–1122. doi: 10.1046/j.1365-2958.2002.03227.x

Dumas Z, Ross-Gillespie A, Kummerli R (2013) Switching between apparently redundant iron-uptake mechanisms benefits bacteria in changeable environments. Proc R Soc B Biol Sci 280:20131055–20131055. doi: 10.1098/rspb.2013.1055

Dyballa N, Metzger S (2009) Fast and sensitive colloidal Coomassie G-250 staining for proteins in polyacrylamide gels. J Vis Exp. doi: 10.3791/1431

Fillat MF (2014) The FUR (ferric uptake regulator) superfamily: Diversity and versatility of key transcriptional regulators. Arch Biochem Biophys 546:41–52. doi: 10.1016/j.abb.2014.01.029

Foster RA, Kuypers MMM, Vagner T, et al (2011) Nitrogen fixation and transfer in open ocean diatom–cyanobacterial symbioses. ISME J 5:1484–1493. doi: 10.1038/ismej.2011.26

Fukui T, Ohsawa K, Mifune J, et al (2011) Evaluation of promoters for gene expression in polyhydroxyalkanoate-producing *Cupriavidus necator* H16. Appl Microbiol Biotechnol 89:1527–1536. doi: 10.1007/s00253-011-3100-2

Griffith KL, Wolf RE (2002) Measuring β-galactosidase activity in bacteria: Cell growth, permeabilization, and enzyme assays in 96-well arrays. Biochem Biophys Res Commun 290:397–402. doi: 10.1006/bbrc.2001.6152

Hallegraeff GM (2010) Ocean climate change, phytoplankton community responses, and harmful algal blooms: A formidable predictive challenge. J Phycol 46:220–235. doi: 10.1111/j.1529-8817.2010.00815.x

Haynes K, Hofmann TA, Smith CJ, et al (2007) Diatom-derived carbohydrates as factors affecting bacterial community composition in estuarine sediments. Appl Environ Microbiol 73:6112–6124. doi: 10.1128/AEM.00551-07

Hermenau R, Ishida K, Hoffmann B, et al (2018) Gramibactin – a bacterial siderophore with a diazeniumdiolate ligand system. Nat Chem Biol

Hider RC, Kong X (2010) Chemistry and biology of siderophores. Nat Prod Rep 27:637. doi: 10.1039/b906679a

Homann VV, Sandy M, Tincu JA, et al (2009) Loihichelins A−F, a suite of amphiphilic siderophores produced by the marine bacterium *Halomonas* LOB-5. J Nat Prod 72:884–888. doi: 10.1021/np800640h

Ito Y, Butler A (2005) Structure of synechobactins, new siderophores of the marine cyanobacterium *Synechococcus* sp. PCC 7002. Limnol Oceanogr 50:1918–1923. doi: 10.4319/lo.2005.50.6.1918

Jutras BL, Verma A, Stevenson B (2012) Identification of novel DNA-binding proteins using DNA-affinity chromatography/pull down. In: Coico R, McBride A, Quarles JM, et al. (eds) Current Protocols in Microbiology. John Wiley & Sons, Inc., Hoboken, NJ, USA, p 1F.1.1-1F.1.13

Kohlmann Y (2015) Charakterisierung des Proteoms von *Ralstonia eutropha* H16 unter lithoautotrophen und anaeroben Bedingungen. Dissertation, Humboldt University of Berlin

Kouzuma A, Watanabe K (2015) Exploring the potential of algae/bacteria interactions. Curr Opin Biotechnol 33:125–129. doi: 10.1016/j.copbio.2015.02.007

Kreutzer MF, Kage H, Nett M (2012) Structure and biosynthetic assembly of cupriachelin, a photoreactive siderophore from the bioplastic producer *Cupriavidus necator* H16. J Am Chem Soc 134:5415–5422. doi: 10.1021/ja300620z

Kümmerli R, Schiessl KT, Waldvogel T, et al (2014) Habitat structure and the evolution of diffusible siderophores in bacteria. Ecol Lett 17:1536–1544. doi: 10.1111/ele.12371

Kurth C, Kage H, Nett M (2016a) Siderophores as molecular tools in medical and environmental applications. Org Biomol Chem 14:8212–8227. doi: 10.1039/C6OB01400C

Kurth C, Schieferdecker S, Athanasopoulou K, et al (2016b) Variochelins, lipopeptide siderophores from *Variovorax boronicumulans* discovered by genome mining. J Nat Prod 79:865–872. doi: 10.1021/acs.jnatprod.5b00932

Liao CH, McCallus DE, Wells JM, et al (1996) The *repB* gene required for production of extracellular enzymes and fluorescent siderophores in *Pseudomonas viridiflava* is an analog of the *gacA* gene of *Pseudomonas syringae*. Can J Microbiol 42:177–182

Livny J, Waldor MK (2007) Identification of small RNAs in diverse bacterial species. Curr Opin Microbiol 10:96–101. doi: 10.1016/j.mib.2007.03.005

Lowry R (2018) VassarStats: Website for statistical computation

Martin JD, Ito Y, Homann VV, et al (2006) Structure and membrane affinity of new amphiphilic siderophores produced by *Ochrobactrum* sp. SP18. JBIC J Biol Inorg Chem 11:633–641. doi: 10.1007/s00775-006-0112-y

Martinez JS (2000) Self-assembling amphiphilic siderophores from marine bacteria. Science 287:1245–1247. doi: 10.1126/science.287.5456.1245

Massé E, Salvail H, Desnoyers G, Arguin M (2007) Small RNAs controlling iron metabolism. Curr Opin Microbiol 10:140–145. doi: 10.1016/j.mib.2007.03.013

Niehus R, Picot A, Oliveira NM, et al (2017) The evolution of siderophore production as a competitive trait: The competitive evolution of siderophores. Evolution 71:1443–1455. doi: 10.1111/evo.13230

Papenfort K, Vogel J (2009) Multiple target regulation by small noncoding RNAs rewires gene expression at the post-transcriptional level. Res Microbiol 160:278–287. doi: 10.1016/j.resmic.2009.03.004

Robertson AW, McCarville NG, MacIntyre LW, et al (2018) Isolation of imaqobactin, an amphiphilic siderophore from the arctic marine bacterium *Variovorax* species RKJM285. J Nat Prod

Schalk IJ, Guillon L (2013) Fate of ferrisiderophores after import across bacterial outer membranes: different iron release strategies are observed in the cytoplasm or periplasm depending on the siderophore pathways. Amino Acids 44:1267–1277. doi: 10.1007/s00726-013-1468-2

Schindelin J, Arganda-Carreras I, Frise E, et al (2012) Fiji: an open-source platform for biological-image analysis. Nat Methods 9:676–682. doi: 10.1038/nmeth.2019

Schwartz E, Henne A, Cramm R, et al (2003) Complete nucleotide sequence of pHG1: A *Ralstonia eutropha* H16 megaplasmid encoding key enzymes of H_2-based lithoautotrophy and anaerobiosis. J Mol Biol 332:369–383. doi: 10.1016/S0022-2836(03)00894-5

Seymour JR, Amin SA, Raina J-B, Stocker R (2017) Zooming in on the phycosphere: the ecological interface for phytoplankton–bacteria relationships. Nat Microbiol 2:17065. doi: 10.1038/nmicrobiol.2017.65

Shevchenko A, Wilm M, Vorm O, Mann M (1996) Mass spectrometric sequencing of proteins from silver-stained polyacrylamide gels. Anal Chem 68:850–858. doi: 10.1021/ac950914h

Stintzi A, Evans K, Meyer J, Poole K (1998) Quorum-sensing and siderophore biosynthesis in *Pseudomonas aeruginosa: lasRllasI* mutants exhibit reduced pyoverdine biosynthesis. FEMS Microbiol Lett 166:341–345. doi: 10.1111/j.1574-6968.1998.tb13910.x

Watnick PI, Eto T, Takahashi H, Calderwood SB (1997) Purification of *Vibrio cholerae* Fur and estimation of its intracellular abundance by antibody sandwich enzyme-linked immunosorbent assay. J Bacteriol 179:243–247

Wichard T (2016) Identification of metallophores and organic ligands in the chemosphere of the marine macroalga *Ulva* (Chlorophyta) and at land-sea interfaces. Front Mar Sci 3:. doi: 10.3389/fmars.2016.00131

497 TABLE 1. Plasmids used in this study and their features and origin.

Plasmid	**Features**	**Origin**
pRANGER-BTB-3	pBBR1, *cat*, *araC*	Lucigen
pMLB1034	pMB1, *bla*, *lacZ*	ATCC
pGEX-6P-2	pBR322, *bla*, *tacp*	GE Healthcare Life Sciences
pCK01	pBBR1, *cat* (pRANGER-BTB-3 without *araC*)	This study
pCK02	pBBR1, *cat*, *lacZ* (without promoter)	This study
pCK03	pBBR1, *cat*, *lacZ* with arabinose-inducible promoter *araBp*	This study
pCK04	pBBR1, *cat*, *lacZ* with artificial promoter *tacp*	This study
pCK05	pBBR1, *cat*, *lacZ* with cupriachelin biosynthesis gene promoter *cucJp*	This study

498

Figure captions

Fig. 1 Proposed mutualistic photoreactive siderophore-based iron sharing between bacteria and algae. *C. necator* H16 secretes cupriachelin under iron-deficient conditions. The ferrisiderophore will likely be taken up by *C. necator* H16 in the dark. In the light, however, the ferrisiderophore will undergo photolytic cleavage, thereby releasing Fe^{2+} into the environment. The solubilized iron is then also available to the surrounding planktonic community (e.g., *N. pelliculosa*). In exchange for the iron, the alga may provide the bacterium with dissolved organic carbon (DOC).

Fig. 2 (A) β-Galactosidase activity of *C. necator*:pCK05 on three successive days after inoculation in H-3 mineral medium with different iron concentrations. The values represent the means and standard deviations for samples tested in triplicates. Statistical significance was assessed via one-way ANOVA with Tukey´s post hoc test ($P<0.05$) for every day comparison. Statistical differences are denoted by different letters within each day. (B) β-Galactosidase activity of *C. necator*:pCK05 on the second day after inoculation in H-3 mineral medium plotted against iron concentration in the medium. The values represent the means and standard deviations for samples tested in triplicates. The β-glactosidase activity was significantly (t-test, $P < 0.05$) different at low iron (1 μM) compared to replete conditions (10 μM).

Fig. 3 β-Galactosidase activity of *C. necator*:pCK05 on days 3 and 4 after inoculation in a 1:1 mixture of H-3 mineral medium and culture supernatant of *N. pelliculosa* grown under iron starvation (0.15 μM; grey bar) or iron replete conditions (10 μM; black bar) or modified WC medium (control; white bar). The values represent means and standard deviations of nine replicates (each of three algal culture supernatants distributed amongst triplicate reporter strains). Statistical significance was assessed via one-way ANOVA with Tukey´s post hoc test ($P<0.05$) for every day comparison. Statistical differences are denoted by different letters within each day.

Fig. 4 SDS-PAGE of proteins of the DNA-protein pulldown assays performed with *C. necator* H16 grown with culture supernatant of *N. pelliculosa* (s) or with medium (c). E1 and E2 refer to eluates with increasing NaCl concentrations (200 mM and 300 mM, respectively). Protein bands clearly visible in the supernatant samples (s), but less pronounced medium samples (c), or vice versa were subjected to MALDI-TOF/TOF MS analysis (see arrows). The identified proteins are given in the table below. PageRuler Unstained Protein Ladder (Thermo Fisher Scientific) was used as marker (M). The numbers indicate protein masses in kDa.

531 **Figure 1.**

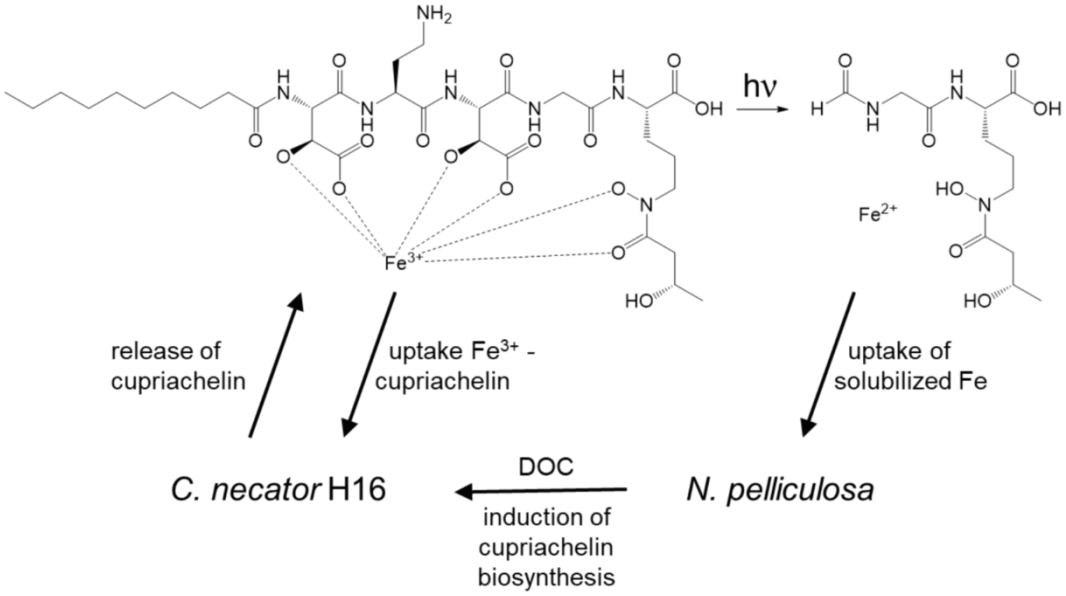

532

533

534 **Figure 2.**

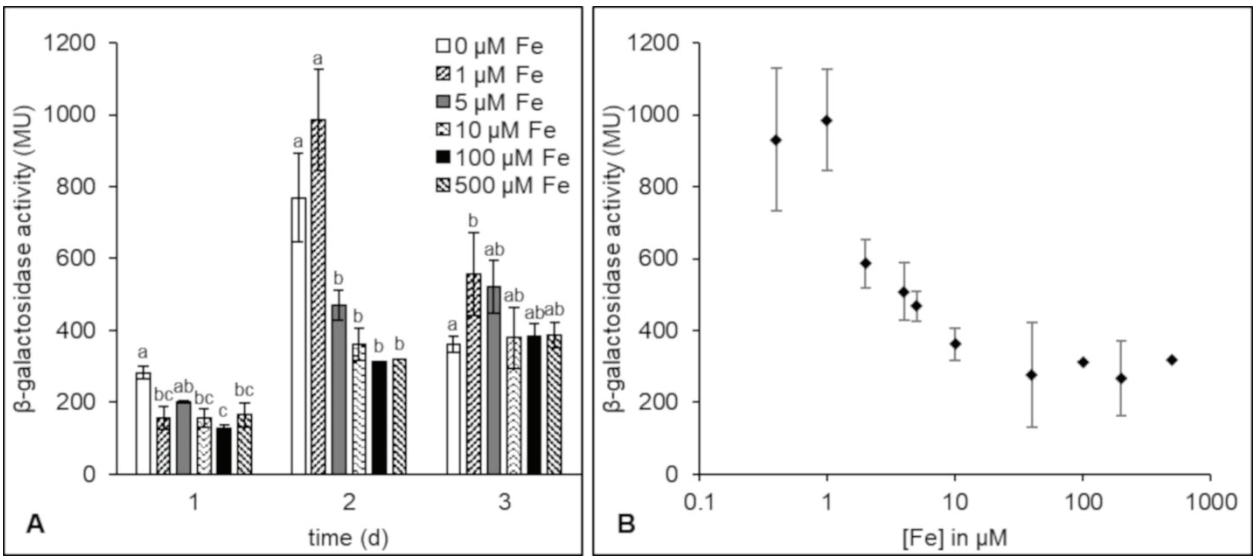

535

Figure 3.

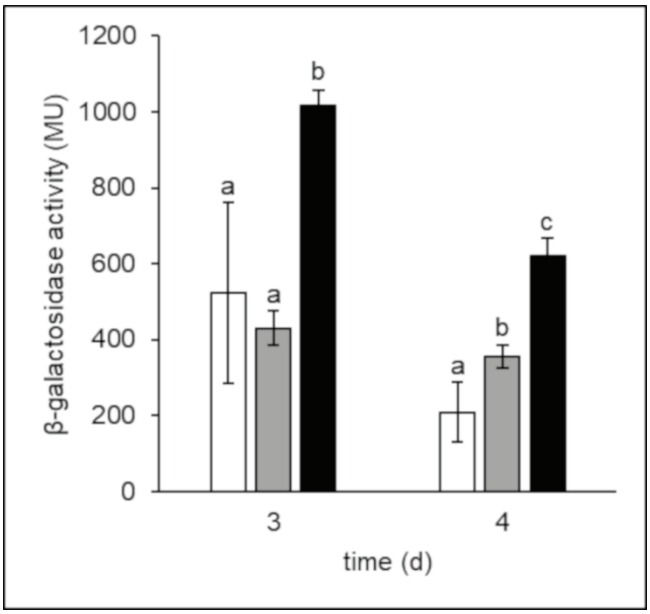

Figure 4.

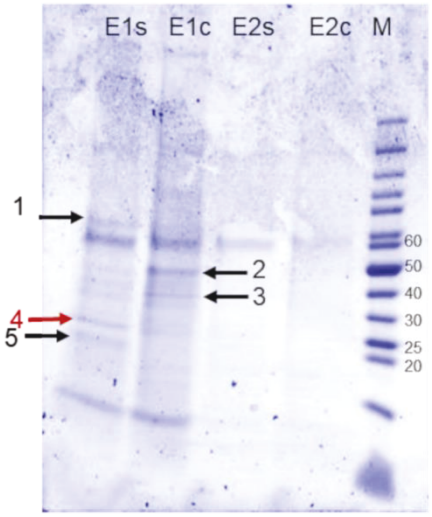

No.	Identified protein (accession no.)	MW [kDa]
1	Dihydrolipoyl dehydrogenase (WP_011615030.1)	62.1
2	Dihydroorotase (KUE90283.1)	45.3
3	Aspartate carbamoyltransferase (Q0K7N2.1)	35.3
4	Response regulator NarL family (AEI76745.1)	23.4
5	Hypothetical protein ASL20_18650 (KUE87334.1)	20.4

541 Algae Induce Siderophore Biosynthesis in the Freshwater Bacterium *Cupriavidus necator*

542 H16

543

544 Colette Kurth,[a] Ina Wasmuth,[b] Thomas Wichard,[b] Georg Pohnert,[b] and Markus Nett[c]#

545

546 [a]Leibniz Institute for Natural Product Research and Infection Biology, Hans Knöll Institute,

547 Beutenbergstr. 11a, 07745 Jena, Germany

548 [b]Institute of Inorganic and Analytical Chemistry, Friedrich Schiller University, Lessingstrasse

549 8, D-07743 Jena, Germany

550 [c]Department of Biochemical and Chemical Engineering, Laboratory of Technical Biology,

551 TU Dortmund University, Emil-Figge-Strasse 66, 44227 Dortmund, Germany

552

553

554 Table of contents

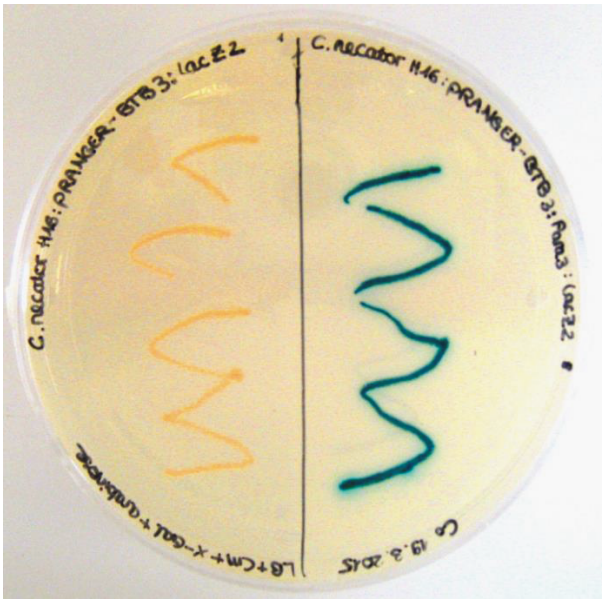

Fig. S1 *C. necator* H16 control strains for β-galactosidase activity. When plated on LB agar containing 10 mM arabinose and 0.1 mg/mL X-Gal, *C. necator* H16:pCK02 forms white colonies (left), while *C. necator* H16:pCK03 forms blue colonies (right). The blue color indicates β-galactosidase activity and thus confirms the functionality of *lacZ* as reporter gene in *C. necator* H16.

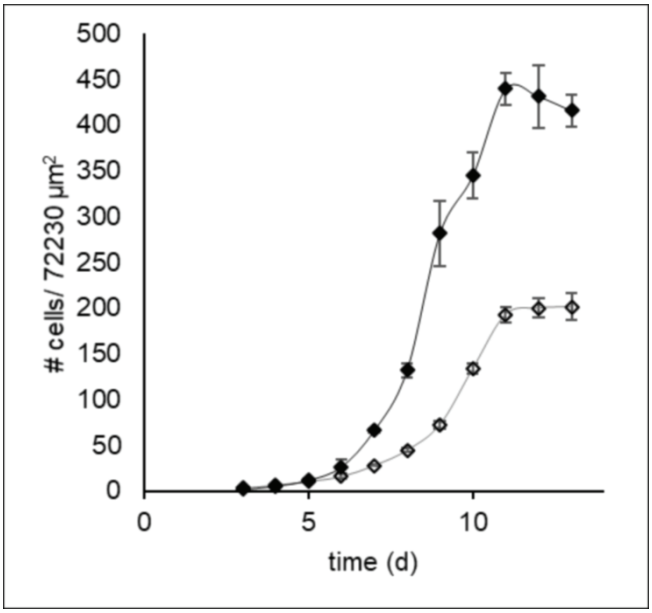

Fig. S2 Growth curve of *N. pelliculosa* grown under iron-limited (0.15 µM Fe; white diamonds) and iron-replete (10 µM; black diamonds) conditions. The values represent means and standard deviations of triplicates.

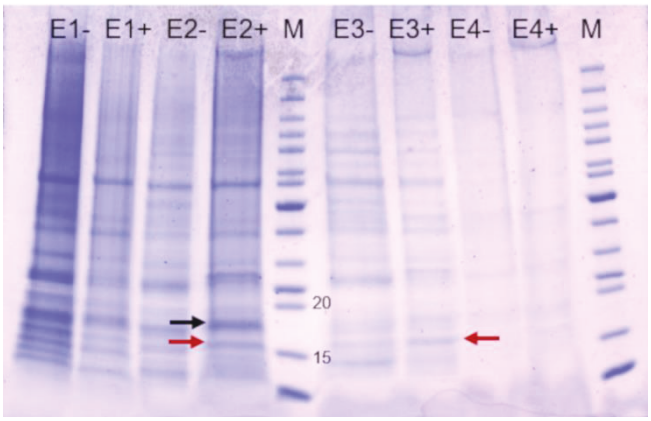

Fig. S3 SDS-PAGE of proteins of the DNA-protein pulldown assays performed with *C. necator* H16 grown without (-) and with 190 µM Fe (+). E1 to E4 indicate the elution steps with increasing NaCl concentrations (200 mM, 500 mM, 750 mM, 1,000 mM, respectively). Proteins between 15 kDa and 20 kDa, the molecular mass of *C. necator* H16 Fur proteins, were analyzed via MALDI-TOF/TOF MS (see arrows). The red arrows denote the protein bands identified as H16_A3143 (Fur). PageRuler Unstained Protein Ladder (Thermo Fisher Scientific) was used as marker (M). The numbers indicate protein masses in kDa.

3.3 Manuscript C

Kurth C, Kage H, Nett M

Siderophores as molecular tools in medical and environmental applications. *Organic & Biomolecular Chemistry* 14 (2016): 8212-8227.

Organic & Biomolecular Chemistry

REVIEW

View Article Online
View Journal | View Issue

CrossMark click for updates

Cite this: *Org. Biomol. Chem.*, 2016, **14**, 8212

Siderophores as molecular tools in medical and environmental applications

Colette Kurth,[a] Hirokazu Kage[b] and Markus Nett*[b]

Received 28th June 2016,
Accepted 29th July 2016

DOI: 10.1039/c6ob01400c

www.rsc.org/obc

Almost all life forms depend on iron as an essential micronutrient that is needed for electron transport and metabolic processes. Siderophores are low-molecular-weight iron chelators that safeguard the supply of this important metal to bacteria, fungi and graminaceous plants. Although animals and the majority of plants do not utilise siderophores and have alternative means of iron acquisition, siderophores have found important clinical and agricultural applications. In this review, we will highlight the different uses of these iron-chelating molecules.

Introduction

Iron is the fourth most abundant element in the Earth's crust. Although it represents a rather soft metal in its pure, equilibrium state, the microstructure of iron can be changed to endow the material with a variety of properties.[1] Due to this plasticity, iron and its alloys are widely used in engineering.[2] In biology, iron plays a pivotal role, which can be largely ascribed to its unique coordination and redox chemistry. The electronic configuration of iron is [Ar] $3d^6 4s^2$, and the two most frequent oxidation states of the transition metal are +2 (d^6) and +3 (d^5), which are also referred to as ferrous and ferric, respectively. Further oxidation states, among them +1, +4 and +5, have been described as reaction intermediates during enzymatic transformations.[3]

The interconversion of iron redox states is the basis for electron transfer processes and the binding of different organic ligands. In protein active sites, mono- or binuclear iron species can be directly coordinated by amino acid residues. As a hard Lewis acid, ferric iron (Fe^{3+}) favours hard-base ligands such as charged oxygen atoms from the side chains of aspartate and glutamate. In contrast, ferrous iron (Fe^{2+}) represents a Lewis acid on the borderline between hard and soft and thus prefers nitrogen and sulfur ligands, such as histidine, cysteine and methionine. Apart from iron-only centres, metalloenzymes can also possess sulfide-linked iron cofactors (*e.g.*, [2Fe–2S]

[a]*Leibniz Institute for Natural Product Research and Infection Biology, Hans-Knöll-Institute, Adolf-Reichwein-Str. 23, D-07745 Jena, Germany*
[b]*Technical University Dortmund, Department of Biochemical and Chemical Engineering, Technical Biology, Emil-Figge-Str. 66, D-44227 Dortmund, Germany. E-mail: markus.nett@bci.tu-dortmund.de; Tel: +49 231 755 4742*

Colette Kurth

Colette Kurth was born in Gelsenkirchen, Germany, in 1988. She received her B.Sc. degree in Biology from the Ruhr University of Bochum in 2012 in the group of Professor Dominik Begerow. Colette continued her M.Sc. studies at the Friedrich Schiller University Jena. There, she joined the research group of Professor Markus Nett. Her PhD project is integrated in the Jena Collaborative Research Centre Chemical Mediators in Complex Biosystems *and deals with photoreactive siderophores from freshwater bacteria.*

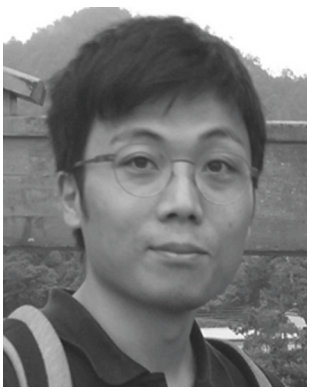

Hirokazu Kage

Hirokazu Kage received his PhD from the Graduate School of Medical and Pharmaceutical Sciences of Chiba University, Japan, in 2009. He became a postdoctoral fellow of the Jena School for Microbial Communication and continued his research studies with Professor Markus Nett at the Leibniz Institute for Natural Product Research and Infection Biology. In 2016, he moved to the Technical University Dortmund. His main research interests are in the field of biosynthesis with a particular focus on siderophore pathways.

and [4Fe–4S] clusters) or iron porphyrin complexes, the so-called heme groups.[4] Since the ligand environment influences the electronic spin state and redox potential in both ferric and ferrous forms, iron represents an extremely versatile prosthetic component. Fundamental biological pathways including respiration, photosynthesis, nitrogen fixation, and methanogenesis depend on iron-containing proteins for the transport and storage of oxygen, electron transfer, as well as substrate oxidation and reduction.[5]

In the early history of life, the use of iron in biological processes was likely favoured by its general availability and chemical properties. Since then, however, Earth underwent dramatic changes. With the onset of photosynthesis, the oxygen levels in the atmosphere began slowly to rise, as the oxygen was initially being depleted by the oxidation of methane and metals. The surface iron was converted from the relatively soluble ferrous state (0.1 M at pH 7.0) to the extremely insoluble ferric form (10^{-18} M at pH 7.0). Organisms now living in aerobic environments had to learn to cope with a rather low pool of bioavailable iron while still satisfying their need for this life-sustaining metal. Simultaneously, the uptake of the transition metal had to be tightly regulated to prevent excess accumulation and a Fenton-induced radical damage.[6]

Iron homeostasis can be achieved by different means. A common strategy of bacteria,[7] fungi[8] and even some plants[9] involves the secretion of small molecules that coordinate ferric iron with high affinity. Once such an iron carrier or siderophore has bound the metal ion, the resulting complex is actively transported back into the cell, where the coordinated ion is released by a reductive or hydrolytic mechanism.[10] In recent years, evidence has accumulated that siderophores not only maintain cellular iron levels, but also fulfil additional biological functions, be it the structuring of microbial communities,[11,12] or the suppression of host defense mechanisms, which has been reported for pathogenic siderophore producers.[13,14]

This review is intended to give readers an overview of the chemistry and biosynthesis of siderophores. Furthermore, we will present the different applications that siderophores have found in recent years. Potential uses that are not exploited yet will also be discussed in order to highlight possible directions in which siderophore research is currently heading.

Chemistry of siderophores

High affinity and selectivity for the binding of ferric iron are important criteria, which must be met by a siderophore to exert its biological function. Since negatively charged oxygen atoms establish extremely tight interactions with Fe^{3+}, it is no surprise that catecholates, hydroxamates and α-hydroxycarboxylates, which each feature two oxygen donor atoms, are frequent constituents of siderophores. Bidentate ligands, involving nitrogen or sulfur as donor atoms, do also occur but exhibit a lower selectivity.[15] Siderophores featuring such moieties are therefore often less restrictive when it comes to the complexation of metal ions other than ferric iron.[16]

Chelate effects maximize the stability of Fe^{3+}-siderophore complexes. In water, ferric ions spontaneously form octahedral $Fe(H_2O)_6^{3+}$ complexes. As the full displacement of the six coordinated water molecules by a single hexadentate ligand is greatly favoured in terms of entropy, many siderophores possess six possible coordination sites. The respective donor atoms are typically distributed over three bidentate ligand groups and have been integrated into a conformationally restrained scaffold that adopts an octahedral or pseudooctahedral geometry around the Fe^{3+} centre (Fig. 1).[19] Although hexadentate siderophores prevail in Nature, ligands with less than six coordination sites are not uncommon. Since single molecules of the latter are unable to satisfy the preferred octahedral geometry of Fe^{3+}, coordination of the metal ion can involve bi- and multinuclear complexes.[20] Still, hexadentate ligands can be expected to form more stable Fe^{3+} complexes by virtue of the entropic contribution. This is also reflected in their high iron affinities. The affinities of different siderophores for Fe^{3+}

Markus Nett

After studying pharmacy at the University of Bonn, Markus Nett joined the group of Professor Gabriele König, where he was working on the structure elucidation of natural products. Upon completion of his PhD, he became a postdoctoral fellow of Professor Bradley Moore at the Scripps Institution of Oceanography in La Jolla. In 2009, he started his independent research at the Leibniz Institute for Natural Product Research and Infection Biology in Jena. Since 2016, he has been a Professor of Technical Biology at the Technical University Dortmund. His research focuses on the analysis and engineering of bacterial biosynthetic pathways.

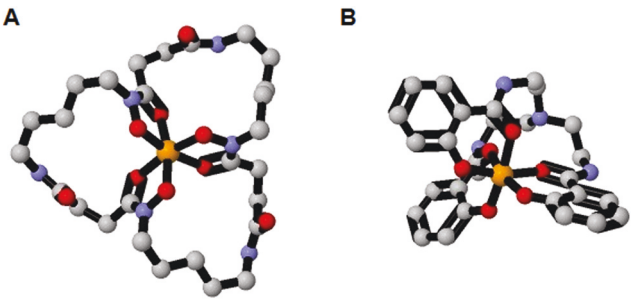

Fig. 1 Ball-and-stick structures of the Fe^{3+} complexes of ferrioxamine E (A) and a model tris-salicylate ligand (B). Crystallographic data were obtained from the Cambridge Structural Database (CCDC # 1154884 and 102066, respectively).[17,18]

are usually compared on the basis of their complex formation constants (K_f values), which can range over 30 orders of magnitude.[21] Care has to be taken in the interpretation of these data considering the differences in the pH sensitivity of Fe^{3+}-siderophore complexes.[22] Metal chelation competes with the protonation of the donor atoms and, thus, depends on the pH of the environment and the pK_a values of the ligands. Donors with low pK_a values, such as carboxylates, are more efficient iron chelators in an acidic environment (pH 3.0 to 5.0), where catecholates and hydroxamates are still fully protonated. At higher pH, however, the situation reverses.[23] Therefore, the pH-dependent pFe parameter, which is defined as the negative decadic logarithm of the free ferric iron concentration, generally enables a more reliable assessment of the iron affinity.[17] It must be noted that the iron affinity of a siderophore is also connected with the redox potential of the coordinated ferric iron. By approximation, a higher pFe value will come along with a more negative redox potential.[15] The latter value is a good means to estimate the selectivity of a siderophore for ferric iron over ferrous iron. Furthermore, the redox potential has direct implications for the cellular release mechanism of the coordinated metal ion, especially whether a reduction with biological reducing agents, such as NAD(P)H or flavins, is possible.[23]

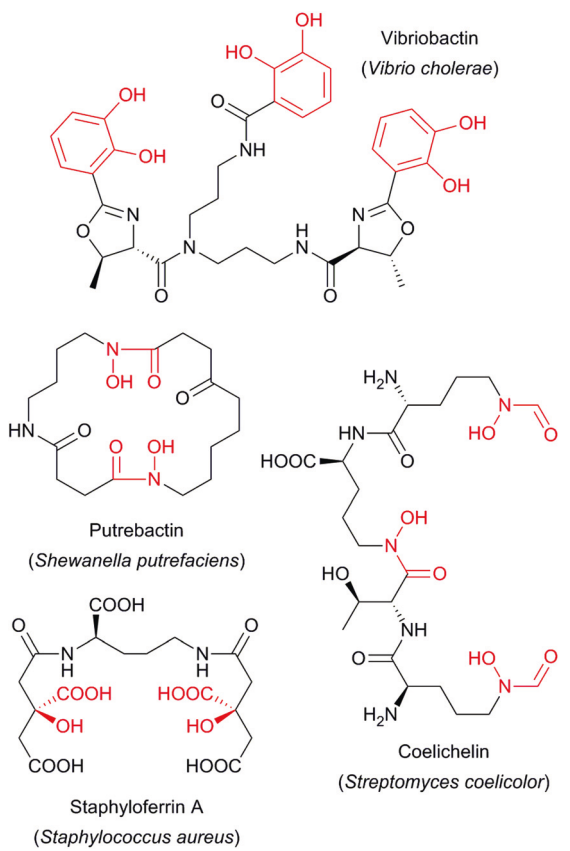

Fig. 2 Selected examples of catecholate, hydroxamate and α-hydroxycarboxylate siderophores. The respective ligand groups are highlighted in red. The producing organisms are set in parentheses.

Structurally, siderophores show an enormous diversity, which results from the many possible combinations of ligand groups and the variations in their linkages. While some siderophores exclusively possess catecholate, hydroxamate, or α-hydroxy-carboxylate residues as ferric chelating groups, many others exhibit mixtures of different ligands. These functions can be incorporated in both linear and cyclic structures (Fig. 2). The heterogeneity of siderophores together with the evolution of specialized uptake systems underlines the competitive nature of iron acquisition as well as an environment-dependent specialisation.

Biosynthesis of siderophores

The production of a siderophore requires the preparation of suitable ligand groups and their incorporation into a larger molecular scaffold that can accommodate a ferric ion. For this, the structural backbone must integrate defined spacer groups to support the creation of an octahedral binding site. The biosynthetic linkage of ligand and spacer groups typically involves amide or ester bond formations. Prior to introducing the enzymes that are responsible for catalysing the latter reactions, we will first take a closer look at the origin of the different ferric chelating groups.

The most commonly used catechol-containing precursor in siderophore biosynthesis is 2,3-dihydroxybenzoate (DHBA). It is derived from the shikimate pathway with chorismate representing the relevant branching point. An enzyme known as isochorismate synthase catalyses a 1,5-double-S_N2 displacement of the 4-hydroxyl group in chorismate with water. The product of this reaction is then subjected to a hydrolytic cleavage of its enolpyruvyl group, before an alcohol dehydrogenase converts the cyclohexadienone intermediate into the more stable aromatic catechol.[24] Hydroxamate residues are usually made from lysine or ornithine moieties. In a two-step conversion, the side chain amino group is first oxidized by a flavin adenine dinucleotide (FAD)-dependent monooxygenase to give an intermediary hydroxylamine and, subsequently, acylated by an acyl coenzyme A transferase.[25] Compared to the DHBA and hydroxamate pathways, the preparation of α-hydroxycarboxylates is even less complex. Citrate, which features an α-hydroxycarboxylate moiety, is a ubiquitous intermediate in the TCA cycle and can be readily recruited for siderophore production, as exemplified in aerobactin biosynthesis.[25] In addition, the reduction of α-ketoglutarate and the hydroxylation of aspartic acid provide access to alternative α-hydroxycarboxylate building blocks.[26,27] Another ligand that is particularly widespread in bacterial siderophores is salicylate. The phenolate moiety is typically linked to a nitrogen heterocycle ligand, *e.g.* a thiazoline or an oxazoline. With a single exception,[28,29] the salicylate building block is derived from isochorismate by the loss of pyruvate.[30]

The assembly of the siderophore backbone is carried out by either of two distinct enzyme classes, namely nonribosomal peptide synthetases (NRPS) or NRPS-independent siderophore

(NIS) synthetases. The former are large proteins that exhibit a modular organisation and follow a thiotemplate-based enzymatic logic.[31] From a biosynthetic perspective NRPS modules can be regarded as discrete functional units, each of which is responsible for the attachment of a single amino acid to the growing peptide chain. To fulfil this function, every NRPS harbors a defined set of catalytic domains. An adenylation (A) domain acts as a gatekeeper by selecting the correct substrate for incorporation. It activates the respective amino acid using ATP and covalently tethers the resulting acyl adenylate (Fig. 3A). The required docking site is located in a peptidyl carrier protein (PCP) domain and must have undergone a phosphopantetheinylation in order to provide an active thiol group for the binding of the amino acid. The intrinsic chain elongation is eventually carried out by a condensation (C) domain. It catalyzes an amide bond formation between the peptidyl-S-PCP of the preceding module and the aminoacyl-S-PCP of the active module. Since the aminoacyl-S-PCP serves as the attacking, acceptor substrate, the extension of the peptide chain also involves its translocation. After the condensation reaction, the new peptidyl-S-PCP is ready for another elongation cycle by the C domain of the following module (Fig. 3B).[31]

In addition to the essential C, A and PCP domains, NRPS modules can possess further domains, which contribute to the structural diversity of NRPS-derived siderophores. Examples include methyltransferase (MT) domains, as well as epimerization (E) domains, which invert the configuration of the amino acid monomers at their α-carbon atoms. The presence of D-amino acids not only increases the proteolytic stability of a peptidic siderophore, but is often also important for conformational reasons to enable the binding of ferric iron. Occasionally, the C domain is replaced by a cyclization (Cy) domain in cysteine, serine or threonine-selecting modules. Upon amide bond formation, the bifunctional Cy domain catalyses an intramolecular cyclodehydration that gives rise to thiazoline or oxazoline rings. Further redox adjustments of these heterocycles are achieved through the catalytic action of oxidase (Ox) or reductase (Red) domains. A thioesterase (TE) domain terminates the biosynthesis by hydrolysing the thioester-bound compound from the enzyme. Alternatively, a reductive chain release is possible.[32]

Recent studies on the bacterial siderophores pyoverdine and pyochelin suggest a clustering of their NRPS biosynthetic enzymes in the immediate vicinity of the cytoplasmic membrane.[33,34] It has been proposed that this type of cellular organisation facilitates the transfer of siderophore intermediates as well as the secretion of the final product.[35] Similar observations were made in fungi, where siderophore biosynthesis is localised in peroxisomes.[36]

Unlike NRPS, NIS synthetases are autonomously acting enzymes that utilise free intermediates as substrates. In an ATP-driven reaction, they first convert a selected carboxylic acid into an acyl adenylate. Afterwards, an amine or alcohol substrate displaces adenosine monophosphate from the adenylate *via* an S_N2-type mechanism to give an amide or ester.[37] Although the substrate activation of NIS synthetases is reminiscent of NRPS adenylation domains, the respective proteins are structurally different.[38] Sequence analyses revealed that NIS synthetases fall into three main families, corresponding to their carboxylic acid substrate preferences. While type A enzymes are specific for citric acid, type B enzymes utilise α-ketogluaric acid as a substrate. On the other hand, type C enzymes catalyse condensation reactions of citric or succinic acid-derivatives.[25]

Medical applications

Due to their metal binding properties, siderophores are promising agents for medical applications. Starting with the treatment of iron overload, we will introduce possible pharmacological targets and therapeutic fields for siderophores.

Siderophores in iron chelation therapy

Iron is an essential element for sustaining biological processes, but an excess accumulation must be prevented, as it can cause severe health problems. The human body stores between 3 and 4 g of iron, which is largely bound to porphyrin in heme-containing proteins, such as hemoglobin, myoglobin and ferritin, or to cysteinyl sulfur in Fe–S complexes. Iron mobilized from the tissue storage pool is distributed in the body by the plasma protein transferrin, which is normally only 25–50% saturated with the metal. Due to the low solubility of iron, homeostasis cannot exclusively be maintained by excretion. Rather, the iron uptake needs to be tightly regulated so that it approximates the physiological losses. The balance between iron absorption from diet and iron excretion from the body is kept around 1 to 2 mg a day.[39] Therefore, regular blood infusions can put a patient at the risk of iron overload.

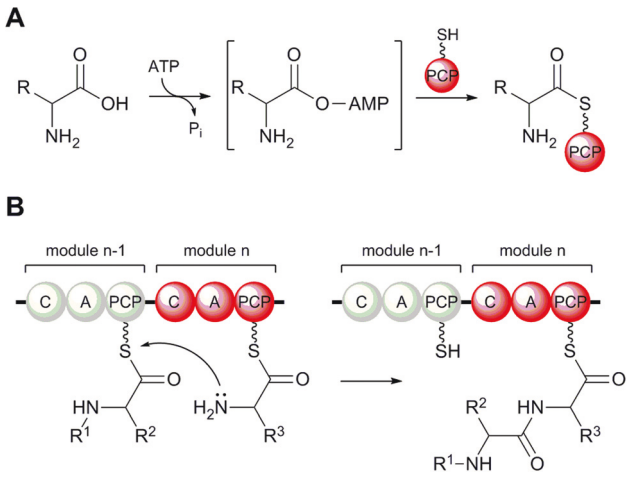

Fig. 3 ATP-driven activation of an amino acid substrate and tethering of the resulting aminoacyl adenylate to a peptidyl carrier protein domain (A). Reaction catalysed by an NRPS condensation domain (B).

In particular the non-transferrin-bound plasma iron, is highly redox-active and promotes the formation of reactive oxygen species (ROS) by the Fenton reaction.[40,41] This ROS generation causes cell impairment in the body, ultimately resulting in fatal organ failures. To prevent these undesired side-effects, excess plasma iron must be removed. The treatment of transfusion-dependent patients thus often involves an accompanying iron chelation therapy.[42]

Desferrioxamine B (DFO, Fig. 4), a hydroxamate-based siderophore originally isolated from *Streptomyces pilosus*,[43] was the first agent to be used for the treatment of iron overload in the early 1960s,[44] and is also included in the WHO list of essential medicines.[45] Owing to its low oral availability, DFO must be administered intravenously or subcutaneously.[42] Moreover, the siderophore is rapidly metabolized,[46] has a short half-life in blood plasma and, thus, requires repeated dosing each day.[42] These unfavourable properties have led to the development of improved drugs for clinical use, namely deferiprone (DFP) and deferasirox (DFX). The two synthetic iron chelators are given orally and they also exhibit an increased half-life as well as improved cell permeability in comparison with DFO.[42] Interestingly, the combination of DFO and DFP was found to be superior to a monotherapy of either drug, and significantly decreased a patient's mortality.[47] It has been speculated that the additive or even synergistic effect of DFO and DFP could be due to a shuttle mechanism. According to this theory, DFP would be responsible for removing cellular iron, which is subsequently forwarded to DFO for excretion in urine or feces.[48]

Recently, a novel promising iron-chelator, deferitazole, has entered phase 1 and phase 2 clinical trials.[49] Deferitazole might possess an even larger therapeutic window than DFP and DFX. Noteworthily, its structure was inspired by the naturally occurring siderophore desferrithiocin.[50,51]

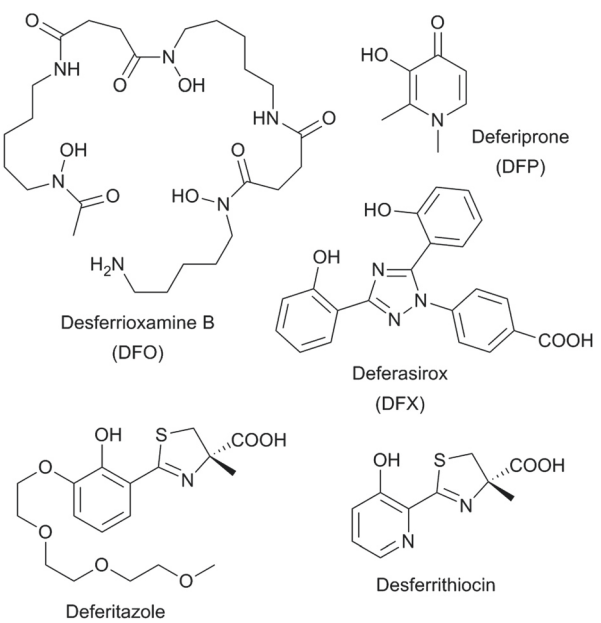

Fig. 4 Compounds used in iron chelation therapy, as well as the new drug candidate deferitazole and its natural product template, desferrithiocin.

Siderophores as antibiotic carriers

Sideromycins are antibiotic conjugates, in which the active warhead is covalently linked with a siderophore moiety. The term "sideromycin" was introduced by Zähner *et al.* in 1960,[52] although the discovery of the first member of this compound class dates back to 1947, when Reynolds and coworkers isolated an antibacterial compound named "grisein" from a strain of *Streptomyces griseus*.[53] Later it turned out that grisein was structurally identical to the sideromycin, albomycin, from *Actinomyces subtropicus*.[54,55] Further naturally occurring sideromycins are ferrimycin, danomycin, salmycin, and MccE492m (Fig. 5).[56–59] Exploiting the natural transporter systems for siderophores, sideromycins gain entry to bacterial cells. During the uptake, the antibiotic is typically cleaved off from the siderophore moiety *via* hydrolysis of an ester or amide bond in the linker region.[60] In the case of salmycins, however, the drug release was proposed to occur *via* an intramolecular cyclisation process upon iron reduction.[61] Irrespective of the mechanism involved, the cleavage step is crucial for the activation of the antibiotic.[60] The smart delivery system of sideromycins, which has also been referred to as a 'Trojan horse' strategy, can dramatically reduce the inhibitory concentration of an antibiotic.[62,63] This advantageous property as well as the possibility to bypass bacterial resistance due to enhanced antibiotic uptake has inspired the synthetic design of new siderophore-based antibiotics. For this, two different strategies have been pursued, *i.e.*, the replacement of the antibiotic in a naturally occurring sideromycin or, alternatively, the *de novo*-design of a sideromycin, involving an unprecedented combination of siderophore and antibiotic moieties.[64–68]

In the following, the focus shall be placed on the latter approach, because it enables the development of narrow-range therapeutic agents, which integrate selected antibiotics and pathogen-specific siderophores as carrier molecules. An illustrative example in this context is the generation of a mycobactin–artemisinin conjugate (Fig. 6).[69] A synthetic analogue of mycobactin T, a siderophore produced by *Mycobacterium tuberculosis*,[70] provides access to the pathogen's cell, while artemisinin serves as the antibiotic pharmacophore. Undoubtedly, the plant-derived artemisinin is not a prototypical antibacterial agent, but rather known for its potent antimalarial effects,[71] which are likely triggered by an iron-induced reductive cleavage of its *endo*-peroxide bond.[72] A treatment with artemisinin alone cannot suppress the growth of *M. tuberculosis*. In conjunction with the mycobactin T analogue, however, sufficient iron is transported and released in the mycobacterial cell to evoke its toxicity.

Apart from *M. tuberculosis*, the development of siderophore–drug conjugates for the treatment of *Pseudomonas aeruginosa* infections has received considerable attention, as this

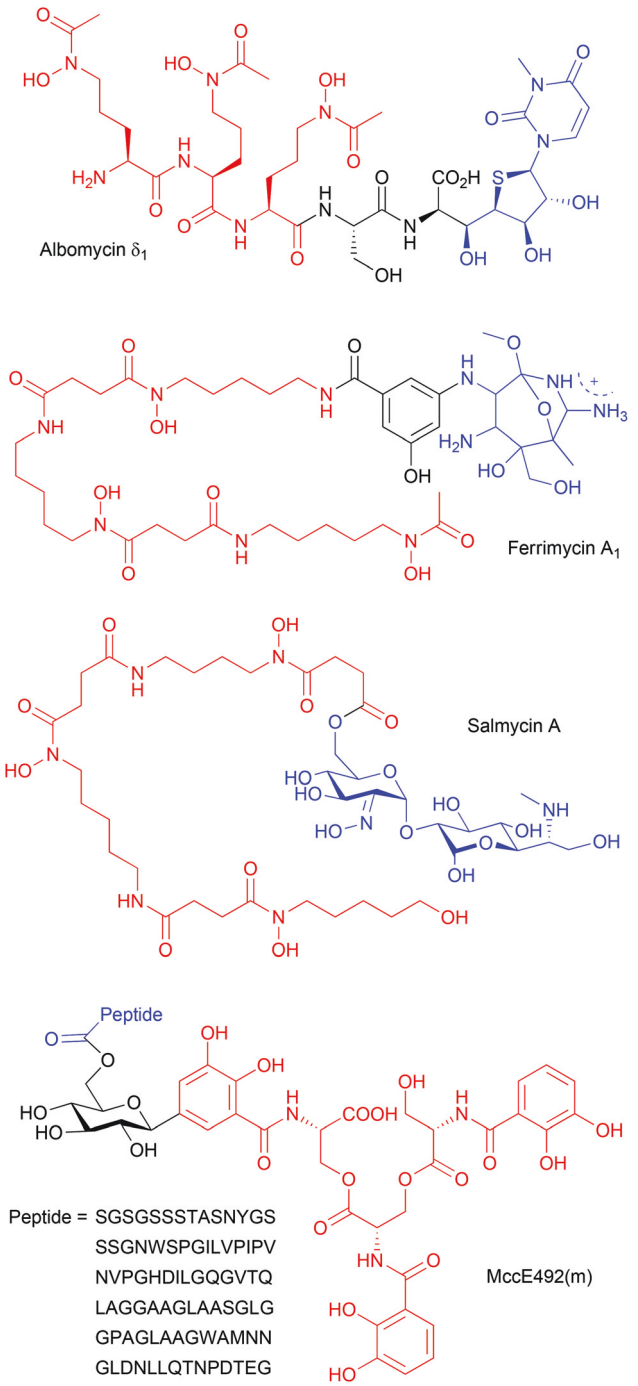

Fig. 5 Chemical structures of natural sideromycins. Siderophore and antibiotic moieties are depicted in red and blue, respectively.

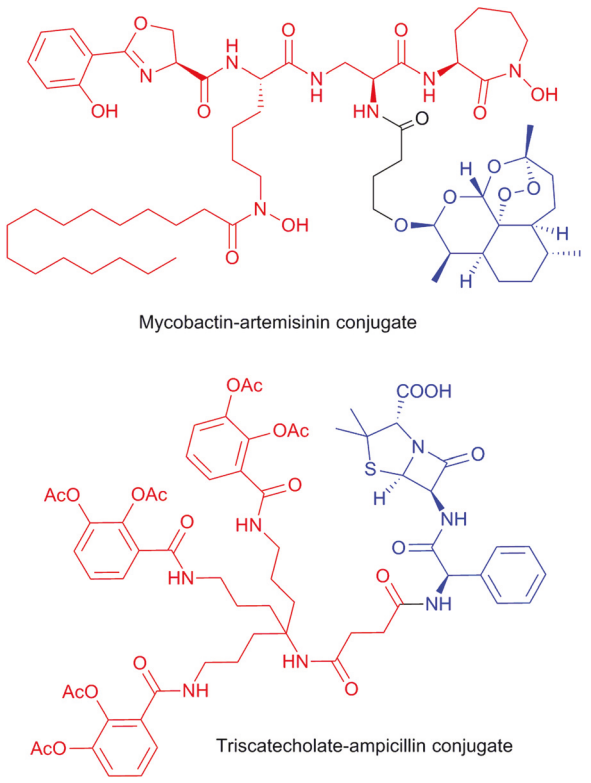

Fig. 6 Examples for artificial sideromycins. Siderophore and antibiotic moieties are depicted in red and blue, respectively.

Gram-negative opportunistic pathogen is intrinsically resistant to most antibiotics.[73] Using natural siderophores from *P. aeruginosa*, namely pyoverdines, as vehicles, it became possible to kill the otherwise β-lactam resistant bacterium with ampicillin.[74] Unfortunately, however, the *P. aeruginosa* strains tested were found to discriminate between different types of pyoverdine siderophores, excluding the development of a broadly applicable conjugate.[74] Much more successful was the approach to link ampicillin (and amoxicillin) with an artificial tris-catecholate siderophore (Fig. 6).[75] The latter serves as a surrogate for enterobactin, which is utilised by *P. aeruginosa*, even though the bacterium does not produce this siderophore on its own.[76] The tested drug conjugates exhibited significant *in vitro* activities against different strains of *P. aeruginosa* with minimal inhibitory concentrations (MICs) ranging from 0.05 to 0.39 μM.[75]

Despite these promising examples it must be noted that many artificial sideromycins were found to be less active against the targeted bacteria than free antibiotics without a conjugated siderophore.[65,66] Recent investigations have provided possible explanations for this inconsistency. First, the linkage of a siderophore to an antibiotic can affect the interaction of the former with its transporter. Consequently, it is possible that the iron-loaded siderophore–antibiotic conjugate is not effectively transported into the cell.[77] Second, some siderophores are known to shuttle iron into the bacterial periplasm.[78] Antibiotics linked to these iron carriers might thus not reach their cytoplasmic target. Third, the antibiotic is not released from the conjugate upon cellular uptake.[79] Its activity will hence decrease due to insufficient target binding. Clearly, these eventualities must be considered when designing non-natural sideromycins. Another challenge not to be forgotten is the rapid resistance development against sideromycins. The fact that most microbial pathogens possess alternative routes for iron acquisition facilitates the spread of mutation-induced

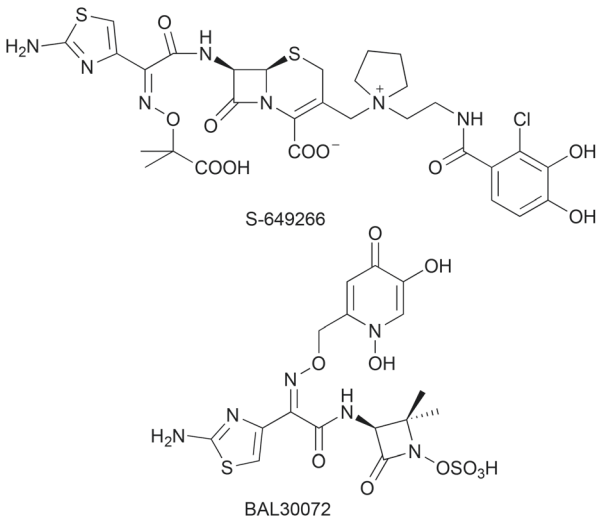

Fig. 7 Siderophore–antibiotic conjugates in clinical trials.

resistance. An interesting concept to overcome such issues was the design of siderophore–antibiotic conjugates with mixed ligand groups. These conjugates are capable of entering bacterial cells through different outer membrane transporters, thereby rendering transport-related resistance development less likely.[80]

Although sideromycins are not used in therapy yet, two siderophore-conjugated β-lactam antibiotics have entered clinical trials (Fig. 7), among them S-649266, a catechol-substituted cephalosporin, which has already reached phase III,[81] and BAL30072, a siderophore monosulfactam in phase I.[82]

Siderophores as inhibitors of metalloenzymes

Nearly half of all proteins found in nature are classified as metalloproteins. These proteins are involved in a number of diverse biological reactions, and their dysregulation is often associated with the onset of diseases, such as cancer, inflammation, hypertension, bacterial and viral infections.[83] The metal centres of metalloproteins serve as cofactors and, in general, have fundamental catalytic functions. It is hence unsurprising that metal binding groups are common motifs in metalloprotein inhibitors, as exemplified by the FDA approved drugs zileuton[84] and vorinostat.[85] The structural diversity of siderophores together with their different degrees of Fe^{3+} specificity make these natural products promising candidates for the identification and design of new drugs targeting metalloproteins.

The zinc-containing matrix metalloproteinases (MMPs) degrade extracellular matrixes as well as other enzymes and play a pivotal role in a number of cellular processes, including cell migration, proliferation, apoptosis and morphogenesis.[86–88] Due to their involvement in inflammatory diseases and certain types of cancer, MMPs have become important therapeutic targets.[89–91] In an early study, microbial siderophores, among them DFO, ferrichrome, and rhodotorulic acid showed a concentration-dependent inhibition of MMP-2, which is possibly involved in tumor cell invasion as well as tissue destruction during periodontitis.[92] Likewise, pyoverdine-type siderophores from *Pseudomonas* spp. were reported as MMP-2 inhibitors.[93,94] The biscatechol myxochelin A (Fig. 8) was originally isolated from the myxobacterium *Stigmatella aurantiaca* upon cultivation under low iron conditions.[95] Later, the siderophore was rediscovered in the culture broths of other bacteria due to its potent antitumoural effects.[96,97] While the antimetastatic properties of myxochelin A could be associated with an inhibition of MMP-2 and MMP-9,[98] the preferential antileukemic activity of the siderophore was traced to an inhibition of human 5-lipoxygenase (5-LO).[97,99] The latter enzyme, whose active site harbours a non-heme iron atom, has a key role in the biosynthesis of leukotrienes. Leukotrienes are generally known as mediators of inflammatory reactions, but are also known to promote the pathogenesis of myeloid leukemia.[100,101]

Apart from 5-LO, class I ribonucleotide reductases (RNRs) are further iron-containing metalloenzymes with a proven role in carcinogenesis.[102] RNRs catalyse the conversion of ribonucleotides into 2′-deoxyribonucleotides, which are necessary building blocks for DNA synthesis and repair. For this, the

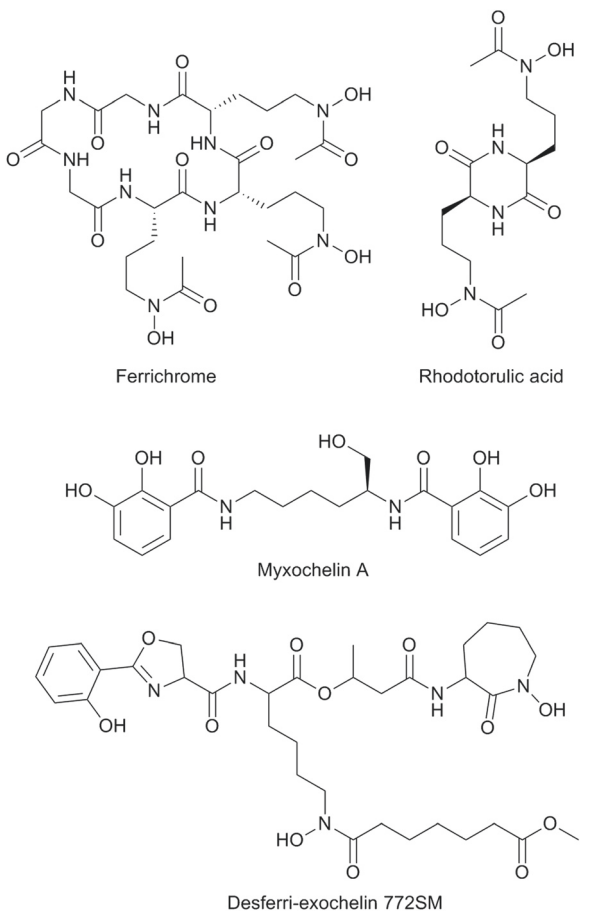

Fig. 8 Structures of selected siderophores inhibiting metalloproteins.

RNR iron centre reacts with molecular oxygen to generate a tyrosyl radical, which then initiates substrate activation. Already more than 20 years ago, the siderophore DFO was supposed to interfere with this reaction.[103–105] Later, the mycobactin-type siderophore desferri-exochelin 772SM was shown to induce apoptosis in breast cancer cell lines due to RNR inhibition.[106,107]

Non-medical applications of siderophores

Siderophores have a great potential for bioremediation of contaminated ecosystems. They can assist in the removal of heavy metals from contaminated areas, enhance the contaminant degradation abilities of microbes or they can be used as biocontrol agents. Other promising fields of application are the recovery of rare earth elements for high-tech applications such as photovoltaics and wind power, as well as surface modifications. These aspects will be discussed in the following sections.

Soil bioremediation

Siderophore-assisted bioremediation has been addressed in a vast number of studies and different approaches have been developed to remove contaminants from soil. Many siderophores have the ability to bind metals other than iron[108] and, in some bacteria, their biosynthesis is even stimulated by different heavy metals.[109–111] Siderophores were found to solubilise heavy metals and make them bioavailable. This can be harnessed in technical applications, where the solubilised heavy metals are concentrated by siderophores and separated from the soil matrix. Different bioreactors have been developed for this purpose.[112] Diels *et al.* reported an up to 16-fold reduction of heavy metals in soil treated in a bioreactor with *Cupriavidus metallidurans*,[112] which is known to produce the citrate siderophore staphyloferrin B.[113] In another study, Nair and colleagues demonstrated the soil-purifying potential of a catecholate-hydroxamate siderophore produced by *Pseudomonas azotoformans*.[114] Washing of As-contaminated soil with the siderophore removed 92.8% of As in comparison with 33.8% removed by washing with medium only. The siderophore was also more potent than EDTA in As-removal and exhibits the further advantage of being environmentally safe. Although the aforementioned soil remediation techniques are highly efficient, they require excavation of the contaminated soil, which is environmentally and economically costly. *In situ* soil bioremediation, in contrast, is less invasive. One possibility is bioaugmentation, *i.e.*, the directed inoculation of microorganisms into contaminated soil. The choice of the microorganism to be used for bioaugmentation is complex and requires consideration of the microbe's metal tolerance, ability to grow in contaminated soil and efficiency to mobilise metals.[115] A major challenge is the persistence and ongoing metal solubilisation ability of the chosen microbe in its new environment.[116] To promote these properties, cells can be immobilised in beads. In this way, the introduced bacterium is protected from predators and competitors. Furthermore, a certain iron deficiency necessary for siderophore production can be guaranteed.[117] Supply of nutrients and buffers within the beads can additionally increase the metal accumulation potential of the strain.[118,119]

Combining bioaugmentation with phytoextraction has recently proven highly beneficial for the remediation of contaminated soil. Siderophore-producing rhizosphere bacteria seem particularly well-suited for bioaugmentation, since they enhance plant growth and metal accumulation in multiple ways. First of all, bacterial siderophores can increase the iron supply of a plant. Phytosiderophores, such as mugineic acid[120] and avenic acid[121] (Fig. 9), may not always be sufficient to satisfy the plant's need for iron, especially in heavy metal-contaminated soils.[122] Some plants are, however, capable of accessing iron from bacterial siderophore complexes by direct uptake, chelate degradation, or ligand exchange reactions.[123] Since many siderophores also bind metals different from iron, they can also increase accumulation of these metals in plants. Braud *et al.* reported that bioaugmentation of polluted soil with *Ralstonia metallidurans* and *Pseudomonas aeruginosa* increased Cr-accumulation in maize plants up to 5.4 times.[119] Similarly, Dimkpa *et al.* found that *Streptomyces tendae* F4 culture filtrates containing siderophores enhanced Cd and Fe uptake in sunflower and promoted plant growth.[124] Siderophore-producing rhizosphere bacteria also indirectly act on plant heavy metal uptake through their effects on plant growth dynamics.[122] For instance, they can lower the level of growth-inhibiting stress ethylene and reduce oxidative stress in plants,[125,126] thereby protecting (microbial) auxins from degradation and resulting in increased plant biomass.[127]

The success of phytoremediation is essentially determined by the amount of plant biomass produced and the heavy metal concentrations in plant tissues.[128] As illustrated by the above examples, both factors can be enhanced by microbial siderophores. Lebeau *et al.* reported that biomass of plants grown on bioaugmented contaminated soil was increased up to four times in the majority of the studies they reviewed.[129] Also the metal concentration within the shoots of these plants was increased by up to three times. Siderophores thus turn out to be highly efficient in solubilising heavy metals, providing

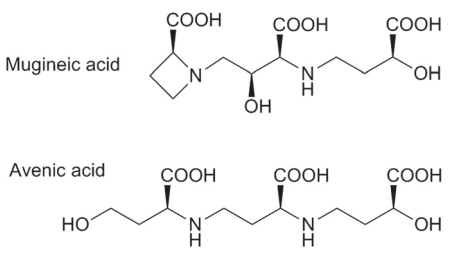

Fig. 9 Phytosiderophores commonly produced by *Graminaceae*.

them to plants and thereby lowering their concentration in the soil environment.

Removal of petroleum hydrocarbons from the marine environment

The influx of hydrocarbons into the ocean is a serious environmental problem and bioremediation is regarded as an effective treatment of petroleum-polluted ocean areas.[130] Siderophores contribute to hydrocarbon biodegradation by supplying the participating microorganisms with iron. Indeed, the availability of nutrients, especially nitrogen, phosphorus and iron, directly affects the rate of hydrocarbon degradation.[131] Numerous studies have reported increased iron requirements of hydrocarbon-degrading bacteria when hydrocarbons are used as the carbon source.[132,133] Further, Sabirova *et al.* found that genes required for alkane oxidation and iron uptake are linked in *Alcanivorax borkumensis*, being exclusively expressed when the bacterium uses alkanes as the carbon source compared to pyruvate.[134] The reason for the increased iron requirement during hydrocarbon degradation is the alkane oxidizing enzymes. AlkB oxidizes the majority of medium- and long-chain alkanes,[135] and synthesis and functioning of this enzyme strictly depend on iron.[132]

The influx of hydrocarbons has a significant impact on the indigenous microbial community structure. Mason *et al.* surveyed the microbial composition after the explosion of the oil rig Deepwater Horizon in 2010 and found a rather low microbial diversity in the oil plume, enriched in species capable of alkane utilisation.[136] The entire pathway for degradation of *n*-alkanes, including genes for iron uptake, was represented and abundant in the metagenome data of the plume. *Alcanivorax borkumensis* is the most abundant microbe in oil-polluted waters.[137] It produces two distinct siderophores, amphibactins and pseudomonines (Fig. 10), which maintain the bacterium's hydrocarbon-degradation efficiency under iron-limiting conditions.[138] Another important oil-degrading microbe is *Marinobacter hydrocarbonoclasticus*. It produces petrobactin[139] and petrobactin sulfonate.[140] Amphibactins have also been detected as siderophores of some hydrocarbon-utilizing *Vibrio* species.[131] The amphiphilic character of these siderophores allows them to act as biosurfactants. They can thus support alkane degradation in two ways: (i) by aiding the iron uptake process of alkane-degrading microbes and thus enhancing their degradation potential as described above; (ii) by emulsifying the alkanes and thus increasing the solubility of the oil at the bacterial surface.

In summary, siderophores appear to play an important role in bioremediation of oil-polluted ocean areas. Directed application of siderophore-producing hydrocarbon-degraders thus seems a promising approach to "clean" the oceans.

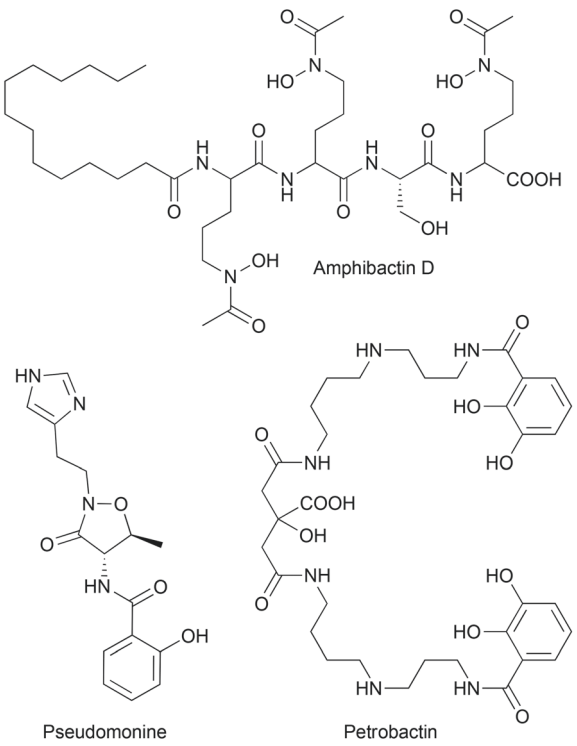

Fig. 10 Siderophores produced by different oil-degrading bacteria.

Biocontrol of algal blooms

A more hypothetical environmental application of siderophores is the biocontrol of toxic algal blooms. On the one hand, siderophores can deprive harmful algae from iron and thus inhibit them in their growth. Naito *et al.* investigated 13 species of abundant red tide algae in their ability to grow when iron was complexed to the microbial siderophores ferrichrome and ferrioxamine.[141] None of the species was able to use Fe-ferrichrome and only three species exhibited growth, when iron was bound to ferrioxamine. Only a few eukaryotic microalgae have been found to produce iron-complexing ligands on their own (*e.g.*, *Chattonella antiqua* and *Skeletonema costatum*).[142,143] It has been proposed that picoeukaryotic algae of the genus *Ostreococcus* could possibly take up iron from microbial siderophores by ligand-exchange or even by direct uptake of the Fe-siderophore complex.[144] Experimental evidence verifying this assumption is, however, still missing. In contrast, iron acquisition has been thoroughly studied in diatoms of the genus *Thalassiosira*. It was found to be similar to the iron uptake system of *Saccharomyces cerevisiae*, where chelate-bound or free Fe^{3+} is reduced by surface reductases, resulting in the accumulation of Fe^{2+} on the cell surface. This ferrous iron can then be transported across the cell membrane.[145] Such reductive iron removal is efficient in the case of weak chelators, but is very slow in the case of strong iron chelators, such as siderophores. As a result, siderophores can induce iron limitation in eukaryotic algae.[146]

On the other hand, photoreactive siderophores can increase iron bioavailability for the microbial community. These intriguing molecules are common in the marine

environment,[26,147,148] and have recently also been found to occur in freshwater and soil.[27,149–151] They are characterized by an α-hydroxycarboxylate function, which confers the molecule photoreactive properties. While the free ligand is photochemically stable, the Fe^{3+}-siderophore complex rapidly undergoes photooxidative cleavage once exposed to sunlight (Fig. 11). As a result, ferrous iron is released into the environment, though it will rapidly reoxidize to ferric iron under aerobic conditions. The free inorganic iron species are readily available for many members of the microbial community. There is increasing evidence for mutualistic relationships between marine bacteria and phytoplankton, where iron and carbon are shared and exchanged.[11] Thus, photoreactive siderophores certainly have the potential to shape microbial communities by favouring certain species and indirectly hindering the growth of others. It might be even possible to utilise selected bacterial siderophore producers as biocontrol agents against algal blooms. However, interactions are highly complex and the effect of siderophore-addition has to be carefully considered, before applying such biocontrol agents to the field. To date, our knowledge about iron-uptake by eukaryotic plankton is scarce and it seems that various mechanisms exist.[145,152] The complexity of siderophore-based microbial interactions is further increased by the fact that different siderophore photoproducts exhibit different iron-chelating capabilities. Some photoproducts, such as "photodegraded" petrobactin, exhibit an even stronger affinity for iron than the parent siderophore,[153] while others, such as the vibrioferrin photoproduct, forfeit their siderophore function.[154] In different open ocean studies, petrobactin and vibrioferrin were detected as highly abundant molecules,[155,156] illustrating their importance in marine iron cycling.

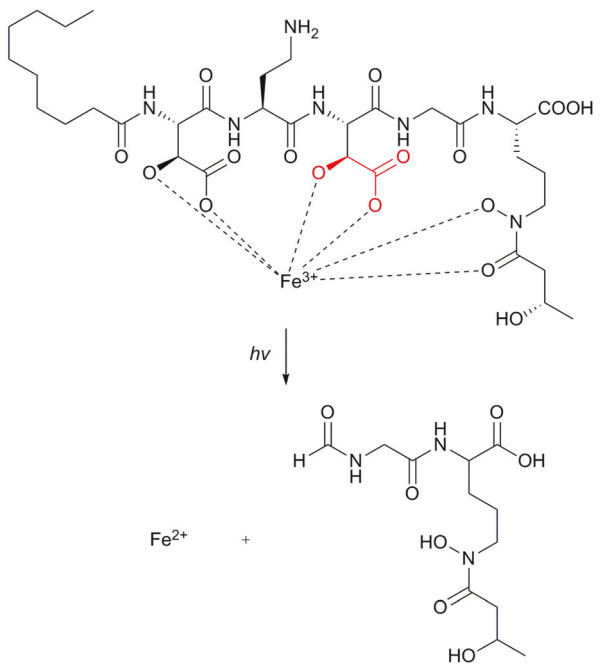

Fig. 11 Reaction scheme for the UV photolysis of Fe^{3+}-cupriachelin.[27] The α-hydroxycarboxylate function responsible for the photoreaction is marked in red.

Promotion of plant growth

Siderophores produced by rhizosphere bacteria have positive effects on plant growth, as already discussed in the phytoremediation section. First, siderophore-producing bacteria can act as biofertilizers by supplying plants with iron.[157] Several studies illustrate the link between increased iron uptake *via* bacterial siderophores and increased plant growth. For instance, Masalha *et al.* showed that maize and sunflowers grown under non-sterile conditions showed far better iron nutrition than plants grown under sterile conditions,[158] an effect that the authors attributed to bacterial siderophores. Similarly, Sharma *et al.* reported that *Pseudomonas* strain GRP_3 could reduce chlorotic symptoms and enhance chlorophyll levels in mung beans.[159] Katiyar and Goel developed a siderophore-overproducing strain of *Pseudomonas fluorescens* ATCC 13525, which proved highly efficient in plant growth promotion.[160] Inoculation of the rhizosphere with the mutant resulted in 29% increase of plant root length compared to the wild type strain. This mutant was further cold resistant and showed growth at 10 °C, making it highly interesting for agricultural applications in certain climate zones.

Siderophore-producing rhizosphere bacteria can further be used as biopesticides,[157] as they can competitively exclude plant pathogens by depriving them of iron.[161,162] This effect is corroborated by numerous studies. Kloepper *et al.* found that addition of a *Pseudomonas* strain or its siderophore to disease-conducive soil inoculated with plant pathogenic fungi rendered the soil disease-suppressive.[163] This effect was revoked, when iron was added to the soils, supposedly due to suppressed siderophore production. Another study investigated *Pseudomonas* sp. mutants with altered siderophore production levels regarding their biocontrol potential against wilt disease-causing *Ralstonia solanacearum*.[164] The mutants with higher siderophore production suppressed disease to a greater degree than the wild type, confirming the role of siderophores in the biocontrol mechanism. Kumar *et al.* isolated the siderophore-producing strains *Sinorhizobium fredii* KCC5 and *Pseudomonas fluorescens* LPK2 from the rhizosphere and assessed a growth-inhibiting effect of these isolates on plant pathogenic *Fusarium udum*.[165] In another study, the siderophore-producer *Pseudomonas putida* WCS358 was shown to suppress growth of *Fusarium oxysporum*.[166] However, siderophore knock-out mutants of the strain were also able to suppress wilt disease to a similar extent, indicating that another plant protection mechanism must also be involved. Indeed, rhizobacteria use a variety of different ways to promote plant growth in addition to siderophore production, including the production of indole acetic acid, ammonia and hydrogen cyanide and phosphate solubilisation.[167,168] Siderophore-mediated iron deprivation of pathogens works better at higher pH, than at lower pH, where iron is more soluble and more easily available to the pathogens.[162]

It thus makes sense to combine plant growth promoting bacteria with different biocontrol mechanisms to combat plant pathogens. Nevertheless, siderophores represent an eco-friendly and cost-effective way to enhance plant growth and prevent plant diseases. Optimizing siderophore production of selected strains in the soil *via* a supply of different minerals and carbon sources may further increase the success of this technique.[169]

Biocontrol of fish pathogens

The increase in aquaculture in the last few decades goes along with disease outbreaks caused by different pathogens.[170] The use of probiotics has appeared to be an efficient, well-applicable and mild method to prevent such diseases. The main mode of action of probiotic bacteria seems to be the production of siderophores, and thus the iron deprivation of pathogens. Indeed, iron is essential for virulence and bacterial communication of pathogens.[171] Fish usually use iron-binding proteins to make iron unavailable to potential pathogenic microorganisms,[172] but many pathogens are able to retrieve iron from these proteins by using transferrins.[173] Siderophores produced by probiotic bacteria would then be able to recover this iron, resulting in attenuated virulence of the pathogen. Gram *et al.* effectively found a positive correlation between the production of siderophores and a decrease in pathogen prevalence.[174]

A lot of effort has been made to find potential probiotics for use in aquaculture and resolve their mode of action. Fuente *et al.* tested 80 strains isolated from fish farms for their ability to inhibit fish pathogens.[175] All the ten positive strains belonged to the genus *Pseudomonas*, of which nine were found to produce siderophores. This corroborates the assumption that siderophores are important, but not the sole mode of action of probiotic bacteria against pathogens. Similarly, Korkea-aho *et al.* found that two closely related *Pseudomonas* strains were active against pathogenic *Flavobacterium psychrophilum*, but exhibited different modes of action, using siderophore production and immunostimulatory effects on fish, respectively.[176,177] An earlier study reported culture supernatants of iron-limited *Pseudomonas fluorescens* to inhibit growth of *Vibrio anguillarum*, while supernatants of iron-replete cultures did not.[174] The probiotic effect could also be observed *in vivo*, where mortality of rainbow trout exposed to *V. anguillarum* was significantly reduced in animals previously exposed to the *P. fluorescens*. Another promising biocontrol candidate is *Bacillus cereus*.[178] It was shown to competitively exclude pathogenic *Aeromonas hydrophila*. Even though the pathogen is capable of siderophore production, *B. cereus* was far more efficient, thus starving its competitor of iron. *Bacillus* sp. JB-1 and *Aeromonas sobria* are further promising siderophore producers for aquaculture.[179] *Pseudoalteromonas* sp. releases several compounds with inhibitory activity against *Vibrio parahaemolyticus*.[180] This effect could be overcome by the pathogen under iron-replete conditions suggesting, again, the involvement of siderophores.

It has to be considered that some fish pathogens also acquire iron *via* siderophores and that their exclusion by probiotics may be more difficult.[181] Osorio *et al.* reported that the complete gene cluster for biosynthesis and transport of the siderophore piscibactin is encoded on a transmissible plasmid in the genome of the pathogen *Photobacterium damselae*.[182] Horizontal transfer of such genes can facilitate pathogen emergence. In these cases, affinity constants of the competing siderophores, as well as possible other modes of action, will decide, whether probiotic bacteria can protect fish from disease or not. In any case, the use of probiotics in aquaculture seems to be advantageous over vaccines or antibiotics, which is also reflected in their increasing application.

Recovery of rare earth elements

The rare earth elements (REEs) are a group of metals that comprise the 15 lanthanides, yttrium and scandium. REEs exhibit unique physical and chemical properties and have become indispensable for a vast number of high-tech applications, such as in computers, auto converters, catalysis, photovoltaics and wind turbines.[183] Global demands for these elements are rapidly increasing and mining is almost exclusively performed in China, the largest REE deposit in the world being located in Baotou, Inner Mongolia, China.[184] REEs are usually extracted from ores *via* chemical leaching, which are however rather non-specific and have drastic impact on the environment.[185] Siderophores could be used in a more specific and environmentally friendly way to extract these elements. Siderophores have indeed been found to bind REEs.[186–188] Most studies focused on desferrioxamine, a naturally occurring and ubiquitous siderophore. The smaller the radius of the lanthanide (*i.e.* the higher its atomic number), the stronger the binding affinity of desferrioxamine towards it.[189] Mohwinkel *et al.* tested desferrioxamine for its ability to leach trace metals from ocean ferromanganese nodules and crusts.[188] The metals of interest being mainly concentrated in the iron oxide phase, a siderophore – a ligand specialized in the dissolution of iron oxides – seemed a promising candidate for the selective leaching of the enclosed REEs. The technique proved highly successful for lithium and molybdenum with a total mobilisation of 60% and 40%, respectively. The values were lower for the actual REEs, with a maximum of 7% reached for cerium. Even though REE-desferrioxamine stability constants are rather high, the complex formation is likely inhibited by the huge amount of competing cations in the surrounding, such as Fe^{3+}. Changing parameters like pH, temperature and the used siderophore could further increase selectivity and efficiency of siderophore leach. Follow-up studies should also work on the separation of the metals present in the leach mixture.[188] It should also be considered that recycling REEs will gain increasing importance in the future, when mines become depleted. In 2007, the overall use of REEs was estimated at 120 Gg, while the in-use stocks totaled around 440 Gg,[183] reflecting the huge potential of recycling. Recycling appears feasible for

metallurgical applications, such as magnets, wind turbines and automobiles, where La, Ce, Nd and Pr are present in high quantities. However, recycling of other REEs present in smaller quantities, *e.g.*, in screens, appears more challenging. Whether siderophores can be used for such purposes remains elusive and should become a prospect for future studies.

Modification of surfaces

Siderophores can dissolve iron oxides and other iron-bearing minerals by means of a progressive ligand exchange reaction.[190–193] This surface controlled process is assumed to have a key role in mineral weathering as well as biological iron acquisition.[194] Recently, the surface binding properties of siderophores have been explored with respect to potential applications in materials sciences.[195] Biofouling, *i.e.*, the non-specific adsorption of microorganisms and biological macromolecules to wetted surfaces, is of great concern in various areas, ranging from medicine to the shipping industries.[196] In order to prevent biofouling, surfaces can be coated with poly (ethylene glycol) (PEG).[197] For this, covalent as well as electrostatic coupling strategies have been developed. A promising biomimetic approach involves the usage of catechol ligand groups in order to mediate the binding of PEG to metal oxide surfaces.[198,199] Catecholates are well known to possess adhesive functions in nature.[200] Mussels use at least six different proteins for adhesion, all of which contain the catechol-bearing amino acid 3,4-dihydroxyphenylalanine.[201] Also, the bacterium *Pseudomonas aeruginosa* was assumed to use the catechol siderophore pyoverdine for initial adhesion during biofilm formation.[202] In an exemplary study, the iron-chelating 6,7-dihydroxy-1,1-dimethyl-1,2,3,4-tetrahydroquinolin-1-ium chromophore of the siderophore anachelin was attached to PEG and surfaces were coated with this conjugate by a simple "dip-and-rinse" procedure.[199] Since the conjugate displayed favorable properties, further studies were carried out to replace the anachelin motif by structurally less complex derivatives.[203] Another interesting development in this context was the linkage of the antibiotic vancomycin with the anachelin-derived conjugate.[204] The resulting hybrid compound can be used for the functionalisation of surfaces, endowing them with antimicrobial properties. Antimicrobial surfaces, in general, have significant potential to prevent undesired biofilm formation on medical devices, such as catheters, implants and stents.[205] Recent studies even demonstrate that the binding properties and stability of catecholate-based antifouling coatings can be further improved by mimicking the tripodal siderophore topology.[206,207]

Conclusions

Siderophores are extremely versatile molecules that capture iron from the environment to ensure microbial iron homeostasis. Humans have been exploiting these molecules for medical and environmental applications for many years. In the medical field, highly satisfactory progress has been achieved and siderophores are routinely used in the clinic to treat iron overload diseases. Siderophore-conjugated antibiotics are now tested in clinical trials to overcome bacterial resistance and improve anti-infective therapy. Siderophores could also be used to inhibit metalloenzymes, of which many are responsible for disease pathologies, an aspect that still requires a lot of research. In the environmental field, ideas for the application of siderophores are vast. They have been found to support plant and fish health and are thus applied in both agriculture and aquaculture. Many auspicious propositions have also been made with respect to their potential to remediate contaminated environments, which could be illustrated in numerous studies. However, the complexity of nature compared to the studied laboratory systems makes the actual application of siderophores challenging. Thus, the complexity of the investigated systems has to be increased, *e.g.*, by adding further organisms, in order to be able to foresee the consequences of applying siderophores to an ecosystem. All in all, we summarized studies that depict siderophores as intriguing molecules with numerous possible applications, far beyond their natural function.

Acknowledgements

We thank the Deutsche Forschungsgemeinschaft (DFG) for funding our research on siderophores within the Collaborative Research Centre *Chemical Mediators in Complex Biosystems* (CRC 1127, ChemBioSys).

Notes and references

1 R. J. D. Tilley, *Understanding solids – the science of materials*, Wiley, Chichester, 2004.
2 A. Stwertka, *A guide to the elements*, Oxford University Press, New York, Oxford, 2002.
3 T. C. Johnstone and E. M. Nolan, *Dalton Trans.*, 2015, **44**, 6320.
4 F. W. Outten and E. C. Theil, *Antioxid. Redox Signaling*, 2009, **5**, 1029.
5 S. C. Andrews, A. K. Robinson and F. Rodríguez-Quiñones, *FEMS Microbiol. Rev.*, 2003, **27**, 215.
6 W. H. Koppenol, *Redox Rep.*, 2001, **6**, 229.
7 M. Sandy and A. Butler, *Chem. Rev.*, 2009, **109**, 4580.
8 H. Haas, *Nat. Prod. Rep.*, 2014, **31**, 1266.
9 C. Curie, G. Cassin, D. Couch, F. Divol, K. Higuchi, M. Le Jean, J. Misson, A. Schikora, P. Czernic and S. Mari, *Ann. Bot.*, 2009, **103**, 1.
10 K. N. Raymond, B. E. Allred and A. K. Sia, *Acc. Chem. Res.*, 2015, **48**, 2496.
11 S. A. Amin, D. H. Green, M. C. Hart, F. C. Küpper, W. G. Sunda and C. J. Carrano, *Proc. Natl. Acad. Sci. U. S. A.*, 2009, **106**, 17071.
12 M. F. Traxler, M. R. Seyedsayamdost, J. Clardy and R. Kolter, *Mol. Microbiol.*, 2012, **86**, 628.

13 V. I. Holden and M. A. Bachman, *Metallomics*, 2015, **7**, 986.
14 A. Paauw, M. A. Leverstein-van Hall, K. P. van Kessel, J. Verhoef and A. C. Fluit, *PLoS One*, 2009, **4**, e8240.
15 R. C. Hider and X. Kong, *Nat. Prod. Rep.*, 2010, **27**, 637.
16 K. S. Chaturvedi, C. S. Hung, J. R. Crowley, A. E. Stapleton and J. P. Henderson, *Nat. Chem. Biol.*, 2012, **8**, 731.
17 D. van der Helm and M. Poling, *J. Am. Chem. Soc.*, 1976, **98**, 82.
18 S. M. Cohen, M. Meyer and K. N. Raymond, *J. Am. Chem. Soc.*, 1998, **120**, 6277.
19 H. Drechsel and G. Winkelmann, Iron chelation and siderophores, in *Transition metals in microbial metabolism*, ed. G. Winkelmann and C. J. Carrano, Harwood Academic Publishers, 1997, p. 1.
20 H. Boukhalfa, T. J. Brickman, S. K. Armstrong and A. L. Crumbliss, *Inorg. Chem.*, 2000, **39**, 5591.
21 H. Boukhalfa and A. L. Crumbliss, *BioMetals*, 2002, **15**, 325.
22 Z. D. Liu and R. C. Hider, *Coord. Chem. Rev.*, 2002, **232**, 151.
23 M. Miethke and M. A. Marahiel, *Microbiol. Mol. Biol. Rev.*, 2007, **71**, 413.
24 C. T. Walsh, J. Liu, F. Rusnak and M. Sakaitani, *Chem. Rev.*, 1990, **90**, 1105.
25 G. L. Challis, *ChemBioChem*, 2005, **6**, 601.
26 A. Butler and R. M. Theisen, *Coord. Chem. Rev.*, 2010, **254**, 288.
27 M. F. Kreutzer, H. Kage and M. Nett, *J. Am. Chem. Soc.*, 2012, **134**, 5415.
28 H. Kage, M. F. Kreutzer, B. Wackler, D. Hoffmeister and M. Nett, *Chem. Biol.*, 2013, **20**, 764.
29 H. Kage, E. Riva, J. S. Parascandolo, M. F. Kreutzer, M. Tosin and M. Nett, *Org. Biomol. Chem.*, 2015, **13**, 11414.
30 B. S. Moore and C. Hertweck, *Nat. Prod. Rep.*, 2002, **19**, 70.
31 J. H. Crosa and C. T. Walsh, *Microbiol. Mol. Biol. Rev.*, 2002, **66**, 223.
32 N. Gaitatzis, B. Kunze and R. Müller, *Proc. Natl. Acad. Sci. U. S. A.*, 2001, **98**, 11136.
33 F. Imperi and P. Visca, *FEBS Lett.*, 2013, **587**, 3387.
34 O. Cunrath, V. Gasser, F. Hoegy, C. Reimmann, L. Guillon and I. J. Schalk, *Environ. Microbiol.*, 2015, **17**, 171.
35 V. Gasser, L. Guillon, O. Cunrath and I. J. Schalk, *J. Inorg. Biochem.*, 2015, **148**, 27.
36 M. Gründlinger, S. Yasmin, B. E. Lechner, S. Geley, M. Schrettl, M. Hynes and H. Haas, *Mol. Microbiol.*, 2013, **88**, 862.
37 D. Oves-Costales, N. Kadi and G. L. Challis, *Chem. Commun.*, 2009, 6530.
38 S. Schmelz, N. Kadi, S. A. McMahon, L. Song, D. Oves-Costales, M. Oke, H. Liu, K. A. Johnson, L. G. Carter, C. H. Botting, M. F. White, G. L. Challis and J. H. Naismith, *Nat. Chem. Biol.*, 2009, **5**, 174.
39 T. Ganz, *Physiol. Rev.*, 2013, **93**, 1721.
40 Z. I. Cabantchik, W. Breuer, G. Zanninelli and P. Cianciulli, *Best Pract. Res., Clin. Haematol.*, 2005, **18**, 277.
41 C. Winterbourn, *Toxicol. Lett.*, 1995, **82–83**, 969.
42 C. N. Kontoghiorghe and G. J. Kontoghiorghes, *Drug Des., Dev. Ther.*, 2016, **10**, 465.
43 H. Bickel, R. Bosshardt, E. Gäumann, P. Reusser, E. Vischer, W. Voser, A. Wettstein and H. Zähner, *Helv. Chim. Acta*, 1960, **43**, 2118.
44 R. M. Bannerman, S. T. Callender and D. L. Williams, *Br. Med. J.*, 1962, **2**, 1573.
45 19th WHO Model List of Essential Medicines.
46 S. Singh, R. C. Hider and J. B. Porter, *Anal. Biochem.*, 1990, **187**, 212.
47 A. Hoffbrand, A. Taher and M. Cappellini, *Blood*, 2012, **120**, 3657.
48 W. Breuer, M. J. Ermers, P. Pootrakul, A. Abramov, C. Hershko and Z. I. Cabantchik, *Blood*, 2001, **97**, 792.
49 R. C. Hider, X. Kong, V. Abbate, R. Harland, K. Conlon and T. Luker, *Dalton Trans.*, 2015, **44**, 5197.
50 H.-U. Naegeli and H. Zähner, *Helv. Chim. Acta*, 1980, **63**, 1400.
51 R. J. Bergeron, J. Wiegand, J. S. McManis and N. Bharti, *J. Med. Chem.*, 2014, **57**, 9259.
52 H. Bickel, E. Gäumann, W. Keller-Schierlein, V. Prelog, E. Vischer, A. Wettstein and H. Zähner, *Experientia*, 1960, **16**, 129.
53 D. M. Reynolds, A. Schatz and S. A. Waksman, *Proc. Soc. Exp. Biol. Med.*, 1947, **64**, 50.
54 G. F. Gause, *Br. Med. J.*, 1955, **2**, 1177.
55 J. Turková, O. Mikeš and F. Šorm, *Collect. Czech. Chem. Commun.*, 1966, **31**, 2444.
56 W. Sackmann, P. Reusser, L. Neipp, F. Kradolfer and F. Gross, *Antibiot. Chemother.*, 1962, **12**, 34.
57 H. Tsukiura, M. Okanishi, T. Ohmori, H. Koshiyama, T. Miyaki, H. Kitazima and H. Kawaguchi, *J. Antibiot.*, 1964, **17**, 39.
58 L. Vértesy, W. Aretz, H.-W. Fehlhaber and H. Kogler, *Helv. Chim. Acta*, 1995, **78**, 46.
59 X. Thomas, D. Destoumieux-Garzón, J. Peduzzi, C. Afonso, A. Blond, N. Birlirakis, C. Goulard, L. Dubost, R. Thai, J.-C. Tabet and S. Rebuffat, *J. Biol. Chem.*, 2004, **279**, 28233.
60 T. A. Wencewicz, U. Möllmann, T. E. Long and M. J. Miller, *BioMetals*, 2009, **22**, 633.
61 J. M. Roosenberg and M. J. Miller, *J. Org. Chem.*, 2000, **65**, 4833.
62 V. Braun, A. Pramanik, T. Gwinner, M. Köberle and E. Bohn, *BioMetals*, 2009, **22**, 3.
63 T. Zheng and E. M. Nolan, *J. Am. Chem. Soc.*, 2014, **136**, 9677.
64 T. A. Wencewicz, T. E. Long, U. Möllmann and M. J. Miller, *Bioconjugate Chem.*, 2013, **24**, 473.
65 G. H. Vondenhoff, B. Gadakh, K. Severinov and A. Van Aerschot, *ChemBioChem*, 2012, **13**, 1959.
66 S. Noël, V. Gasser, B. Pesset, F. Hoegy, D. Rognan, I. J. Schalk and G. L. Mislin, *Org. Biomol. Chem.*, 2011, **9**, 8288.

67 A. Souto, M. A. Montaos, M. Balado, C. R. Osorio, J. Rodríguez, M. L. Lemos and C. Jiménez, *Bioorg. Med. Chem.*, 2013, **21**, 295.
68 S. J. Milner, A. Seve, A. M. Snelling, G. H. Thomas, K. G. Kerr, A. Routledge and A.-K. Duhme-Klair, *Org. Biomol. Chem.*, 2013, **11**, 3461.
69 M. J. Miller, A. J. Walz, H. Zhu, C. Wu, G. Moraski, U. Möllmann, E. M. Tristani, A. L. Crumbliss, M. T. Ferdig, L. Checkley, R. L. Edwards and H. I. Boshoff, *J. Am. Chem. Soc.*, 2011, **133**, 2076.
70 A. F. Vergne, A. J. Walz and M. J. Miller, *Nat. Prod. Rep.*, 2000, **17**, 99.
71 Y. Y. Tu, M. Y. Ni, Y. R. Zhong, L. N. Li, S. L. Cui, M. Q. Zhang, X. Z. Wang and X. T. Liang, *Yaoxue Xuebao*, 1981, **16**, 366.
72 B. Meunier and A. Robert, *Acc. Chem. Res.*, 2010, **43**, 1444.
73 G. L. A. Mislin and I. J. Schalk, *Metallomics*, 2014, **6**, 408.
74 O. Kinzel, R. Tappe, I. Gerus and H. Budzikiewicz, *J. Antibiot.*, 1998, **51**, 499.
75 C. Ji, P. A. Miller and M. J. Miller, *J. Am. Chem. Soc.*, 2012, **134**, 9898.
76 K. Poole, L. Young and S. Neshat, *J. Bacteriol.*, 1990, **172**, 6991.
77 T. Zheng, J. L. Bullock and E. M. Nolan, *J. Am. Chem. Soc.*, 2012, **134**, 18388.
78 I. J. Schalk and L. Guillon, *Amino Acids*, 2013, **44**, 1267.
79 T. Zheng and E. M. Nolan, *Bioorg. Med. Chem. Lett.*, 2015, **25**, 4987.
80 A. Ghosh, M. Ghosh, C. Niu, F. Malouin, U. Moellmann and M. J. Miller, *Chem. Biol.*, 1996, **3**, 1011.
81 N. Kohira, J. West, A. Ito, T. Ito-Horiyama, R. Nakamura, T. Sato, S. Rittenhouse, M. Tsuji and Y. Yamano, *Antimicrob. Agents Chemother.*, 2015, **60**, 729.
82 M. G. P. Page, *Ann. N. Y. Acad. Sci.*, 2013, **1277**, 115.
83 M. Rouffet and S. M. Cohen, *Dalton Trans.*, 2011, **40**, 3445.
84 K. A. McGill and W. W. Busse, *Lancet*, 1996, **348**, 519.
85 P. A. Marks and R. Breslow, *Nat. Biotechnol.*, 2007, **25**, 84.
86 R. Visse and H. Nagase, *Circ. Res.*, 2003, **92**, 827.
87 A. Page-McCaw, A. J. Ewald and Z. Werb, *Nat. Rev. Mol. Cell Biol.*, 2007, **8**, 221.
88 R. P. Verma and C. Hansch, *Bioorg. Med. Chem.*, 2007, **15**, 2223.
89 W. C. Parks and C. L. Wilson, *Nat. Rev. Immunol.*, 2004, **4**, 617.
90 C. Gialeli, A. D. Theocharis and N. K. Karamanos, *FEBS J.*, 2011, **278**, 16.
91 K. Kessenbrock, V. Plaks and Z. Werb, *Cell*, 2010, **141**, 52.
92 R. Gendron, D. Grenier, T. Sorsa, V.-J. Uitto and D. Mayrand, *J. Periodontal Res.*, 1999, **34**, 50.
93 Y. Shinozaki, Y. Akutsu-Shigeno, T. Nakajima-Kambe, S. Inomata, N. Nomura, T. Nakahara and H. Uchiyama, *Appl. Microbiol. Biotechnol.*, 2004, **64**, 840.
94 Y. Shinozaki-Tajiri, Y. Akutsu-Shigeno, T. Nakajima-Kambe, S. Inomata, N. Nomura and H. Uchiyama, *J. Biosci. Bioeng.*, 2004, **97**, 281.
95 B. Kunze, N. Bedorf, W. Kohl, G. Höfle and H. Reichenbach, *J. Antibiot.*, 1989, **42**, 14.
96 S. Miyanaga, T. Obata, H. Onaka, T. Fujita, N. Saito, H. Sakurai, I. Saiki, T. Furumai and Y. Igarashi, *J. Antibiot.*, 2006, **59**, 698.
97 S. Schieferdecker, S. König, A. Koeberle, H.-M. Dahse, O. Werz and M. Nett, *J. Nat. Prod.*, 2015, **78**, 335.
98 S. Miyanaga, H. Sakurai, I. Saiki, H. Onaka and Y. Igarashi, *Bioorg. Med. Chem.*, 2009, **17**, 2724.
99 J. Korp, S. König, S. Schieferdecker, H.-M. Dahse, G. M. König, O. Werz and M. Nett, *ChemBioChem*, 2015, **16**, 2445.
100 Y. Chen, Y. Hu, H. Zhang, C. Peng and S. Li, *Nat. Genet.*, 2009, **41**, 783.
101 J. Roos, C. Oancea, M. Heinssmann, D. Khan, H. Held, A. S. Kahnt, R. Capelo, E. la Buscato, E. Proschak, E. Puccetti, D. Steinhilber, I. Fleming, T. J. Maier and M. Ruthardt, *Cancer Res.*, 2014, **18**, 5244.
102 M. Kolberg, K. R. Strand, P. Graff and K. K. Andersson, *Biochim. Biophys. Acta*, 2004, **1699**, 1.
103 J. Barankiewicz and A. Cohen, *Biochem. Pharmacol.*, 1987, **36**, 2343.
104 K. P. Hoyes, R. C. Hider and J. B. Porter, *Cancer Res.*, 1992, **52**, 4591.
105 C. E. Cooper, G. R. Lynagh, K. P. Hoyes, R. C. Hider, R. Cammack and J. B. Porter, *J. Biol. Chem.*, 1996, **271**, 20291.
106 P. M. B. Pahl, M. A. Horwitz, K. B. Horwitz and L. D. Horwitz, *Breast Cancer Res. Treat.*, 2001, **69**, 69.
107 Y. K. Hodges, W. E. Antholine and L. D. Horwitz, *Biochem. Biophys. Res. Commun.*, 2004, **315**, 595.
108 M. F. Kreutzer, H. Kage, P. Gebhardt, B. Wackler, H. P. Saluz, D. Hoffmeister and M. Nett, *Appl. Environ. Microbiol.*, 2011, **77**, 6117.
109 I. J. Schalk, M. Hannauer and A. Braud, *Environ. Microbiol.*, 2011, **13**, 2844.
110 H. Fones and G. M. Preston, *FEMS Microbiol. Rev.*, 2013, **37**, 495.
111 E. Schütze, E. Ahmed, A. Voit, M. Klose, M. Greyer, A. Svatoš, D. Merten, M. Roth, S. J. M. Holmström and E. Kothe, *Environ. Sci. Pollut. Res.*, 2015, **22**, 19376.
112 L. Diels, S. Van Roy, S. Taghavi and R. Van Houdt, *Antonie Van Leeuwenhoek*, 2009, **96**, 247.
113 M. Münzinger, K. Taraz and H. Budzikiewicz, *Z. Naturforsch.*, 1999, **54**, 867.
114 A. Nair, A. A. Juwarkar and S. Devotta, *J. Hazard. Mater.*, 2008, **152**, 545.
115 A. M. Braud, M. Hubert, P. Gaudin and T. A. Lebeau, *J. Appl. Microbiol.*, 2015, **119**, 435.
116 I. P. Thompson, C. J. van der Gast, L. Ciric and A. C. Singer, *Environ. Microbiol.*, 2005, **7**, 909.
117 A. Braud, K. Jézéquel, M. A. Léger and T. Lebeau, *Biotechnol. Bioeng.*, 2006, **94**, 1080.
118 A. Braud, K. Jézéquel and T. Lebeau, *J. Hazard. Mater.*, 2007, **144**, 229.

119 A. Braud, K. Jézéquel, S. Bazot and T. Lebeau, *Chemosphere*, 2009, **74**, 280.
120 T. Takomoto, K. Nomoto, S. Fushiya, R. Ouchi, G. Kusano, H. Hikino, S. Takagi, Y. Matsuura and M. Kakudo, *Proc. Jpn. Acad., Ser. B*, 1978, **54**, 469.
121 S. Fushiya, Y. Sato, S. Nozoe, K. Nomoto, T. Takemoto and S. I. Takagi, *Tetrahedron Lett.*, 1980, **21**, 3071.
122 Y. Ma, M. N. V. Prasad, M. Rajkumar and H. Freitas, *Biotechnol. Adv.*, 2011, **29**, 248.
123 W. Schmidt, *New Phytol.*, 1999, **141**, 1.
124 C. O. Dimkpa, D. Merten, A. Svatoš, G. Büchel and E. Kothe, *J. Appl. Microbiol.*, 2009, **107**, 1687.
125 B. R. Glick, *Biotechnol. Adv.*, 2003, **21**, 383.
126 C. O. Dimkpa, D. Merten, A. Svatoš, G. Büchel and E. Kothe, *Soil Biol. Biochem.*, 2009, **41**, 154.
127 C. O. Dimkpa, A. Svatoš, P. Dabrowska, A. Schmidt, W. Boland and E. Kothe, *Chemosphere*, 2008, **74**, 19.
128 M. Rajkumar, N. Ae, M. N. V. Prasad and H. Freitas, *Trends Biotechnol.*, 2010, **28**, 142.
129 T. Lebeau, A. Braud and K. Jézéquel, *Environ. Pollut.*, 2008, **153**, 497.
130 I. M. Head and R. P. Swannell, *Curr. Opin. Biotechnol.*, 1999, **10**, 234.
131 M. P. Kem, H. K. Zane, S. D. Springer, J. M. Gauglitz and A. Butler, *Metallomics*, 2014, **6**, 1150.
132 I. E. Staijen and B. Witholt, *Biotechnol. Bioeng.*, 1998, **57**, 228.
133 I. J. T. Dinkla, E. M. Gabor and D. B. Janssen, *Appl. Environ. Microbiol.*, 2001, **67**, 3406.
134 J. S. Sabirova, A. Becker, H. Lünsdorf, J. M. Nicaud, K. N. Timmis and P. N. Golyshin, *FEMS Microbiol. Lett.*, 2011, **319**, 160.
135 R. N. Austin and J. T. Groves, *Metallomics*, 2011, **3**, 775.
136 O. U. Mason, T. C. Hazen, S. Borglin, P. S. Chain, E. A. Dubinsky, J. L. Fortney, J. Han, H. Y. Holman, J. Hultman, R. Lamendella, R. Mackelprang, S. Malfatti, L. M. Tom, S. G. Tringe, T. Woyke, J. Zhou, E. M. Rubin and J. K. Jansson, *ISME J.*, 2012, **6**, 1715.
137 J. S. Sabirova, M. Ferrer, D. Regenhardt, K. N. Timmis and P. N. Golyshin, *J. Bacteriol.*, 2006, **188**, 3763.
138 R. Denaro, F. Crisafi, D. Russo, M. Genovese, E. Messina, L. Genovese, M. Carbone, M. L. Ciavatta, M. Ferrer, P. Golyshin and M. M. Yakimov, *Mar. Genom.*, 2014, **17**, 43.
139 K. Barbeau, G. Zhang, D. H. Live and A. Butler, *J. Am. Chem. Soc.*, 2002, **124**, 378.
140 S. J. H. Hickford, F. C. Küpper, G. Zhang, C. J. Carrano, J. W. Blunt and A. Butler, *J. Nat. Prod.*, 2004, **67**, 1897.
141 K. Naito, I. Imai and H. Nakahara, *Phycol. Res.*, 2008, **56**, 58.
142 K. Naito, M. Suzuki, S. Mito, H. Hasegawa, I. Imai, Y. Sohrin and M. Matsui, *Anal. Sci.*, 2001, **17**, i817.
143 H. Hasegawa, T. Maki, K. Asano, K. Ueda and K. Ueda, *Anal. Sci.*, 2004, **20**, 89.
144 B. Palenik, J. Grimwood, A. Aerts, P. Rouzé, A. Salamov, N. Putnam, C. Dupont, R. Jorgensen, E. Derelle, S. Rombauts, K. Zhou, R. Otillar, S. S. Merchant, S. Podell, T. Gaasterland, C. Napoli, K. Gendler, A. Manuell, V. Tai, O. Vallon, G. Piganeau, S. Jancek, M. Heijde, K. Jabbari, C. Bowler, M. Lohr, S. Robbens, G. Werner, I. Dubchak, G. J. Pazour, Q. Ren, I. Paulsen, C. Delwiche, J. Schmutz, D. Rokhsar, Y. Van de Peer, H. Moreau and I. V. Grigoriev, *Proc. Natl. Acad. Sci. U. S. A.*, 2007, **104**, 7705.
145 Y. Shaked, A. B. Kustka and F. M. M. Morel, *Limnol. Oceanogr.*, 2005, **50**, 872.
146 B. M. Hopkinson and F. M. M. Morel, *BioMetals*, 2009, **22**, 659.
147 J. S. Martinez, G. P. Zhang, P. D. Holt, H. T. Jung, C. J. Carrano, M. G. Haygood and A. Butler, *Science*, 2000, **287**, 1245.
148 A. Butler, *BioMetals*, 2005, **18**, 369.
149 M. F. Kreutzer and M. Nett, *Org. Biomol. Chem.*, 2012, **10**, 9338.
150 F. Rosconi, D. Davyt, V. Martínez, M. Martínez, J. A. Abin-Carriquiry, H. Zane, A. Butler, E. M. de Souza and E. Fabiano, *Environ. Microbiol.*, 2013, **15**, 916.
151 C. Kurth, S. Schieferdecker, K. Athanasopoulou, I. Seccareccia and M. Nett, *J. Nat. Prod.*, 2016, **79**, 865.
152 D. A. Hutchins, A. E. Witter, A. Butler and G. W. Luther, *Nature*, 1999, **400**, 858.
153 R. J. Abergel, A. M. Zawadzka and K. N. Raymond, *J. Am. Chem. Soc.*, 2008, **130**, 2124.
154 S. A. Amin, D. H. Green, F. C. Küpper and C. J. Carrano, *Inorg. Chem.*, 2009, **48**, 11451.
155 A. Gärdes, C. Triana, D. H. Green, A. Romano, L. Trimble and C. J. Carrano, *BioMetals*, 2013, **26**, 507.
156 K. Yarimizu, G. Polido, A. Gärdes, M. L. Carter, M. Hilbern and C. J. Carrano, *Metallomics*, 2014, **6**, 1156.
157 J. K. Vessey, *Plant Soil*, 2003, **255**, 571.
158 J. Masalha, H. Kosegarten, Ö. Elmaci and K. Mengel, *Biol. Fertil. Soils*, 2000, **30**, 433.
159 A. Sharma, B. N. Johri, A. K. Sharma and B. R. Glick, *Soil Biol. Biochem.*, 2003, **35**, 887.
160 V. Katiyar and R. Goel, *Plant Growth Regul.*, 2004, **158**, 239.
161 J. W. Kloepper, J. Leong, J. Teintze and M. N. Schroth, *Nature*, 1980, **286**, 885.
162 D. Haas and G. Défago, *Nat. Rev. Microbiol.*, 2005, **3**, 307.
163 J. W. Kloepper, J. Leong, J. Teintze and M. N. Schroth, *Curr. Microbiol.*, 1980, **4**, 317.
164 K. S. Jagadeesh, J. H. Kulkarni and P. U. Krishnaraj, *Curr. Sci.*, 2001, **81**, 882.
165 H. Kumar, V. K. Bajpai, R. C. Dubey, D. K. Maheshwari and S. C. Kang, *Crop Prot.*, 2010, **29**, 591.
166 M. de Boer, P. Bom, F. Kindt, J. J. B. Keurentjes, I. van der Sluis, L. C. van Loon and P. A. H. M. Bakker, *Phytopathology*, 2003, **93**, 626.
167 B. Joseph, R. R. Patra and R. Lawrence, *Int. J. Plant Prod.*, 2007, **2**, 141.
168 F. Ahmad, I. Ahmad and M. S. Khan, *Microbiol. Res.*, 2008, **163**, 173.
169 B. K. Duffy and G. Défago, *Appl. Environ. Microbiol.*, 1999, **65**, 2429.
170 A. Irianto and B. Austin, *J. Fish Dis.*, 2003, **26**, 59.
171 C. Ratledge and L. G. Dover, *Annu. Rev. Microbiol.*, 2000, **54**, 881.

172 I. Frans, C. W. Michiels, P. Bossier, K. A. Willems, B. Lievens and H. Rediers, *J. Fish Dis.*, 2011, **34**, 643.
173 E. Ahmed and S. J. M. Holmström, *Microb. Biotechnol.*, 2014, **7**, 196.
174 L. Gram, J. Melchiorsen, B. Spanggaard, I. Huber and T. F. Nielsen, *Appl. Environ. Microbiol.*, 1999, **65**, 969.
175 M. D. L. Fuente, C. D. Miranda, P. Jopia, G. González-Rocha, N. Guiliani, K. Sossa and H. Urrutia, *J. Aquat. Anim. Health*, 2015, **27**, 112.
176 T. L. Korkea-aho, J. Heikkinen, K. D. Thompson, A. von Wright and B. Austin, *J. Appl. Microbiol.*, 2011, **111**, 266.
177 T. L. Korkea-aho, A. Papadopoulou, J. Heikkinen, A. von Wright, A. Adams and K. D. Thompson, *J. Appl. Microbiol.*, 2012, **113**, 24.
178 R. Lalloo, G. Moonsamy, S. Ramchuran, J. Görgens and N. Gardiner, *Lett. Appl. Microbiol.*, 2010, **50**, 563.
179 J. Brunt, A. Newaj-Fyzul and B. Austin, *J. Fish Dis.*, 2007, **30**, 573.
180 C. P. Aranda, C. Valenzuela, J. Barrientos, J. Paredes, P. Leal, M. Maldonado, F. A. Godoy and C. G. Osorio, *World J. Microbiol. Biotechnol.*, 2012, **28**, 2365.
181 Z. Zhou, L. Zhang and L. Sun, *Vet. Microbiol.*, 2015, **175**, 145.
182 C. R. Osorio, A. J. Rivas, M. Balado, J. C. Fuentes-Monteverde, J. Rodríguez, C. Jiménez, M. L. Lemos and M. K. Waldor, *Appl. Environ. Microbiol.*, 2015, **81**, 5867.
183 X. Du and T. E. Graedel, *Environ. Sci. Technol.*, 2011, **45**, 4096.
184 Y. Pan and H. Li, *Environ. Manage.*, 2016, **57**, 879.
185 E. A. Sholkovitz, *Chem. Geol.*, 1989, **77**, 47.
186 E. A. Christenson and J. Schijf, *Geochim. Cosmochim. Acta*, 2011, **75**, 7047.
187 M. Bau, N. Tepe and D. Mohwinkel, *Earth Planet. Sci. Lett.*, 2013, **364**, 30.
188 D. Mohwinkel, C. Kleint and A. Koschinsky, *Appl. Geochem.*, 2014, **43**, 13.
189 T. Yoshida, T. Ozaki, T. Ohnuki and A. Francis, *Chem. Geol.*, 2014, **212**, 239.
190 S. M. Kraemer, *Aquat. Sci.*, 2004, **66**, 3.
191 P. M. Borer, B. Sulzberger, P. Reichard and S. M. Kraemer, *Mar. Chem.*, 2005, **93**, 179.
192 N. Carrasco, R. Kretzschmar, M.-L. Pesch and S. M. Kraemer, *Environ. Sci. Technol.*, 2007, **41**, 3633.
193 J. G. Wiederhold, S. M. Kraemer, N. Teutsch, P. M. Borer, A. N. Halliday and R. Kretzschmar, *Environ. Sci. Technol.*, 2006, **40**, 3787.
194 P. U. Reichard, R. Kretzschmar and S. M. Kraemer, *Geochim. Cosmochim. Acta*, 2007, **71**, 5635.
195 K. Gademann, *Acc. Chem. Res.*, 2015, **48**, 731.
196 W. J. Costerton and M. Wilson, *Biofilms*, 2004, **1**, 1.
197 M. J. Roberts, M. D. Bentley and J. M. Harris, *Adv. Drug Delivery Rev.*, 2002, **54**, 459.
198 J. L. Dalsin, B. H. Hu, B. P. Lee and P. B. Messersmith, *J. Am. Chem. Soc.*, 2003, **125**, 4253.
199 S. Zürcher, D. Wäckerlin, Y. Bethuel, B. Malisova, M. Textor, S. Tosatti and K. Gademann, *J. Am. Chem. Soc.*, 2006, **128**, 1064.
200 J. Sedó, J. Saiz-Poseu, F. Busqué and D. Ruiz-Molina, *Adv. Mater.*, 2013, **25**, 653.
201 J. H. Waite, *Integr. Comp. Biol.*, 2002, **42**, 1172.
202 M. J. McWhirter, P. J. Bremer, I. L. Lamontand and A. J. McQuillan, *Langmuir*, 2003, **19**, 3575.
203 K. Gademann, J. Kobylinska, J.-Y. Wachand and T. M. Woods, *BioMetals*, 2009, **22**, 595.
204 J.-Y. Wach, S. Bonazzi and K. Gademann, *Angew. Chem., Int. Ed.*, 2008, **47**, 7123.
205 F. Siedenbiedel and J. C. Tiller, *Polymer*, 2012, **4**, 46.
206 E. Franzmann, F. Khalil, C. Weidmann, M. Schröder, M. Rohnke, J. Janek, B. M. Smarsley and W. Maison, *Chem. – Eur. J.*, 2011, **17**, 8596.
207 F. Khalil, E. Franzmann, J. Ramcke, O. Dakischew, K. S. Lips, A. Reinhardt, P. Heisig and W. Maison, *Colloids Surf., B*, 2014, **117**, 185.

4 Additional results

4.1 Co-cultivation of *C. necator* H16 and *N. pelliculosa*

The postulated "carbon for iron mutualism" implies that the cupriachelin-released iron has a positive growth effect on *N. pelliculosa*. This was tested in a co-cultivation study, where algal growth was monitored after inoculation with *C. necator* H16. For this purpose, *N. pelliculosa* SAG 1050-3 (SAG culture collection, Göttingen, Germany) was grown in non-shaking culture in cell culture flasks (12.5 mL, Sarstedt) at 18 °C in modified WC medium[98] supplemented with 0.05 µM ferric chloride (or 10 µM as control). Light was provided by a "JBL Solar Reptil Sun T8" tube covering the UV-Vis range from 200-800 nm. A light regime of 12:12 (light/dark) with 30–50 µmol/m^2/s light intensity was used. Seed cultures consisted of *N. pelliculosa* cells in their exponential growth phase and constituted 2% (v/v) of the final culture volume. Growth was monitored by daily microscopic cell counts. For this purpose, micrographs were taken every day on ten randomly chosen spots of every cell culture flask and the number of cells per monitored area (~72,000 µm^2) was counted using ImageJ.[99] *C. necator* H16 was grown in iron-free modified WC medium[98] supplemented with 2% fructose at 28 °C with moderate shaking. When both, algae and bacteria, had reached exponential growth phase, co-cultures were started. For this, the spent algal growth medium was replaced by fresh medium. Since algal cells were strongly attached to the bottom of the cell culture flasks, this medium exchange was performed in the same cell culture flask in which algal cultures had initially been inoculated. *C. necator* H16 was then added to algae in different cell number ratios (1:1, 1:10 and 10:1). For the controls, the spent algal growth medium was replaced by fresh medium as described before, but no bacteria were added. The media contained either 0.05 µM ferric chloride, corresponding to the co-cultures (≙ iron deficiency) or 10 µM ferric chloride (≙ iron repletion). Co-cultures and controls were incubated as previously described for algal cultures. Algal growth was monitored by daily cell counts as outlined before.

The co-cultivation study confirmed that *C. necator* H16 exerts a positive growth effect on *N. pelliculosa* SAG 1050-3. When grown in co-culture with the bacterium under iron deficiency, the alga reached similar cell densities as in monoculture under iron repletion (Fig. 7). In contrast, algal monocultures grew to lower cell densities under iron deficiency. This positive growth effect corroborates the assumption of a mutualism that might involve cupriachelin. The ferrisiderophore would release Fe^{2+} upon light exposure, which would be taken up by *N. pelliculosa*, resulting in the observed positive growth effect. Other compounds released from

C. necator H16, such as CO_2 and vitamins, may further contribute to this effect. The recorded growth curve thus supports the hypothesized mutualism between *C. necator* H16 and *N. pelliculosa*. However, the involvement of cupriachelin would need to be confirmed in iron uptake experiments.[100–102]

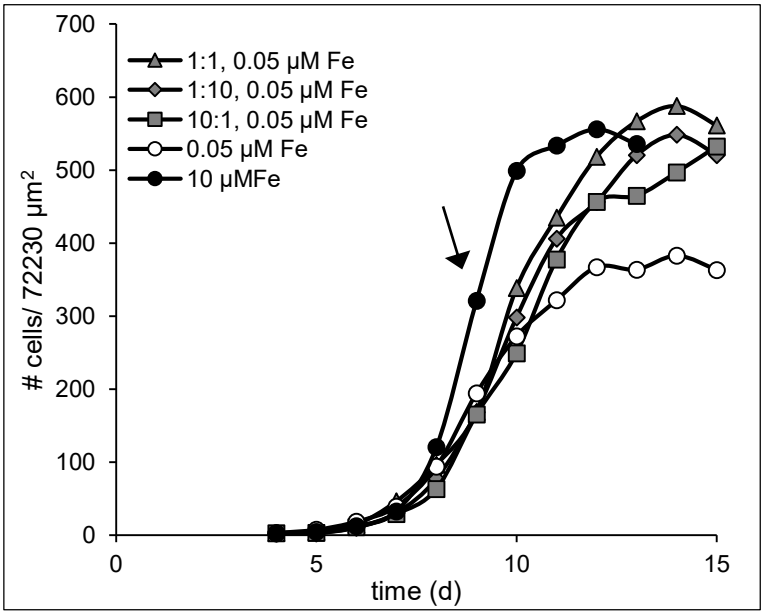

Fig. 7: Growth curves of *N. pelliculosa* grown in co-culture with *C. necator* H16 in different algal: bacterial cell number ratios (1:1, 1:10, 10:1) under iron deficiency (0.05 µM Fe) or in monoculture under iron deficiency (0.05 µM Fe) or iron repletion (10 µM Fe). Co-cultures were started on day 9 (see arrow).

4.2 Photoreactivity of cupriachelin

In order to confirm that Fe^{2+} is released from Fe^{3+}-cupriachelin under the chosen laboratory light conditions ("JBL Solar Reptil Sun T8" tube covering the UV-Vis range from 200-800 nm), the bathophenanthrolinedisulfonic acid (BPDS) assay was performed. Cupriachelin isolation and Fe^{3+}-complexation, as well as the BPDS assay, were conducted as described by Kreutzer et al.[66], with the exception that Fe^{3+}-cupriachelin samples were exposed to light/dark conditions for 30 h. Results demonstrate that Fe^{2+} is indeed released from the siderophore upon light exposure (Fig. 8). This corroborates the assumption that cupriachelin-solubilized iron is at least partly responsible for the positive growth effect of *C. necator* H16 on *N. pelliculosa* described in section 4.1.

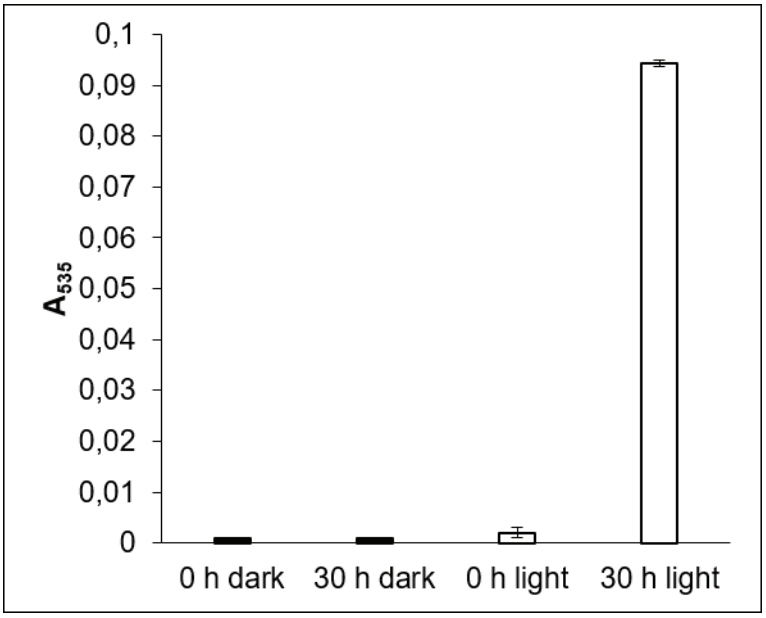

Fig. 8: BPDS assay of Fe^{3+}-cupriachelin exposed to dark or laboratory light conditions. Initially, A_{535} is low for both conditions and remains at the same level after 30 h in the dark. In the light, A_{535} clearly raises within 30 h, indicating the formation of Fe^{2+}-$BPDS_3$ complexes (i.e., the release of Fe^{2+} from Fe^{3+}-cupriachelin).

4.3 Effect of *Chlamydomonas reinhardtii* culture supernatants on cupriachelin transcription levels

Bacterial siderophore biosynthesis is highly dependent on environmental conditions, especially on the availability of iron. The finding that culture supernatants of *N. pelliculosa* also induce cupriachelin biosynthesis (manuscript B) is highly interesting and raises the question for the species specificity of this effect. Therefore, the influence of a second alga, the green alga *C. reinhardtii*, on cupriachelin biosynthesis was investigated using the β-galactosidase assay. First, *C. reinhardtii* was inoculated to a cell density of 10,000 cells/mL into modified WC medium[98] supplemented with 0.1 µM ferric chloride and grown for 7 days under the conditions described before for *N. pelliculosa* (section 4.1). Cells were then removed by centrifugation and the supernatants were added to *C. necator* H16 reporter strains as described in manuscript B. β-Galactosidase assays were performed on day 10 after inoculation as described in manuscript B. Interestingly, no significant effect of *C. reinhardtii* culture supernatants on cupriachelin transcription levels could be observed (Fig. 9). It seems plausible that this indicates a certain species specificity for the influence of algae on bacterial siderophore biosynthesis. While diatoms and bacteria are known to establish particularly intimate interactions,[13] these may be less pronounced between green algae and bacteria. Testing the effect of supernatants of other

algal species on cupriachelin biosynthesis should further clarify this aspect. An alternative explanation for the lack of an observable effect of *C. reinhardtii* culture supernatants on cupriachelin transcription levels may be the experimental design. The β-galactosidase assay was only performed once, on day 10 after inoculation. However, cupriachelin transcription levels are growth phase- and time-dependent (manuscript B), and different results could be obtained, if the β-galactosidase assay was performed at different time points.

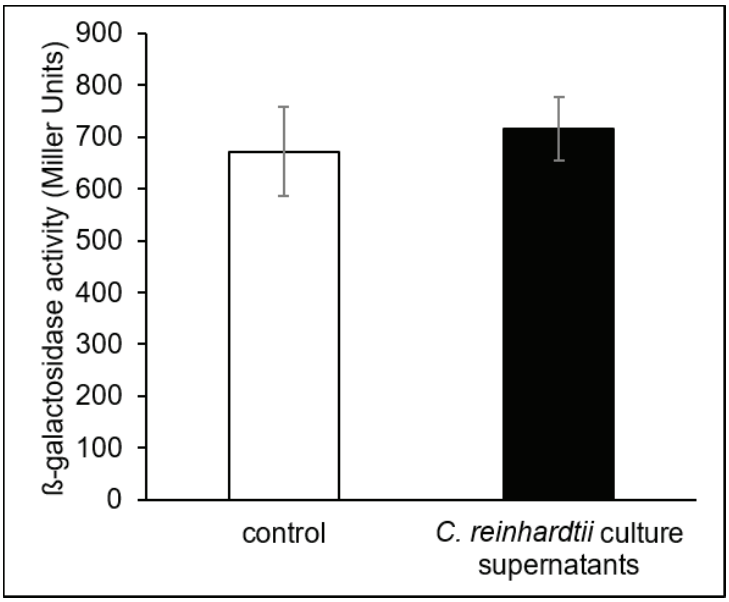

Fig. 9: β-Galactosidase activity of *C. necator* H16 on day 10 after inoculation in a 1:1 mixture of H-3 mineral medium and culture supernatant of *C. reinhardtii* or modified WC medium (control). The values represent means and standard deviations of nine replicates (each of three algal culture supernatants distributed amongst triplicate reporter strains).

4.4 Effect of natural pond water on cupriachelin transcription levels

The ratio of bacterial to algal cells in natural assemblages is poorly studied and is probably highly variable. The algal culture supernatants of *N. pelliculosa* (manuscript B) and *C. reinhardtii* (section 4.3) applied in the β-galactosidase assays probably contained higher metabolite concentrations than can be found in many natural freshwaters. It is thus interesting to test the effect of natural pond water on cupriachelin transcription levels. The Erlkönig pond in Jena was chosen for this purpose. Water samples were taken on 11/03/2016, filtered through a 0.2 µM filter and the iron concentration was measured using AAS (2.37 µM). Pond water was then added to *C. necator* H16 reporter strains as described for *N. pelliculosa* culture supernatants in manuscript B. β-Galactosidase assays were performed on days 4, 6, 8 and 11

after inoculation, according to the protocol in manuscript B. On all tested days, bacteria showed lower cupriachelin transcription levels when grown with pond water than with modified WC medium (Fig. 10). Also, the measured β-galactosidase activities were highly variable for each of the measured time points. This experiment thus cannot confirm that natural plankton assemblages induce siderophore biosynthesis in *C. necator* H16. Nevertheless, it also does not refute it. Planktic communities are highly dynamic, following a seasonal succession.[103] Sampling at another time point or another pond can therefore lead to different results, due to different plankton and metabolites present in the water. This experiment therefore clearly mirrors the complexity of planktic communities.

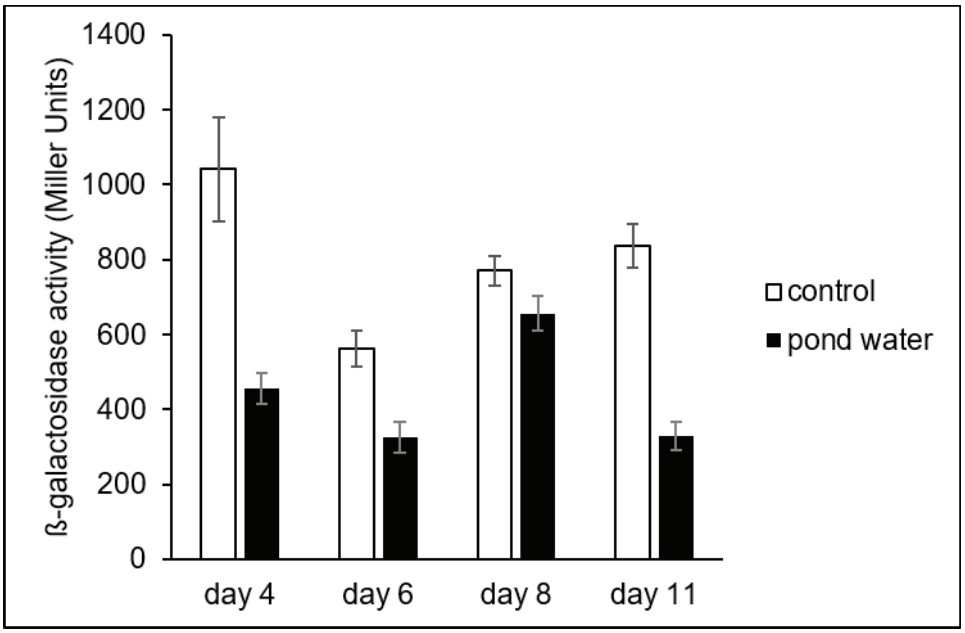

Fig. 10: β-Galactosidase activity of *C. necator* H16 on days 4, 6, 8 and 11 after inoculation in a 1:1 mixture of H-3 mineral medium and pond water or modified WC medium (control). The values represent means and standard deviations of triplicates.

4.5 Dependence of Fur transcription levels in *C. necator* H16 on iron concentrations

Single-cell prokaryotes are exposed to instant and dramatic environmental changes, making a highly responsive gene regulation crucial for survival.[104] Little is known about the expression levels of genes encoding transcription factors. A certain basal expression seems plausible, allowing for fast cellular responses upon sudden environmental changes. However, up- or downregulation under certain environmental conditions may also be reasonable. Fur, for instance, acts as transcriptional repressor on siderophore biosynthesis under iron repletion. *Fur*

may thus be upregulated under iron repletion, while being downregulated under iron deficiency. This was tested for *h16_a3143*, encoding one of the Fur proteins produced by *C. necator* H16.

For this purpose, the Fur promoter *h16_a3143p* was cloned in front of *lacZ* in pCK02 (manuscript B). The promoter region was amplified via PCR from *C. necator* H16 genomic DNA using the primers *h16_a3143p*_F (5'-ctcacgccctcggtgttcag-3') and *h16_a3143p*_R (5'-ggactcggcatgtgggtgact-3'). The subsequent cloning steps were performed as described in manuscript B, yielding the reporter strain *C.* necator:pCK06. Along with the control strains harboring pCK02 and pCK04 (manuscript B), this strain was used for β-galactosidase assays. For this, the reporter strain was grown in H-3 mineral medium[105] supplemented with 1 mg/mL aspartate, 50 µg/mL chloramphenicol, and $FeCl_3$ in varying concentrations (0 µM, 1 µM, 5 µM, 10 µM, 100 µM, 500 µM). A culture volume of 2-4 mL was harvested by centrifugation (1 min, 15,700 x *g*, room temperature) for each assay and resuspended in 200 µL phosphate-buffered saline pH 7.4 (8 g/L NaCl, 0.2 g/L KCl, 1.44 g Na_2HPO_4, 0.24 g KH_2PO_4). The β-galactosidase assay was performed as previously described by Griffith and Wolf,[106] with the exception that microplates were incubated at 28 °C instead of room temperature.

In *C. necator* H16, *fur* expression was not found to be highly dependent on the iron concentration present in the bacterial growth medium (Fig. 11). Only on the first day after inoculation, expression levels showed a positive correlation with iron concentrations, as expected. On the second and third day after inoculation however, no clear relationship between the measured β-galactosidase activity and the iron concentration could be assessed. Only the culture growing in medium without any addition of iron (0 µM Fe) consistently showed the lowest *fur* expression levels. Under such iron starvation conditions, siderophore biosynthesis is indispensable for bacterial growth and Fur should not be involved in the repression of siderophore biosynthesis genes. The low β-galactosidase activity measured for these cultures probably could mirror the basal expression level of the transcription factor. In case iron-starved cells suddenly encounter high iron concentration, these basal Fur levels will help preventing ROS damage to the cells. The lacking connection between *fur* expression and iron concentration for all other samples (1 µM – 500 µM Fe) may reflect the global regulatory role of the protein. Since Fur is involved in the regulation of numerous other genes than those involved in siderophore biosynthesis,[78] its own expression level probably does not only depend on iron concentrations. This was also found for Fur proteins in *Vibrio cholerae*.[107] Fur concentrations were constantly high but seemed independent of extracellular iron concentrations. Instead, they varied mainly according to the bacterium's growth phase. While intracellular Fur

concentrations were lower in exponential growth phase (~2500 Fur monomers/cell), they were higher (~7500 Fur monomers/cell) in stationary growth phase.[107] These results are consistent with the *h16_a3143* expression levels observed for *C. necator* H16 (Fig. 11). In summary, the intracellular Fur concentrations in *C. necator* H16 is rather high and almost independent of the iron concentration in the bacterial growth medium. In this way, Fur can act as global regulator and induce fast cellular responses to environmental changes.

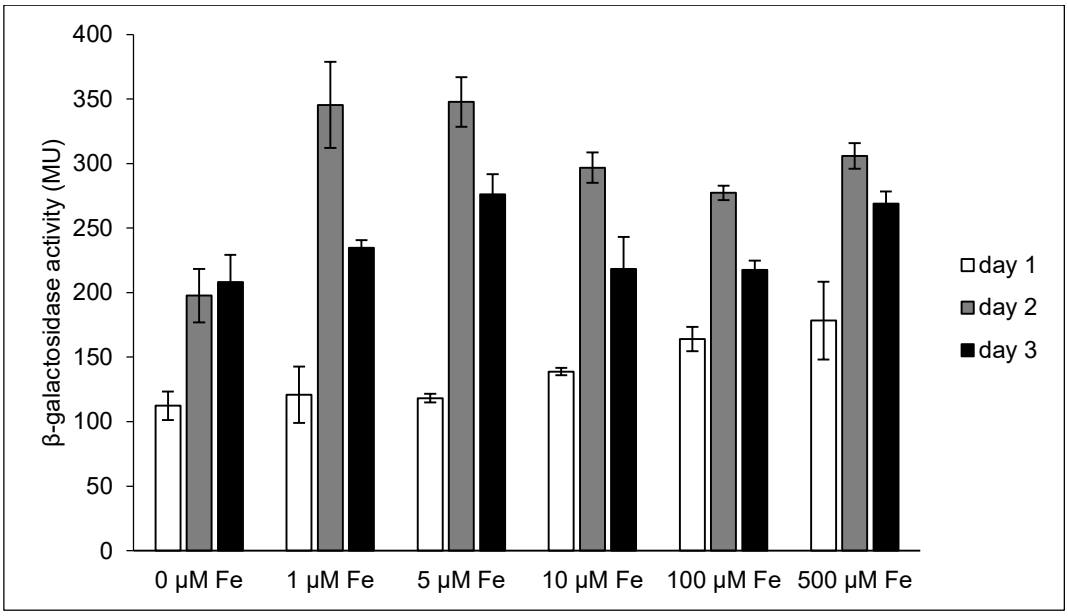

Fig. 11: β-Galactosidase activity of *C. necator*:pCK06 on days 1, 2 and 3 after inoculation in H-3 mineral medium supplemented with 0 µM, 1 µM, 5 µM, 10 µM, 100 µM and 500 µM $FeCl_3$. The values represent means and standard deviations of triplicates.

5 Discussion

5.1 Occurrence of photoreactive lipopeptide siderophores in freshwater

To date, only few siderophores from freshwater bacteria are known, which partly has to be attributed to the lack of cultivability of these organisms.[108] Studies based on 16S rDNA sequencing revealed that most freshwater bacteria belong to the groups of cyanobacteria, bacteroidetes, α-, β- and γ-proteobacteria and actinobacteria.[109,110] Another important finding of these studies is that the bacterioplankton communities found in freshwaters clearly differ from the ones found in other environments, especially in the ocean.[109,110] This suggests that freshwater bacteria may also produce different siderophores. But it is also possible that they use siderophores known from other environments. This could be interpreted as the result of common evolutionary ancestors, convergent evolution or horizontal gene transfer. The latter becomes relevant when bacteria are transported across the Earth e.g. in huge dust events. Taxonomically diverse bacteria have been reported to travel over 5,000 km via these "atmospheric bridges".[111] Some of them retain their growth potential[112] and could therefore horizontally transfer siderophore biosynthesis genes to other bacteria in their new habitat. Vibrioferrin, for example, was first isolated from several marine bacteria, such as *Vibrio parahaemolyticus*[113] and different *Marinobacter* species[52] before being rediscovered in the soil bacterium *Azotobacter vinelandii*.[114] Similarly, aerobactin is produced by phylogenetically and ecologically diverse organisms, such as enteric *Klebsiella aerogenes*[115] and marine *Vibrio* species.[116] Nevertheless, novel bacterial species represent a promising source for the discovery of structurally unprecedented siderophores. The search for freshwater siderophores is thus not only interesting for assessing their ecological relevance, but also for the discovery of novel compounds.

Until the discovery of cupriachelins,[66] photoreactive lipopeptide siderophores were thought to be restricted to the marine environment. Siderophores harboring citric acid-derived moieties are actually known for a long time. They represent a rather small group and are predominately produced by soil and pathogenic bacteria,[117] which are not likely to be exposed to UV light. For this reason, their photoreactive properties remained neglected for several decades. Aerobactin, for instance, was characterized in 1969,[115] but its photoreactivity was only described some 35 years later.[93] In comparison, siderophores harboring β-hydroxy aspartate residues are rare in non-marine environments. Among the few exceptions are the ornibactins produced by

Burkholderia cepacia.[118] Akin to the citrate siderophores, photoreactivity was not recognized until recently.[66]

Amphiphilic siderophores are scarcely found in terrestrial environments. In contrast to water, soil represents a rather structured habitat. Here producers and their metabolites stay associated relatively easily, abolishing the need for amphiphilic metabolites.[119] In this respect, freshwaters lie between terrestrial and marine habitats. Although diffusion plays an important role in freshwater environments, it is less pronounced than in the ocean, due to an increased substrate-to-water ratio.[119] Accordingly, the diffusion length of terrestrial and freshwater siderophores and their water solubility are generally higher compared to siderophores from marine habitats and the fraction of siderophores binding to lipid membranes are generally lower.[119] The amphiphilicity of a lipopeptide siderophore is determined by both, the size of the peptidic head group and the length of the fatty acid chain. For most marine siderophores several derivatives with fatty acids of different chain lengths are known.[120] In terrestrial bacteria, this phenomenon is rare. Ornibactins once more represent an example here, but their short fatty acid chain lengths of C_4 to C_8 clearly distinguish them from the marine siderophores, which harbor much longer acyl chains.[120] Some mycobacteria have also been reported to produce amphiphilic siderophores of varying fatty acid chain lengths. *Mycobacterium tuberculosis*, for example, secretes exochelins into the medium that bind Fe^{3+} and shuttle it to the membrane-associated myochelins. Both siderophores share the same core structure, but differ in polarity and thereby their diffusivity.[121]

While the discovery of cupriachelins revealed that photoreactive lipopeptide siderophores also occur in freshwater, the discovery of variochelins foreshadows that these molecules may even be widely distributed in these environments. It proves that cupriachelins are not an exception and motivates further research to focus on these intriguing molecules. The finding of other freshwater photoreactive lipopeptide siderophores will further illustrate their ecological relevance, which was persuasively commenced by the present study.

5.2 Genome mining – a valuable tool for the discovery of novel photoreactive lipopeptide siderophores

Genome mining has proven a valuable tool for the discovery of novel natural products. The enormous potential of this method is reflected in its figurative name: Just like “real” mining, genome mining can unearth hidden, unforeseen and precious compounds. The term was coined

in the beginning of the genomics era and describes the exploitation of genomic information for the screening, isolation and structure elucidation of novel natural products.[122] Compared to traditional approaches for compound discovery, it has several advantages. While the success of bioassay-guided methods in detecting novel compounds was largely driven by chance for much of its history, genome mining now represents a highly targeted approach.[123] By connecting genes to their metabolites, the rediscovery of already known compounds can be eliminated. Furthermore, gene clusters involved in the biosynthesis of new chemical entities can be readily identified. Such orphan loci represent a huge and largely untapped resource for natural product discovery.[124,125] *Streptomyces* genomes, for example, harbor an average of about 30 biosynthetic gene clusters, but only two or three were known in the time before the onset of genome mining.[126]

Traditionally, siderophores were detected in the chrome azurol S (CAS) assay.[127] CAS, hexadecyltrimethylammonium bromide and Fe^{3+} form a blue complex. When a strong chelator (e.g., a siderophore) removes Fe^{3+} from the complex, its color changes from blue to orange. This assay is highly sensitive and is still widely used for siderophore detection. Another approach to discover siderophores from organisms which genomes have not been sequenced is "PrISM" (Proteomic Investigation of Secondary Metabolites).[128] It involves the cultivation of the organism of interest under different conditions followed by the analysis of its proteome. Larger proteins (>150 kDa) often represent NRPSs or polyketide synthases (PKSs) and are further analyzed. The genetic information of the expressed biosynthetic gene cluster can then be reconstructed and lead to the discovery of novel compounds. In that way, gobichelins were found, without the genome of the siderophore-producing *Streptomyces* strain being sequenced.[128]

Siderophore biosynthesis can usually be triggered by cultivating the respective organism under iron starvation.[129] As a result, the isolation of siderophores is relatively easy compared to many other metabolites, for which suitable cultivation conditions first have to be established. This knowledge, along with the well-established CAS-assay, led to the description of several hundred siderophores, even before the onset of genome mining.[51] However, when searching for siderophores with special features, such as photoreactivity and amphiphilicity, genome mining is extremely helpful. This is illustrated by the discovery of cupriachelins[66] and taiwachelins.[130] In both cases, genome mining targeted the enzymes involved in supplying the siderophore with the β-hydroxy aspartate residue and the fatty acid side chain. In fact, searching for genes encoding enzymes putatively involved in the biosynthesis of secondary metabolites, represents

the most "classical" variant of genome mining.[126] NRPSs represent good targets, due to their high degree of conservation of core enzymes, the collinearity of the modular organization and the synthesized peptide, and the possibility to predict the substrate specificity of A domains.[126] In certain cases, tailoring enzymes can also serve as genome mining probes.[126] Both enzyme classes were used in this PhD project in order to find novel photoreactive lipopeptide siderophores from freshwater bacteria. The CucG A domain that activates aspartate in cupriachelin biosynthesis and the CucF TauD domain that conducts its hydroxylation were chosen as probes for photoreactivity. Fatty acid activation can be executed by external ligases, as in the case of cupriachelins and amphibactins. Alternatively, this biosynthetic step can be performed by fatty acyl-AMP ligases (FAALs), as in the case of taiwachelins[124] and marinobactins.[95,131] The CucF starter C domain from cupriachelin biosynthesis and the TaiD FAAL domain from taiwachelin biosynthesis thus served as probes for amphiphilicity. The search was further focused on freshwater bacteria, in particular on β-proteobacteria, due to their abundance and key role in freshwater ecosystems.[132] The success of the approach is not only mirrored in the discovery of variochelins, but also of seven further putative photoreactive lipopeptide siderophore biosynthesis clusters in freshwater and soil bacteria (manuscript A, Table S1). The putative siderophores from *Achromobacter spanius* CGMCC9173, *Burkholderia sordidicola* S170, *Cupriavidus gilardii* CR3, *Janthinobacterium agaricidamnosus* NBRC102515, *Variovorax paradoxus* B4, *V. paradoxus* EPS and *V. paradoxus* S110 still await discovery and will certainly contribute to our understanding of the function of this compound class outside of the marine environment. Their finding reflects the power of genome mining, which is still formidably growing along with the availability of publically available genomes.

5.3 Photoreactivity of variochelins

The assumed photoreactive property of variochelin was experimentally confirmed via high-resolution mass spectrometry (HRMS) and the BPDS assay. HRMS revealed the decomposition of Fe^{3+}-variochelin into multiple fragments upon light exposure. Two fragments were predominant and could be assigned to distinct photoproducts (Fig. 12). A key fragment results from cleavage in the vicinity of the β-hydroxy aspartate residue, as it was also reported for the aquachelins[49] and cupriachelins.[66] However, the cleavage of variochelins differs from the established route in that it occurs at the N-terminal side of the amino acid, in contrast to the C-terminal side (Figs. 5, 12). As a result, the identified variochelin photoproduct still harbors the

fatty acid side chain, while this is not the case for the aquachelin and cupriachelin photoproducts. A second variochelin fragment results from the decarboxylation of the β-hydroxy aspartate residue leading to the aldehyde, as reported before.[133] Of the numerous other masses detected by HRMS in light-exposed Fe^{3+}-variochelin samples, none could be matched to specific fragments. The situation is comparable for the cupriachelins, where only one photoproduct could be identified, while the fate of the remaining molecule fragments remained obscure.[66] This reflects our limited understanding of the actual photoreactive process. It further mirrors the complexity of photolytic cleavage.

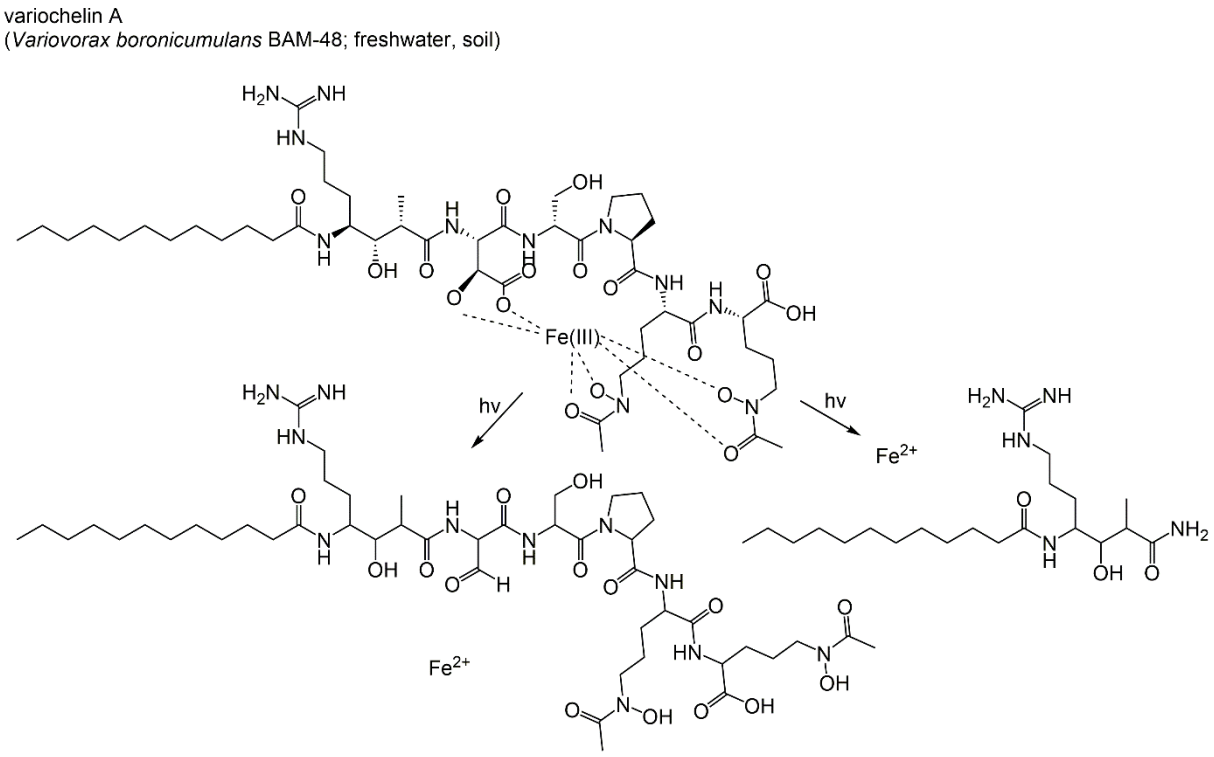

Fig. 12: Reaction scheme for the photolysis of ferric variochelin A.

Of the "classical" Fe^{3+}-binding siderophore moieties, only hydroxamates appear photochemically stable. Siderophores comprising α-hydroxy carboxylate moieties are stable when Fe^{3+}-free, but become photolabile once they have complexed the metal – a situation that is inversed in catecholate-type siderophores.[134] The fact that most photoreactive siderophores belong to a mixed type further adds complexity to the possible photoproducts. For aquachelins exhibiting two photochemically inert hydroxamate functions and one α-hydroxy carboxylate moiety, the situation is relatively simple. Only when ferrated, the siderophore will be cleaved by sunlight, yielding only one major photoproduct.[49] For petrobactin, which is a bis-catecholate α-hydroxy carboxylate siderophore, the situation appears more complicated. When iron-free,

the catechols are readily photooxidized to quinones or semiquinones. Although this reaction is reversible, it temporarily decreases the ligand binding strength of the siderophore. When ferrated, photooxidation occurs at the citrate moiety. This effect is quite localized and does not significantly reduce the siderophore's Fe^{3+}-binding properties.[134] Photodegradation can be more extensive, as soon as the siderophores harbor more than a single α-hydroxy carboxylate function. Examples include the alterobactins and the cupriachelins, which feature two β-hydroxy aspartates besides a catecholate or hydroxamate function, respectively.[66,135] Photoreactive siderophores and their photoproducts thus likely represent an important portion of the organic ligands that complex most Fe^{3+} in surface waters.[136]

The BPDS assay further confirmed the photoreactive properties of variochelins and, more precisely, the associated reduction and release of Fe^{3+} from the complex. BPDS specifically binds Fe^{2+}, forming a photometrically tractable product. The release of Fe^{2+} into the environment is highly interesting from an ecological point of view. By this means, interspecific interactions can arise, which will be discussed in the following chapters.

5.4 Role of photoreactive lipopeptide siderophores in freshwater and soil

Following the discovery of variochelins and the genome mining-based corroboration of the hypothesis that photoreactive lipopeptide siderophores are common in freshwater bacteria (manuscript A), their ecological function in these habitats needs to be addressed. A role comparable to the one of marine siderophores is verisimilar. Freshwater photoreactive siderophores would thus have a dual function by delivering iron to the siderophore producer mainly in the dark, while also providing other organisms with this essential metal in the light. The amphiphilic property would help retaining the siderophore in the vicinity of the producing cell. A clear correlation between habitat structure and diffusivity has been observed. Bacteria living in highly structured habitats produce highly diffusible siderophores, while bacteria living in aquatic environments rather produce siderophores with reduced diffusivity.[119] Also, the severity of iron starvation was found to impact siderophore diffusivity, with hydrophilic siderophores found in regions where iron is not limiting and poorly diffusible siderophores found in region with a severe lack of iron.[137]

C. necator H16 and *V. boronicumulans* have both been described as freshwater and soil bacteria.[97,138] This further raises the question of the ecological function of photoreactive lipopeptide siderophores in soil. In these habitats, exposure to UV light is a rare or even never

occurring event. As a result, α-hydroxy carboxylate-containing ferrisiderophores should remain intact. The solubilized iron is thus delivered only to the siderophore producer and possibly to certain siderophore-pirating species, while mutualistic iron-sharing cannot be expected. However, it has to be considered that bacteria can be transported over great distances, e.g. through aerosols, and can occur in diverse habitats as a result.[139] Furthermore, bacterial habitats are highly dynamic and bacteria isolated from soil will likely also be found e.g. on the soil surface, where photoreactions may happen. The serobactin-producer *Herbaspirillum seropedicae*, for instance, was initially isolated from plant endosphere,[140] but has subsequently also been found on the surface of leaves.[141] The bacterium thus occurs in "dark", as well as sunlight-exposed environments, suggesting that the photoreactive property of serobactins is ecologically relevant, at least under certain circumstances. The fate of the solubilized iron released upon photooxidative siderophore cleavage has not been investigated in soil. An effect on the bioavailability of iron to other organisms and resulting interspecific interactions are well conceivable and should be addressed in the future. A recent study showed that the siderophore gramibactin produced by plant-associated bacteria can be taken up and utilized by the host plants.[142] Gramibactin harbors an α-hydroxy carboxylate function and its photoinduced cleavage should further alter the bioavailability of iron to the plant. This siderophore thus represents a good starting point for the investigation of photoreactive siderophore-based bacteria-plant interactions. Other (micro-)organisms should also be considered in this context.

Diffusion is much less relevant in soil compared to water,[119] suggesting that amphiphilicity of metabolites may have distinct roles in these environments. Lipopeptides have indeed been found to be crucial for bacterial swarming in several soil-colonizing bacterial speices.[143,144] Rather than preventing diffusion, amphiphilicity of siderophores could therefore have an important function in bacterial motility in soil. This implies a dual role as iron chelators and biosurfactants, an interesting aspect that should become the object of further studies.

The suggested ecological roles of photoreactive lipopeptide siderophores in freshwater and soil are speculative and require experimental confirmation. Alternatively, photoreactivity and amphiphilicity of siderophores may simply represent an evolutionary relict in non-marine bacteria. This implies common ancestors with marine bacteria and/or horizontal gene transfer.

5.5 Importance of iron for phytoplankton

The importance of iron for phytoplankton is particularly well-illustrated by the iron hypothesis, formulated by Martin in the 1990s.[28] Martin postulated that iron is the limiting factor for primary production in vast areas of the ocean and that iron fertilization would lead to massive phytoplankton blooms. Iron concentrations in open ocean surface waters range from 0.02 to 1 nM.[145] Considering the fact that phytoplankton requires iron for numerous fundamental cellular processes, such as photosynthesis, chlorophyll synthesis and detoxification of ROS, it is no surprise that such concentrations generally mean severe iron paucity for these organisms. In coastal areas and freshwaters, iron concentrations are usually higher, reaching up to 100 nM.[146,147] In diatoms, low iron concentrations were found to lead to reduced cellular growth rates, chlorophyll *a* contents and cell sizes.[148] However, clear differences could be observed between oceanic and coastal diatoms in their response to iron limitation. While oceanic diatoms can thrive with chronically low concentrations of this vital element, coastal diatoms struggle to do so.[146] This can be attributed to two important aspects. First, oceanic diatoms are often smaller than their coastal counterparts, resulting in a larger surface to biomass ratio and thereby more efficient iron uptake rates.[148] Secondly, they are able to reduce their demand for cellular iron to a substantially higher degree than coastal diatoms.[148] This is effectuated by the different architecture of their photosynthetic apparatus. In fact, most of the iron required by phytoplankton is needed for photosynthetic iron transport. Photosystem (PS) II requires two, the cytochrome b_6f complex six and PSI twelve iron atoms per complex. While the PSII:PSI ratio is about 1:1 in land plants, it is about 2:1 in coastal diatoms and 10:1 in oceanic diatoms.[149] Furthermore, the amount of cytochrome b_6f complex present in oceanic diatoms is reduced in comparison to coastal diatoms.[149] In this way, oceanic diatoms markedly decrease their cellular iron requirements, while maintaining high photosynthesis rates.[149]

Iron requirements of freshwater diatoms are poorly studied. Since iron levels are similar in freshwater and coastal environments, it can however be expected that the inhabiting diatoms' needs for iron are also similarly high. Regardless their habitat, diatoms thus have to cope with growth-limiting iron concentrations. Any extra portion of iron, which can be obtained from mutualistic siderophore producers, should ameliorate this situation and boost diatom growth.

5.6 The "carbon for iron mutualism"

The "carbon for iron mutualism" proposes that heterotrophic bacteria provide iron to algae via photoreactive siderophores and obtain organic carbon in exchange.[50] For phytoplankton, iron is the primary limiting factor in aquatic habitats.[25,26] For bacteria, organic carbon was found to be the primary limiting factor, even in iron-poor waters. Only when carbon limitation was alleviated, iron rapidly became a limiting growth factor for bacteria.[150] Both interaction partners may thus provide each other with the nutrient they most urgently need, corroborating the assumption of a mutualism with major ecological impact.

The speciation of iron is crucial for the ability of phytoplankton to take it up. Reductive iron uptake is widely distributed in algae and its efficiency is highly dependent on the stability of Fe^{3+}-complexes. While weak complexes are easily reduced, strong complexes, such as photochemically inert Fe^{3+}-siderophores, are generally much less accessible for phytoplanktic iron uptake.[151] The siderophore desferrioxamine B, for instance, was found to completely deprive the diatom *Skeletonema costatum* of iron, resulting in a strong negative growth effect.[152] Photoreactive siderophores, in contrast, dramatically alter iron speciation by releasing Fe^{2+} upon light exposure and by forming photoproducts with altered affinity for Fe^{3+} compared to the respective parent siderophores. Both aspects likely enhance the bioavailability of iron to phytoplankton. This was illustrated in a study on natural planktic assemblages, which exhibited far higher iron uptake rates from photoreactive Fe^{3+}-aerobactin than from non-photoreactive Fe^{3+}-desferrioxamine B.[153] The persistence time of photoreactive siderophore-released Fe^{2+} depends on several factors, including pH and temperature. In air-equilibrated seawater at pH 8, dissolved Fe^{2+} was calculated to persist for just 2 min at 30 °C, but for more than 3 h at 0 °C.[154] Fe^{2+} can account for a surprisingly high fraction (> 60%) of dissolved iron in the ocean, which is maintained by constant redox cycling and putative Fe^{2+} ligands.[151,155] The iron affinity of siderophore photoproducts has a major impact on iron availability to phytoplankton. Vibrioferrin appears special in this context due to the apparent lack of iron binding properties of its photoproduct.[52] Vibrioferrin-producing bacteria were found to be highly abundant in the ocean, especially during algal blooms.[156] This suggests that the siderophore is highly involved in delivering iron to the blooming algae, which further supports the "carbon for iron mutualism".

The positive growth effect of *C. necator* H16 on the growth of *N. pelliculosa* assessed in this study (section 4.1) is suggestive of a "carbon for iron mutualism" occurring between both organisms. If so, this would confirm that freshwater photoreactive lipopeptide siderophores are

considerably involved in iron cycling and interspecific interactions. This would allocate them a major ecological role, akin to marine siderophores. However, the presented growth curves are not statistically hedged. Also, it cannot be excluded that the observed positive growth effect is due to other factors rather than cupriachelin-mediated iron release. At this point, it can only be concluded that a "carbon for iron mutualism" based on freshwater photoreactive lipopeptide siderophores can be anticipated, but requires further experimental confirmation.

5.7 Algae can induce the biosynthesis of photoreactive siderophores in *C. necator* H16

The finding that algae can induce cupriachelin biosynthesis in *C. necator* H16 (manuscript B) is in line with the "carbon for iron mutualism". It suggests that cupriachelin is advantageous to *N. pelliculosa* and that the benefit is so important that the alga invests in producing compounds that further upregulate the biosynthesis of the precious siderophore. The assumed extra iron supply will boost algal growth and thereby photosynthesis rates. As a result, *C. necator* H16 will supposably be able to acquire more fixed carbon from *N. pelliculosa*. This study represents a novel approach to support the hypothesis of mutualistic siderophore-based iron sharing. Amin et al. had chosen a more direct approach, demonstrating algal iron utilization via the bacterial siderophores by uptake experiments.[50] In their study, vibrioferrin was complexed with radioactive ^{55}Fe and fed to algal cultures. As soon as exposed to attenuated sunlight, algae incorporated this iron at extremely high rates, as reflected in high intracellular ^{55}Fe levels. Evidence for the uptake of algal organic carbon by the siderophore-producing bacterium was found on the genetic level, by identifying genes involved in transport and utilization of algal exudates. Also, iron uptake by the bacterium was tested and found to be more efficient in sunlight (i.e., from "free" Fe^{2+} or Fe^{3+}) than in the dark (from Fe^{3+}-vibrioferrin).[50] Such metal uptake experiments are well-established[100–102] and could readily confirm photoreactive siderophore-based iron sharing. They shed light on the fate of photoreactive siderophore-complexed iron and should also be conducted with Fe^{3+}-cupriachelin in future studies.

Another aspect that should be addressed in the future is the nature of the compounds that are released by *N. pelliculosa* and that induce cupriachelin transcription in *C. necator* H16. The secretion of compounds that directly act as transcription factors in the bacterium is unlikely, since this would require corresponding bacterial uptake systems. Directly applying algal culture supernatants to *cucJp* in DNA protein pulldown assays did not yield any visible proteins after SDS-PAGE (data not shown). This confirms that the alga does not produce any protein that

directly binds to *cucJp* as transcription factor. Instead, a signaling cascade involving several steps can be expected, with the detected NarL-type response regulator H16_A1372 as final effector protein. A first step in identifying the algal compounds of interest could be the fractionation of algal culture supernatants. The discrete fractions could then be applied to *C. necator* H16 reporter strains, followed by β-galactosidase assays. The increased β-galactosidase activities detected for non-fractionated algal supernatants compared to the control (manuscript B, Fig. 3) should be recovered in the fraction(s) of interest. In this way, the compounds present in algal culture supernatants could be narrowed down to the one or few compound(s) inducing cupriachelin transcription.

Phytoplankton produces saccharides that accumulate to high concentrations in aquatic environments. Due to hydroxyl and carboxyl functions and certain heteroatoms, these compounds exhibit a weak binding affinity towards iron, thereby increasing the bioavailability of the metal for eukaryotic phytoplankton.[157,158] It seems unlikely that saccharides can compete with siderophores for iron, due to their relatively low iron binding capacities. However, their abundance may be decisive in this context. If so, the cupriachelin biosynthesis-inducing compounds produced by *N. pelliculosa* may simply be saccharides. These would compete for iron with cupriachelin, thereby decreasing iron availability to *C. necator* H16 and inducing higher siderophore production levels. This would however imply a competitive rather than a mutualistic interaction between both organisms, which seems unlikely, especially in the context of the photoreactivity of cupriachelins.

Interactions between bacteria and diatoms are often highly species-specific, reflecting their long coevolution.[13,20,21] A drawback of the present study is that *C. necator* H16 and *N. pelliculosa* have not been isolated from the same environment. Testing whether even stronger positive effects can be assessed between *C. necator* H16 and a co-isolated alga would thus prove highly valuable. The main difficulty in this context is the small number of freshwater algae available from culture collections, notably as axenic cultures. Nevertheless, both *C. necator* and *N. pelliculosa* have been described as widely distributed freshwater plankton species, making their encounter in nature a plausible event. This is also corroborated by the seemingly intimate observed interaction. Planktic cross-talk is well-documented on a substrate exchange basis, but the gene regulative interaction described here goes one step beyond and suggests species specificity.

The finding of a two-component system involved in the regulation of cupriachelin transcription is highly interesting. In the DNA-protein pulldown assay, the NarL-type response regulator

H16_A1372 seemed more abundant when *C. necator* H16 was cultivated with algal culture supernatants compared to the control (manuscript B, Fig. 4). Since the former was also the conditions, where higher cupriachelin transcription levels were detected (manuscript B, Fig. 2), H16_A1372 is anticipated to act as transcriptional activator. This may easily be verified by cloning the corresponding promoter region *h16_a1372p* upstream of *lacZ* in the corresponding *C. necator* reporter strain. Up- or downregulation of the response regulator under different conditions should allow such conclusions. This approach was chosen for Fur (section 4.5). Acting as transcriptional repressor for siderophore biosynthesis, expression of this protein was expected to be upregulated under iron repletion, while being downregulated under iron deficiency. This was however not the case (Fig. 11) and no clear iron-dependent expression pattern could be observed. A possible explanation may be the global regulatory function of Fur, which requires a consistent basal level of protein.[77]

In summary, it was found that bacteria and algae can influence each other's growth dynamics also at the transcriptional level. Addressing this aspect also in marine environments, where photoreactive siderophores are already well-established, will further broaden our understanding of these compounds in interkingdom interactions.

5.8 Siderophores as biocontrol agents against harmful algal blooms

Harmful algal blooms have become an increasingly serious problem in the last few decades that now affect every coastal country in the world. The responsible algae cause damage either by toxin production or simply by their gigantic biomass that entails devastating effects on other organisms.[159] Harmful algal blooms have been known for centuries, but their constant increase indicates that their origin is nowadays very often anthropogenic. Their expansion can thus be attributed to storms and currents, but also to pollution, ship ballast water and extensive aquaculture. Toxins are dangerous in that they accumulate via the food chain, thereby poisoning various animals, including fish, shellfish, seabirds, sea lions, whales and humans.[160] Dinoflagellates are prominent toxin producers, causing numerous gastrointestinal and neurological diseases.[159] Cyanobacteria also represent potentially dangerous blooming algae.[161] Diatoms were believed to be free of toxins for a long time, until the discovery that *Pseudo-nitzschia* species produce the potent neurotoxin domoic acid.[162] Only recently, a *Pseudo-nitzschia* bloom covering the whole North American west coast resulted in the largest recorded outbreak of this neurotoxin.[163] Control of such harmful algal blooms is challenging. Mechanical

strategies are used in Korea, where clay is dispersed over the water surface.[164,165] The clay particles then aggregate with algal cells, removing them via sedimentation. Chemical control has also been used,[159] but has to be regarded as environmentally inacceptable, due to unspecific poisoning of aquatic life. Biological control may achieve better results here and the present dissertation aims at understanding plankton dynamics in this respect. The emphasis lies on the tremendous role of iron in shaping planktic communities. The nature and concentration of iron ligands are crucial for the bioavailability of the metal to different species.[166] The elaborated role of photoreactive siderophores herein suggests, that these molecules can shift plankton community equilibria from certain species to others, i.e., from harmful bloom-forming to harmless algae (manuscript C). However, using photoreactive siderophores and/or their producers for biocontrol purposes requires a profound understanding of the complex planktic interaction, which appears an almost unsurmountable task at present. This PhD thesis represents one of the first steps on the long path into this direction.

Summary

Photoreactive lipopeptide siderophores are intriguing compounds that are well-known from the marine environment. Once they have complexed Fe^{3+}, these compounds rapidly undergo photooxidative cleavage, thereby releasing Fe^{2+} into the environment. As a result, the solubilized iron is not only available to the siderophore producer, but to the whole microbial community. This can result in mutualistic interactions, with bacteria providing siderophore-solubilized iron to phytoplankton and obtaining photosynthetically fixed carbon in exchange. This is known as the "carbon for iron mutualism".

Photoreactive lipopeptide siderophores are widely distributed in the marine environment, but have recently also been found in freshwater and soil. The discovery of cupriachelins from *C. necator* H16 was followed by taiwachelin from *Cupriavidus taiwanensis* and serobactins from *H. seropedicae*. In this study, variochelins from *V. boronicumulans* are presented as further example. In addition, seven freshwater and soil bacteria are designated that are expected to produce such siderophores based on genome mining results. These findings corroborate the assumption that photoreactive lipopeptide siderophores are also widely distributed outside of the marine environment, raising the interest for their ecological role. In soil, where light exposure is not very likely, the photoreactive property may rather represent an evolutionary relict. In freshwater, mutualistic iron sharing, as described from the marine environment, is well-conceivable and may have a major ecological impact. This is addressed in the second part of the present study. Here, the cupriachelin-based interaction between the β-proteobacterium *C. necator* H16 and the diatom *N. pelliculosa* is investigated. Since iron usually represents a limiting factor for algal growth, diatoms are expected to strongly benefit from a "carbon for iron mutualism". If so, they could further maximize their advantage by manipulating (i.e., increasing) siderophore biosynthesis by the bacterium. Effectively, not only iron starvation, but also culture supernatants of *N. pelliculosa* were found to induce cupriachelin transcription levels in *C. necator* H16. Planktic interactions are well-documented on a substrate exchange basis, but this is one of the few studies reporting crosstalk on a transcriptional level. In conclusion, photoreactive siderophores play an important role in iron cycling in aquatic environments. They form a basis for interspecies interactions and thereby have the potential to shape planktic communities. This knowledge could be used for the biocontrol of harmful algal blooms.

Zusammenfassung

Photoreaktive Lipopeptidsiderophore sind fazinierende Moleküle, die aus marinen Habitaten bekannt sind. Sobald sie Fe^{3+} komplexiert haben, werden sie unmittelbar durch Sonnenlicht gespalten, wobei sie Fe^{2+} in die Umwelt freisetzen. Das gelöste Eisen ist somit nicht nur für den Siderophorproduzenten, sondern für die gesamte mikrobielle Gemeinschaft verfügbar. Dies kann zu mutualistischen Interaktionen führen, bei denen Bakterien Phytoplankton mit Siderophor-gelöstem Eisen versorgen und im Gegenzug photosynthetisch fixierten Kohlenstoff erhalten. Dies ist als „Kohlenstoff-für-Eisen-Mutualismus“ bekannt.

Photoreaktive Lipopeptidsiderophore sind in marinen Habitaten weit verbreitet, wurden jedoch kürzlich auch im Süßwasser und im Boden beschrieben. Der Entdeckung von Cupriachelinen von *C. necator* H16 folgten die von Taiwachelin von *Cupriavidus taiwanensis* und von Serobactinen von *H. seropedicae*. In der vorliegenden Studie werden Variocheline von *V. boronicumulans* als weiteres Beispiel präsentiert. Außerdem werden sieben Süßwasser- und Bodenbakterien genannt, die Genome Mining Ergebnissen zufolge in der Lage sind, solche Siderophore zu produzieren. Diese Ergebnisse unterstützen die Annahme, dass photoreaktive Lipopeptidsiderophore auch außerhalb von marinen Habitaten verbreitet sind, was die Frage nach ihrer ökologischen Rolle aufwirft. Im Boden, wo der Einfluss von Licht eher unbedeutend ist, könnte die Photoreaktivität lediglich ein evolutionäres Relikt darstellen. Im Süßwasser hingegen ist mutualistisches Teilen von Eisen, wie aus marinen Habitaten bekannt, durchaus denkbar und könnte eine wichtige ökologische Rolle spielen. Dies wird im zweiten Teil der vorliegenden Studie adressiert. Hier wird die Cupriachelin-basierte Interaktion zwischen dem β-Proteobakterium *C. necator* H16 und der Diatomee *N. pelliculosa* untersucht. Da Eisen meist einen limitierenden Faktor für Algenwachstum darstellt, wird erwartet, dass Diatomeen in hohem Maße von einem “Kohlenstoff-für-Eisen-Mutualismus“ profitieren. Wenn dem so sein sollte, könnten sie ihren Vorteil weiter maximieren, indem sie die Siderophorbiosynthese des Bakteriums manipulieren (d.h. erhöhen). Tatsächlich wurde festgestellt, dass nicht nur Eisenmangel, sondern auch Kulturüberstände von *N. pelliculosa*, Cupriachelin-Transkriptionslevel induzieren. Planktoninteraktionen sind auf Substrataustauschbasis gut dokumentiert, aber dies ist eine der wenigen Studien, die solche Interaktionen auf dem Level der Genregulation beschreibt. Zusammenfassend spielen photoreaktive Siderophore eine wichtige Rolle im aquatischem Eisenkreislauf. Sie bilden die Basis für interspezifische Interaktionen und haben somit das Potential, Planktongemeinschaften zu formen. Dieses Wissen könnte für die Biokontrolle schädlicher Algenblüten genutzt werden.

Theses

1. Photoreactive lipopeptide siderophores are not only common in the marine environment, but are also produced by many freshwater bacteria.

2. Freshwater photoreactive siderophores play similar ecological roles as their marine counterparts. The iron concentration is generally higher in freshwater than in the ocean, but iron starvation is similarly severe in both environments, due to different iron requirements of the inhabiting plankton species.

3. Photoreactive siderophores form the basis for interspecific planktic interactions. There is a "carbon for iron mutualism", where bacteria obtain photosynthetically fixed carbon from algae in exchange for the solubilized iron.

4. Photoreactive siderophore-based iron sharing can only be beneficial to bacteria, if the corresponding partners are mutualists. The interaction is rather species-specific and the partners recognize each other by the secretion of certain metabolites.

5. Diatoms strongly benefit from iron solubilized by bacterial photoreactive siderophores. In order to maximize their advantage, they can manipulate (i.e., increase) the siderophore biosynthesis by the bacterium.

6. Due to their potential to shape planktic communities, photoreactive siderophores are promising candidates for the biocontrol of toxic algal blooms. This depends on the degree to which selected species can benefit from the siderophore-solubilized iron.

7. In a tripartite interaction between a photoreactive siderophore-producing bacterium, a diatom and a non-photoreactive siderophore-producing cyanobacterium, the former two partners will be mutualists ("carbon for iron mutualism"). The cyanobacterium will not profit from either partner, since it is dependent neither on photoreactive siderophore-solubilized iron nor on carbon fixed by the diatom. This disadvantage can impair its growth compared to the other organisms, which can be regarded as positive, if the cyanobacterium causes harmful blooms.

References

1. Hay, M. E. Marine chemical ecology: Chemical signals and cues structure marine populations, communities, and ecosystems. *Annu. Rev. Mar. Sci.* **1,** 193–212 (2009).

2. Yim, G., Huimi Wang, H. & Davies FRS, J. Antibiotics as signalling molecules. *Philos. Trans. R. Soc. B Biol. Sci.* **362,** 1195–1200 (2007).

3. Asai, N., Fusetani, N., Matsunaga, S. & Sasaki, J. Sex pheromones of the hair crab *Erimacrus isenbeckii*. Part 1: Isolation and structures of novel ceramides. *Tetrahedron* **56,** 9895–9899 (2000).

4. Hardege, J. *et al.* Novel behavioural assay and partial purification of a female-derived sex pheromone in *Carcinus maenas*. *Mar. Ecol. Prog. Ser.* **244,** 179–189 (2002).

5. Atema, J., Jacobson, S., Karnofsky, E., Oleszko-Szuts, S. & Stein, L. Pair formation in the lobster, *Homarus americanus:* Behavioral development pheromones and mating. *Mar. Behav. Physiol.* **6,** 277–296 (1979).

6. Karlson, P. & Butenandt, A. Pheromones (ectohormones) in insects. *Annu. Rev. Entomol.* **4,** 39–58 (1959).

7. Schneider, D. Insect olfaction: Deciphering system for chemical messages. *Science* **163,** 1031–1037 (1969).

8. Sakurai, T. *et al.* Identification and functional characterization of a sex pheromone receptor in the silkmoth *Bombyx mori*. *Proc. Natl. Acad. Sci. U. S. A.* **101,** 16653–16658 (2004).

9. Tebben, J. *et al.* Chemical mediation of coral larval settlement by crustose coralline algae. *Sci. Rep.* **5,** (2015).

10. Spoerner, M., Wichard, T., Bachhuber, T., Stratmann, J. & Oertel, W. Growth and thallus morphogenesis of *Ulva mutabilis* (Chlorophyta) depends on a combination of two bacterial species excreting regulatory factors. *J. Phycol.* **48,** 1433–1447 (2012).

11. Weiss, A., Costa, R. & Wichard, T. Morphogenesis of *Ulva mutabilis* (Chlorophyta) induced by *Maribacter species* (Bacteroidetes, Flavobacteriaceae). *Bot. Mar.* **60,** (2017).

12. Wolfram, S., Nejstgaard, J. C. & Pohnert, G. Accumulation of polyunsaturated aldehydes in the gonads of the copepod *Acartia tonsa* revealed by tailored fluorescent probes. *PLoS ONE* **9,** e112522 (2014).

13. Amin, S. A., Parker, M. S. & Armbrust, E. V. Interactions between diatoms and bacteria. *Microbiol. Mol. Biol. Rev.* **76,** 667–684 (2012).

14. Bowler, C. *et al.* The *Phaeodactylum* genome reveals the evolutionary history of diatom genomes. *Nature* **456,** 239–244 (2008).

15. Paul, C., Mausz, M. A. & Pohnert, G. A co-culturing/metabolomics approach to investigate chemically mediated interactions of planktonic organisms reveals influence of bacteria on diatom metabolism. *Metabolomics* **9,** 349–359 (2013).

16. Croft, M. T., Lawrence, A. D., Raux-Deery, E., Warren, M. J. & Smith, A. G. Algae acquire vitamin B12 through a symbiotic relationship with bacteria. *Nature* **438,** 90–93 (2005).

17. Amin, S. A. *et al.* Interaction and signalling between a cosmopolitan phytoplankton and associated bacteria. *Nature* **522,** 98–101 (2015).

18. Bruckner, C. G., Bahulikar, R., Rahalkar, M., Schink, B. & Kroth, P. G. Bacteria associated with benthic diatoms from Lake Constance: Phylogeny and influences on diatom growth and secretion of extracellular polymeric substances. *Appl. Environ. Microbiol.* **74,** 7740–7749 (2008).

19. Grossart, H.-P., Levold, F., Allgaier, M., Simon, M. & Brinkhoff, T. Marine diatom species harbour distinct bacterial communities. *Environ. Microbiol.* **7,** 860–873 (2005).

20. Sison-Mangus, M. P., Jiang, S., Tran, K. N. & Kudela, R. M. Host-specific adaptation governs the interaction of the marine diatom, *Pseudo-nitzschia* and their microbiota. *ISME J.* **8,** 63–76 (2014).

21. Schäfer, H., Abbas, B., Witte, H. & Muyzer, G. Genetic diversity of 'satellite' bacteria present in cultures of marine diatoms. *FEMS Microbiol. Ecol.* **42,** 25–35 (2002).

22. Bell, W. & Mitchell, R. Chemotactic and growth responses of marine bacteria to algal extracellular products. *Biol. Bull.* **143,** 265–277 (1972).

23. Seymour, J. R., Amin, S. A., Raina, J.-B. & Stocker, R. Zooming in on the phycosphere: the ecological interface for phytoplankton–bacteria relationships. *Nat. Microbiol.* **2,** 17065 (2017).

24. Uitz, J., Claustre, H., Gentili, B. & Stramski, D. Phytoplankton class-specific primary production in the world's oceans: Seasonal and interannual variability from satellite observations. *Glob. Biogeochem. Cycles* **24,** n/a-n/a (2010).

25. Martin, J. H. & Fitzwater, S. E. Iron deficiency limits phytoplankton growth in the north-east Pacific subarctic. *Nature* **331,** 341–343 (1988).

26. Martin, J. H., Gordon, M. & Fitzwater, S. E. The case for iron. *Limnol. Oceanogr.* **36,** 1793–1802 (1991).

27. Pitchford, J. Iron limitation, grazing pressure and oceanic high nutrient-low chlorophyll (HNLC) regions. *J. Plankton Res.* **21,** 525–547 (1999).

28. Martin, J. H. Glacial-interglacial CO_2 change: The Iron Hypothesis. *Paleoceanography* **5,** 1–13 (1990).

29. Boyd, P. W. *et al.* Mesoscale iron enrichment experiments 1993-2005: Synthesis and future directions. *Science* **315,** 612–617 (2007).

30. John R. Chipperfield & Ratledge, C. Salicylic acid is not a bacterial siderophore: a theoretical study. *Biometals* **13,** 165–168 (2000).

31. Beinert, H. Iron-sulfur clusters: Nature's modular, multipurpose structures. *Science* **277,** 653–659 (1997).

32. Waldron, K. J., Rutherford, J. C., Ford, D. & Robinson, N. J. Metalloproteins and metal sensing. *Nature* **460,** 823–830 (2009).

33. Andrews, S. C., Robinson, A. K. & Rodríguez-Quiñones, F. Bacterial iron homeostasis. *FEMS Microbiol. Rev.* **27,** 215–237 (2003).

34. Posey, J. E. Lack of a role for iron in the lyme disease pathogen. *Science* **288,** 1651–1653 (2000).

35. Archibald, F. *Lactobacillus plantarum*, an organism not requiring iron. *FEMS Microbiol. Lett.* **19,** 29–32 (1983).

36. Hudson, R. J. M. & Morel, F. M. M. lron transport in marine phytoplankton: Kinetics of cellular and medium coordination reactions. *Limnol. Oceanogr.* **35,** 1002–1020 (1990).

37. McQuaid, J. B. *et al.* Carbonate-sensitive phytotransferrin controls high-affinity iron uptake in diatoms. *Nature* **555,** 534–537 (2018).

38. Morrissey, J. *et al.* A novel protein, ubiquitous in marine phytoplankton, concentrates iron at the cell surface and facilitates uptake. *Curr. Biol.* **25,** 364–371 (2015).

39. Gledhill, M. The organic complexation of iron in the marine environment: a review. *Front. Microbiol.* **3,** (2012).

40. Shaked, Y., Kustka, A. B. & Morel, F. M. M. A general kinetic model for iron acquisition by eukaryotic phytoplankton. *Limnol. Oceanogr.* **50,** 872–882 (2005).

41. Kustka, A. B., Allen, A. E. & Morel, F. M. M. Sequence analysis and transcriptional regulation of iron acquisition genes in two marine diatoms. *J. Phycol.* **43,** 715–729 (2007).

42. Van Ho, A., Ward, D. M. & Kaplan, J. Transition metal transport in yeast. *Annu. Rev. Microbiol.* **56,** 237–261 (2002).

43. Peers, G., Quesnel, S.-A. & Price, N. M. Copper requirements for iron acquisition and growth of coastal and oceanic diatoms. *Limnol. Oceanogr.* **50,** 1149–1158 (2005).

44. Maldonado, M. T. *et al.* Copper-dependent iron transport in coastal and oceanic diatoms. *Limnol. Oceanogr.* **51,** 1729–1743 (2006).

45. Maldonado, M. T. & Price, N. M. Reduction and transport of organically bound iron by *Thalassiosira oceanica* (Bacillariophyceae). *J. Phycol.* **37,** 298–310 (2001).

46. Kazamia, E. *et al.* Endocytosis-mediated siderophore uptake as a strategy for Fe acquisition in diatoms. *Sci. Adv.* **4,** eaar4536 (2018).

47. Jickells, T. D. Global iron connections between desert dust, ocean biogeochemistry, and climate. *Science* **308,** 67–71 (2005).

48. Marchetti, A. *et al.* Ferritin is used for iron storage in bloom-forming marine pennate diatoms. *Nature* **457,** 467–470 (2009).

49. Barbeau, K., Rue, E. L., Bruland, K. W. & Butler, A. Photochemical cycling of iron in the surface ocean mediated by microbial iron(III)-binding ligands. *Nature* **413,** 409–413 (2001).

50. Amin, S. A. *et al.* Photolysis of iron-siderophore chelates promotes bacterial-algal mutualism. *Proc. Natl. Acad. Sci.* **106,** 17071–17076 (2009).

51. Hider, R. C. & Kong, X. Chemistry and biology of siderophores. *Nat. Prod. Rep.* **27,** 637 (2010).

52. Amin, S. A., Green, D. H., Küpper, F. C. & Carrano, C. J. Vibrioferrin, an unusual marine siderophore: Iron binding, photochemistry, and biological implications. *Inorg. Chem.* **48,** 11451–11458 (2009).

53. Cobessi, D., Celia, H. & Pattus, F. Crystal structure at high resolution of ferric-pyochelin and its membrane receptor FptA from *Pseudomonas aeruginosa*. *J. Mol. Biol.* **352,** 893–904 (2005).

54. Boukhalfa, H. & Crumbliss, A. L. Chemical aspects of siderophore mediated iron transport. *Biometals* **15,** 325–339 (2002).

55. Llamas, M. A. *et al.* The heterologous siderophores ferrioxamine B and ferrichrome activate signaling pathways in *Pseudomonas aeruginosa*. *J. Bacteriol.* **188,** 1882–1891 (2006).

56. Poole, K. & McKay, G. A. Iron acquisition and its control in *Pseudomonas aeruginosa*: many roads lead to Rome. *Front. Biosci.* **8,** d661–d686 (2003).

57. Faraldo-Gómez, J. D. & Sansom, M. S. P. Acquisition of siderophores in Gram-negative bacteria. *Nat. Rev. Mol. Cell Biol.* **4,** 105–116 (2003).

58. Fukushima, T. *et al.* Gram-positive siderophore-shuttle with iron-exchange from Fe-siderophore to apo-siderophore by *Bacillus cereus* YxeB. *Proc. Natl. Acad. Sci. U. S. A.* **110,** 13821–13826 (2013).

59. Fukushima, T., Allred, B. E. & Raymond, K. N. Direct evidence of iron uptake by the Gram-positive siderophore-shuttle mechanism without iron reduction. *ACS Chem. Biol.* **9,** 2092–2100 (2014).

60. Schalk, I. J. & Guillon, L. Fate of ferrisiderophores after import across bacterial outer membranes: different iron release strategies are observed in the cytoplasm or periplasm depending on the siderophore pathways. *Amino Acids* **44,** 1267–1277 (2013).

61. Crosa, J. H. & Walsh, C. T. Genetics and assembly line enzymology of siderophore biosynthesis in bacteria. *Microbiol. Mol. Biol. Rev.* **66,** 223–249 (2002).

62. Wang, H., Fewer, D. P., Holm, L., Rouhiainen, L. & Sivonen, K. Atlas of nonribosomal peptide and polyketide biosynthetic pathways reveals common occurrence of nonmodular enzymes. *Proc. Natl. Acad. Sci.* **111,** 9259–9264 (2014).

63. Walsh, C. T. Polyketide and nonribosomal peptide antibiotics: Modularity and versatility. *Science* **303,** 1805–1810 (2004).

64. Marahiel, M. A., Stachelhaus, T. & Mootz, H. D. Modular peptide synthetases involved in nonribosomal peptide synthesis. *Chem. Rev.* **97,** 2651–2674 (1997).

65. Marahiel, M. A. Protein templates for the biosynthesis of peptide antibiotics. *Chem. Biol.* **4,** 561–567 (1997).

66. Kreutzer, M. F., Kage, H. & Nett, M. Structure and biosynthetic assembly of cupriachelin, a photoreactive siderophore from the bioplastic producer *Cupriavidus necator* H16. *J. Am. Chem. Soc.* **134,** 5415–5422 (2012).

67. de Lorenzo, V., Bindereif, A., Paw, B. H. & Neilands, J. B. Aerobactin biosynthesis and transport genes of plasmid ColV-K30 in *Escherichia coli* K-12. *J. Bacteriol.* **165,** 570–578 (1986).

68. de Lorenzo, V. & Neilands, J. B. Characterization of *iucA* and *iucC* genes of the aerobactin system of plasmid ColV-K30 in *Escherichia coli*. *J. Bacteriol.* **167,** 350–355 (1986).

69. Challis, G. L. A widely distributed bacterial pathway for siderophore biosynthesis independent of nonribosomal peptide synthetases. *ChemBioChem* **6,** 601–611 (2005).

70. Tanabe, T. *et al.* Identification and characterization of genes required for biosynthesis and transport of the siderophore vibrioferrin in *Vibrio parahaemolyticus*. *J. Bacteriol.* **185,** 6938–6949 (2003).

71. Lynch, D. *et al.* Genetic organization of the region encoding regulation, biosynthesis, and transport of Rhizobactin 1021, a siderophore produced by *Sinorhizobium meliloti*. *J. Bacteriol.* **183,** 2576–2585 (2001).

72. Franza, T., Mahé, B. & Expert, D. *Erwinia chrysanthemi* requires a second iron transport route dependent of the siderophore achromobactin for extracellular growth and plant infection: Achromobactin-dependent iron acquisition virulence in *E. chrysanthemi*. *Mol. Microbiol.* **55,** 261–275 (2004).

73. Kang, H. Y., Brickman, T. J., Beaumont, F. C. & Armstrong, S. K. Identification and characterization of iron-regulated *Bordetella pertussis* alcaligin siderophore biosynthesis genes. *J. Bacteriol.* **178,** 4877–4884 (1996).

74. Barry, S. M. & Challis, G. L. Recent advances in siderophore biosynthesis. *Curr. Opin. Chem. Biol.* **13,** 205–215 (2009).

75. Cabiscol, E., Tamarit, J. & Ros, J. Oxidative stress in bacteria and protein damage by reactive oxygen species. *Int. Microbiol.* **3,** 3–8

76. Bagg, A. & Neilands, J. B. Molecular mechanism of regulation of siderophore-mediated iron assimilation. *Microbiol. Rev.* **51,** 509–518 (1987).

77. Hantke, K. Iron and metal regulation in bacteria. *Curr. Opin. Microbiol.* **4,** 172–177 (2001).

78. Escolar, L., Pérez-Martín, J. & de Lorenzo, V. Opening the iron box: transcriptional metalloregulation by the Fur protein. *J. Bacteriol.* **181,** 6223–6229 (1999).

79. de Lorenzo, V., Wee, S., Herrero, M. & Neilands, J. B. Operator sequences of the aerobactin operon of plasmid ColV-K30 binding the ferric uptake regulation (fur) repressor. *J. Bacteriol.* **169,** 2624–2630 (1987).

80. Deng, Z. *et al.* Mechanistic insights into metal ion activation and operator recognition by the ferric uptake regulator. *Nat. Commun.* **6,** (2015).

81. Troxell, B. & Hassan, H. M. Transcriptional regulation by Ferric Uptake Regulator (Fur) in pathogenic bacteria. *Front. Cell. Infect. Microbiol.* **3,** (2013).

82. Masse, E. & Gottesman, S. A small RNA regulates the expression of genes involved in iron metabolism in *Escherichia coli*. *Proc. Natl. Acad. Sci.* **99,** 4620–4625 (2002).

83. Porcheron, G. & Dozois, C. M. Interplay between iron homeostasis and virulence: Fur and RyhB as major regulators of bacterial pathogenicity. *Vet. Microbiol.* **179,** 2–14 (2015).

84. Sheldon, J. R. & Heinrichs, D. E. Recent developments in understanding the iron acquisition strategies of gram positive pathogens. *FEMS Microbiol. Rev.* **39,** 592–630 (2015).

85. Love, J. F. *et al.* Genetic and biophysical studies of diphtheria toxin repressor (DtxR) and the hyperactive mutant DtxR(E175K) support a multistep model of activation. *Proc. Natl. Acad. Sci.* **101,** 2506–2511 (2004).

86. Butler, A. & Theisen, R. M. Iron(III)–siderophore coordination chemistry: Reactivity of marine siderophores. *Coord. Chem. Rev.* **254,** 288–296 (2010).

87. Ito, Y. & Butler, A. Structure of synechobactins, new siderophores of the marine cyanobacterium *Synechococcus* sp. PCC 7002. *Limnol. Oceanogr.* **50,** 1918–1923 (2005).

88. Homann, V. V. *et al.* Loihichelins A−F, a suite of amphiphilic siderophores produced by the marine bacterium *Halomonas* LOB-5. *J. Nat. Prod.* **72,** 884–888 (2009).

89. Martin, J. D., Ito, Y., Homann, V. V., Haygood, M. G. & Butler, A. Structure and membrane affinity of new amphiphilic siderophores produced by *Ochrobactrum* sp. SP18. *JBIC J. Biol. Inorg. Chem.* **11,** 633–641 (2006).

90. Barbeau, K., Zhang, G., Live, D. H. & Butler, A. Petrobactin, a photoreactive siderophore produced by the oil-degrading marine bacterium *Marinobacter hydrocarbonoclasticus*. *J. Am. Chem. Soc.* **124,** 378–379 (2002).

91. Robertson, A. W. *et al.* Isolation of imaqobactin, an amphiphilic siderophore from the arctic marine bacterium *Variovorax* species RKJM285. *J. Nat. Prod.* (2018).

92. Hardy, C. D. & Butler, A. β-Hydroxyaspartic acid in siderophores: biosynthesis and reactivity. *JBIC J. Biol. Inorg. Chem.* (2018). doi:10.1007/s00775-018-1584-2

93. Küpper, F. C., Carrano, C. J., Kuhn, J.-U. & Butler, A. Photoreactivity of iron(III)−aerobactin: Photoproduct structure and iron(III) coordination. *Inorg. Chem.* **45,** 6028–6033 (2006).

94. Martinez, J. S. *et al.* Structure and membrane affinity of a suite of amphiphilic siderophores produced by a marine bacterium. *Proc. Natl. Acad. Sci.* **100,** 3754–3759 (2003).

95. Martinez, J. S. *et al.* Self-assembling amphiphilic siderophores from marine bacteria. *Science* **287,** 1245–1247 (2000).

96. Schwartz, E. *et al.* Complete nucleotide sequence of pHG1: A *Ralstonia eutropha* H16 megaplasmid encoding key enzymes of H_2-based lithoautotrophy and anaerobiosis. *J. Mol. Biol.* **332,** 369–383 (2003).

97. Pohlmann, A. *et al.* Genome sequence of the bioplastic-producing "Knallgas" bacterium *Ralstonia eutropha* H16. *Nat. Biotechnol.* **24,** 1257–1262 (2006).

98. Guillard, R. R. L. & Lorenzen, C. J. Yellow-green algae with chlorophyllide C. *J. Phycol.* **8,** (1972).

99. Lowry, R. *VassarStats: Website for statistical computation*. (2018).

100. Bellenger, J. P., Wichard, T., Kustka, A. B. & Kraepiel, A. M. L. Uptake of molybdenum and vanadium by a nitrogen-fixing soil bacterium using siderophores. *Nat. Geosci.* **1,** 243–246 (2008).

101. Bellenger, J. P., Wichard, T. & Kraepiel, A. M. L. Vanadium requirements and uptake kinetics in the dinitrogen-fixing bacterium *Azotobacter vinelandii*. *Appl. Environ. Microbiol.* **74,** 1478–1484 (2008).

102. Wichard, T., Bellenger, J.-P., Morel, F. M. M. & Kraepiel, A. M. L. Role of the siderophore azotobactin in the bacterial acquisition of nitrogenase metal cofactors. *Environ. Sci. Technol.* **43,** 7218–7224 (2009).

103. Sommer, U. *et al.* Beyond the plankton ecology group (PEG) model: Mechanisms driving plankton succession. *Annu. Rev. Ecol. Evol. Syst.* **43,** 429–448 (2012).

104. Huffman, J. L. & Brennan, R. G. Prokaryotic transcription regulators: More than just the helix-turn-helix motif. *Curr. Opin. Struct. Biol.* **12,** 98–106 (2002).

105. Pfennig, N. *Rhodopseudomonas globiformis*, sp. n., a new species of the Rhodospirillaceae. *Arch. Microbiol.* **100,** 197–206 (1974).

106. Griffith, K. L. & Wolf, R. E. Measuring β-galactosidase activity in bacteria: Cell growth, permeabilization, and enzyme assays in 96-well arrays. *Biochem. Biophys. Res. Commun.* **290,** 397–402 (2002).

107. Watnick, P. I., Eto, T., Takahashi, H. & Calderwood, S. B. Purification of *Vibrio cholerae* Fur and estimation of its intracellular abundance by antibody sandwich enzyme-linked immunosorbent assay. *J. Bacteriol.* **179,** 243–247 (1997).

108. Eiler, A. & Bertilsson, S. Composition of freshwater bacterial communities associated with cyanobacterial blooms in four Swedish lakes. *Environ. Microbiol.* **6,** 1228–1243 (2004).

109. Zwart, G., Crump, B., Kamst-van Agterveld, M., Hagen, F. & Han, S. Typical freshwater bacteria: an analysis of available 16S rRNA gene sequences from plankton of lakes and rivers. *Aquat. Microb. Ecol.* **28,** 141–155 (2002).

110. Glöckner, F. O. *et al.* Comparative 16S rRNA analysis of lake bacterioplankton reveals globally distributed phylogenetic clusters including an abundant group of actinobacteria. *Appl. Environ. Microbiol.* **66,** 5053–5065 (2000).

111. Kellogg, C. A. & Griffin, D. W. Aerobiology and the global transport of desert dust. *Trends Ecol. Evol.* **21,** 638–644 (2006).

112. Yamaguchi, N., Ichijo, T., Sakotani, A., Baba, T. & Nasu, M. Global dispersion of bacterial cells on Asian dust. *Sci. Rep.* **2,** (2012).

113. Yamamoto, S., Okujo, N., Yoshida, T., Matsuura, S. & Shinoda, S. Structure and iron transport activity of vibrioferrin, a new siderophore of *Vibrio parahaemolyticus*. *J. Biochem. (Tokyo)* **115,** 868–874 (1994).

114. Baars, O., Zhang, X., Morel, F. M. M. & Seyedsayamdost, M. R. The siderophore metabolome of *Azotobacter vinelandii*. *Appl. Environ. Microbiol.* **82,** 27–39 (2016).

115. Gibson, F. & Magrath, D. I. The isolation and characterization of a hydroxamic acid (aerobactin) formed by *Aerobacter aerogenes* 62-1. *Biochim. Biophys. Acta BBA - Gen. Subj.* **192,** 175–184 (1969).

116. Haygood, M. G., Holt, P. D. & Butler, A. Aerobactin production by a planktonic marine *Vibrio* sp. *Limnol. Oceanogr.* **38,** 1091–1097 (1993).

117. Budzikiewicz, H. Bacterial citrate siderophores. *Mini-Rev. Org. Chem.* **2,** 119–124 (2005).

118. Stephan, H. *et al.* Ornibactins-a new family of siderophores from *Pseudomonas*. *Biometals Int. J. Role Met. Ions Biol. Biochem. Med.* **6,** 93–100 (1993).

119. Kümmerli, R., Schiessl, K. T., Waldvogel, T., McNeill, K. & Ackermann, M. Habitat structure and the evolution of diffusible siderophores in bacteria. *Ecol. Lett.* **17,** 1536–1544 (2014).

120. Butler, A. Marine siderophores and microbial iron mobilization. *BioMetals* **18,** 369–374 (2005).

121. Gobin, J. & Horwitz, M. A. Exochelins of *Mycobacterium tuberculosis* remove iron from human iron-binding proteins and donate iron to mycobactins in the *M. tuberculosis* cell wall. *J. Exp. Med.* **183,** 1527–1532 (1996).

122. Nett, M. Genome mining: Concept and strategies for natural product discovery. in *Progress in the Chemistry of Organic Natural Products 99* (eds. Kinghorn, A. D., Falk, H. & Kobayashi, J.) **99,** 199–245 (Springer International Publishing, 2014).

123. Bachmann, B. O., Van Lanen, S. G. & Baltz, R. H. Microbial genome mining for accelerated natural products discovery: is a renaissance in the making? *J. Ind. Microbiol. Biotechnol.* **41,** 175–184 (2014).

124. Gross, H. Genomic mining--a concept for the discovery of new bioactive natural products. *Curr. Opin. Drug Discov. Devel.* **12,** 207–219 (2009).

125. Paterson, J. *et al.* The contribution of genome mining strategies to the understanding of active principles of PGPR strains. *FEMS Microbiol. Ecol.* **93,** fiw249 (2017).

126. Ziemert, N., Alanjary, M. & Weber, T. The evolution of genome mining in microbes – a review. *Nat. Prod. Rep.* **33,** 988–1005 (2016).

127. Schwyn, B. & Neilands, J. B. Universal chemical assay for the detection and determination of siderophores. *Anal. Biochem.* **160,** 47–56 (1987).

128. Chen, Y. *et al.* Gobichelin A and B: mixed-ligand siderophores discovered using proteomics. *Med Chem Commun* **4,** 233–238 (2013).

129. Vizcaino, M. I., Guo, X. & Crawford, J. M. Merging chemical ecology with bacterial genome mining for secondary metabolite discovery. *J. Ind. Microbiol. Biotechnol.* **41,** 285–299 (2014).

130. Kreutzer, M. F. & Nett, M. Genomics-driven discovery of taiwachelin, a lipopeptide siderophore from *Cupriavidus taiwanensis*. *Org. Biomol. Chem.* **10,** 9338 (2012).

131. Kem, M. P. & Butler, A. Acyl peptidic siderophores: structures, biosyntheses and post-assembly modifications. *BioMetals* **28,** 445–459 (2015).

132. Parveen, B. *et al.* Diversity and dynamics of free-living and particle-associated *Betaproteobacteria* and *Actinobacteria* in relation to phytoplankton and zooplankton communities: *Betaproteobacteria* and *Actinobacteria* attached to particles. *FEMS Microbiol. Ecol.* **77,** 461–476 (2011).

133. Grabo, J. E., Chrisman, M. A., Webb, L. M. & Baldwin, M. J. Photochemical reactivity of the iron(III) complex of a mixed-donor, α-hydroxy acid-containing chelate and its biological relevance to photoactive marine siderophores. *Inorg. Chem.* **53,** 5781–5787 (2014).

134. Barbeau, K., Rue, E. L., Trick, C. G., Bruland, K. W. & Butler, A. Photochemical reactivity of siderophores produced by marine heterotrophic bacteria and cyanobacteria based on characteristic Fe(III) binding groups. *Limnol. Oceanogr.* **48,** 1069–1078 (2003).

135. Holt, P. D., Reid, R. R., Lewis, B. L., Luther, G. W. & Butler, A. Iron(III) coordination chemistry of alterobactin A: A siderophore from the marine bacterium *Alteromonas luteoviolacea*. *Inorg. Chem.* **44,** 7671–7677 (2005).

136. Vraspir, J. M., Holt, P. D. & Butler, A. Identification of new members within suites of amphiphilic marine siderophores. *BioMetals* **24,** 85–92 (2011).

137. Boiteau, R. M. *et al.* Siderophore-based microbial adaptations to iron scarcity across the eastern Pacific Ocean. *Proc. Natl. Acad. Sci.* **113,** 14237–14242 (2016).

138. Satola, B., Wübbeler, J. H. & Steinbüchel, A. Metabolic characteristics of the species *Variovorax paradoxus*. *Appl. Microbiol. Biotechnol.* **97,** 541–560 (2013).

139. Ravva, S. V., Hernlem, B. J., Sarreal, C. Z. & Mandrell, R. E. Bacterial communities in urban aerosols collected with wetted-wall cyclonic samplers and seasonal fluctuations of live and culturable airborne bacteria. *J Env. Monit* **14,** 473–481 (2012).

140. Baldani, J. I., Baldani, V. L. D., Seldin, L. & Dobereiner, J. Characterization of *Herbaspirillum seropedicae* gen. nov., sp. nov., a root-associated nitrogen-fixing bacterium. *Int. J. Syst. Bacteriol.* **36,** 86–93 (1986).

141. Gyaneshwar, P., James, E. K., Reddy, P. M. & Ladha, J. K. *Herbaspirillum* colonization increases growth and nitrogen accumulation in aluminium-tolerant rice varieties. *New Phytol.* **154,** 131–145 (2002).

142. Hermenau, R. *et al.* Gramibactin – a bacterial siderophore with a diazeniumdiolate ligand system. *Nat. Chem. Biol.* (2018).

143. Berti, A. D., Greve, N. J., Christensen, Q. H. & Thomas, M. G. Identification of a biosynthetic gene cluster and the six associated lipopeptides involved in swarming motility of *Pseudomonas syringae* pv. tomato DC3000. *J. Bacteriol.* **189,** 6312–6323 (2007).

144. Kearns, D. B. A field guide to bacterial swarming motility. *Nat. Rev. Microbiol.* **8,** 634–644 (2010).

145. Reid, R. T., Livet, D. H., Faulkner, D. J. & Butler, A. A siderophore from a marine bacterium with an exceptional ferric ion affinity constant. *Nature* **366,** 455–458 (1993).

146. Sunda, W. G., Swift, D. G. & Huntsman, S. A. Low iron requirement for growth in oceanic phytoplankton. *Nature* **351,** 55–57 (1991).

147. Xing, W. & Liu, G. Iron biogeochemistry and its environmental impacts in freshwater lakes. *Fresenius Environ. Bull.* **20,** 1339–1345 (2011).

148. Sunda, W. G. & Huntsman, S. A. Iron uptake and growth limitation in oceanic and coastal phytoplankton. *Mar. Chem.* **50,** 189–206 (1995).

149. Strzepek, R. F. & Harrison, P. J. Photosynthetic architecture differs in coastal and oceanic diatoms. *Nature* **431,** 689–692 (2004).

150. Kirchman, D. L. *et al.* Carbon versus iron limitation of bacterial growth in the California upwelling regime. *Limnol. Oceanogr.* **45,** 1681–1688 (2000).

151. Sunda, W. G. Feedback interactions between trace metal nutrients and phytoplankton in the ocean. *Front. Microbiol.* **3,** (2012).

152. Sanchez, N. *et al.* Effect of siderophore on iron availability in a diatom and a dinoflagellate species: Contrasting response in associated bacteria. *Front. Mar. Sci.* **5,** (2018).

153. Buck, K. N., Selph, K. E. & Barbeau, K. A. Iron-binding ligand production and copper speciation in an incubation experiment of Antarctic Peninsula shelf waters from the Bransfield Strait, Southern Ocean. *Mar. Chem.* **122,** 148–159 (2010).

154. Santana-Casiano, J. M., González-Dávila, M. & Millero, F. J. Oxidation of nanomolar levels of Fe(II) with oxygen in natural waters. *Environ. Sci. Technol.* **39,** 2073–2079 (2005).

155. Roy, E. G., Wells, M. L. & King, D. W. Persistence of iron(II) in surface waters of the western subarctic Pacific. *Limnol. Oceanogr.* **53,** 89–98 (2008).

156. Yarimizu, K. *et al.* Evaluation of photo-reactive siderophore producing bacteria before, during and after a bloom of the dinoflagellate *Lingulodinium polyedrum*. *Metallomics* **6,** 1156–1163 (2014).

157. Benner, R. Loose ligands and available iron in the ocean. *Proc. Natl. Acad. Sci.* **108,** 893–894 (2011).

158. Hassler, C. S., Schoemann, V., Nichols, C. M., Butler, E. C. V. & Boyd, P. W. Saccharides enhance iron bioavailability to Southern Ocean phytoplankton. *Proc. Natl. Acad. Sci.* **108,** 1076–1081 (2011).

159. Anderson, D. M. Approaches to monitoring, control and management of harmful algal blooms (HABs). *Ocean Coast. Manag.* **52,** 342–347 (2009).

160. Lefebvre, K. A., Bargu, S., Kieckhefer, T. & Silver, M. W. From sanddabs to blue whales: The pervasiveness of domoic acid. *Toxicon* **40,** 971–977 (2002).

161. Watson, S. B., Ridal, J. & Boyer, G. L. Taste and odour and cyanobacterial toxins: Impairment, prediction, and management in the Great Lakes. *Can. J. Fish. Aquat. Sci.* **65,** 1779–1796 (2008).

162. Rao, D. V. S., Quilliam, M. A. & Pocklington, R. Domoic acid - a neurotoxic amino acid produced by the marine diatom *Nitzschia pungens* in culture. *Can. J. Fish. Aquat. Sci.* **45,** 2076–2079 (1988).

163. McCabe, R. M. *et al.* An unprecedented coastwide toxic algal bloom linked to anomalous ocean conditions. *Geophys. Res. Lett.* **43,** 10,366-10,376 (2016).

164. Sengco, M. R., Li, A., Tugend, K., Kulis, D. & Anderson, D. M. Removal of red- and brown-tide cells using clay flocculation.: I. Laboratory culture experiments with *Gymnodinium breve* and *Aureococcus anophagefferens*. *Mar. Ecol. Prog. Ser.* **210,** 41–53 (2001).

165. Sengco, M. R., Hagström, J. A., Granéli, E. & Anderson, D. M. Removal of *Prymnesium parvum* (Haptophyceae) and its toxins using clay minerals. *Harmful Algae* **4,** 261–274 (2005).

166. Naito, K., Imai, I. & Nakahara, H. Complexation of iron by microbial siderophores and effects of iron chelates on the growth of marine microalgae causing red tides. *Phycol. Res.* **56,** 58–67 (2008).

Eigenständigkeitserklärung

Hiermit erkläre ich, dass ich die vorliegende Arbeit selbst verfasst und keine anderen als die angegebenen Quellen und Hilfsmittel verwendet habe. Die geltende Promotionsordnung der Fakultät für Biowissenschaften der Friedrich-Schiller-Universität Jena ist mir bekannt. Die Hilfe eines Promotionsberaters wurde nicht in Anspruch genommen. Es haben Dritte weder mittelbar noch unmittelbar geldwerte Leistungen für Arbeiten erhalten, die im Zusammenhang mit der vorgelegten Dissertation stehen. Diese schriftliche Arbeit wurde in gleicher oder ähnlicher Form noch bei keiner anderen Hochschule als Dissertation eingereicht und auch nicht als Prüfungsarbeit für eine staatliche oder andere wissenschaftliche Prüfung verwendet.

Jena, den 28.09.2018 _____

Colette Kurth

Abbreviations

A	adenylation
AAS	atomic absorption spectroscopy
ACP	Acyl carrier protein
BPDS	bathophenanthrolinedisulfonic acid
C	condensation
CAS	chrome azurol S
DtxR	diphteria toxin repressor
FAAL	fatty acyl-AMP ligase
Fur	ferric uptake regulator
HRMS	high-resolution mass spectrometry
ISIP	iron starvation-induced protein
MALDI	matrix-assisted lased desorption/ionization
MS	mass spectrometry
NIS	NRPS-independent siderophore
NMR	nuclear magnetic resonance
NRPS	non-ribosomal peptide synthetase
PKS	polyketide synthase
PrISM	proteomic investigation of secondary metabolites
PS	photosystem
ROS	reactive oxygen species
SDS-PAGE	sodium dodecyl sulfate polyacrylamide gel electrophoresis
TE	thioesterase
TOF	time of flight

Acknowledgements

First of all, I would like to equally thank my two supervisors Prof. Markus Nett and Prof. Georg Pohnert for giving me the opportunity to work in their research groups, supervising my projects, sharing their knowledge and always having time for questions. I spent wonderful first two years of my PhD in the junior research group “Secondary Metabolism of Predatory Bacteria” at the Hans Knöll Institute, thanks to many people. I am especially grateful to Dr. Hirokazu Kage, who was an excellent teacher for cloning and protein work. I would also like to thank Heike Heinecke, Andrea Perner and Till Kindel for numerous NMR, LC/MS and MALDI-TOF/MS measurements, respectively.

I had the chance to spent the last two years of my PhD in the Department of Bioorganic Analytics of the Friedrich Schiller University. I am deeply grateful to Markus for letting me leave his group, while still always taking a lot of time for me and my research. Also, I would like to thank Georg for readily accepting me in his group. I would like to thank all the people of the Department of Bioorganic Analytics for such enjoyable and unforgettable time.